School of Molecular Medical Sciences

MOLECULAR ANALYSIS OF THE ROLE OF *Haemophilus influenzae* PORIN P2 IN HOST-PATHOGEN INTERACTIONS

by

Mahde Saleh Abdulrahman Assafi

BSc, MSc

Thesis submitted to the University of Nottingham for the degree of Doctor of Philosophy

Molecular Bacteriology and Immunology Group

Centre for Biomolecular Sciences

November 2012

UK

Declaration

I hereby declare that all the work described in this thesis is my own, unless otherwise stated, and that this thesis has not been submitted, neither in whole or in part, elsewhere for another degree.

Mahde Saleh Abdulrahman Assafi

PhD Student

Molecular Bacteriology and Immunology Group

University of Nottingham

November 2012

Acknowledgement

Praise is due to almighty ALLAH for all he has given me, his compassion and mercifulness to allow me to complete this PhD project. I would like to acknowledge and I am grateful to all who have contributed to this piece of work and provided me with insights into several areas. The completion of this thesis would not have been possible without their generous help.

I would first and foremost like to thank my supervisors, Professor Dlawer Ala'Aldeen and Dr. Karl Wooldridge for giving me the opportunity to study for a PhD and complete this research in such a prominent research group. Without their kind supervision, goodwill and mentoring over the years, this thesis would not have been completed.

I owe Dr. Neil Oldfield a special debt of gratitude for his advice provided to me throughout my Ph.D. His invaluable knowledge, immense technical support, continual guidance and support over the years have given me great confidence and have been essential in undertaking this project.

I would also like to express my sincerest gratitude to Dr Jafar Mahdavi for his advice both in the lab and outside of it. His scientific discussions, motivation, encouragement, constructive criticism and suggestions proved most valuable.

I owe a great deal to Dr. Lee Wheldon for providing invaluable training and for the help I received from him during the cell culture experiments and confocal microscopy imaging. Additionally, I gratefully acknowledge Dr. Akhmed Aslam who gave generously of his time, support and contributing to the thesis through his broad knowledge of protein purification.

My gratitude is also directed toward Dr. Shaun Morroll, Dr. Jeroen Stoof, Dr. Nawfal, Dr. Noha, Dr. Sarfraz, Dr. Nader and Dr. Harry, for their technical support, the countless scientist discussions, collaboration, laboratory advice and encouragement, especially during my first year of study.

I am also indebted to Dr Adrian Robins and I really appreciate his willingness to share his knowledge and expertise with me to perform the FACS assay.

My thanks are due to the following members of the MBIG group and my friends in Nottingham for their support, advice and for tolerating the disarray of my social life during this period of study: Falwa, Sheyda, Heba, Ahmed, Sozan, Suha, Dina, Sheryl, Khiyam, Borgel, Kate, Ameer, Amin, Maher, Pierre, Matthew, Shaker, Farhad, Rebee, Nareman the list is endless.

I am thankful to the Ministry of Higher Education of Iraq for providing funding for this study. In a similar way, I am grateful to the members of the Iraqi cultural attaché in London, particularly thanks must go to Ali, for all the help and kindness they provided to me. Similarly, I want to express my gratitude towards the University of Nottingham for giving me this opportunity. Additionally, many thanks must go towards the Biology department at the University of Zakho for the encouragements and permission to do my PhD in Nottingham. In this respect, I thank Dr. Lazgin, Dr. Omar, Dr. Yousif, Dr. Samira, Dr. Samir, Dr. Intsar and Dr. Ezat.

Last but not least, I am extremely grateful to my family, especially my parents for their love, support, patience and encouragement throughout this study. Their faith and belief in me were my motivation, inspiration and strength. This thesis is dedicated to you.

Lastly, I wish to acknowledge all of those who are not mentioned, who supported me in any respect during the completion of my study. Thank you very much to all!

Publication

Abouseada N. M, Assafi, M. S. A, Mahdavi, J, Oldfield, N. J., Wheldon, L. M., Wooldrige, K. G., Ala'Aldeen, D. A. A. (2012). Mapping the laminin receptor binding domains of *Neisseria meningitidis* PorA and *Haemophilus influenzae* OmpP2. PLoS One. 2012; 7(9): e46233.

Posters

Mahde S Assafi, Neil Oldfield, Jafar Mahdavi, Karl Wooldridge & Dlawer Ala'Aldeen. Molecular and Functional Analysis of *Haemophilus influenzae* Porin P2 and Investigation into its Role in Host-Pathogen Interactions. Submitted to the Society of General Microbiology conference (SGM). 30 Mrch - 2 April 2009. Yourkshire, UK.

Mahde S Assafi, Neil Oldfield, Jafar Mahdavi, Karl Wooldridge & Dlawer Ala'Aldeen. Molecular and Functional Analysis of *Haemophilus influenzae* Porin P2 and Investigation into its Role in Host-Pathogen Interactions. Submitted to the 112th American Society of Microbiology conference (ASM). 21-24 May 2011. Louisiana, UAS.

Noha M. Abouseada, Mahde Saleh A. Assafi, Jafar Mahdavi, Neil J. Oldfield, Lee M. Wheldon, Karl G. Wooldridge and Dlawer A. A. Ala'Aldeen. Mapping the laminin receptor binding domains of *Neisseria meningitidis* PorA and *Haemophilus influenzae* OmpP2. Submitted to XVIIIth International Pathogenic Neisseria Conference (IPNC). 09-14 September 2012, Würzburg/Germany.

Abbreviations

A&A	Antibiotic-antimycotic	**JNK**	**c-Jun N-terminal kinases**
ABTS	2, 2'-azino-bis; 3-ethylbenzthiazoline-6-sulphonic acid	**kb**	Kilobase
ATCC	American Type Culture Collection	**kDa**	Kilodalton
AVV	Adeno-Associated Virus	**L**	Litre
***BamH*I**	Restriction endonuclease enzyme from *Bacillus amyloliquefaciens* H	**LAMP-1**	Human lysosomal-associated membrane protein 1
BBB	Blood-brain barrier	**LAS**	Leukocyte aggregation score
BCIP/NBT	5-bromo-4-chloro-3-indolyl phosphate/nitro blue tetrazolium	**LB**	Lysogeny Broth
bex	b capsule expression	**LOS**	Lipooligosaccharide
***Bgl*II**	Restriction endonuclease enzyme from *Bacillus globigii*	**LPS**	Lipopolysaccharide
BHI	Brain-heart infusion	**LamR**	37/67-kDa non-integrin laminin receptor
BMECs	Brain microvascular endothelial cells	**LR**	The 67-kDa laminin receptor
BSA	Bovine serum albumin	**LRP**	The 37-kDa laminin receptor precursor
bp	Base pair	**MAC**	Membrane attack complex
CbpA	Choline-binding protein A	**MAPK**	Mitogen-activated protein kinase
CFU	colony-forming units	**Megabase**	Mb
CIE	Counter-immunoelectrophoresis	**mg**	Milligram
CRP	C-reactive protein	**min**	Minute
CSF	Cerebrospinal fluid	**ml**	Millilitre
CT	Computerised tomographic scans	**MR**	Magnetic resonance
DIG-NHS	Digoxigenin-3-0-succinyl-ε-aminocaproic acid-N-hydroxy-succinimide ester Protein labeling kit	**NAD**	Nicotinamide adenine dinucleotide
DMEM	Dulbecco's MOD Eagle	***Not*I**	Restriction

	Medium		endonuclease enzyme from *Nocardia otitidis-caviarum*
DNA	Deoxyribonucleic acid	**NTHi**	Non-typeable *H. influenzae*
ECGS	Endothelial cell growth supplement	**OapA**	Opacity-associated Protein A
ECM	Extracellular matrix molecule	**OD**	Optical density
EIAs	Enzyme immunoassays	**OG**	*n*-Octyl-ß-D-glucopyranoside
ELISA	Enzyme-linked ImmunoSorbent Assay	**OMP**	Outer membrane protein
FACS	Fluorescent-activated cell sorter	**OP**	Opening pressure
FCS	Fetal calf serum	**ORF**	Open reading frame
FH	Factor H	**PAF**	Platelet-activating factor
FHL-1	Factor H-like protein 1	**PAI-1**	Plasminogen activator inhibitor type I
FHR1	Factor H -related protein 1	**PBS**	Phosphate Buffered Saline
g	Gram	**PCR**	Polymerase chain reaction
GBS	Group B streptococcus	***p*NPP**	*p*-nitrophenyl phosphate
GLC	Gas-liquid chromatography	**PRP**	polyribosyl ribitol phosphate
Gln	Glutamine	**PrP^c**	Cellular prion protein
Glu	Glutamic acid	**PRP-D**	PRP conjugated to diphtheria toxoid
h	Hour	**PRP-T**	PRP conjugated to tetanus toxoid
Hap	*Haemophilus* adherence and penetration	**RNA**	Ribonucleic acid
HBMECs	Human brain microvascular endothelial cells	***rnh***	Ribonuclease H
HbOC	Haemophilus b conjugate vaccine	**ROI**	Republic of Ireland
HEp-2	Human epithelial cell line 2	**s**	Second
Hia	*Haemophilus influenzae* adhesin	***Sal*I**	Restriction endonuclease enzyme from *Streptomyces albus* G
Hib	*Haemophilus influenzae*	**SDS-PAGE**	Sodium dodecyl

	type b		sulfate-polyacrylamide gel electrophoresis
Hif	*Haemophilus influenzae* fimbriae	**SE**	Standard error
HMW	High-molecular-weight proteins	**TLR**	Toll-like receptor
HRP	Horseradish peroxidase	**TNFα**	Tumour necrosis factor-alpha
Hsf	*Haemophilus* surface fibrils	**VCAM-1**	Vascular cell adhesion molecule-1
ICAM-1	Intercellular adhesion molecule 1	**VEE**	Venezuelan Equine Encephalitis Virus
Ig	immunoglobulin	**VOPBA**	Virus overlay protein binding assay
IL	Interleukin	**WBC**	White blood cell
IPCR	Inverse polymerase chain reaction	**WHO**	World health organization

Contents

List of Figures

List of Tables

Abstract

Haemophilus influenzae type b (Hib) was a main cause of bacterial meningitis. Together with *Neisseria meningitidis* and *Streptococcus pneumoniae,* it occurred with comparable frequency prior to the introduction of conjugated polysaccharide vaccines against Hib. Despite the fact that the introduction of conjugated vaccines against Hib has virtually eradicated infection in many areas of the globe, this pathogen still causes many infections in developing countries and a number of cases of infection have been reported in fully vaccinated children in developed countries. Recent studies have focused on the mechanisms by which these pathogens invade the central nervous system through the blood brain barrier (BBB). One study revealed that the outer membrane protein OmpP2 of *H. influenzae* interacted with the 37/67-kDa non-integrin laminin receptor (LamR) of human brain microvascular endothelial cells (HBMECs). In this study, OmpP2 of *H. influenzae* was expressed and purified and its interactions with purified recombinant LamR (rLamR) were analysed. OmpP2, which is predicted to contain eight extracellular loops, was expressed in two parts: OmpP2Δ1-4, lacking loops 1-4, and OmpP2Δ5-8, lacking loops 5-8. The protein fragments were purified and their interaction with rLamR was investigated by ELISA. The LamR binding site of OmpP2 was found to be restricted to loops 1-4. Therefore, *ompP2* derivatives encoding OmpP2 lacking loops 1, 2, 3 and 4 individually, were constructed. The OmpP2 derivatives were expressed and tested in rLamR-binding assays to determine which of these loops is required for LamR binding. Only OmpP2ΔL2 showed dramatically decreased binding to rLamR. Accordingly, loop 2 of OmpP2 may play an important role in the interaction of *H. influenzae* with LamR.

Therefore, *ompP2* and *ompP2ΔL2* null mutants were generated in *H. influenzae* strain Rd KW20 and utilized in subsequent characterization experiments to facilitate a study of the potential role of OmpP2 and its second loop in the pathogenesis of *H. influenzae*. The interaction of *H. influenzae* and its derivative mutants to LamR was investigated using a combination of molecular and immunological techniques, including ELISA, whole cell lysate pull-down assays, invasion and association assays and flow cytometry. *H. influenzae* cells either lacking OmpP2 or expressing OmpP2ΔL2 showed significantly reduced rLamR-binding compared to the wild type. Furthermore, synthetic peptides based on the loop 2 sequence coupled to micro-beads mediated adherence of the beads to HBMECs. The amino acid sequence of OmpP2 loop 2 was found to be highly conserved in Hib isolates, but not in non-typeable *H. influenza*e, which rarely cause invasive disease. The potential roles of OmpP2 and Loop 2 in *H. influenzae* pathogenesis are discussed.

CHAPTER ONE: General Introduction

CHAPTER ONE

1. GENERAL INTRODUCTION

1.1 Meningitis

Meningitis is an inflammation of the meninges: the pia mater, the arachnoid mater and the dura mater. It is characterised by the presence of polymorphonuclear cells in the cerebrospinal fluid (CSF). Inflammation of these membranes may be caused by a number of pathogenic microbes including viruses, fungi, parasites and bacteria, which are capable of entry into the central nervous system (CNS). Although several bacteria are able to invade the CNS and cause meningitis, the majority of cases are caused by *Neisseria meningitidis, Haemophilus influenzae,* and *Streptococcus pneumoniae* and, in newborns, *Escherichia coli* K1 and Group B streptococcus (1999; Harvey *et al.*, 1999; Huang *et al.*, 2000).

1.2 Clinical Presentation of Bacterial Meningitis

The signs and symptoms among patients with bacterial meningitis can be variable, subtle, non-specific, or even absent and somewhat dependent on the age (Kim, 2010; Mace, 2008). They are more subtle and atypical in the younger patient (Saez-Llorens & McCracken, 2003). The common manifestations noted at any age are fever (85% of patients) which is more common in adults than in children, headache, neck stiffness, nausea and altered mental status (Kaplan, 1999; Rosenstein *et al.*, 2001). Other symptoms which can be seen in older children and adults including: vomiting, irritability, neck or back pain, photophobia, anorexia, lethargy, malaise and maybe accompanied by Kernig's (flexing the hip and

extending the knee to elicit pain in the back and legs), and/or Brudzinski's signs (passive flexion of the neck elicits flexion of the hips) (Kaplan, 1999; Tunkel & Scheld, 1995). In addition, signs include cerebral dysfunction (confusion, delirium, or declining consciousness) which are found in 85% of patients who present with acute bacterial meningitis, cranial nerve palsies and focal cerebral signs occur in 10-20% of cases. Buccal or periorbital cellulitis, delirium, drowsiness, and coma can also develop (Kaplan, 1999; Tunkel & Scheld, 1995). Seizures occur more commonly in children (20% to 30%) than in adults (0-12%) and occur more frequently with *S. pneumoniae* or *H. influenzae* type b (Hib) than with meningitis caused by *N. meningitidis* (Tunkel & Scheld, 1995; Geiseler *et al.*, 1980; Kaplan, 1999; Saez-Llorens & McCracken, 2003). Occasionally, hearing loss or balance disorder were found as initial symptoms in older patients. Petechiae or purpura are noted in adults with *N. meningitidis*, *S. pneumoniae* and Hib. Arthritis, pneumonia, and pericarditis are examples of other suppurative signs of bacterial meningitis (Kaplan, 1999). The signs and symptoms in infants who have meningitis are often non-specific and include irritability, diarrhoea, lethargy, fever, stiff neck, poor feeding, seizures, apnea, a rash, or bulging fontanelles (Galiza & Heath, 2009; Kim, 2010).

1.3 Laboratory Diagnosis of Bacterial Meningitis

Blood and CFS (from lumbar puncture) cultures along with morphologic and chemical examination of CSF (cell count, glucose and protein concentrations) are used for the routine laboratory diagnosis of bacterial meningitis. Gram's stain is employed for initial assessment of CSF; other stains, such as Acridine orange and

Wayson stain also can be used (Daly *et al.*, 1985). CSF findings suggestive of bacterial meningitis are: Glucose less than 40 mg/dL or ratio of CSF/blood glucose less than 0.40, protein greater than 200 mg/dL, white blood cells (WBC) greater than 1000/µL, greater than 80% polymorphonuclear neutrophils, opening pressure (OP) of greater than 300 mm (Mace, 2008). In addition, many non-culture tests are used, such as latex agglutination (Gray & Fedorko, 1992), loop-mediated isothermal amplification (Kim *et al.*, 2011), microarray or biochip (Ben *et al.*, 2008). PCR has been used to detect microbial DNA in the CSF of a patient with suspected bacterial meningitis (primers are available for detection of the most common organisms, such as *N. meningitidis*, *S. pneumoniae*, and Hib (Chiba *et al.*, 2009; Kotilainen *et al.*, 1998; Poppert *et al.*, 2005). Leukocyte aggregation score (LAS) in the CSF was described as a cheap, simple and rapid method to detect and differentiate diagnosis of bacterial or meningitis (Garty *et al.*, 1997). Computerised tomographic (CT) scans or magnetic resonance (MR) imaging of the head are being used to detect a number of anatomic abnormalities in patients with bacterial meningitis (Kline & Kaplan, 1988; Steele *et al.*, 1985; Chen & Jiang, 2011). The presence of *S. pneumoniae*, *N. meningitidis*, or Hib can be confirmed using the Quellung procedure by mixing drop of CSF with antisera specific for the capsular polysaccharides of each of these three bacteria; the presence of the bacterial capsules can be detected under microscopic examination (Gray & Fedorko, 1992). Furthermore, Counter-immunoelectrophoresis (CIE) (Naiman & Albritton, 1980), Gas-liquid chromatography (GLC) (Thadepalli *et al.*, 1982), EIA Enzyme immunoassays (EIAs) (Salih *et al.*, 1989) have been used for the detection of suspected bacterial meningitis.

1.4 Epidemiology and Incidence of Bacterial Meningitis

In spite of the introduction and widespread use of antibiotics and other advances in medical care, meningitis still has a high morbidity and mortality (Durand *et al.*, 1993). Bacterial meningitis is an even more significant problem in many areas of the world, especially in developing countries. Despite the fact that many microbes that are pathogenic to humans have the potential to cause meningitis, relatively few of them are responsible for most cases of bacterial meningitis; these include *S. pneumoniae*, *N. meningitidis*, group B streptococcus, Hib, *E. coli* K1, *Mycobacterium tuberculosis*, and *Listeria monocytogenes* (Thigpen *et al.*, 2011). Between 1998 and 2007, more than 3000 patients with bacterial meningitis were identified in eight surveillance area in the United States (about 17.4 million persons), 14.8% of them died (Thigpen *et al.*, 2011). Of the 1670 cases reported in the same study during 2003–2007, *S. pneumoniae* was the predominant infective species (58.0%), followed by group B streptococci (18.1%), *N. meningitidis* (13.9%), *H. influenzae* (6.7%), and *L. monocytogenes* (3.4%) (Thigpen *et al.*, 2011).

More generally, *S. pneumoniae*, *N. meningitidis*, and Hib are the most common etiologic agents, which account for 90% of reported cases of acute bacterial meningitis (Peltola, 2000; CDC, 2002). In England and Wales, these three pathogens counted for 60% of the episodes (Bedford *et al.*, 2001). In the United States during the 1950s, 1960s, and 1970s they were identified to be responsible for the majority of the incidence of bacterial meningitis cases (70%) (Brouwer *et al.*, 2010).

Despite the change in the range of causative infecting bacteria, the rate of incidence has not changed dramatically around the world, in England and Wales from 1985 through 1987, the incidence was 0.22 per 1,000 live births (de Louvois *et al.*, 1991), 0.25 to 2.66 cases per 1,000 live births in Costa Rica (Odio, 1995), and 0.25 per 1,000 in Philadelphia and 0.36 to 1.11 in South Africa (Adhikari *et al.*, 1995). Between 1986 and 2001 in Kaohsiung-Taiwan, *H. influenzae*, Salmonella species, *Strep. agalactiae*, and *E. coli* were identified as the most causative agents of bacterial meningitis (about 59%) in 80 cases of reported bacterial meningitis in children of 1 month to one year of age (Chang *et al.*, 2004). The annual incidence in children younger than 5 years of age between 1995 and 2000 in Kenyans increased from 120 to 202 per 100,000 (Mwangi *et al.*, 2002). The predominant causes were *S. pneumoniae* (43.1%) and *H. influenzae* (41.9%) (Mwangi *et al.*, 2002). Recently, in a study performed in Turkey, 408 CSF samples were collected for a one year period (2005-2006) from children aged 1-17 months. Bacterial meningitis was identified in 243 samples. *N. meningitidis* was the most common causative bacterial agent (56.5%) followed by *S. pneumoniae* (22.5%) then Hib (20.5%). Among *N. meningitidis*–positive CSF samples, 42.7%, 31.1%, 2.2%, and 0.7% belonged to serogroups W-135, B, Y, and A, respectively (Ceyhan *et al.*, 2008). From 1981 to 1996, 7078 cases of bacterial meningitis were identified in Niger (lies within the African meningitis belt), the majority were caused by *N. meningitidis* (57.7%), followed by *S. pneumoniae* (13.2%) and Hib (9.5%) (Campagne *et al.*, 1999). Between 2002 and 2005, a surveillance study was performed to determine the incidence of childhood bacterial meningitis in children between 2 months to 5 years of age in Ulaanbaatar, Mongolia. 201

suspected meningitis cases were identified in residents of Ulaanbaatar. The average annual incidence rate for confirmed and probable bacterial meningitis was 68 cases per 100,000 children aged 2 months to 5 years. The average annual incidence rate of confirmed cases was 28 cases per 100,000 children for Hib meningitis, 11 cases per 100,000 children for pneumococcal meningitis, and 13 cases per 100,000 children for meningococcal meningitis (Mendsaikhan *et al.*, 2009).

1.5 Epidemiology and Incidence of *H. influenzae*

Before the advent of *H. influenzae* type b (Hib) conjugate vaccines, *H. influenzae* type b meningitis was the leading cause of bacterial meningitis in childhood (Mendsaikhan *et al.*, 2009; Howie *et al.*, 2007). The incidence of Hib meningitis was 26-43/100,000 per year in Denmark, Norway, Finland, Sweden and Iceland (Claesson, 1993). The highest rates of Hib meningitis occur in the first year of life. Most cases were in children aged 3 months to 3 years, as most infants are protected by passively acquired maternal antibodies during the first few months of life and they naturally develop immunity to *H. influenzae* after 3 years of age (Munson *et al.*, 1989b; Saez-Llorens & McCracken, 2003). Prior to the availability of *H. influenzae* type b conjugate vaccines in the United States, Hib was the most frequent cause of bacterial meningitis (45 to 48%) (peak incidence, 6 to 12 months of age) (Schlech *et al.*, 1985). A prospective, laboratory-based surveillance project obtained accurate data on meningitis in a population of 34 million people during 1986; *H. influenzae* was the most common cause of bacterial meningitis (45%), followed by *S. pneumoniae* (18%), and *N.*

meningitidis (14%) (Wenger *et al.*, 1990). The annual incidence for Hib meningitis in the Oxford region between 1985 and 1990 was 25.1 per 100,000 children aged less than 5 years with overall mortality was 4.3% and the majority of cases (71%) occurred in children younger than 2 years of age (Booy *et al.*, 1993). In the Republic of Ireland (1991 to 1993), the mean annual incidence rate of *H. influenzae* meningitis in children under five years was 25.4 per 100,000 with peak incidence (65-8 per 100,000) in the 6-11 months age-group (Fogarty *et al.*, 1995).

During the past 25 years and due to the introduction of programs for immunizing infants with conjugate Hib vaccines, the incidence of bacterial meningitis and other forms of invasive disease caused by Hib have greatly reduced in several parts of the world (Bisgard *et al.*, 1998; Schuchat *et al.*, 1997; van Alphen *et al.*, 1997; Slack *et al.*, 1998; Wenger, 1998; Garpenholt *et al.*, 2000; Daza *et al.*, 2006; Cowgill *et al.*, 2006; Lagos *et al.*, 1998; Robbins *et al.*, 1996; Dery & Hasbun, 2007). Since the introduction of the Hib conjugate vaccine in 1990 in the United States, the incidence of bacterial meningitis has declined by 55% (Dery & Hasbun, 2007; Thigpen *et al.*, 2011). Most industrialised countries use a 3-dose schedule in early infancy (2, 3, and 4 months) with a further dose at 11–18 months (Campbell *et al.*, 2009; Peltola *et al.*, 2005; Rijkers *et al.*, 2003). Following three doses of conjugate Hib vaccines; polyribosyl-ribitol-phosphate (PRP) conjugated to tetanus toxoid (PRP-T), diphtheria toxoid (PRP-D), the non-toxic variant of diphtheria toxin CRM_{197} (HbOC), in infancy showed 83–100% protection against invasive Hib infections (Black *et al.*, 1991; Vadheim *et al.*, 1993; Booy *et al.*, 1994). Higher estimates of efficacy were obtained after a booster dose in the

second year of life (Trotter *et al.*, 2008; Fitzgerald *et al.*, 2005). After the introduction of Hib vaccines into the routine infant immunization schedule, the median age of persons with bacterial meningitis increased greatly, from 15 months in 1986 to 25 years in 1995 and recently increased to 39 years of age in the United States (Bisgard *et al.*, 1998; Schuchat *et al.*, 1997).

1.6 Bacterial Meningitis Vaccines

Available vaccines against Hib, *N. meningitidis* (except *N. meningitidis* serogroup B) and *S. pneumoniae* are based on the polysaccharide capsule of the bacteria (Trotter *et al.*, 2008). The polysaccharide capsules of these pathogens are composed of repeating saccharide units, the chemical nature of which defines the capsular type of the organism (Pollard *et al.*, 2009). The disadvantages of polysaccharide vaccines are that they generally produce weak T-cell-independent immune responses which provide short-term protection and they are not generally immunogenic in infants (Trotter *et al.*, 2008; Smith *et al.*, 1973; Coutinho & Moller, 1973). In order to improve immunogenicity, polysaccharide vaccines were conjugated to different carrier proteins, such as tetanus toxoid or mutated diphtheria toxin CRM_{197} (which contains a glycine to glutamic acid point mutation at position 52 in the A subunit of diphtheria toxoid). These conjugate vaccines are immunogenic in children aged under 2 years and are able to induce a T-cell dependent immune response which provides long-term immunity through the production of new memory B cells (Bulkow *et al.*, 1993; Trotter & Ramsay, 2007; Bar-Zeev & Buttery, 2006).

1.6.1 *H. influenzae* Type b (Hib) Conjugate Vaccine Use and Effectiveness

Newborn babies and infants are protected until approximately 6 months of age by maternal antibodies which were supplied through transplacental transfer; after this age they become susceptible to invasive Hib disease (Ulanova & Tsang, 2009). The Hib capsular polysaccharide was the first vaccine to be licensed for use against Hib in 1985. It was composed of polyribosyl ribitol phosphate (PRP) (Morris *et al.,* 2008). Despite the fact that the PRP vaccine provided adequate protection in children above 2 years, it provided little protection in infants younger than 18 months (Peltola *et al.,* 1977). Polysaccharides are not recognized by T cells in children < 18 months, and therefore this cohort has poor immune responses to T-cell-independent antigens (McVernon *et al.,* 2004b; Pollard *et al.,* 2009; Coutinho & Moller, 1973). Consequently, new vaccines based on PRP chemically conjugated to a carrier protein were developed, such as diphtheria toxoid PRP-D, tetanus toxoid PRP-T or outer membrane protein of *N. meningitidis* PRP-OMP (Trotter *et al.,* 2008; Pollard *et al.,* 2009).

Helper T cells are needed to generate an anamnestic response, and also to induce class switching, are able to recognise a peptide linked to the antigen recognised by a B cell (McVernon *et al.,* 2004a). These new Hib vaccines have the ability to induce immunological memory B cells; such cells induce the secondary immune response on re-exposure to Hib antigen (McVernon *et al.,* 2003b). These vaccines are highly immunogenic in young children; anti-PRP antibody is induced in infants as young as 2 months of age (Trollfors *et al.,* 1992).

Immunisation with Hib conjugate vaccines was introduced in the United Kingdom and the Republic of Ireland (ROI) in 1992. In the UK, it was recommended at 2, 3, and 4 months of age and in the ROI, it is recommended at 2, 4, and 6 months of age (Heath *et al.*, 2000). There was also a catch-up campaign, in which a single dose was given to those aged < 4 years (Ramsay *et al.*, 2003). The vaccination program enhanced the control of Hib infection in England and Wales (Ramsay *et al.*, 2003). In England and Wales the incidence of invasive Hib disease has dramatically declined in children < 5 years of age since the annual incidence was 20.5–22.9 per 100,000 in 1990 and by 1998 it had fallen to 0.65 per 100,000 (Johnson *et al.*, 2006).

The most commonly used Hib conjugated vaccines consist of PRP conjugated to tetanus toxoid (PRP-T), diphtheria toxoid (PRP-D), the non-toxic variant of diphtheria toxin CRM_{197} (HbOC), or an outer membrane protein of *N. meningitidis* (PRP-OMP) (Heath, 1998). *H. influenzae* vaccines, PRP–T, PRP–OMP and HbOC are highly efficacious (WHO, 2006). Two injections are needed for such vaccines to induce protective antibody response, except for PRP-OMP which induces a protective response in 2-month-old infants after a single dose (Ulanova & Tsang, 2009). Singleton *et al.* indicated that in addition to decreasing Hib disease in Alaska, by using PRP-OMP in children > 5 years of age, Hib carriage also decreased in unvaccinated children, thus revealing a herd immunity effect (Singleton *et al.*, 2006). Herd immunity is a consequence of unvaccinated children deriving benefit from lower carriage rates in the community and hence reduced risk of exposure to Hib. Hib vaccines are now routinely administrated in 119 countries; however, just 42% of the population in developing countries and

only 8% of the population in the poorest developing countries are routinely vaccinated (Morris *et al.*, 2008; WHO, 2008).

Despite the remarkable efficacy of Hib conjugate vaccines, failures were reported in different areas of the world (Rijkers *et al.*, 2003; McVernon *et al.*, 2003b; Garpenholt *et al.*, 2000). Furthermore, Hib vaccines are not effective against non-type b *H. influenzae*. Recent studies showed that Hib bacterial meningitis is still causing high rates of incidence and mortality throughout the world (Mendsaikhan *et al.*, 2009; Pelkonen *et al.*, 2009). Since 1999, the incidence of Hib infection increased predominantly in vaccinated children (Trotter *et al.*, 2003; McVernon *et al.*, 2004c). There have been reports of true Hib disease vaccine failures cases in children in United Kingdom (Garner & Weston, 2003; Heath *et al.*, 2000). Between 1993 and 2001, 363 cases of Hib infection were reported in fully vaccinated children in England and Wales (Ramsay *et al.*, 2003). The increase in invasive Hib disease incidence in the UK was believed to be due to the combination of Hib vaccines with acellular pertussis (DTaP-Hib) (McVernon *et al.*, 2003a). In Ireland from 1996 to 2005, the annually reported cases of Hib disease in fully vaccinated children were increased from 1 to 10 cases respectively (Fitzgerald *et al.*, 2005) and acellular pertussis combinations were not used prior to 2005. In the Gambia, a recent report suggests that the number of cases of Hib disease may be increasing 8 years after vaccine introduction, highlighting the need for continued surveillance (Howie *et al.*, 2007). Therefore, improved vaccines containing additional well conserved antigens may lead to a greater reduction in *H. influenzae* disease burden; OmpP2 as a non-capsular outer membrane antigen is might be candidate vaccine against Hib infection.

1.7 The Genus *Haemophilus*

The genus *Haemophilus* is classified as a member of the family Pasteurellaceae. This family, together with another two families (Enterobacteriaceae and Vibrionaceae), belong to the facultatively anaerobic Gram-negative rods group (Holt *et al.*, 1994). The family Pasteurelleceae contains two main genera of interest to human disease; *Haemophilus* and *Actinobacillus* (Holt *et al.*, 1994). *Haemophilus* are Gram negative pleomorphic, rod-shaped bacteria, which are non-motile, aerobic but facultatively anaerobic and generally oxidase and catalase positive. *Haemophilus* species reduce nitrate, ferment sugars and grow optimally at 37°C in an environment supplemented with CO_2, on enriched media such as nutrient or chocolate agar. The genus name is derived from the Greek word "blood-loving" alluding to their requirement for heme. *Haemophilus* species require one or both of two growth factors: X factor (hemin) or V factor (β-nicotinamide adenine dinucleotide). These growth factors are required because strains are unable to convert δ-aminolaevulinic acid to protoporphyrin (Collee *et al.*, 1996; Cown & Talaro, 2009; Tortora & Case, 2009). Some species of *Haemophilus,* such as *H. influenzae*, *H. aegyptius* and *H. haemolyticus* require both of these growth factors. In contrast, *H. ducreyi* requires only X factor, whilst *H. parainfluenzae* and *H. parahymolyticus* needs only V factor for survival (Ward *et al.*, 2009; William *et al.*, 2005).

1.7.1 *Haemophilus* Species

Haemophilus species are obligate commensals of the mucous membranes of humans and animals. Ten species are associated with humans: *H. influenzae*; *H.*

parainfluenzae; *H. haemolyticus*; *H. parahymolyticus*; *H. aprophilus*; *H. paraphrophilus*; *H. paraphrohaemolyticus*; *H. aegyptius*; *H. segnis*; and *H. ducreyi* (Mahon & Manuselis, 2000). *Haemophilus* species constitute approximately 10% of the total bacterial flora in the human upper respiratory trac, with the majority being *H. parainfluenzae* and non-encapsulated *H. influenzae*. Six species are associated with animals: *H. parasuis* (swine); *H. paragallinarum* (poultry); *H. paracuniculus* (rabbits); *H. haemoglobinophilus* (dogs); and *H. felis* (cats) amongst others (Mahon & Manuselis, 2000).

1.7.1.1 ***H. influenzae***

H. influenzae forms part of the normal commensal flora of the throat and nasopharynx of between 25-75% of healthy people and acts opportunistically as a secondary invader in a variety of respiratory tract infections (Collee *et al.*, 1996). *H. influenzae* transmission is believed to occur from person to person by contact with infected respiratory droplets (Marrs *et al.*, 2001). *H. influenzae* species are divided into two groups: encapsulated and non-encapsulated. Encapsulated *H. influenzae* can cause severe systemic infections including epiglottitis, pneumonia, meningitis, osteomyelitis, septic arthritis and orbital cellulitis. Non-encapsulated *H. influenzae* are often associated with localised infections including acute otitis media in children, sinusitis in adults and children, and community-acquired pneumonia, especially in the elderly and in those with chronic obstructive pulmonary disease [COPD] (Goering *et al.*, 2008; Marrs *et al.*, 2001). The *H. influenzae* capsule is composed of polysaccharide and six antigenically distinct capsular types are recognized (a-f). Using an animal infection model with

genetically constructed isogenic mutants transformed with serotype-specific capsule-associated DNA from all six serotypes [a–f], serotype b was demonstrated to be the most virulent, followed by serotype a, which is in turn more virulent than serotypes c–f (Zwahlen *et al.*, 1989).

1.7.2 *H. influenzae* Genome

The *H. influenzae* Rd KW20 genome was the first complete genome sequence of a free-living organism which reported by Fleischmann *et al*., (1995). The complete nucleotide sequence of the chromosomal DNA is 1.83 Megabase (Mb), with a G+C content of 38% (Fleischmann *et al.*, 1995). The number of predicted coding regions is 1,743 and the functional predictions were reported for 58% of the putative *H. influenzae* proteins (Fleischmann *et al.*, 1995). The *H. influenzae* Rd KW20 metabolic genotype contains 488 metabolic reactions operating on 343 metabolites (Fleischmann *et al.*, 1995; Edwards & Palsson, 1999).

1.7.3 *H. influenz*ae Type b

WHO reported that *H. influenzae* type b is responsible for more than 90% of infections among the six capsular types of (WHO, 2006). The peak incidence of disease is among those aged between 4 months and 18 months, however Hib disease is occasionally observed in infants aged less than 3 months (WHO, 2006). The highest frequency of invasive disease among unvaccinated children in developing countries happens between 6 and 7 months of age (Morris *et al.*, 2008). Before the era of the Hib conjugate vaccine, most cases of Hib-related morbidity and mortality were due to meningitis and pneumonia, but other severe invasive infections caused by Hib include epiglottitis, osteomyelitis, septic

arthritis, septicaemia, cellulitis, and pericarditis (William *et al.*, 2005). For example, data collected from 357 Hib cases in Wales between 1988-1993 showed that meningitis and epiglottitis were the most common outcome of infection (51.2% and 16.8%, respectively), followed by pneumonia (9.5%), bone and joint infections (5.9%), bacteraemia (5.6%), cellulitis (6.7%) and miscellaneous (3.1%) (Collee *et al.*, 1996).

More recently, Peltola (2000) analysed the data from 3,931 patients from 21 studies worldwide in the 1970s to 1990s and concluded that above 90% of invasive Hib infections manifested as six classical entities: meningitis; bacteremic pneumonia; epiglottitis; septicaemia; cellulitis; and osteoarticular infections (more often septic arthritis than osteomyelitis). Other clinical manifestations constituted only 3% of the total number, whereas multifocal cases were diagnosed in 6%. Notably, meningitis represented 52% of the entire Hib disease spectrum (Peltola, 2000).

1.8 Virulence Factors and Pathogenesis of *H. influenzae*

H. influenzae possesses several virulence factors, which are related to transmission, adherence, colonization, and invasion. Some of these factors are found in all strains, whilst some are only found in sub-populations of strains (Vitovski *et al.*, 2002). *H. influenzae* pathogenesis begins with colonization of the nasopharynx, which requires that the organism overcomes host clearance mechanisms (van Alphen & van Ham, 1994). This colonisation may be transitory or bacteria may remain for several months with no obvious deleterious effects to the host (asymptomatic carriage). Bacterial adherence to the respiratory

epithelium represents a mechanism to circumvent clearance, whereas invasion into host cells and the mucosa of the upper respiratory tract may allow evasion of immune function and subsequent entry into the blood. Hib was identified within epithelial cells several hours after inoculation of infant monkeys (Smith, 1987). Organisms may enter directly into the bloodstream from the nasopharynx via mucosal or sub-mucosal blood vessels or they may be transported to regional lymph nodes, where some may replicate, and result in bacteraemia (Rubin & Moxon, 1983). Subsequently, the bacteria spread in the bloodstream to distant sites in the body. Finally, meningitis-causing strains must cross the blood-brain barrier (BBB) in order to gain entry to the cerebrospinal fluid (CSF) and brain (Polin & Harris, 2001; Quagliarello & Scheld, 1992; Tunkel *et al.*, 1992). Bacteria can traverse the BBB and consequently enter the brain transcellularly, paracellularly and/or in infected phagocytes (Kim, 2008).

The BBB maintains the environment of the brain and spinal column by regulating the influx and efflux of molecules as well as protecting the central nervous system (CNS) from microorganisms and toxins that are circulating in the blood by separating the blood contained in the cerebral microvessels from the cerebrospinal fluid which surrounds the CNS (Rubin & Staddon, 1999; Leib & Tauber, 1999a). The BBB is formed by astrocytes and pericytes and brain microvascular endothelial cells (BMECs), which have tight junctions (Chaudhuri, 2000; Unkmeir *et al.*, 2002). Studies have revealed that receptors for some meningeal pathogens such as *H. influenzae* are present on the choroid plexus cells, which supported bacterial entrance into the subarachnoid space and CSF at this site (Tunkel & Scheld, 1993). Once bacteria enter the CSF, they multiply and induce

the release of pro-inflammatory and toxic compounds, which lead to increased BBB permeability, induce transfer of neutrophils and protein into the subarachnoid space, as well as inducing an inflammatory response leading to many of the pathophysiologic consequences of bacterial meningitis, pleocytosis, encephalopathy, cerebral oedema, increased intracranial pressure, and altered cerebral blood flow (Kim, 2008; Molyneux *et al.*, 2002). White blood cells are entrapped in fibrin, which cannot cross the villi, consequently producing arachnoid villus dysfunction; such dysfunction results in many of the signs and symptoms of Hib meningitis. Some of the major virulence factors that contribute to these processes are discussed below:

1.8.1 Capsule

The capsule is an essential virulence factor for the six encapsulated types (a, b, c, d, e and f) and its structure relates directly to the structure of the *H. influenzae cap* locus (17-kb). This consists of three regions; Regions 1 and 3 are similar while region 2 is different and is a type specific (Luong *et al.*, 2004; Pittman, 1931). According to capsular polysaccharide structure: types a and b are composed of a neutral sugar, an alcohol (ribitol), and a phosphodiester bond; types c and f are composed of an *N*-acetylated amino sugar, another saccharide, and a phosphodiester bond; types d and e have a repeat unit of an *N*-acetylglucosamine and *N*-acetylmannosamine uronic acid (Figure 1.1) (Jin *et al.*, 2007). The type b capsule is composed of a linear teichoic acid containing ribose, ribitol (a five-carbon sugar alcohol), and phosphate linked by phosphodiester bonds and is named PRP (polyribosyl-ribitol-phosphate). The Hib capsule is unique in that it

contains two pentose monosaccharides rather than hexose sugars as subunit carbohydrates (Winn *et al.*, 2006).

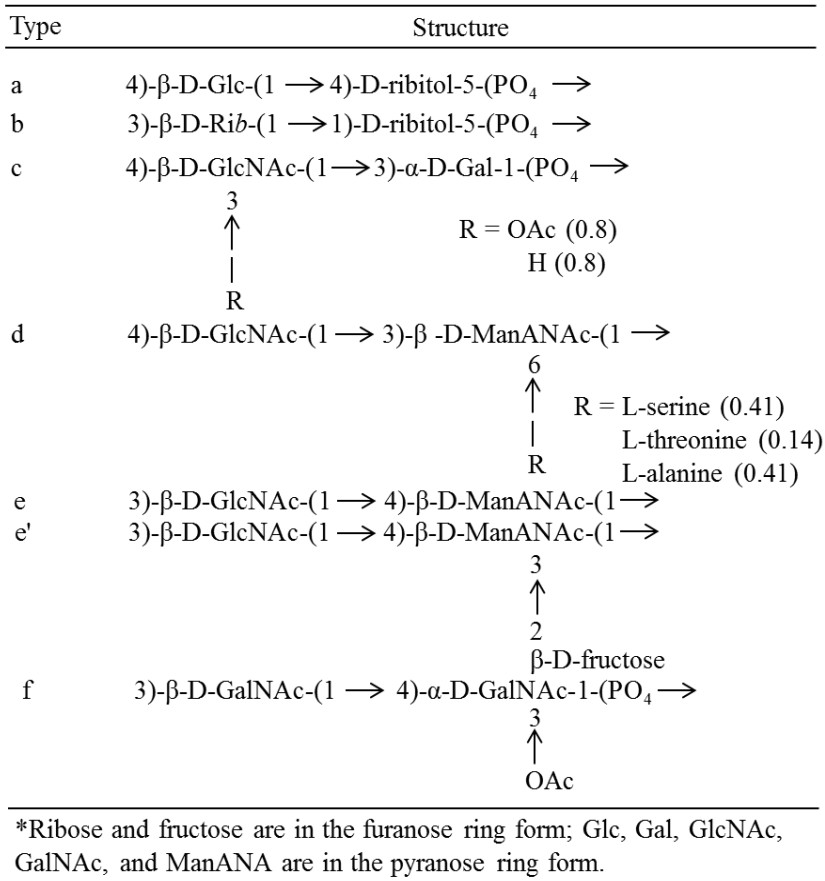

Figure 1.1. Structures of *H. influenzae* capsular polysaccharide*. Reported from (Sutton *et al*., 1982) .

Polysaccharide capsules are thought to protect the organism from desiccation, potentially facilitating transmission between hosts. Capsule polysaccharide also enhances survival in the blood by interfering with the binding of opsonising antibodies and complement to the bacterial surface (Marrs *et al.*, 2001). Thus, encapsulated *H. influenzae* can evade phagocytosis and

complement-mediated lysis in the non-immune host (Mahon & Manuselis, 2000).

As previously mentioned, the genes responsible for the biosynthesis and surface expression of the *H. influenzae* capsule are located in the *cap* locus, which contains three functionally distinct regions (Kroll *et al.*, 1991). Region 1 contains the genes *bexA*, *bexB*, *bexC*, and *bexD* genes and encodes an ABC transporter system involved in the export of capsular polysaccharide to the bacterial surface (Kroll *et al.*, 1990). Region 2 contains serotype-specific biosynthesis genes that appear to be unique to each of the six capsule types. The cap b region 2 contains the genes *orf1* to *orf4* which encode enzymes involved in the biosynthesis of ribose-ribitol-5-phosphate disaccharide subunit (Van Eldere *et al.*, 1995). Region 3 contains *hcsA* and *hcsB*, which have been shown to be involved in capsule transport across the outer membrane (Sukupolvi-Petty *et al.*, 2006).

In many *H. influenzae* strains the *cap* region contains two tandem copies of the cap locus, including one copy that is intact and a second copy that is complete except for a partial deletion of *bexA* (Kroll *et al.*, 1988). In the remaining *H. influenzae* isolates, a single copy of the *cap* locus is present. The significance of this duplication is unclear, but gene dosage effects may result in higher capsule expression levels in strains containing the *cap* duplication (Kroll *et al.*, 1988).

1.8.2 Adhesins

1.8.2.1 Fimbriae

Fimbriae are filamentous organelles that extend from the bacterial surface and are found on encapsulated type b strains and on about 30-40% of non-typeable strains

(Gilsdorf *et al.*, 1997). These organelles are peritrichous, hair-like helical structures approximately 5 nm in diameter and up to 450 nm in length (Stull, 1984). Fimbriae are thought to mediate the initial bacterial attachment to human oropharyngeal epithelial cells, thus facilitating respiratory tract colonization (reviewed in (St Geme & Falkow, 1990). Spontaneous mutants that lacked surface fibrils were deficient in attachment to cultured human epithelial cells (Joseph & David, 1995). *H. influenzae* fimbriae are complex structures composed of molecules of the major subunit protein, HifA, and two minor tip proteins, HifD and HifE (McCrea *et al.*, 1997). Like P pili and type 1 pili, *H. influenzae* pili are assembled via a chaperone/usher pathway (Bruant *et al.*, 2002). HifA, HifD, and HifE bind to the HifB putative chaperone in the periplasm, so protecting them from degradation during export from the cell. These proteins are assembled at the bacterial surface through interactions with the HifC assembly platform protein. The genes encoding these proteins (*hifA*, *hifD*, and *hifE*) exist as a single-copy cluster along with *hifC* and *hifB* (Bruant *et al.*, 2002).

Mutants lacking HifA were shown to have a reduced ability to bind human mucin; furthermore, antibodies against HifA could block binding (Kubiet *et al.*, 2000). HifE, which is found at the tip of the pilus, also has adhesive properties since mutations in *hifE* resulted in the production of fimbriae that had a reduced ability to cause hemagglutination and to adhere to epithelial cells (McCrea *et al.*, 1994). In addition, antibodies against HifE hindered the binding of Hib to human erythrocytes (McCrea *et al.*, 1998). A potential role for HifD remains unclear, but mutations in *hifD* resulted in strains expressing pili which were unable to agglutinate erythrocytes (McCrea *et al.*, 1998). Moreover, it was reported that

purified Hib fimbriae interacted with two heparin-binding extracellular matrix proteins: human fibronectin and heparin-binding growth-associated molecule (Virkola *et al.*, 2000).

1.8.2.2 HMW1 and HMW2

High-molecular-weight proteins HMW-1 (160 kDa) and HMW2 (155 kDa) are members of the auto-transporter family of proteins and are found in 70-80% of non-typeable *H. influenzae* but are rarely present in encapsulated strains (Winn *et al.*, 2006). The HMW-1 and HMW-2 proteins are encoded by separate chromosomal loci, *hmw1* and *hmw2*, respectively, each containing an *hmwA* gene, which encodes the structural protein, and two accessory genes, called *hmwB* and *hmwC,* encoding proteins involved in processing and surface localization of the HMW adhesins (Barenkamp & St Geme, 1994). These proteins were shown to have a role in adherence to human epithelial cells and are important colonization factors (St Geme & Falkow, 1993). St Geme & Falkow demonstrated that mutations in HMW-1 or HMW-2, or both in non-typeable *H. influenzae* led to a reduction in adherence to cultured human epithelial cells (St Geme & Falkow, 1993). Furthermore, the HMW-1 and HMW-2 proteins exhibit different cellular binding specificities; HMW-1 binds to sialylated glycoproteins, whereas the receptor for HMW-2 remains unknown (St Geme, 1994). The amino acids sequences 555–914 of HMW-1 (1,536 amino acids) was defined to be the domain which is responsible for interacting with epithelial cell receptors while in HMW-2 (1,477 amino acids) it was the region 553–916 (Dawid *et al.*, 2001). Animals

immunized with purified HMW-1/HMW-2 were protected against otitis media (Barenkamp, 1996).

1.8.2.3 Hia and Hsf

Hia (*H. influenzae* adhesin) is a trimeric autotransporter protein expressed in non-typeable *H. influenzae* strains and in some types a, e, and f strains (Rodriguez *et al.*, 2003). Hia promotes adherence to respiratory epithelial cells via two homologous binding domains, named HiaBD1 and HiaBD2 (Yeo *et al.*, 2004). Barenkamp & St Geme reported that a *hia* mutant showed reduced attachment to various human epithelial cell types (Barenkamp & St Geme, 1996). Interestingly, Hia is 81% identical to the Hsf protein (*H.* surface fibrils), an adhesin found in type b strains (St Geme *et al.*, 1996). Hsf also plays an essential role in respiratory tract colonization (St Geme *et al.*, 1996). Hsf strongly adheres to vitronectin and the active vitronectin binding domains of Hsf were suggested to be between 608–1351 and 1536–2414 (Hallstrom *et al.*, 2006). Furthermore, the Hia and Hsf proteins appear to recognize the same host cell receptor structure (St Geme *et al.*, 1996).

1.8.2.4 Hap Adhesin

The Hap (*H.* adherence and penetration) adhesin is ubiquitous among isolates of *H. influenzae* and is also a member of the autotransporter family of proteins. Hap is synthesized as a 155-kDa pre-protein encompassing a 110-kDa passenger domain, Hap_S, and a 45-kDa β-barrel domain, Hap_β (Hendrixson *et al.*, 1997). The Hap_S passenger domain has been shown to promote adhesion to human respiratory cells as well as to extracellular matrix proteins such as fibronectin, laminin, and

collagen IV (Fink *et al.*, 2002). Hap_S is also responsible for bacterial aggregation via Hap-Hap interactions, contributing to microcolony formation (Doran *et al.*, 2003). Immunization of mice with Hap_S led to reduction in nasopharyngeal colonization when mice were subsequently challenged with a non-typeable *H. influenzae* (Cutter *et al.*, 2002).

In addition to adhesive properties, Hap_S functions as a protease directing auto-proteolytic cleavage of Hap_S from Hap_β, resulting in release of the former from the cell surface (Fink *et al.*, 2001). Hap protease activity can be blocked by human respiratory secretions which contain protease inhibitors, such as secretory leukocyte protease inhibitor (Hendrixson & St Geme, 1998). Inhibition results in retention of Hap_S on the bacterial surface, increased adherence to epithelial cells, increased adherence to extracellular matrix proteins, increased bacterial aggregation, and increased microcolony formation (Hendrixson & St Geme, 1998).

1.8.2.5 Opacity-associated Protein A (OapA)

OapA is a 47-kDa adhesin found in all *H. influenzae* strains and it is responsible for an opaque colonial phenotype (Weiser *et al.*, 1995; Prasadarao *et al.*, 1999). Prasadarao *et al.* showed that OapA mediated attachment to Chang epithelial cells as binding was significantly reduced by mutating *oapA* (Prasadarao *et al.*, 1999). Furthermore, both recombinant OapA and polyclonal anti-OapA antiserum blocked the binding of *H. influenzae* to Chang epithelial cells (Prasadarao *et al.*, 1999).

1.8.3 IgA Protease

IgA1 protease is an extracellular autotransported enzyme that is capable of inactivating human immunoglobulin AI (Marrs *et al.*, 2001). IgA1 protease was found to be produced by several species of pathogenic bacteria including *H. influenzae*, *S. pneumoniae*, *N. gonorrhoeae* and *N. meningitidis* (Mistry & Stockley, 2006). *Neisseria gonorrhoeae* IgA1 protease was shown to cleave an amino acid sequence of human lysosomal-associated membrane protein 1 (LAMP-1) (Hauck & Meyer, 1997). IgA1 protease also has many effects on the immune system as Lorenzen *et al* have indicated, for example, it stimulates the release of cytokines such as tumour necrosis factor *α* (TNFα), interleukin-1ß (IL-1ß), interleukin-6 (IL6), and interleukin-8 (IL8) (Lorenzen *et al.*, 1999). The IgA1 proteases are therefore thought to be an important virulence factor, which influence colonisation and infection by bacteria at the mucosal surfaces. IgA1 protease is encoding by the gene *iga*, which is present in 97% of *H. influenzae*, however it is missing from non-pathogenic *Haemophilus* species (Fernaays *et al.*, 2006). Vitovski *et al*. found that IgA1 protease activity in strains isolated from sputum, blood, CSF, or normally sterile tissue of symptomatic individuals was considerably higher than in those isolated from throat swabs of asymptomatic carriers (Vitovski *et al.*, 2002). However, the precise role of IgA1 protease in the pathogenesis of *H. influenzae* infection has not yet been elucidated. Recently a second IgA1 protease gene, *igaB* has been identified, which is present in around one-third of isolated strains (Fernaays *et al.*, 2006). The contribution of this second IgA protease to pathogenesis has not yet been determined.

1.8.4 Lipooligosaccharide

Lipooligosaccharide (LOS) of *H. influenzae* is an outer membrane-associated glyco-lipid composed of lipid A joined via 2-keto-3-deoxyoctulosonic acid to a core polysaccharide polymer and is analogous to the lipopolysaccharide of many Gram-negative bacteria (Swords *et al.*, 2000). Innate responses to lipid A are mediated by Toll-like receptor 4 (TLR4) and are important for the containment of non-typeable *H. influenzae* (NTHi) infections in the airway and in the generation of the inflammatory response that is induced in chronic airway infections (Wang *et al.*, 2002). The interaction between bacteria and host cells is affected by LOS structure, which varies considerably between strains and also among bacterial cells within a strain. LOS containing phosphorylcholine (ChoP) promotes adherence in the upper airway (Swords *et al.*, 2000), and sialylated LOS promotes biofilm formation and persistence in the middle ear and lung (Swords *et al.*, 2001). Furthermore, these additions have been shown to help the bacteria to survive in the nasopharynx and evade phagocytosis by mimicking molecular structures usually found in the host (Weiser *et al.*, 1997). Moreover, NTHi invade host cells by binding to the platelet-activating factor (PAF) receptor via LOS glycoforms containing ChoP (Swords *et al.*, 2001). Mutations affecting the oligosaccharide region of LOS or the incorporation of ChoP considerably reduce the adherence to and invasion of bronchial cells by NTHi (Swords *et al.*, 2000).

1.8.5 Outer Membrane Porins

Outer membrane porins of Gram-negative bacteria are trimeric proteins which are mainly responsible for the molecular sieve properties of the outer membrane.

They act as a permeability barrier to the free diffusion of molecules across the cell envelope; they form water-filled channels, which allow the diffusion of hydrophilic molecules into the periplasm (Galdiero, 2007; Srikumar *et al.*, 1992b; Vachon *et al.*, 1985). Porins have both hydrophilic and hydrophobic features; the side in contact with the membrane is hydrophobic and the other side is hydrophilic so as to provide a hydrophilic lining to the pore. Loops are exposed to the aqueous environment on either side of the membrane will tend to be predominantly hydrophilic. In addition, they are composed of amphipathic membrane-spanning beta strands separating short periplasmic loops and longer and more variable extracellular loops (Srikumar *et al.*, 1992b). Porins have characteristics of selective permeability to permit the uptake of nutrients into the cell. Solutes lower in molecular weight than the pore size such as sugars, amino acids, nucleosides, and small antibiotics diffuse readily through outer membrane, whereas substances such as proteins, detergents, and large antibiotics molecular do not readily gain access to the periplasm (Srikumar *et al.*, 1997). The variety of porins and their exclusion limits differ from one bacterial genus to another (Srikumar *et al.*, 1992); for example, the pore formed by the Hib OmpP2 porin has a molecular size exclusion limit of *ca.* 1,400 Da (Cope *et al.*, 1990).

Porin OmpP2 of Hib is one of the best-characterized porins in terms of its functional characteristics and is the most abundant outer membrane protein (OMP) in both non-typeable *H. influenzae* (NTHi) and Hib. Its molecular mass varies between 36 and 42 kDa, and it is present in all strains. OmpP2 contains 16 anti-parallel β-strands crossing the outer membrane, eight large loops, termed L1-L8, of variable length on the external surface of the bacterial membrane, and

seven short periplasmic turns (Munson & Tolan, 1989; Srikumar *et al.*, 1992b; Srikumar *et al.*, 1997). Loops L1, L2, and L4 are important for monomer-monomer interactions within the porin trimer. Pore size is determined by folding of the longest loop (L3) into the channel, leaving a gap in the wall between strands β4 and β7 (Figure 1.2); Loop L4 is the second longest loop after internal loop L3, it is oriented toward the central axis of the pore and deletions in this loop widen the pore entrance; loops L5, L6, and L7 are superficial; loop L8, which is the third longest loop, seems to fold back into the barrel interior and to contribute to the formation of the channel opening at the external side (Galdiero *et al.*, 2003; Srikumar *et al.*, 1997). Sequence comparisons of *ompP2* genes indicate that all trans-membrane regions are relatively conserved among strains, whilst considerable heterogeneity exists in loop regions. It is likely that selective pressure imposed by the immune system is responsible for the heterogeneity of the extracellular loops (Bell *et al.*, 1994).

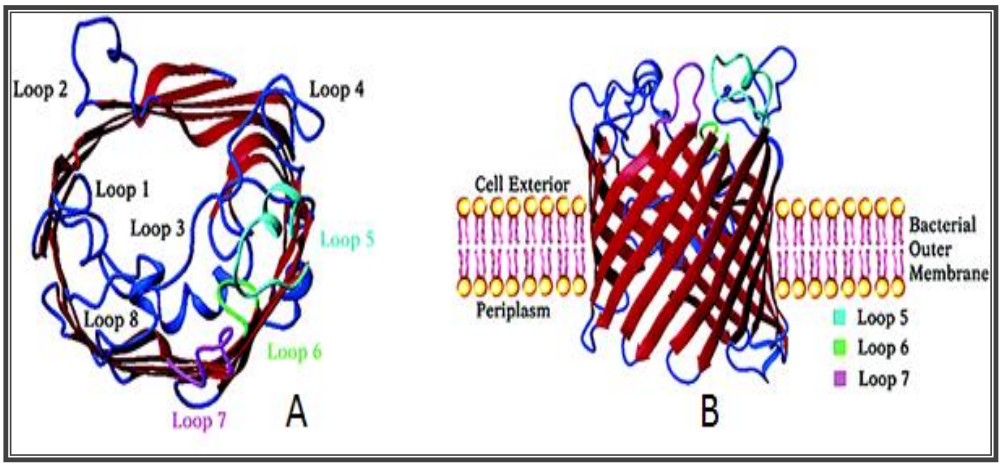

Figure 1.2. Three-dimensional model of the OmpP2 monomer from Hib. A slice horizontally through the barrel; loops. (B) Overview of the molecule (Galdiero *et al*., 2006).

There is significant evidence that OmpP2 of *H. influenzae* plays an important role in the pathology of infection; studies have revealed that antibodies against the OmpP2 protein are bactericidal in both type b and non-typeable *H. influenzae* strains (Galdiero *et al.*, 2001; Galdiero *et al.*, 2003; Murphy & Bartos, 1988). Cope *et al.* confirmed that an *ompP2* mutant lost the ability to producing bacteraemia in an infant rat model (Cope *et al.*, 1990). Furthermore, antibodies against OmpP2 were shown to be protective in an infant rat model of bacteraemia and a OmpP2 mutant was unable to cause bacteraemia in infant rats (Chong *et al.*, 1993; Duim *et al.*, 1996; Murphy & Bartos, 1988; Yi & Murphy, 1997). Porins also activate host inflammatory signalling cascades; it was demonstrated that whole OmpP2 from Hib and synthetic peptides corresponding to the surface exposed loops L5-L7 were able to activate cell phosphorylation and in particular the JNK and p38 mitogen-activated protein kinase (MAPK) pathways in U937 cells (Galdiero *et al.*, 2003). In contrast, peptides corresponding to the β-barrel of OmpP2 were not able to activate this pathway (Galdiero *et al.*, 2003). Moreover,

studies have suggested that OmpP2 and its loops are capable of activating signal transduction pathways such as MEK1-MEK2/MAP and JNK and the synthesis and secretion of inflammatory cytokines including IL-6 and TNF (Vitiello *et al.*, 2008).

A more recent study by Vitiello *et al.,* (2008) deduced that inoculation with loop L7 of OmpP2 from Hib induced significant patho-physiological changes in rats. Inoculation with L7 and whole OmpP2, but not a scrambled L7 peptide significantly induced E-selectin, a marker of endothelial injury, hyperglycemia and inflammatory cytokine production. In contrast, the coagulative/fibrinolytic cascade was impaired as shown by elevations of plasminogen activator inhibitor type I (PAI-1) levels (Vitiello *et al.*, 2008).

It was recently reported that *H. influenzae* binds laminin receptor (LamR) on human brain microvascular endothelial cells, suggesting that LamR binding is required for *H. influenzae* to invade the vascular endothelium of the blood brain barrier (Orihuela *et al.*, 2009). LamR may also be important in infection since some pathogens use the 67-kDa laminin receptor (67LR) as cell-surface receptors to enter their host's cells as part of their life cycles (Anderson *et al.*, 2000; Nelson *et al.*, 2008; Tio *et al.*, 2005; Chung *et al.*, 2003). The LamR protein on the surface of microvascular endothelial cells was identified to be a common receptor for the meningeal pathogens *N. meningitidis*, *H. influenzae* and *S. pneumoniae*. Moreover, mutagenesis studies indicated that the corresponding bacterial LamR-binding adhesins were pneumococcal CbpA, meningococcal PilQ and PorA, and OmpP2 of *H. influenzae* (Orihuela *et al.*, 2009). Each of the bacterial meningeal

pathogens (pneumococcus, meningococcus, and *H. influenzae*) were shown to interact with LamR and the interaction was severely decreased in the presence of soluble LamR. Furthermore, adherence of the three pathogens to the rat brain endothelial cell line rBCEC6 cells was reduced by antibody against the LamR C-terminus. Mutant *H. influenzae* which lack to OmpP2 (*ΔompP2*) showed dramatically less adherence to LamR. Moreover, when the expression of LamR was reduced by transfection of rBCEC6 cells with LamR siRNA, bacterial binding was significantly decreased compared with that of control transfected cells (Orihuela *et al.*, 2009). LamR acts as receptor protein for alphaviruses, such as the Sindbis virus (Wang *et al*., 1992), the major dengue virus serotypes (Tio *et al*., 2005), Venezuelan Equine Encephalitis Virus (VEE) (Ludwig *et al*., 1996), and several serotypes of Adeno-Associated Virus (AVV) (Akache *et al*., 2006). LamR was identified as important receptor for developing bacterial meningitis caused by *E. coli* K1 (Kim *et al*., 2005). Furthermore, it was demonstrated that it is a receptor for both PrP^{c} and PrP^{Sc} on the surface of mammalian cells (Nikles *et al.*, 2008; Gauczynski *et al.*, 2001).

1.9 *H. influenzae* and the Immune Response

The complement system is the first line of defence against pathogenic microorganisms, particularly against Gram-negative bacteria, and activation of the cascade leads to C3 deposition on the bacterial surface, phagocytosis and formation of the membrane attack complex (MAC) (Schneider *et al.*, 2007; Hallstrom *et al.*, 2008; Joiner, 1988). The complement system is organized into

three activation pathways; the alternative, the lectin and the classical pathway (Prescott *et al.*, 2005).

The ability of pathogens to survive in the human host and to circumvent the innate immune system including the complement system has role in their pathogenesis (Hallstrom & Riesbeck, 2010). Pathogenic microbes increase their serum resistance by interacting with complement components. For instance, *H. influenzae*, *N. meningitidis* and *E. coli* interfere with the classical complement activation pathway by binding to C4BP (Hallstrom & Riesbeck, 2010; Hallstrom *et al.*, 2007).

H. influenzae has developed several efficient strategies to circumvent complement attack such as the capsule, lipooligosaccharides, and several outer membrane proteins play role in bacterial survival by contribution in resistance against complement-mediated attacks and phagocytosis (Hallstrom & Riesbeck, 2010; Noel *et al.*, 1996). Clearance of Hib from blood is associated with the deposition of C3 on these bacteria and is independent of the later complement components (C5-C9) (Crosson *et al.*, 1976; Noel *et al.*, 1988).

It was shown that the interaction of Hib with factor H (FH) and factor H-like protein 1 (FHL-1), the inhibitors of the alternative pathway, increased its survival (Hallstrom *et al.*, 2008). Similarly, the outer membrane protein Hib surface fibrils (Hsf) has been reported to bind vitronectin that prevents complement deposition and formation of the membrane attack complex (MAC) (Hallstrom *et al.*, 2006). In addition, *H. influenzae* protein E (PE) interferes with complement-mediated

bacterial killing by capturing vitronectin (Singh *et al.*, 2011; Hallstrom *et al.*, 2009).

1.10 Laminin Receptor

The 67-kDa laminin receptor (67LR) is a non-integrin cell surface receptor for the laminin (Ardini *et al.*, 1998; Rao *et al.*, 1983). The 67-kDa laminin receptor was first isolated and identified as a laminin-binding protein in 1983 (Malinoff & Wicha, 1983; Lesot *et al.*, 1983; Rao *et al.*, 1983; Terranova *et al.*, 1983).

Laminin is one of the components of the extracellular matrix molecule (ECM) and is the major glycoprotein of the basement membrane from all types of tissues (Nelson *et al.*, 2008). In addition to its primary role as cell-matrix attachment, several biological activities have been demonstrated, such as nerve regeneration, tumour growth and metastasis, promoting cell growth and migration (Malinda & Kleinman, 1996).

37/67-kDa laminin receptor (LamR) protein can be found to be expressed in a wide variety of mammalian cells (Ardini *et al.*, 1998; Sobel, 1993; Garcia-Hernandez *et al.*, 1994; Nelson *et al.*, 2008). It is established that three regions of the C-terminal domain of 67LR are involved in the interaction with the laminin and these include: TEDWS-containing C-terminal repeats, residues 205–229 and a heparan-sulfate-dependent laminin-binding region from 161–180 (peptide G) (Castronovo *et al.*, 1991; Kazmin *et al.*, 2000). Recently, the residues Phe32, Glu35, and Arg155 of the LamR were identified as a laminin binding site (Jamieson *et al.*, 2011).

The exact structure of the 67LR is unclear; this receptor is believed to be formed from a 295-amino-acid 37-kDa precursor, while its observed molecular mass is approximately of 67-kDa on denaturing polyacrylamide gels. The corresponding gene has been identified and encodes a protein with a calculated molecular mass of approx. 37-kDa, a protein that is also observed in mammalian cells on SDS-PAGE (Wewer *et al.*, 1986; Wang *et al.*, 1992) and is thought to be the precursor of the 67-kDa variant of the protein. The mechanism by which 37 laminin receptor precursor (LRP) gives rise to its mature form (cell-membrane-embedded 67LR) has not been elucidated to date. LRP has been localized to the cytoplasmic, perinuclear and perichromosomal regions of the cell and also in the ribosomes of several tissues, such as heart, uterus, ovary, brain, liver, skeletal muscle and retina (Taylor *et al.*, 2003; Bortoluzzi *et al.*, 2001; Auth & Brawerman, 1992; Sato *et al.*, 1996; Kinoshita *et al.*, 1998). One hypothesis could be that the protein undergoes some form of post-translational modification in order to become the mature protein (Nelson *et al.*, 2008). Post-translational modification of the LRP including fatty acylation of the protein has been proposed to be a prerequisite of 67LR formation (Landowski *et al.*, 1995; Akache *et al.*, 2006; Scheiman *et al.*, 2010). It has also been proposed that the 67LR is a heterodimer between LRP and galectin-3 (Buto *et al.*, 1998). However, it has been shown that both LRP and 67LR are present on the plasma membrane of a cell line N2a, which does not express galectin-3 (Gauczynski *et al.*, 2001).

67-kDa laminin receptors have been shown to play an important role in tumour invasion and metastasis of a variety of tumours (Menard *et al.*, 1997; Pelosi *et al.*, 1997; Barsky *et al.*, 1984). An increase in the expression of 67LR (compared with

the corresponding normal tissue) has been found in a variety of common cancers, such as breast, colon, cervical, gastric, lung, hepatocellular, pancreatic, thyroid, carcinomas, ovary and prostate (Castronovo, 1993; Martignone *et al.*, 1993; Ménard *et al.*, 1998; Sanjuan *et al.*, 1996; al-Saleh *et al.*, 1997; Ozaki *et al.*, 1998; Fontanini *et al.*, 1997; Pelosi *et al.*, 1997; Montuori *et al.*, 1999; Rao *et al.*, 1989).

1.11 Aims of the Project

The general aim of the current study was to dissect the molecular interactions of *H. influenzae* outer membrane protein P2 and the human 37/67-kDa laminin receptor. More specfically, the initial aim was to define the LR-binding site(s) on OmpP2 by expressing specific regions of OmpP2 and investigating the ability of these recombinant proteins to bind to LamR. Having defined the extra-cellular loop 2 as the LamR-binding region (Chapter 3), a further aim was to produce and charaterise the LR-binding of an OmpP2 loop 2 deletion mutant of *H. influenzae* strain Rd KW20 (Chapter 4). Finally, the role of OmpP2 loop 2 in interactions with host cells was investigated using a combination of synthetic peptides, recombinant proteins and *H. influenzae* strains (Chapter 5).

CHAPTER TWO: Materials and Methods

CHAPTER TWO

2. MATERIAL AND METHODS

2.1 Bacterial Strains, Growth Conditions, and Media

Haemophilus influenzae Winslow Rd [KW20] (LGC/ American Type Culture Collection; ATCC), and its mutant derivatives, were grown at 37°C in either brain heart infusion (BHI) (Oxoid), supplemented with hemin (10 μg ml^{-1}) and NAD (10 μg ml^{-1}) in liquid, agar media or chocolate horse blood agar (Oxoid). *Neisseria meningitidis* serogroup B, strain MC58 (B:15:P1.7.16b) (Tettelin *et al.*, 2000) and its mutant derivatives were cultured on Columbia agar with chocolate horse blood agar (Oxoid) at 37°C, in an atmosphere of air plus 5% CO_2. When grown in suspension, meningococcal strains were grown in brain-heart infusion (BHI) broth (Oxoid) at 37°C with agitation. Broth cultures were aerated by agitation at 200 revolutions per min (rpm) in a shaking incubator. Agar or broth media were supplemented, where appropriate, with antibiotics. Antibiotics used (Sigma) were ampicillin (100 μg ml^{-1}), kanamycin (50 μg ml^{-1}), streptomycin (50 μg ml^{-1}) and spectinomycin (50 μg ml^{-1}). *Escherichia coli* JM109 strains (Promega) were routinely grown at 37°C in Lysogeny Broth (LB) (Bertani, 2004) or on LB agar (Fisher Scientific). These cells were used for the routine propagation of plasmids and for expression of 6 × histidine-tagged recombinant protein fragments. Where appropriate, blue/white selection of transformants in cloning experiments was achieved using IPTG (Roche) and X-gal at 0.5 mM and 80 μg ml^{-1}, respectively.

2.2 DNA Manipulation

2.2.1 Chromosomal DNA Extraction

Chromosomal DNA was isolated using the DNeasy Blood & Tissue kit (Qiagen) using the protocol for bacterial cells according to the manufacturer's instructions. Briefly, following overnight growth cells were harvested using a sterile loop and re-suspended in 180 µl of ATL buffer and 20 µl of Proteinase K was added to disrupt the cells. The sample was then heated at 56°C until the complete lysis of cells was achieved. The lysate was applied to a DNeasy spin column (Qiagen). The bound DNA was washed twice using the buffers provided in the kit. The bound DNA was eluted in 200 µl of nuclease-free deionised water and stored at -20°C.

2.2.2 Extraction of Plasmid DNA

Plasmid extraction was performed in accordance with the manufacturers' instructions using QIAprep Miniprep kit (Qiagen). Briefly, *E. coli* JM109, harboring the desired plasmid, was streaked onto LB agar plates supplemented, where appropriate, with antibiotics and incubated overnight at 37°C. Single colonies of cells were transferred to 5 ml of LB broth containing appropriate antibiotics and cultured overnight with shaking at 200 rpm. The following day, cells were harvested by centrifugation at 13,000 × *g* for 10 min and the pellet re-suspended in 200 µl of re-suspension solution. Then, 200 µl of the lysis buffer was added and mixed gently followed by adding neutralization solution and centrifuged at 13,000 × *g* for 10 min and the supernatant was added to a GenElute

tube and centrifuged for 1 min. After washing, the plasmid DNA was finally eluted in 100 μl of nuclease-free deionised water and stored at -20°C.

2.2.3 Restriction Endonuclease Digestion and Ligation of DNA

To selectively cleave DNA at specific recognition nucleotide sequences, appropriate restriction endonuclease enzymes were purchased from New England Biolab, Promega or Roche and used according to the manufacturer's instructions followed by incubation with T4 DNA ligase (Promega).

2.2.4 Dephosphorylation of DNA Fragments

To prevent the re-circularization of linearized digested vector during ligation with a DNA insert, linearized vectors were dephosphorylated using alkaline phosphatase. Briefly, 50 units of Antarctic Phosphatase (New England Biolabs) was added to 1 μg of plasmid DNA and Antarctic Phosphatase reaction Buffer (10 ×) for 1 h at 37°C and heat inactivated for 5 min at 65°C.

2.2.5 DNA Sequencing

DNA fragments were sequenced on both strands using specific primers using fluorescent-labelled dye terminator reactions on a 3130xl Genetic Analyser (Applied Biosystems) at the Biopolymer Synthesis and Analysis Unit, School of Biomedical Sciences, University of Nottingham. DNAMAN version 3.14 (Lynnon BioSoft) software was used to analyse DNA sequences.

2.3 Quantification of DNA and Protein

The concentration of purified PCR products, plasmid, genomic DNA and recombinant purified proteins was quantified using a NanoDrop (ND-1000) spectrophotometer (Agilent Technologies) by measuring the absorbance at 260 nm for DNA and 280nm for protein; the ratio of the readings at 260 nm and 280 nm was used to determine the purity of the DNA. For more accurate determinations, proteins were quantified using a Pierce BCA protein assay kit (Thermo Scientific; kit 23225) or Bradford assay kit (Bio-Rad) in accordance with the manufacturer's instructions.

2.4 Polymerase Chain Reaction (PCR)

For all experiments, PCR reactions were performed in a 25 µl reaction mixture using a C1000 model Thermal Cycler (BIO-RAD). The components, volumes and concentrations used were: 1 µl of primer in a final concentration 5µM; 10-50 ng μl^{-1} (final concentration) of a plasmid or chromosomal DNA in 1 µl; 0.5 µl of a final concentration of 200 µM dNTPs (deoxyribonucleotide mix, 10 mM each) (Roche); Expand High Fidelity *Taq* DNA polymerase 0.2 µl (3.5 U μl^{-1}) (Roche) or *Taq* DNA polymerase (Roche) and 2.5 µl of 10 × PCR buffer. The reaction mixture was made up to a final volume of 25 µl with nuclease free deionised water. The PCR amplification conditions were: initial template denaturation step of 3 min at 94°C, followed by 33 cycles consisting of 50s of annealing at 50-56°C, extension at 68°C (for Expand High fidelity *Taq* polymerase) or 72°C (for *Taq* polymerase) for varying amouts of time according to the polymerase used (generally 1min/kb of expected product), and 30 s of denaturation at 94°C. The

final cycle consisted of 50s at 50°C for annealing and 10 min at 70°C for extension.

2.5 Primer Design and Analysis

All oligonucleotide sequences for PCR amplification of specific DNA sequences were designed using DNAMAN version 3.14 (Lynnon BioSoft). This software was also used for checking primer sequences for characteristics such as melting temperature and the presence of unique binding sites within templates. All primers used in this study were synthesized by Eurofins MWG GmbH (Germany) and listed in Table 2.1.

Table 2.1. DNA primers utilised in this study.

Primer	Oligonucleotide sequence[a] (5'-3')	Restriction site
mP2_F	CGCTAACATTTCATCAGTAATTCC	--
mP2_R	GACCAAACTAGCGTTGAAACC	--
P2F3	GCCGCGGCCGCTAACATTTCATCAGTAATTCCATGAAC	*Not*I
P2R3_3	CGCGCGGCCGCAATTAAATGGCTGTGGTGGC	*Not*I
F1	CACGCTTTATAGTGATAGCC	--
T7P	TAATACGACTCACTATAGGG	--
SP6	ATTTAGGTGACACTATAGT	--
Fbg	GGAAGATCTCACGCTTTATAGTGATAGCC	*Bgl*II
mP2bg	GGAAGATCTGACCAAACTAGCGTTGAAACC	*Bgl*II
Omg_F	GCGGATCC**AAGTGCGGTCA**AGCAAGGCGAATCGAAAGAT	*Bam*HI
Omg_R	GCGGATCCTCTAACAAATGATTAGAAGTAAACGC	*Bam*HI
P2Δ2I_F	CGCAGATCTGGTGATATTACAAGCAAATATGCTTATG	*Bgl*II
P2Δ2I_R	CGCAGATCTTTTTGTAACAAAACGAGTTTCTAAATAA	*Bgl*II
MegaR	GCAAGTGTTTTTTTCATAATTTGTATTCC	--
R2	CCAGAACTAGAAAGTTTTAC	--
Mega primer	539-bp fragment amplified from *H. influenzae* chromosomal DNA using MegaR/ R2 primers	--
P2R8	GGCATTATCGTCGATGGTGTGCATATCA	--
Kan_CTR	GGTATGACATTGCCTTCTGCG	--
P2R3_2	GCCGCGGCCGCACTTGGTTTACATATTGAAGGACCTTA	*Not*I
P2FR	CGCGCGGCCGCGCGGTAAAAATTATGCGTGAA	*Not*I
P2Δ5-8I_R	CGCGTCGACGTAGTTAGTTCTACCATAAGCAATTTTTGC	*Sal*I
P2F1	CGCGGATCCTATAACAACGAAGGGACTAACG	*Bam*HI
P2R1	CGCGTCGACCAAATGATTAGAAGTAAACGC	*Sal*I
P2Δ1-4I_F	CGCGGATCCAACTACAAATATAACGAAGCTGACG	*Bam*HI
P2Δ1-4I_R	GTCACTATTGTTGAGAACGCC	--
P2Δ5-8I_F	GTGTCTCTAGATAGTGGCTATGC	--
P2ΔL1I_F	CGCAGATCTGGTTCACGTTTCCACATTAAAGC	*Bgl*II
P2ΔL1I_R	CGCAGATCTACTTTGTTCTGCGATAATGCTTAAAC	*Bgl*II
P2ΔL3I_F	CGCAGATCTGGTAATACCGTTGGCTATACTTTT	*Bgl*II
P2ΔL3I_R	CGCAGATCTCGCACGACCAAGTTTTACTTCAC	*Bgl*II
P2ΔL4I_F	CGCAGATCTATAGGTGAAATCAATAATGGAATTCAAG	*Bgl*II
P2ΔL4I_R	CGCAGATCTCTTTTGTGCTAATAAATAATTAGCGCC	*Bgl*II
P2CtHis_F	ATGTATAACAACGAAGGGACTAAC	--
P2CtHis_R	GAAGTAAACGCGTAAACCTACAC	--
P2FF	CGCGCGGCCGCGGGGCGATCTGGCTTAATA	*Not*I
P2R3	GCCGCGGCCGCGTGATGTTTAACGACCAAACTAG	*Not*I
P2R5	GCCGCGGCCGCATTCCACAAAGGCGCAACTTTTG	*Not*I
Rbg	GGAAGATCTCCAGAACTAGAAAGTTTTAC	*Bgl*II
ΔP2F	CGCAGATCTGCGTTTACTTCTAATCATTTG	*Bgl*II

[a] Restriction site is underlined
[b] *H. influenzae* DNA uptake sequences are shown in bold

2.6 PCR Purification

After PCR and restriction digestion reactions, PCR products were purified using QIAquick PCR purification kit (Qiagen) according to the manufacturer's instructions: 5 volume of binding buffer (PBT) was added to the 1 volume of PCR products and the mixture added to the column. This was then centrifuged for 1 min and the flow-through discarded. Then, 750 µl of washing buffer (PE) was added and centrifuged for 1 min and flow-through discarded. After that 50 µl of nuclease free deionised water was added and incubated for 2 min at room temperature. Finally, DNA was eluted by centrifugation for 1 min. Purified DNA fragments then were quantified and stored at -20°C.

2.7 Gel Electrophoresis and Gel Extraction

DNA fragments were separated and visualized by horizontal gel electrophoresis typically using 10 µl of the reaction mixtures at 100 V in a 0.8-1% w/v agarose gels. Before loading the DNA samples into the gel, 2 µl 6 × loading dye was added to each 10 µl DNA sample. Gels were run in 1 × Tris Acetate EDTA (TAE buffer, Sigma) buffer at 5 V/cm. Ethidium bromide (Sigma) was added to the gel at the concentration 10 mg ml^{-1} and DNA fragments were visualized using an ultraviolet trans-illuminator. Afterwards, the sizes of DNA bands in the agarose gel were estimated by comparison to the 2-log DNA molecular weight marker (New England Biolabs). Bands of interest were excised using a clean scalpel blade and extracted from the agarose gel using a QIAquick Gel Extraction kit (Qiagen) according to the manufacturer's instructions.

2.8 Bacterial Transformation

2.8.1 Electro-transformation of *H. influenzae*

Electro-transformation of *H. influenzae* was achieved according the method previously described by Mitchell *et al.,* (1991) as follows:

A) Preparation of electro-competent *H. influenzae* cells. Overnight growth was harvested from chocolate horse blood agar plates into 10 ml of supplemented BHI broth and centrifuged (4,000 × *g* for 4 min). The bacteria were then resuspended in 20 ml of ice-cold S&G buffer (272 mM sucrose, 15% glycerol) before being re-centrifuged. This washing procedure was repeated three times before the bacterial cells were finally resuspended in 1 ml S&G buffer and left on ice until required.

B) Electroporation of *H. influenzae* cells. Purified DNA (1-5 µg) of DNA was added to an electroporation cuvette (0.2 cm inter-electrode distance; Bio-Rad) along with 40 µl of competent *H. influenzae* cells and placed on ice for 10 min. This was then subjected to an electroporation in a Bio-Rad Gene Pulser at a voltage of 2.5 kV and resistance and capacitance of 400 Ω and 25 µF, respectively. The contents of the tube were then added to 2 ml of supplemented BHI broth and incubated at 37°C for 3 h. Aliquots were then plated out onto supplemented Brain Heart Infusion (BHIs) agar plates containing kanamycin (50 µg ml^{-1}) and incubated for up to 2 days at 37°C in air plus 5% CO_2.

2.8.2 Natural Transformation of *H. influenzae*

Based on a previously described method for transformation of *N. meningitidis* (Hoda Abdel *et al.,* 2001) *H. influenzae* strain Rd KW20 was naturally

transformed. Briefly, *H. influenzae* was grown to an optical density of 0.2 at 600nm in supplemented Brain Heart Infusion (BHI) (Oxoid) broth. 200 µl of bacterial culture was added to a 15 ml tube containing BHI agar with NAD and hemin. After incubation for 6 h at 37°C in 5% CO_2, 2 µg of the mutagenic fragment was added to the culture and incubation was continued for a further 16 h. The cells were then harvested and plated onto BHI plates supplemented with NAD (10 µg ml^{-1}), hemin (10 µg ml^{-1}) and kanamycin (50 µg ml^{-1}). Overnight colonies were observed and selected for analysis.

2.8.3 Heat Shock Transformation of *E. coli*

The desired plasmid DNA was transformed into competent *E. coli* JM109 (Promega) using a heat shock approach according to the manufacturers' instructions as follows: 50 µl of bacteria *E. coli* JM109 were thawed on ice for 10 min then 100 ng (5µl) of plasmid DNA was added to cells and mixed gently by stirring with a pipette tip. The mixture was incubated on ice for 10 min and the cells were heat shocked in a 42°C water bath for 45-50 seconds. Immediately after heat treatment, the cells were transferred onto ice for 2 min. 450 µl of room temperature SOC medium (2% tryptone, 0.5% yeast extract, 10 mM sodium chloride, 10 mM magnesium chloride and 20 mM glucose) (Sigma) was added and the cell suspension was incubated at 37°C for 2 h with shaking at 250 rpm. Finally, 100 µl, 150 µl, and 200 µl of the cell suspension was plated onto LB agar containing the appropriate antibiotic and incubated at 37°C overnight.

2.9 Expression of Recombinant Proteins

Recombinant proteins were primarily expressed using *E. coli* JM109 (Promega) harboring the appropriate expression plasmid. *E. coli* BL21 (DE3) pLysS (Promega) contains the plasmid pET28LR was used for expression of recombinant laminin receptor precursor protein (rLRP). Briefly, 10 ml of LB medium containing the appropriate antibiotic was inoculated with 25 ml of an overnight bacterial culture. The cultures were incubated at 37°C with shaking. The optical density (OD) was monitored using a UV-160A spectrophotometer (Shimadzu) to mid log phase (OD600=0.6). Isopropyl-1-thio-β-D-galactopyranoside (IPTG) (Promega) was added to a final concentration of 1 mM. The culture tubes were then incubated at 37°C for 3-4 h with shaking. Aliquots of 1 ml were removed from each culture pre-induction and also at hourly time points after induction, and cell were harvested by centrifugation at 13,000 × *g*. The cell pellets were resuspended in 1 × SDS-PAGE sample buffer (Appendix 1), according to the formula (volume in µl = O.D. × 800/3). The samples were heated to 95°C for 5 min and subsequently resolved by Sodium Dodecyl Sulfate-Polyacrylamide Gel Electrophoresis (SDS-PAGE) (Laemmli, 1970).

2.10 Sodium Dodecyl Sulfate-Polyacrylamide Gel Electrophoresis (SDS-PAGE) and Immunoblot Analysis

2.10.1 SDS-PAGE

Purified recombinant proteins and the whole cell lysates were separated according to their electrophoretic mobility using 10-12% SDS-PAGE gels (Appendix 1)

(Sambrook & Maniatis, 1989). Proteins were dissolved in 1 × SDS-PAGE sample buffer (Appendix 1) and heated for 5 min at 95°C. An aliquot of 10 µl of sample was loaded into a SDS-PAGE gel using Mini- Protean III equipment (BIO-RAD) at a constant 30mA per gel with a 200V voltage limit for approximately 50-60 min using a Power PAC 300 (BIO-RAD). Protein l (Page Ruler^{TM} Plus Prestained Protein Ladder, Fermentas) was used as a protein marker. After separation, proteins were visualized using SimplyBlue^{TM}SafeStain^{TM} (Invitrogen) or PageBlue^{TM} Protein Stain Solution (Fermentas) used according to the manufacturer's instructions. Gels were scanned using a GS-800 calibrated densitometer (BIO-RAD).

2.10.2 Immunoblot Analysis

After SDS-PAGE, proteins were transferred onto a nitrocellulose membrane (Hybond^{TM} –ECL^{TM}, Amersham Biosciences) in semi-dry blotting buffer (Appendix 1) at room temperature using a Trans-Blot SD semidry transfer cell (BIO-RAD) at a constant current of 13 mA for approximately 30 min. After transfer, the nitrocellulose membrane was incubated for 1 h in blocking solution [5% (w/v) skimmed milk powder in 20 ml PBS] (Oxoid, England) or 1% Bovine serum albumin (BSA) (Sigma). The membranes were then probed with the appropriate primary antibody diluted in blocking buffer and incubated overnight with shaking at 4°C. After washing in PBS containing 0.05% Tween-20 (PBST) (Sigma) three times, each for 15 min, the membranes were incubated for 1 h with an appropriate secondary antibody which had been diluted in blocking buffer.

Next, the membrane was washed with PBST and the membrane was then developed using the substrate BCIP/NBT (Perkin Elmer Life Science, USA).

2.11 Protein Purification under Denaturing Conditions

Hispure™ cobalt resin (Thermo) was used to purify his-tagged proteins under denaturing conditions. A single colony of *E. coli* JM109 or *E. coli* BL21 (DE3) pLysS harboring the desired expression plasmid was inoculated into 10 ml LB containing appropriate antibiotic and grown at 37°C overnight. One litre of LB broth containing appropriate antibiotics was then inoculated with 10 ml of an overnight starter culture and grown to mid log phase (OD_{600} = 0.6), and induced by addition of IPTG to a final concentration of 1 mM. After a further 3h of induction the cells were harvested by centrifugation at 9,000 × *g* for 10 min at 4°C using an Allegra™ X-22R centrifuge (Beckman Coulter). Next, the culture pellet from 50 ml culture was resuspended in 5 ml of lysis buffer (8 M urea, 0.1 M NaH_2PO_4, 0.01 M Tris-Cl, pH 8.0). Following incubation at room temperature for 30 min with shaking, the mixture was sonicated (15 s on, 10 s off pulses for 5 min on ice) using a SoniPrep Sonicator 150 (MSE). The lysate from disrupted cells was then centrifuged at 9,000 × *g* for 30 min at 4°C, the soluble phase (supernatant) was filtered using 0.45 µm filters and collected in polypropylene chromatography columns (Sigma) and 500 µl of hispure™ cobalt resin (Thermo) was added. Then a low concentration (20 mM) imidazole solution (Qiagen) was added and the suspension was shaken at 50 rpm for 2 h. The sample was then loaded onto a gravity column (Evergreen) and the cleared lysate allowed to pass through using washing buffer (8 M urea; 0.1 M NaH_2PO_4; 0.01 M Tris.Cl; pH6.3).

Protein was eluted using elution buffer (8 M urea; 0.1 M NaH_2PO_4; 0.01 M Tris.Cl; pH4.5). Urea was removed by buffer exchange using PD-10 desalting columns (GE Health Care) or D-Tube™ Dialyzer Maxi, MWCO 12-14 kDa (Novagen). The protein eluates were stored at -20°C.

2.12 Expression and Purification of Recombinant Proteins in a Cell-free Protein Synthesis System

Recombinant membrane proteins were expressed and purified using the MembraneMax™ Protein Expression Kit (Invitrogen).

Recombinant proteins were synthesized following the manufacturer's recommendations. In brief, samples were prepared containing the following reagents: *E. coli slyD*⁻ Extract, 20 µl; 2.5X IVPS Reaction Buffer (–amino acids), 20 µl; 50 mM Amino Acids (–Met), 1.25 µl; 75 mM Methionine, 1 µl; MembraneMax™, 2 µl; T7 Enzyme Mix, 1 µl; DNA Template (pMSA18 or pMSA19), not added to the negative control, 1 µg. Reactions were performed in a final volume of 50 µl in DNase/RNase-free water. Samples were incubated at 37°C for 30 min then feed buffers (2 × IVPS Feed Buffer, 25 µl; 50 mM Amino Acids (–Met), 1.25 µl; 75 mM Methionine, 1 µl; 10 mM all-trans retinal, 0.5 µl, were added to a final volume of 100 µl and incubation continued up to 4 h and samples analysed.

2.12.1 Analysing Synthesised Recombinant Membrane Protein Sample

Synthesised recombinant membrane proteins were analysed in accordance with the manufacturer's instructions. Briefly, proteins were precipitated using acetone. 5 µl of the samples mixed with 20 µl of acetone and centrifuged at 10,000 × *g* for 5 min at room temperature. The supernatants were removed carefully and pellets were resuspended in 20 µl of sample loading buffer. 10 µl was loaded on a SDS-PAGE gel and, after electrophoretic separation, transferred to nitrocellulose membranes. Membranes were probed with primary antibody diluted 1:5000, in blocking buffer [5% (wt/vol) milk, 1% (vol/vol) phosphate-buffered saline (PBS)] and incubated for overnight at 4°C. After washing in PBS with 0.1% Tween 20 (PBST), membranes were incubated for 1 h with 1:30000-diluted (PBS-BSA) alkaline phosphatase conjugated secondary antibody (Sigma). After washing with PBST, blots were developed using BCIP/NBT-Blue liquid substrate (Sigma).

2.13 Protein Purification Using Ion Exchange and Gel Filtration

Ion exchange and then gel filtration were employed to purify proteins under non-denatured conditions from *H. influenzae* strains. Bacteria cultured overnight on 20 plates of chocolate agar were harvested in 1 × PBS, harvested cells were lysed overnight in 500 ml lysis buffer (50 mM Tris-HCl, 30 mM Zwittergent 3-12, pH 8.5 and 1:500 DNase I) at 4°C, cell lysates then were centrifuged at 100,000 × *g* for 20 min (Aluminum rotor A-841, SORVALL ULTRASPEED). Supernatants were filtered through 0.22 µm filters. Membrane protein extracts were then applied to a Capto Q anion exchange column (GH Healthcare Life Science), with

flow rate 1 ml min^{-1} using an AKTA PrimePlus FPLC, pre-equilibrated with cooled wash buffer (50 mM Tris-HCl, 30 mM Zwittergent 3-12, pH 8.5). Proteins were eluted with a linear gradient of elution buffer 1 (50 mM Tris-HCl, 30 mM Zwittergent 3-12, 2M NaCl, pH 8.5). Protein fractions were applied to a gel filtration column (Superdex™ 200, 130 ml bed volume), flow rate 1 ml min^{-1}, using elution buffer 2 [30 mM *n*-Octyl-ß-D-glucopyranoside (OG) (Calbiochem®) in PBS].

2.14 DIG-labeling of Proteins and Bacteria

DIG-labeling was carried out using the Digoxigenin-3-0-succinyl-ε-aminocaproic acid-N-hydroxy-succinimide ester Protein labeling kit (DIG-NHS; Roche) in accordance to manufacturer's instructions. Briefly, for proteins the pH was adjusted to pH 9.0 by the addition of 2 M sodium carbonate, and DIG-NHS reagent added in a 1:10 molar ratio. Reactions were incubated at room temperature for 1 h, and then unbound DIG-NHS was removed using PD-10 desalting columns (GE Healthcare). For bacteria, cells were harvested from an overnight plate, washed three times in PBS with 0.05% Tween 20 (PBST), resuspended in the sodium carbonate buffer (150 mM; 142 mM $NaHCO_3$, 8 mM Na_2SO_3, pH 9.0) and the optical density adjusted (at 600 nm = 1.0) then labeled with 10 µg ml^{-1} DIG-NHS at room temperature for 30 min. Bacteria were then washed three times with PBST and resuspended in PBS containing 1% bovine serum albumin (BSA; Sigma).

2.15 rLRP Protein Labelling

The Lightning-Link™ Atto680 Conjugation Kit (Innova Biosciences) was used to label the rLRP protein according to the manufactures' instructions. In brief, 1 µl of LL Modifier reagent was added to each 10 µl of protein and mixed gently. 5 µg of Lightning-Link fluorescein was then mixed with every 1 µg protein sample (with added LL-Modifier) and resuspended gently for 3 h in the dark at room temperature. After incubating, 1 µl of LL-Quencher FD reagent was added for every 10 µl of protein and mixed gently for 30 min in the dark at room temperature and stored at 4°C.

2.16 Synthetic peptides

The synthetic OmpP2 peptides (loop 2 and its derivatives) utilised in this study were synthesized (high purity grade; peptide purity > 95%) by GenScript, USA and supplied as a lyophilized powder. Aliquots were prepared in PBS at a final concentration of 2 mg ml^{-1} and stored at -20°C. These are detailed in Table 2.2.

Table 2.2. Synthetic peptides used in this study

Peptide	Peptide sequence
OmpP2L2	CASENGSDNFC [a]
L2-1	ASENGSDNF
L2-2	AAENGSDNF[b]
L2-3	ASANGSDNF[b]
L2-4	ASEAGSDNF[b]
L2-5	ASENASDNF[b]
L2-6	ASENGADNF[b]
L2-7	ASENGSANF [b]
L2-8	ASENGSDAF[b]
L2-9	ASENGSDNA[b]
Scrambled L2	SNGFEDNSA
PorA loop 4[c]	CPIQNSKSAYTPAYYTKNTNNNLTLVPAVVGKPGSC [a]
PorA loop 1[c]	CVEGRNYQLQLTEAQAANGGASGQVKVTKVTKAKSRIRTKIC [a]

[a]Peptide sequence includes terminal cysteine residues to facilitate disulfide bond formation.
[b] The substituted amino acid is highlighted in red.
[c]from previous study

2.17 Enzyme-Linked Immunosorbent Assay (ELISA)

Purified proteins were diluted in coating (carbonate) buffer (142 mM sodium bicarbonate, 8 mM sodium carbonate [pH 9.4]), concentrations were variable according to the experiment performed (typcially 1-5 µg ml^{-1}), before being added in 100 µl aliquots to plate wells (Nunc 96-well plates) for 4 h at room temperature or overnight at 4°C with shaking. Control wells were coated with PBS containing 1% BSA (PBS-BSA) or recombinant PorA (positive control). Plates were washed three times in PBS containing 0.05% v/v Tween 20 (PBST) buffer and the wells

were blocked for 1 h at room temperature with 100µl PBS-BSA. Wells were again washed six times with 3 min soaking intervals with PBST and 100µl of binding protein (5 µg ml^{-1}) was added. Next, the plate was incubated at 4°C for 4 h then washed with PBST six times with 3 min soaking intervals. Rabbit polyclonal antibody (diluted 1:1000) in 1% BSA in PBS was added and plates were shaken overnight at 4°C. Wells were then washed with PBST six times with 3 min soaking intervals. Next, conjugated secondary antibody (Sigma; diluted 1:10,000 in 1% BSA in PBS) was added and plates were shaken for 1 h at room temperature. After washing for six times, 100 µl of 2, 2'-azino-bis; 3-ethylbenzthiazoline-6-sulphonic acid (ABTS; Chemicon international ES004) substrate or *p*-nitrophenyl phosphate (*p*NPP) substrate (Sigma) diluted in alkaline phosphatase buffer (Appendix 1) (1 mg ml^{-1}, 100 µl per well) were used for color development and plate was incubated then read using an ELISA plate reader (BioTek EL800) at 405 nm.

Alternatively, ELISAs were undertaken using DIG-labelled bacteria in the same principles described above. Wells were coated with protein (5 µg ml^{-1}) and incubated for 1 h at room temperature. The plate was then washed three times with PBST and the wells then were blocked for 1 h at room temperature with 1% BSA in PBS followed with 4 washes with PBST. DIG-labeled *H. influenzae* were added (100 µl; optical density at 600 nm = 0.04) for 2 h at room temperature and plates were then washed four times. 100 µl of the anti-digoxigenin HRP conjugate antibody (Roche) (diluted 1:5000 made up in was added to each well and incubated for 1 h at room temperature. Wells were washed four times and ABTS

(Roche) substrate was added and plate was read for different time points with an ELISA reader (Biotek EL800) at an absorbance of 405 nm.

2.18 Sub-cellular Fractionation of *H. influenzae* Cells

Bacterial cell fractionation was undertaken based on a modification of a previously described method (Nossal & Heppel, 1966; Schnaitman, 1971). Briefly, *H. influenzae* cells were grown overnight at 37°C in supplemented BHI. Cells from 10 ml overnight cultures were harvested at 10,000 × *g* for 10 min, the pellet resuspended in 0.4 ml 10 mM Tris-HCl (pH 7.5) and the cells disrupted by sonication (5 min 10/5s cycles). The preparation was centrifuged at 16,000 × *g* for 30 min and the supernatant (periplasmic proteins) was transferred to a fresh tube and stored at -20°C. The pellet was resuspended in 0.2 ml of 10 mM Tris-HCl (pH 7.5), 10 mM $MgCl_2$ then 0.2 ml 10 mM Tris-HCl (pH 7.5), 10 mM $MgCl_2$ 4% Triton X-100 was added and sonicated (2 min 10/5s cycles) and incubated at 37°C for 30 min. The mixture was centrifuged at 16,000 × *g* for 30 min. The supernatant (cytoplasmic membrane-enriched fraction) was transferred to a fresh tube and stored at -20°C. The remaining pellet was resuspended in 0.5 ml 10 mM Tris-HCl (pH 7.5), 10 mM $MgCl_2$ and sonicated (2 min 10/5s cycles), then 0.5 ml 10 mM Tris-HCl (pH 7.5), 10 mM $MgCl_2$ 2% Triton X-100 was added and the sample was incubated at 37°C for 30 min. Finally, the outer membrane protein-enriched fraction was harvest by centrifugation at 16,000 × *g* for 30 min and resuspended in 0.2 ml 10 mM Tris-HCl (pH 7.5) and stored at -20°C.

2.19 Determining the *in vitro* Growth Rate of *H. influenzae* and Its Mutant Derivatives

Bacterial cultures were incubated overnight at 37°C, with shaking at 200 rpm. The following day, the cultures were diluted in fresh BHI and were adjusted to a starting OD_{600} of 0.1 in the 15 ml of BHI. Next, the broth cultures were incubated at 37°C with shaking. The OD_{600} reading was taken at each 1.5 h interval for 16.5 h and then at 24 h. The viable counts of broth cultures were determined by sampling during exponential growth over 24 h in triplicate.

2.20 Flow Cytometry Analysis

The ability of *H. influenzae* and mutants to bind to rLRP protein was determined by flow cytometry using an indirect fluorescence assay. *H. influenzae* strains were grown to mid-log phase (OD_{600} approximately 0.7). Then, they were washed three times with PBS and the concentration of bacterial cells in phosphate-buffered saline (PBS) was adjusted to 2×10^7 colony-forming units (CFU) ml^{-1} aliquots. After centrifugation at 5,000 × *g* for 7 min, 20 µg of fluorescein- conjugated rLRP was added in a total volume of 0.2 ml FACS buffer [0.1% BSA, 0.1% sodium azide and 2% fetal calf serum (FCS) in PBS] and untreated cells were used as a control. After being incubated of 3 h at room temperature in the dark, the samples were washed three times with FACS buffer (centrifugation at 5000 × *g* for 7 min). Finally, samples were re-suspended in 1 ml PBS containing 0.5% formaldehyde to fix the cells. The samples were analysed for fluorescence using a Coulter Altra Flow Cytometer. The cells were detected using forward and log-side scatter dot plots, and a gating region was set to exclude cell debris and aggregates of bacteria.

A total of 50,000 bacteria (events) were analysed for fluorescence signals using Weasel v2.7.4 software.

2.21 Whole Cell lysate Pull-down Assay

Bacterial strains were grown to mid-log phase (OD_{600} approximately 0.7). After washing twice with PBS, the bacterial pellet was resuspended to same OD in PBS and then mixed with soluble purified rLRP (20 µg). After incubation for 3 h at 4°C with shaking, mixtures were washed three times in PBS. Harvested pellets were resuspended in SDS-PAGE loading buffer and run on the SDS-PAGE. Separated proteins transferred to nitrocellulose membrane (section 2.18), blocked for 1 h at room temperature with PBS containing 1% BSA (PBS-BSA). Nitrocellulose membranes were then incubated with anti-LR antibody diluted appropriately in blocking buffer (1:3000) overnight at 4°C. After being washed three times, each for 15 min in PBS containing 0.05% Tween-20 (PBST; Sigma), HRP-conjugated anti-rabbit IgG (Sigma) was added at the concentration of 1:30,000 for 1 h at room temperature. Next, the membrane was washed with PBST for 1 h at room temperature and then was developed using BCIP/NBT-Blue liquid substrate (Sigma).The protein bands were quantitated on a Bio-Rad GS-800 calibrated densitometer employing Quantity One 4.6.5 software.

2.22 Adhesion Assay

Adhesion and invasion assays were undertaken essentially based on the previously described method (Oldfield *et al.*, 2007). In brief, confluent monolayers of human epithelial cell line 2 (HEp-2) cells (passage 55-60) and human brain

microvascolar endothelial cells (HBMECs) (passage 12-19) cells were obtained in 24-well tissue culture plates ($2cm^2$, Costar®, Corning Inc.), in growth media DMEM (Dulbecco's MOD Eagle Medium, Gibco) for HEp-2 and endothelial cell medium (ECM) for HBMECs both were supplemented with 10% fetal calf serum (FCS) (Gibco), and 1% antibiotic-antimycotic solution (Sigma; penicillin and streptomycin) and 1% endothelial cell growth supplement (ECGS) was added to the ECM. After overnight incubation, the media was replaced with 1 ml of DMEM or ECM supplemented with 2% FCS (no antibiotics-antimycotic) and incubated overnight. One loopful of bacterial culture from an overnight plate was suspended in 20 ml of brain heart infusion broth (BHI) and incubated at 37°C for 4 h with shaking. The OD_{600} reading of the bacterial cultures were taken, cultures were equilibrated using BHI, centrifuged at 4,000 × *g* for 5 min. Next, the pellets were thoroughly resuspended in pre-warmed DMEM or ECM supplemented with 2% FCS (no antibiotic-antimycotic) and re-equilibrated in the same medium to similar OD_{600}, adjusted to approximate 1×10^7 CFU ml^{-1} (confirmed retrospectively by plating out aliquots of serially diluted inoculums) and the cells infected with the bacteria in a total volume of 0.5 ml medium. Following the incubation period, 3 h at 37°C 5% CO_2, monolayers were rinsed three times with 1 ml 1 × PBS to remove non-adherent bacteria and then disrupted and homogenised in 1 ml of 0.1% Saponin in PBS. 10 µl volumes of the serial 10-fold dilutions in PBS were plated out on a chocolate agar plates and incubated at 37°C overnight in 5% CO_2. The viable count plates yielded the number of adherent bacteria per monolayer (CFU/well per strain).

2.23 Invasion Assay

To determine the number of bacteria entering the cells of HBMEC and HEp-2 monolayers, invasion assays were performed identically to adhesion assay except that after the initial 3-h incubation, monolayers were rinsed three times with PBS and DMEM or ECM media containing 2% FCS (no antibiotics-antimycotic) and gentamicin (100 µg ml^{-1}) was added. The susceptibility of *H. influenzae* strain to gentamicin at 100 µg ml^{-1} was confirmed prior to testing. To assess cell invasion, tissue culture plates were further incubated for 2 h, rinsed twice with PBS, and then treated with 0.1% saponin in PBS. Well contents were agitated and colony-forming units determined by plating 10 µl spots from appropriate dilutions of the lysates on agar to quantify the number of internalized bacteria per monolayer.

2.24 Micro-beads Adhesion Assay

PolyLink protein coupling kit (Polysciences, Inc.) was used for coupling the microspheres (beads) with the desired proteins according to the manufacturers' instructions. In brief, all buffers were pre-warmed to room temperature. 0.5 ml of microparticles was centrifuged for 10 min at 8,000 × *g* and the pellet was then re-suspended in 0.4 ml PolyLink coupling buffer, samples were centrifuged for 10 min at 8,000 × *g* and the pellet resuspend in 0.17 ml of PolyLink coupling buffer. 200 mg ml^{-1} EDCA solution was prepared by dissolving 10 mg DCA in 50 µl PolyLink coupling buffer and used immediately. After adding 20 µl of the EDCA to the microparticles suspension, it was gently mixed, then 300-350 µg of protein was added and incubated at room temperature for 5 h. After centrifugation for 10 min at 8,000 × *g*, pellet was resuspend in 0.4 ml of wash/storage buffer (10 mM

Tris, pH 8.0, 0.05% bovine serum albumin, 0.05% Proclin® 300) and then centrifugation was repeated again and the pellet was resuspended in 0.4 ml of wash buffer and stored at 4°C.

HBMECs (passage 12-19) were grown on ECM medium supplemented with 1% ECGS, 10% FCS and 1% antibiotic-antimycotic solution (A&A) (penicillin [1 $U.ml^{-1}$], streptomycin [1 $g.ml^{-1}$]). After overnight incubation at 37°C in 5% CO_2 on human fibronectin cellware 75cm^2 flask (BD BioCoat™), confluent cells were harvested, resuspended in ECM medium (1% ECGS, 1% A&A, 5% FCS) and transferred into 12-well plates (1 ml/well) containing sterile coverslips. Cells were then incubated overnight at 37°C with 5% CO_2 followed by the additiona of fresh media (1% ECGS, 1% A&A, 5% FCS) containing the desired recombinant proteins and synthetic loops coupled to micro-beads (5 µl). Cells were incubated at 4°C for 1 h, rinsed once with PBS before fixing with 4% PFA/PBS (500 µl per well) for 10 min at room temperature. Following fixation, cells were washed three times with 1% PBS, blocked with 4% BSA in PBS overnight at 4°C. Cells were incubated for 1 h with 1:150-diluted (4% BSA in PBS) IHLR against anti-37LR or with 1:100-diluted (4% BSA in PBS) Mluc5 IgM mouse against 67LR. After being washed three times with PBS, cells were incubated for 1 h with 1:500-diluted (4% BSA in PBS) with anti-rabbit Alexa 488 (against anti 37LR), anti-mouse IgM 647 1:1000 (against Mluc5 IgM), and also Hoechst 33258 1:1000 (against double-stranded DNA). Following incubation, cells were rinsed three times with PBS and once with dH_2O and coverslips were mounted with Prolong Gold anti-fade (Invitrogen) and images acquired on a Zeiss LSM 700

AxioObserver confocal microscope using a Plan-Apochromat 63 × /1.4 Oil DIC M27 objective. In addition, slides were read using a compound light microscope at 400 × magnification, starting from a spot and moving in a zigzag pattern; micro-beads were counted from a minimum of 15 randomly chosen fields per slide, excluding those in which the monolayer was not confluent.

2.25 RhoA-GTP Assay

2.25.1 Growth and Treatment of HBMECs Cell Line

The G-LISA^{TM} RhoA activation assay biochem kit^{TM} (Cytoskeleton) was used according to the manufacturer's instructions. Briefly, HBMECs (passage 15-19) were cultured in ECM medium supplemented with 10 % FCS, 1% Antibiotic-Antimycotic (A&A) and 1% ECGS overnight at 37°C, 5% CO_2 overnight in human fibronectin cellware 75cm^2 flasks (BD BioCoat^{TM}). Confluent cells were split into 6-well plates and incubated overnight at 37°C in ECM containing 10% FCS, 1% A&A and 1% ECGS. Next, 50-60% confluent cells were rinsed once with pre-warmed serum free medium (ECM) and then re-incubated with fresh ECM medium containing 0.5% FCS, 1% A&A and 1% ECGS for 24 h at 37°C, 5% CO_2. To obtain serum-starved cultures, media was changed to fresh serum-free ECM medium and cells were incubated for 16-24 h at 37°C, 5% CO_2. Cells were treated for 30 min at 37°C 5% CO_2 with 5 µM protein. The medium was then aspirated and cells were washed with ice cold PBS and lysed using cell lysis buffer (70 µl). Cell lysates were harvested with a cell scraper, transferred into

sample tubes on ice, centrifuged at 10,000 × *g*, at 4°C for 2 min, 20 µl was saved for protein quantitation. Samples were stored at -70°C until use.

2.25.2 Protein Concentration Equivalence

For accurate comparison between samples in the Rho activation assay, an equal protein concentration in all samples was desired. 10 µl aliquots of cell extracts were pipetted into a 96-well plate followed by the addition of 300 µl of protein assay reagent, the plate was then read at 600 nm and the absorbance was multiplied by 3.75 to obtain the protein concentration in mg ml^{-1}.

2.25.3 G-LISA™ Assay

Buffer blank sample was prepared (80 µl of lysis buffer diluted with 80 µl of ice cold binding buffer). Positive control sample was prepared by diluting 18 µl of Rho control protein with 72 µl of cell lysis buffer and 90 µl of binding buffer. The powder in the Rho plate was dissolved in 100 µl ice cold water and solution removed from wells and the plate was put back on ice. Then, 1.6 mg ml^{-1} of samples were prepared (0.4 -2 mg ml^{-1} was recommended) in ice-cold lysis buffer and equal amount of ice-cold binding buffer was then added. Immediately 50 µl of equalized cell lysate for each sample was added to triplicate wells and incubated at 4°C for 30 min. Wells were washed with 200 µl of wash buffer at room temperature and then 200 µl of room temperature antigen presenting buffer was added and incubated for 2 min at room temperature. Wells were washed three times with 200 µl of room temperature washing buffer and 50 µl of diluted anti-RhoA primary antibody (1/250 in antibody dilution buffer) was added, incubated

for 45 min at room temperature followed by washing using washing buffer and then 50 µl of diluted secondary antibody (1/62.5 in antibody dilution buffer) was added, incubated for 45 min at room temperature. After washing with 200 µl washing buffer, 50 µl of HRP detection reagent (prepared by mixing same equal of par A and B) was added and incubated at 37°C. The signal was read by measuring absorbance at 490 nm using a microplate spectrophotometer. All incubations were performed on a 150 × *g* shaker.

2.26 Statistical Analysis

Statistical significance of the experimental results was determined by unpaired two-tailed Student's *t*-test using the Excel 2007 or Minitab 15 software program (Minitab). All experiments were performed using three technical replicates and unless otherwise stated and were repeated at least three times. Data were expressed as the mean ± standard error (SE). Differences were considered statistically significant at probability p value < 0.1; highly significant at $p < 0.05$ and very highly significant at $p < 0.01$.

CHAPTER THREE: Localisation of the LamR-Binding Domain(s) of *H. influenzae* OmpP2 Determined Using Purified Recombinant OmpP2 Derivatives

CHAPTER THREE

3. LOCALISATION OF THE LamR-BINDING DOMAIN(S) OF *H. INFLUENZAE* OMPP2 DETERMINED USING PURIFIED RECOMBINANT OMPP2 DERIVATIVES

3.1 Introduction

There is evidence that OmpP2 of *H. influenzae* plays an important role in the pathology of infection (Murphy & Bartos, 1988; Chong *et al.*, 1993; Duim *et al.*, 1996; Yi & Murphy, 1997). Porins can activate host inflammatory signalling cascades and it was demonstrated that whole OmpP2 from *H. influenzae* type b (Hib) and synthetic peptides corresponding to the surface exposed loops L5-L7 were able to activate cell phosphorylation and in particular the JNK and p38 mitogen-activated protein kinase (MAPK) pathways in human monocytic U937 cells (Galdiero *et al.,* 2003). In contrast, peptides corresponding to the β-barrel of OmpP2 were not able to activate this pathway (Galdiero *et al.*, 2003). In a more recent study, using two-dimensional electrophoresis and mass spectrometry proteomic approaches, OmpP2 from Hib and, specifically, its surface exposed loop L7 was shown to induce post-transcriptional alterations in U937 cells (Severino *et al.,* 2009). The study provided a list of candidate proteins with potential relevance to the host immune and inflammatory response. Most of the differentially expressed proteins are involved in metabolic processes, remodelling of cytoskeleton, stress response and signal transduction pathways (Severino *et al.*, 2009).

In an investigation of Hib OmpP2 and its loop 7- induced effects on human astrocytes (U87-MG cells), it was demonstrated that MEK1-MEK2/mitogen-activated protein kinase phosphorylation was induced and also the production of cellular adhesion molecule and interleukin-6 (IL-6) was up-regulated. In addition, the expression of adhesion molecules ICAM-1, VCAM-1 and E-selectin was considerably induced by treatment with either Hib OmpP2 or loop 7 (Vitiello *et al.*, 2011).

To cause bacterial meningitis, *H. influenzae* must cross the blood–brain barrier (BBB) to gain entry to the CNS where it can proliferate. It was recently reported that *H. influenzae* binds 37/67-kDa laminin receptor (LamR) on human brain microvascular endothelial cells, suggesting that LamR binding is required for *H. influenzae* to invade the vascular endothelium of the blood-brain barrier (Orihuela *et al.*, 2009). The LamR protein on the surface of microvascular endothelial cells was identified to be a common receptor for the meningeal pathogens *Neisseria meningitidis*, *H. influenzae* and *Streptococcus pneumoniae*. Moreover, mutagenesis studies indicated that the corresponding bacterial 37/67-kDa laminin receptor (LamR)-binding adhesins were pneumococcal CbpA, meningococcal PilQ and PorA, and OmpP2 of *H. influenzae* (Orihuela *et al.*, 2009). In ELISA experiments, *H. influenzae* was shown to bind recombinant laminin receptor precursor (rLRP) and the interaction was significantly reduced in the presence of soluble rLRP. Furthermore, *H. influenzae* mutants lacking OmpP2 showed dramatically less adherence to rLRP compared to the parental wild-type strain (Orihuela *et al.*, 2009). Further confirmation of OmpP2-mediated rLRP binding by *H. influenzae* was demonstrated by visualizing binding of Cy5-labelled rLRP

to the wild-type but not the Δ*ompP2* derivative, and by the reduction of LamR expression in brain endothelial cells using siRNA; wild-type *H. influenzae* binding was significantly reduced compared with binding to control cells. In contrast, the binding of the Δ*ompP2* mutant was not affected by LamR siRNA (Orihuela *et al.*, 2009).

The aim of the work described in this chapter was to identify the region(s) of *H. influenzae* OmpP2 involved in the interaction with LamR. This was achieved by expressing and purifying recombinant OmpP2 derivatives lacking specific regions or extracellular loops and then investigating their rLRP-binding activities using ELISA.

3.2 Results

3.2.1 Binding of Whole Recombinant OmpP2 of *H. influenzae* to Laminin Receptor

As an initial step towards determining the region(s) of OmpP2 responsible for the interaction with LamR, ELISAs were performed to confirm the previously published results showing that recombinant OmpP2 could bind to recombinant LRP (Orihuela *et al.*, 2009). For these experiments, recombinant PorA, OmpP2 and LRP were purified as previously described (Orihuela *et al.*, 2009). PorA from *N. meningitidis* was used as a comparative positive control. The data obtained showed that both proteins, OmpP2 and PorA, bound to rLRP at similar levels and that the binding was significantly ($p < 0.01$) higher than binding to the negative control (Figure 3.1). This finding confirms the previously described finding that PorA and OmpP2 bind rLRP (Orihuela *et al.*, 2009).

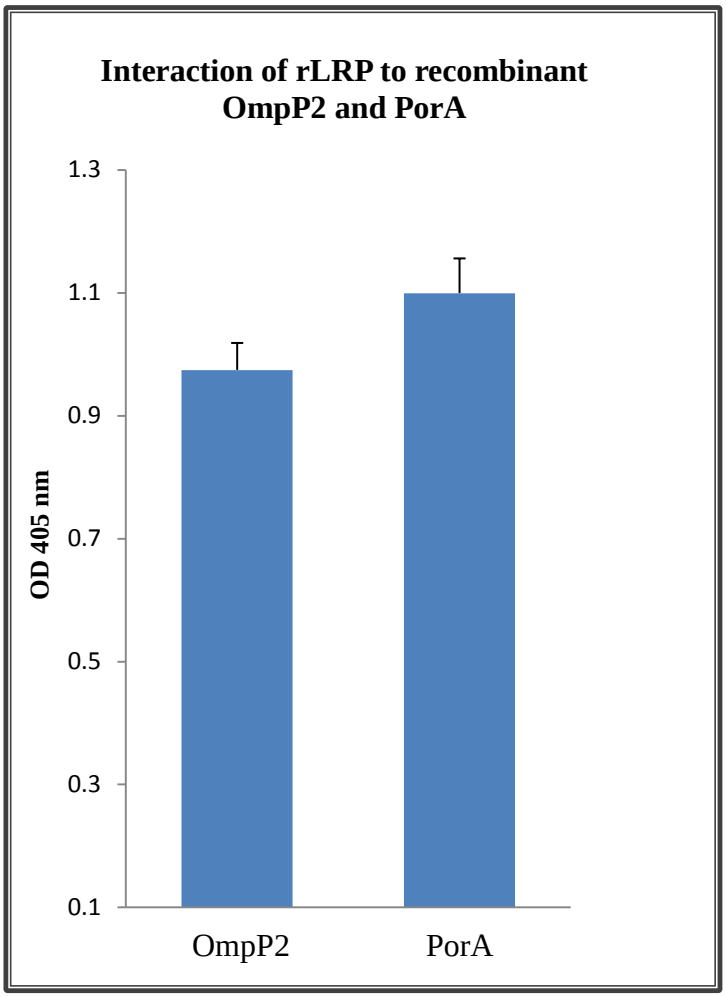

Figure 3.1. Interaction of rLRP with OmpP2 of *H. influenzae* and PorA of *N. meningitidis.* ELISA wells were coated with recombinant OmpP2 or PorA. After blocking, rLRP was added followed by rabbit anti-LR and then anti-rabbit IgG-HRP antibodies. Specific binding of LRP to OmpP2 and PorA-coated ELISA plates was determined by subtracting the absorbance in BSA-coated wells from that in OmpP2 and PorA-coated wells. Data shown are the means of at least three independent experiments, with each sample tested in triplicate. Error bars indicate standard error (SE).

3.2.2 Construction Plasmids of expression OmpP2 Derivatives, OmpP2ΔL1-4 and OmpP2ΔL5-8

After confirmation of the binding of OmpP2 to rLRP, the next step was to identify the region of OmpP2 that was responsible for the binding activity. Therefore, two

fragments; one corresponding to the N-terminal portion of OmpP2 (spanning the first four predicted surface exposed loops and named OmpP2ΔL5-8) and a second corresponding to the C-terminal portion (spanning loops 5-8 and named OmpP2ΔL1-4) were expressed, purified and tested for rLRP binding. Plasmids encoding these OmpP2 derivatives were constructed by inverse PCR deletion of regions of *ompP2* from a previously constructed plasmid pNJO74 (made by Dr. N. J. Oldfield). Briefly, pNJO74 was constructed by amplifying *ompP2* of *H. influenzae* strain Rd KW20, using primers P2F1 and P2R1 (Table 2.1; Figure 3.2; Figure 3.3). The product was digested with *Bam*HI and *Sal*I, and cloned into *Bam*HI- and *Sal*I-digested pQE30 to yield pNJO74. The amplified region of *ompP2* corresponded to amino acids 24-359 of OmpP2, and since the N-terminal signal peptide cleavage site is predicted to be between amino acids 20 and 21, pNJO74 encodes the full length mature OmpP2 minus three N-terminal amino acids and in their place has amino acids MRGSHHHHHHGS (encoded by pQE30).

To obtain OmpP2ΔL1-4 and OmpP2ΔL5-8, two sets of primers (P2Δ1- 4I_F/ P2Δ1- 4I_R and P2Δ5-8I_F/ P2Δ5-8I_R) were designed based on pNJO74 (Table 2.1, Figure 3.2). The resulting PCR products obtained using pNJO74 as template DNA were digested and self-ligated to form pMSA1 and pMSA2 (Figures 3.3 and 3.4).

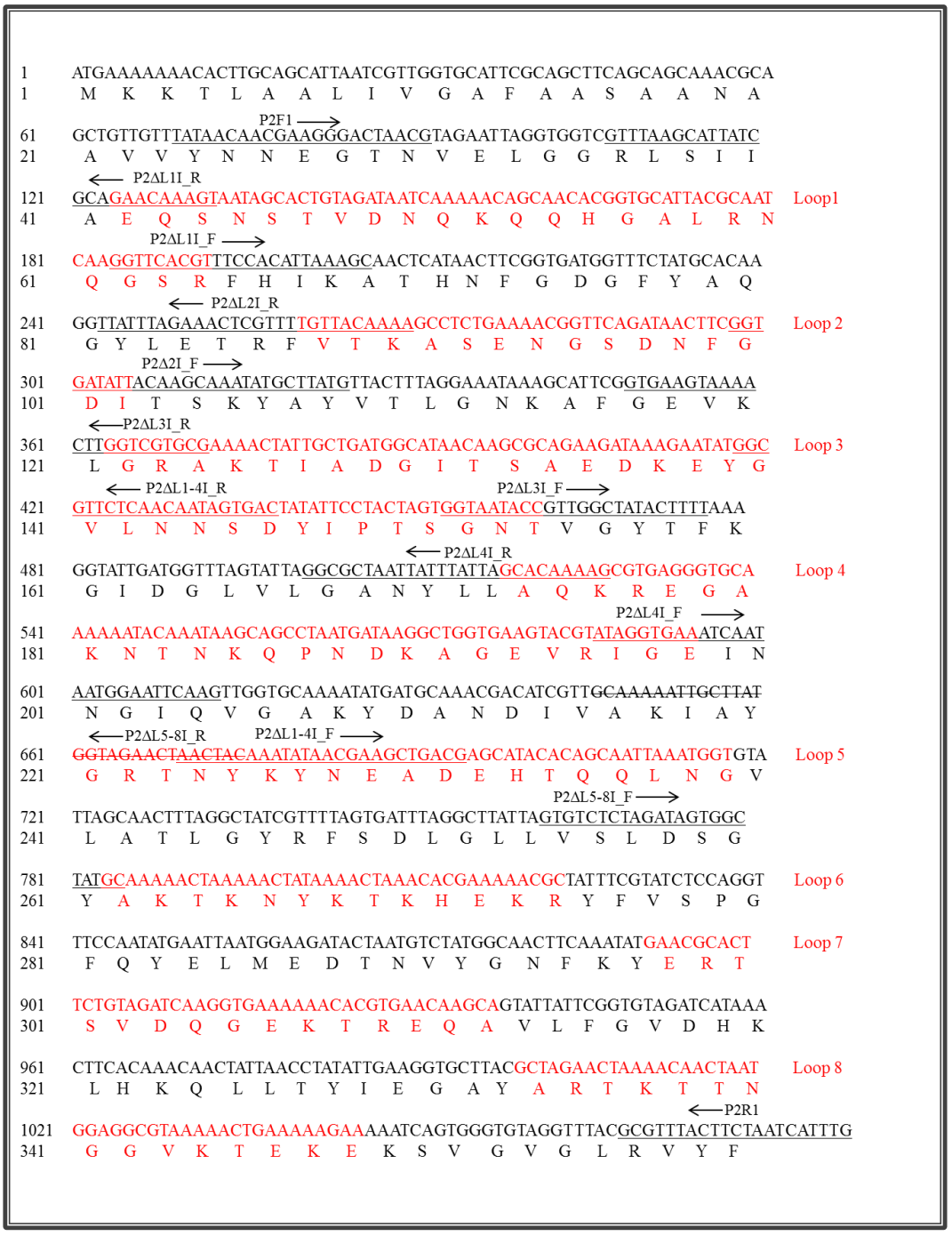

Figure 3.2. Diagram showing the *ompP2* nucleotide and OmpP2 protein sequence, and the annealing sites of primers used in this study. Loops 1-8 are also highlighted in red.

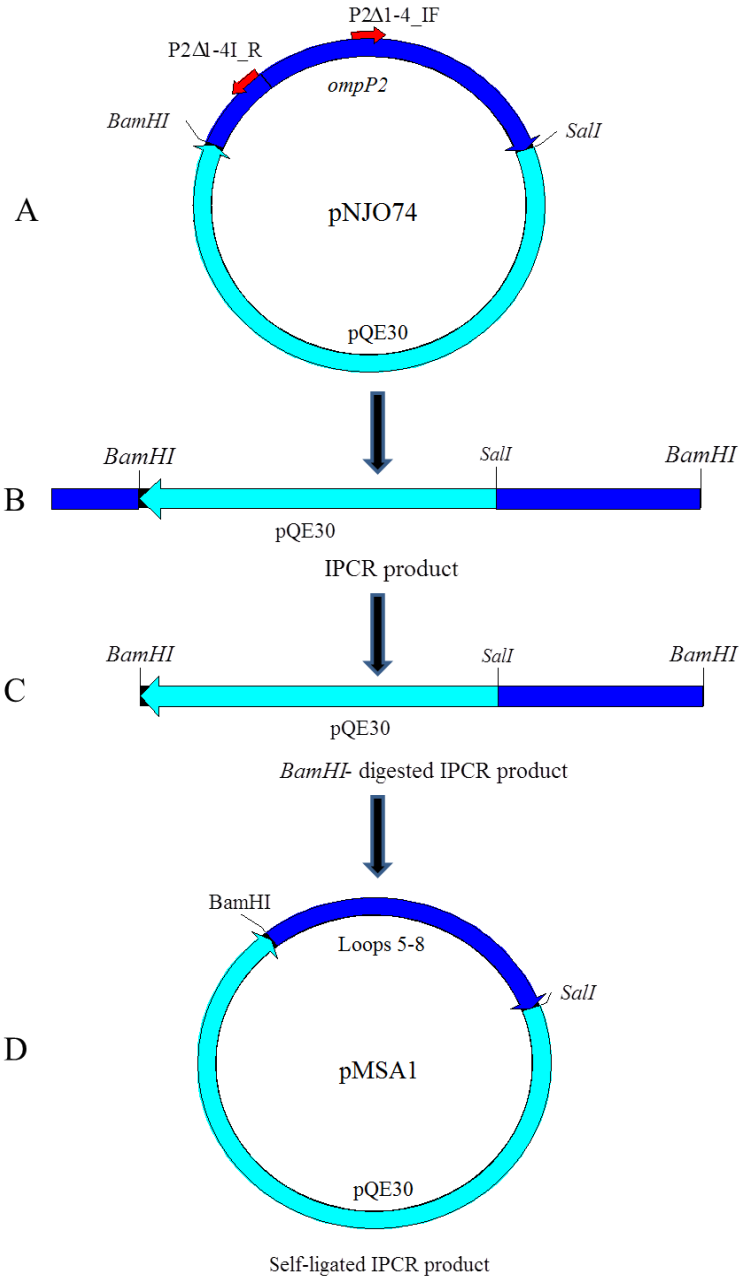

Figure 3.3. A schematic representation of the construction of pMSA1 (encoding OmpP2 lacking loops 1-4). A: IPCR from pNJO74 using P2Δ1- 4I_F, P2Δ1-4I_R primers. B: IPCR product obtained. C: *Bam*HI-digested IPCR product. D: self-ligated *Bam*HI-digested IPCR product to form pMSA1.

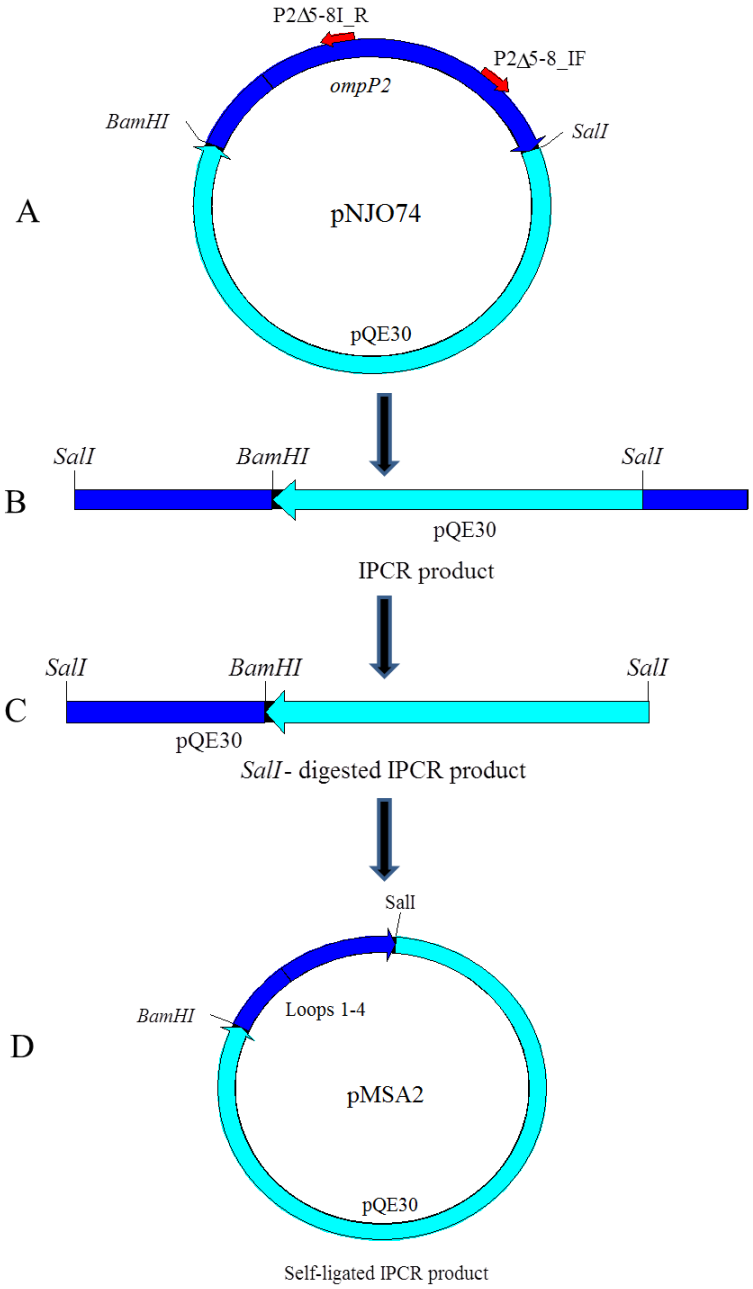

Figure 3.4. A schematic representation of the construction of pMSA2 (encoding OmpP2 lacking loops 5-8). A: IPCR from pNJO74 using P2Δ5-8I_F, P2Δ5-8I_R primers. B: IPCR product obtained. C: *Bam*HI-digested IPCR product. D: self-ligated *Bam*HI-digested IPCR product to form pMSA2.

The first set of primers was P2Δ1-4I_F (forward primer, to anneal to nucleotides 670-694 of *ompP2*) and primer P2Δ1-4I_R (reverse primer, to anneal to nucleotides 418-438 of *ompP2*). These primers, used with pNJO74 as template, yielded a fragment of 4,285 bases (Figure 3.6). The second set of primers was P2Δ5-8I_F and P2Δ5-8I_R, which were designed to anneal to nucleotides 763-785 and 646-675 of *ompP2*, respectively. These two primers yielded a fragment of 4,413 bases when used with pNJO74 as template (Figure 3.5).

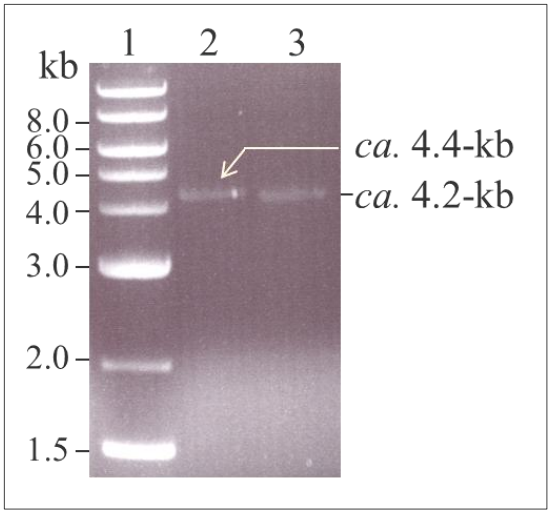

Figure 3.5. Inverse PCR products obtained from the pNJO74 template plasmid (comprising pQE30 with *ompP2*). Lane 2, the amplified fragment with primers P2Δ5-8I_F and P2Δ5-8I_R; lane 3, amplified fragment with primers P2Δ1-4I_F and P2Δ1-4I_R. Molecular mass markers are shown in lane 1.

Amplified fragments were purified, digested with *Bam*HI or *Sal*I as appropriate, then self-ligated and finally transformed into *Escherichia coli* JM109 competent cells. Transformant colonies were selected and screened by *Bam*HI/*Sal*I restriction digestion of the purified plasmids (Figure 3.6). One clone from each

transformation was chosen for further confirmation by DNA sequencing, and then designated pMSA1 or pMSA2.

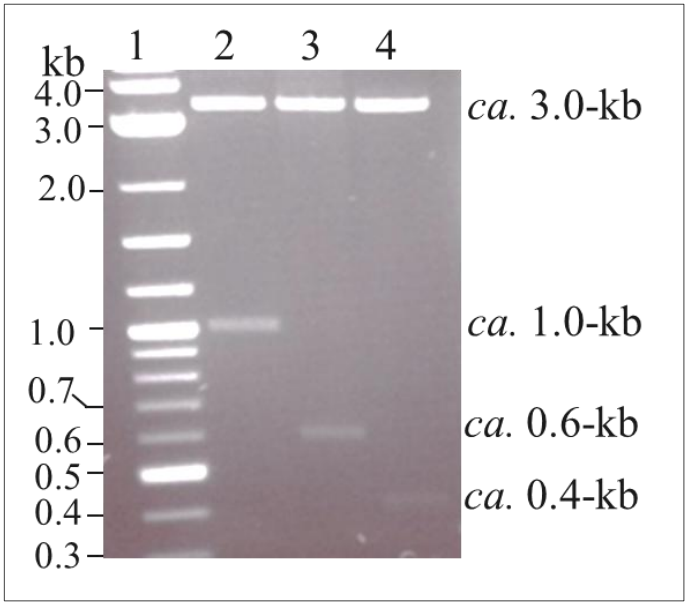

Figure 3.6. Agarose gel electrophoresis showing *Bam*HI/*Sal*I restriction fragments of pNJO74, pMSA1 and pMSA2. Lane 2 is pNJO74 (3.5 kb and 1.017 kb bands are apparent); lane 3 is pMSA2 (3.5 kb and 0.605 kb); lane 4 is pMSA1 (3.5 kb and 0.417 kb). Molecular mass markers are shown in lane 1.

3.2.3 Expression of OmpP2 Truncated Derivatives OmpP2ΔL1-4 and OmpP2ΔL5-8

pMSA1 and pMSA2 were successfully constructed and used to transform *E. coli* JM109 (section 3.2). pMSA1 encoded the vector-derived sequence MRGSHHHHHHGS, followed by *H. influenzae* OmpP2 N24-F359. In contrast, pMSA2 encoded the vector-derived sequence MRGSHHHHHHGS, followed by OmpP2 Y24-Y225, followed by the vector-derived sequence VDLQPSLI. Expression of the recombinant proteins was performed using exponential-phase *E. coli* JM109 harbouring either pMSA1 or pMSA2 and induced with IPTG for 3 h.

Pre-induced and induced samples were solubilized with SDS sample buffer and run on 10% SDS-polyacrylamide gels. Bands of *ca.* 17 kDa and *ca.* 28 kDa were observed in induced samples of cells harbouring plasmids encoding OmpP2ΔL1-4 and OmpP2ΔL5-8 respectively (Figure 3.7A). Histidine-tagged proteins were then detected by immunoblotting using anti-Penta-His antibodies (Figure 3. 7B).

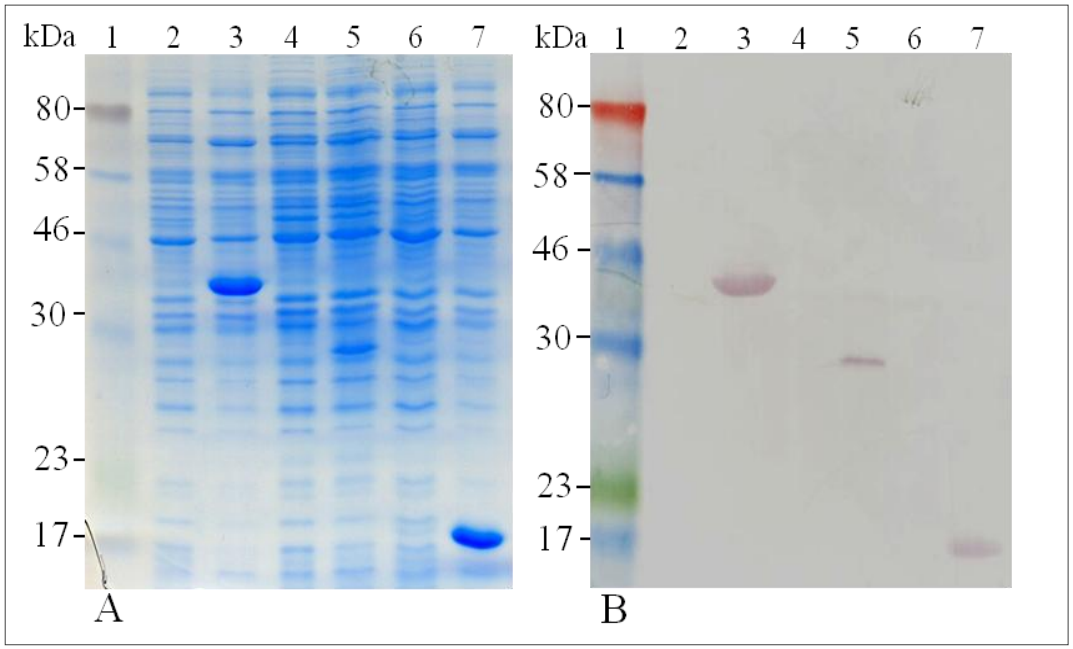

Figure 3.7. SDS-PAGE (A) and immunoblot using penta-his antibodies (B) showing OmpP2, OmpP2ΔL5-8 and OmpP2ΔL1-4 expression. In both panels: Lane 1, protein marker; 2, non-induced *E. coli* JM109 (pNJO74); 3, induced *E. coli* JM109 (pNJO74) (OmpP2); 4, non-induced *E. coli* JM109 (pMSA2); 5, induced *E. coli* JM109 (pMSA2) (OmpP2ΔL5-8); 6, non-induced *E. coli* JM109 (pMSA1); 7, induced *E. coli* JM109 (pMSA1) (OmpP2ΔL1-4).

3.2.4 Protein Purification by Affinity Chromatography

HisPur cobalt resin was used for recombinant protein purification. Due to the insoluble nature of OmpP2, protein purification was performed under denaturing conditions using affinity chromatography as described in section (2.11). To

confirm the purity and identity of the purified proteins, they were analysed by SDS-PAGE and immunoblotting. Recombinant protein bands with apparent molecular weight of *ca.* 17-kDa and 28-kDa corresponding to the OmpP2ΔL1-4 and OmpP2ΔL5-8, respectively, were observed by SDS-PAGE (Figure 3.8A). Immunoblot analysis also detected the tagged recombinant protein, and single bands corresponding to the expected protein size obtained (Figure 3.8B).

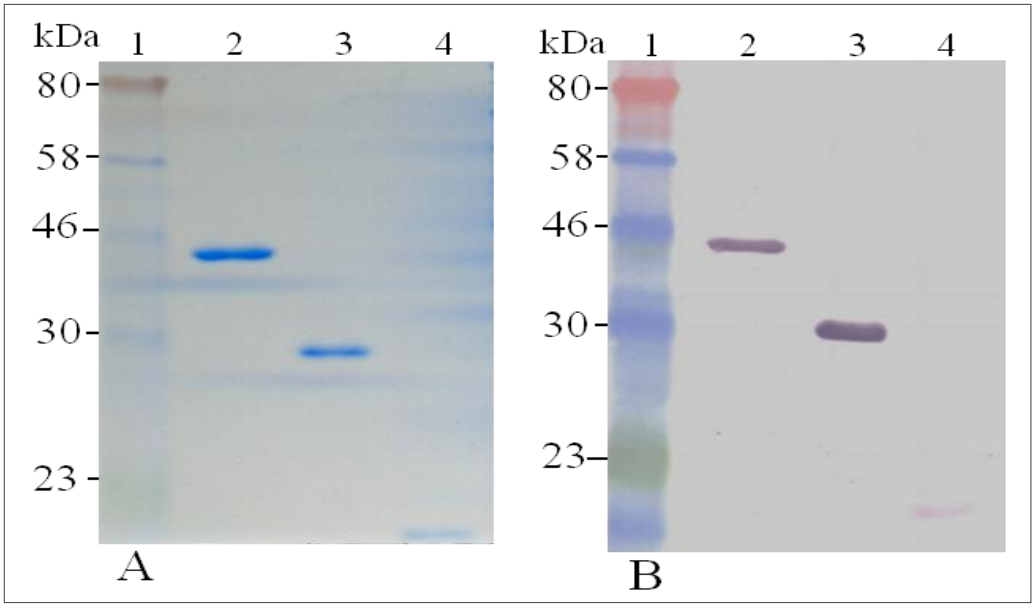

Figure 3.8. 10% SDS-polyacrylamide gel (A) and immunoblot analysis using anti-penta his antibodies (B) demonstrating affinity purification of OmpP2, OmpP2ΔL5-8 and OmpP2ΔL1-4. *E. coli* JM109 harbouring pNOJ74, pMSA1 or pMSA2 were grown to exponential phase and induced with IPTG. After induction, cells were harvested by centrifugation and recombinant protein purified using a Qiagen Ni-NTA spin kit under denaturing conditions. In both panels: Lane 1, protein marker; lane 2, OmpP2; lane 3, OmpP2LΔ5-8; lane 4, OmpP2ΔL1-4.

3.2.5 Binding of Recombinant OmpP2ΔL1-4 and OmpP2ΔL5-8 to Laminin Receptor

The purified truncated OmpP2 proteins were tested for rLRP-binding by ELISA. In these assays, wells were coated with 5 μg ml^{-1} OmpP2 or truncated OmpP2, blocked and later challenged with rLRP (5 μg ml^{-1}). After rigorous washing, anti-LR was added to detect the interaction between the bacterial proteins and rLRP. PorA was used as a positive control for rLR-binding. Each sample was tested at least in triplicate and each test was repeated at least three times. The data obtained showed that the binding of rLRP to OmpP2ΔL1-4 was significantly lower ($p < 0.01$) than binding to whole OmpP2. In contrast, rLRP-binding to PorA or OmpP2ΔL5-8 was not significantly reduced compare to whole OmpP2 (Figure 3.9).

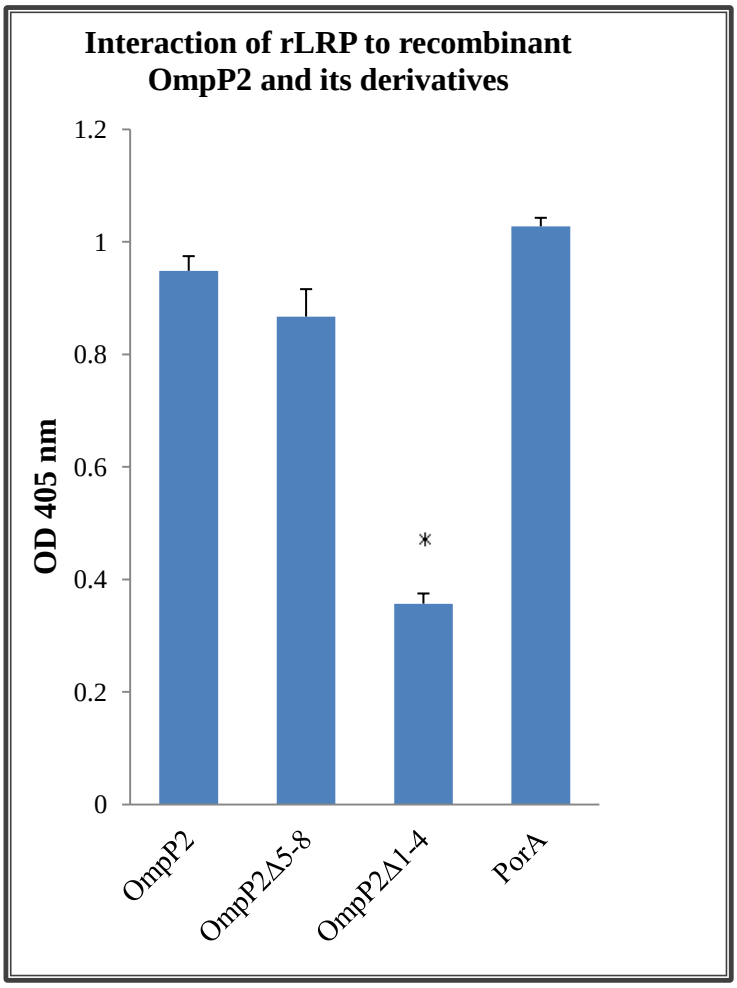

Figure 3.9. Binding of rLRP to OmpP2 and its derivatives. OmpP2, OmpP2ΔL1-4, OmpP2ΔL5-8 and PorA (as a positive control) were used as the solid-phase ligands. After blocking, rLRP was added followed by rabbit anti-LR and then anti-rabbit IgG-HRP antibodies. The absorbance in BSA-coated wells was subtracted from that in OmpP2 and PorA-coated wells. Data shown are the means of at least three independent experiments, with each sample tested in triplicate. *$p < 0.01$ compared with whole OmpP2. Error bars indicate SE.

3.2.6 Construction Plasmids of expression OmpP2 Derivatives: OmpP2ΔL1, OmpP2ΔL2, OmpP2ΔL3 and OmpP2ΔL4

The data shown in Figure 3.9 suggested that the rLRP-binding domain of OmpP2 was localised to the N-terminal portion of the protein. Therefore, further studies

were undertaken to identify the rLRP binding site present in this region. Specifically, plasmids encoding deletions in each of the first four extracellular loops of OmpP2 were constructed, since it was hypothesized that rLRP-binding was likely to be localised to one of the extra-cellular loops. All plasmids encoding OmpP2 loop deletions were derived from the pNOJ74 using inverse PCR methodology. Primers were designed based on the nucleotide sequence of *ompP2* from *H. influenzae*. *Bgl*II restriction sites were incorporated into both forward and reverse primers to facilitate self-ligation of amplified products.

After amplification, all PCR products were visualised on an agarose gel (Figure 3.10). PCR products then were digested using *Bgl*II and self-ligated to yield plasmids pMSA3 (encoding OmpP2 lacking loop 1), pMSA4 (encoding OmpP2 lacking loop 2), pMSA5 (encoding OmpP2 lacking loop 3) and pMSA6 (encoding OmpP2 lacking loop 4). Constructs were confirmed using restriction digest and DNA sequencing (data not shown).

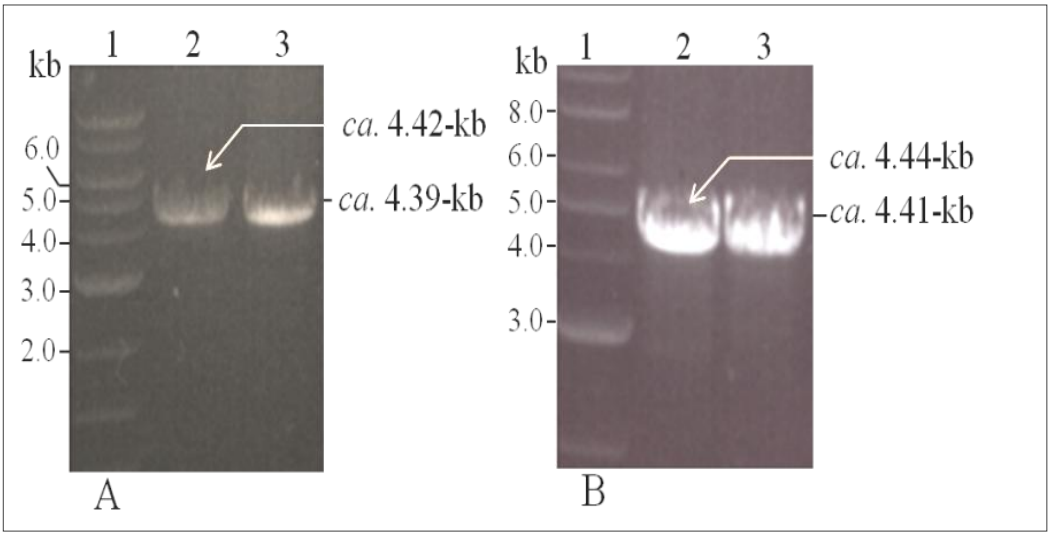

Figure 3.10. Agarose gel analysis showing the inverse PCR amplicons generated from pNJO74. (A) Lane 2, P2ΔL1I_F with P2ΔL1I_R product (loop 1 deletion). Lane 3, P2ΔL3I_F with P2ΔL3I_R product (loop 3 deletion) (B) Lane 2, P2ΔL2I_F with P2ΔL2I_R product (loop 2 deletion). Lane 3, P2ΔL4I_F with P2ΔL4I_R product (loop 4 deletion). In both panels, molecular mass markers are shown in lane 1.

3.2.7 Expression and Purification of OmpP2ΔL1, OmpP2ΔL2, OmpP2ΔL3 and OmpP2ΔL4 Recombinant Proteins

Plasmids pMSA3, pMSA4, pMSA5 and pMSA6 were transformed into *E. coli* JM109 and the transformants used to express recombinant OmpP2 derivatives lacking defined loops as described in section (3.2.6). Whole cell lysates from pre- and post-induced samples were solubilised in SDS sample buffer and run on 10% SDS-polyacrylamide gels. N-terminally 6 × His-tagged recombinant proteins were seen in induced samples of cells harbouring plasmids encoding OmpP2ΔL1, OmpP2ΔL2, OmpP2ΔL3 and OmpP2ΔL4 respectively (Figure 3.11A). Immunoblotting using anti-penta His antibodies confirmed that these proteins were histidine-tagged (Figure 3.11B). Faint immuno-reactive bands were also

observed in un-induced samples. This was probably due to leaky expression of the gene even without induction.

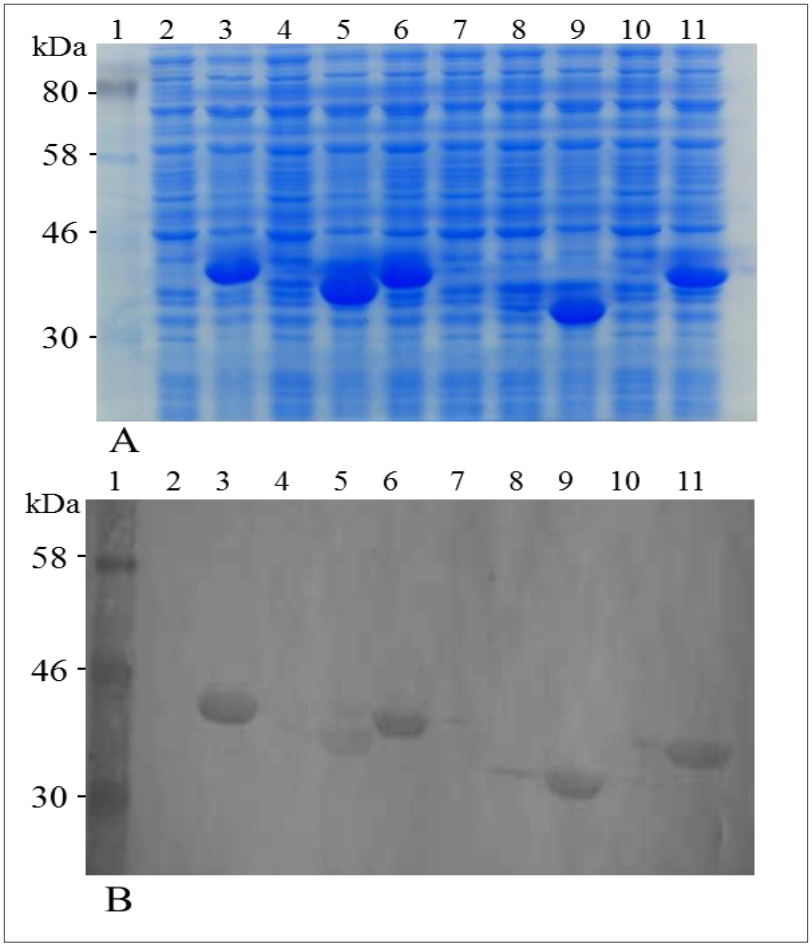

Figure 3.11. SDS-PAGE (A) and immunoblotting analysis using anti-penta His antibodies (B) showing OmpP2, OmpP2ΔL1 and OmpP2ΔL2, OmpP2ΔL3 and OmpP2ΔL4 expression in pre- and post- induced *E. coli* JM109 strains. Lane 1, protein marker. Lanes: 2, 4, 7, 8 and 10 cell are lysates of *E. coli* JM109 harbouring pNJO74, pMSA3, pMSA4, pMSA5 or pMSA6 respectively before induction. Lanes 3, 5, 6, 9 and 11 are corresponding cell lysates of *E. coli* JM109 harbouring pNJO74 (OmpP2), pMSA3 (OmpP2ΔL1), pMSA4 (OmpP2ΔL2), pMSA5 (OmpP2ΔL3) or pMSA6 (OmpP2ΔL4), respectively, after induction with IPTG. Immunoblot analysis shows that recombinant proteins are recognized by anti-penta histidine antibody.

Recombinant proteins were then purified under denaturing conditions and the urea removed using desalting columns or D-TubeTM Dialyzers. Purified proteins were analysed by SDS-PAGE and immunoblotting with anti-penta histidine or anti-OmpP2 antibodies. SDS-PAGE analysis showed single bands corresponding to OmpP2ΔL1, OmpP2ΔL2, OmpP2ΔL3 and OmpP2ΔL4, respectively (Figure 3.12A). Immunoblot analysis confirmed that the purified proteins were histidine-tagged (Figure 3.12B). In addition, the purified recombinant proteins were identified by anti OmpP2 antibody (Figure 3.12C).

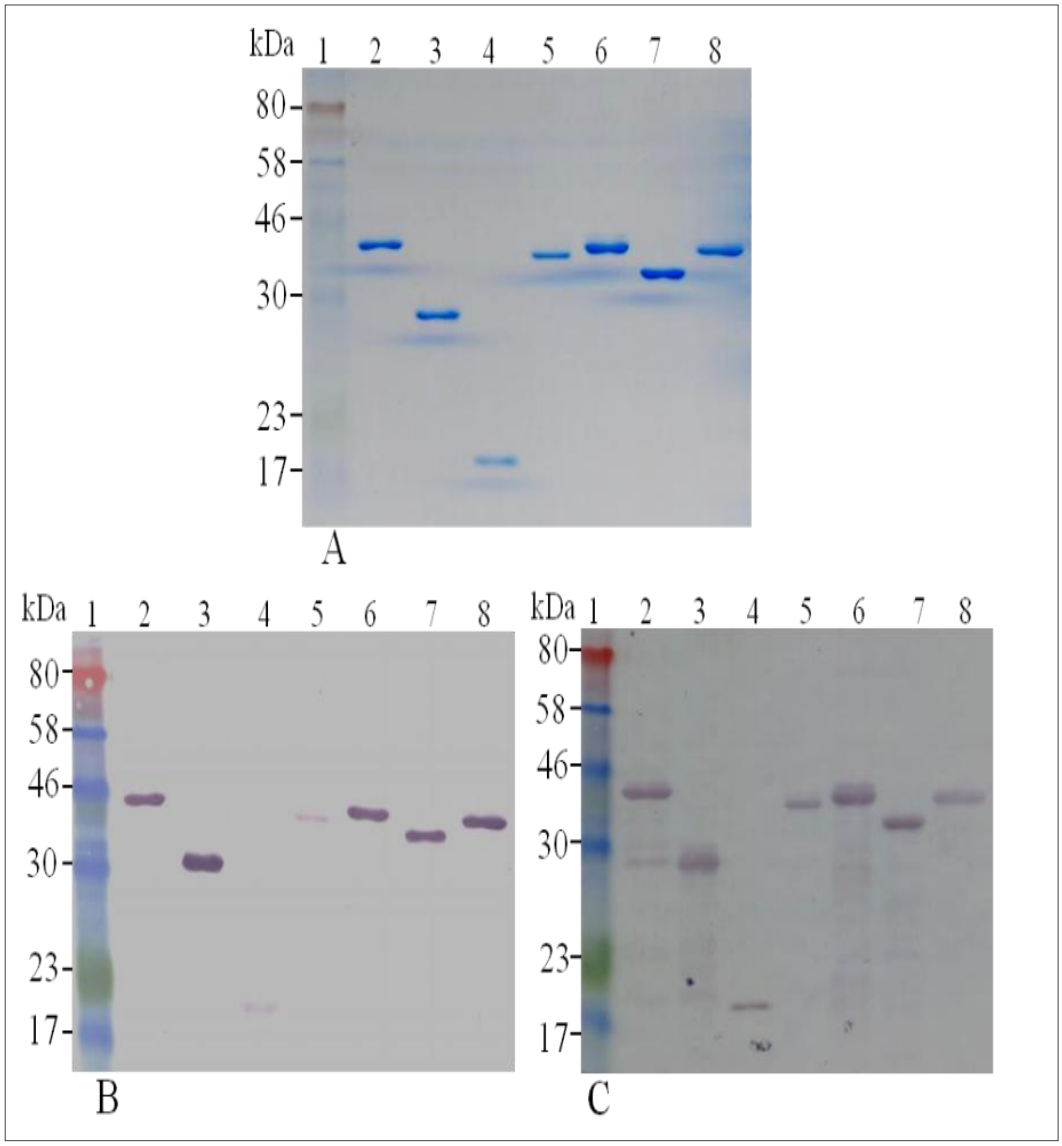

Figure 3.12. SDS-PAGE analysis (A), immunoblotting with anti-penta his (B) or anti-OmpP2 (C) confirming the purity and identity of the purified OmpP2 derivatives lacking specific loops. In all panels: lane 1, protein marker; lane 2, OmpP2; lane 3, OmpP2ΔL5-8; lane 4, OmpP2ΔL1-4, lane 5, OmpP2ΔL1; lane 6, OmpP2ΔL2; lane 7, OmpP2ΔL3; lane 8, OmpP2ΔL4.

3.2.8 Binding of rLRP to Recombinant OmpP2ΔL1, OmpP2ΔL2, OmpP2ΔL3 and OmpP2ΔL4 Using ELISA

The four purified truncated OmpP2 proteins were then tested for rLRP-binding by ELISA. In these assays, wells were coated with 5 μg ml^{-1} OmpP2 or truncated OmpP2, blocked and later challenged with rLRP (5 μg ml^{-1}). After rigorous washing, anti-LR was added to detect the interaction between the bacterial proteins and rLRP. PorA was used as a positive control for rLRP-binding. Each sample was tested at least in triplicate and each test was repeated at least three times. The data obtained showed that the binding of rLRP to OmpP2ΔL2 was significantly lower ($p < 0.01$) than binding to whole OmpP2. In contrast, LRP-binding to OmpP2ΔL1, OmpP2ΔL3 or OmpP2ΔL4 was not significantly reduced compare to whole OmpP2 (Figure 3.13). This data suggested that loop 2 is important for the interaction of OmpP2 with rLRP.

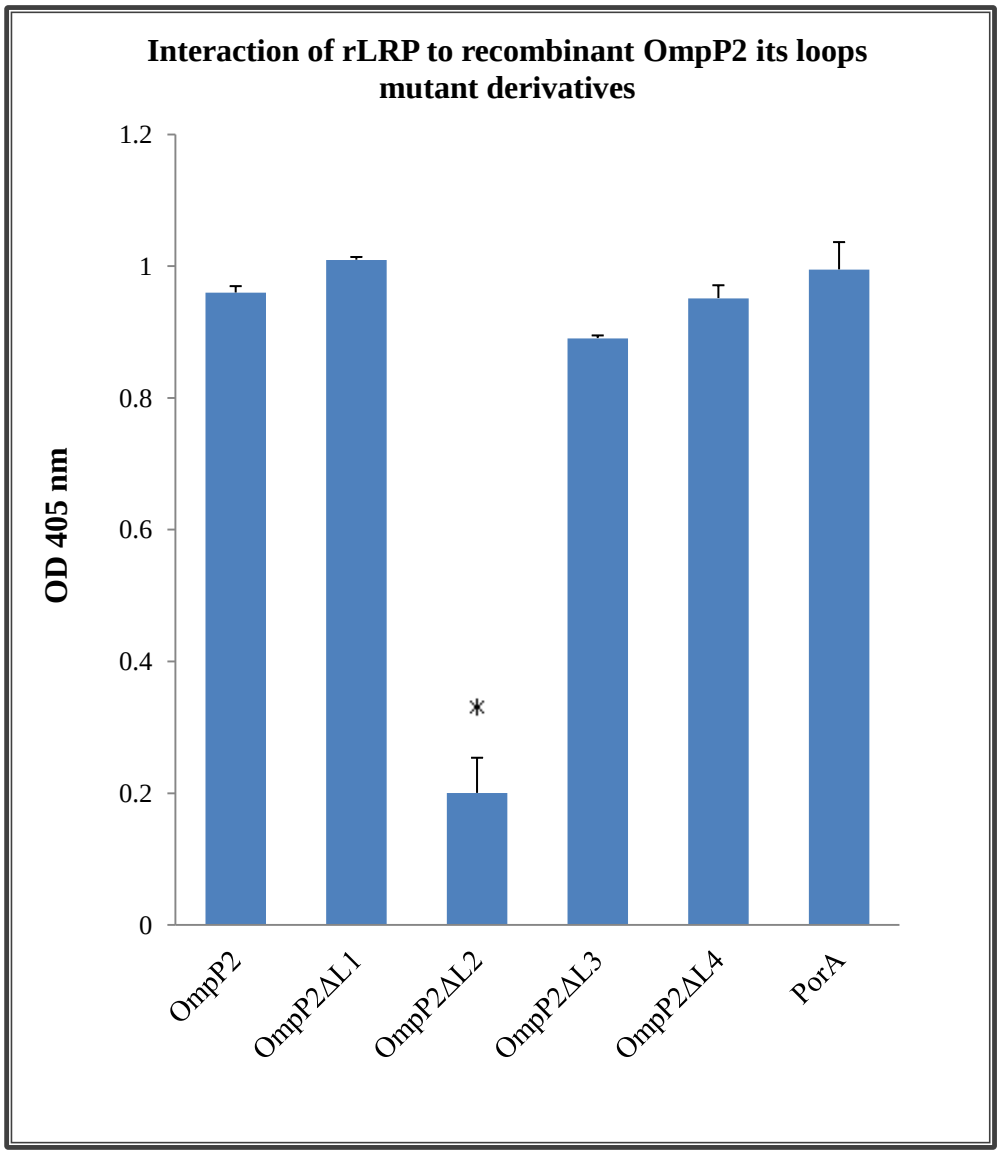

Figure 3.13. Binding of rLRP to OmpP2 and its OmpP2ΔL1, OmpP2ΔL2, OmpP2ΔL3 and OmpP2ΔL4 derivatives. OmpP2, OmpP2ΔL1 (labeled P2ΔL1), OmpP2ΔL2 (labeled P2ΔL2), OmpP2ΔL3 (labeled P2ΔL3), OmpP2ΔL4 (labeled P2ΔL4) were used to coat the wells of an ELISA plate at a concentration of 5 µg ml^{-1}. PorA and BSA-coated wells were included as comparative positive and negative controls respectively. After blocking, rLRP was added followed by rabbit anti-LR and then anti-rabbit IgG-HRP antibodies. The absorbance in BSA-coated wells was subtracted from that in OmpP2 and PorA-coated wells. Data shown are the means of at least three independent experiments, with each sample tested in triplicate. *$p < 0.01$ compared with whole OmpP2. Error bars indicate SE.

3.2.9 Construction of Plasmids for Expressing Native OmpP2 and OmpP2ΔL2 Using a Cell-free Protein Synthesis Methodology

The data shown in Figure 3.13 suggested that loop 2 was important for the interaction of OmpP2 with rLRP. However, the recombinant proteins used in this analysis were purified under denaturing conditions. This could dramatically affect protein structure and thus their biology activity (*i.e.* LRP-binding properties). Therefore, the aim was to purify OmpP2 and OmpP2ΔL2 under non-denatured conditions. If successfully purified these proteins could be tested for LRP-binding, so provide additional confirmation that loop 2 was required for optimal OmpP2 LRP-binding. The MembraneMax™ Protein Expression Kit (Invitrogen) was used for this purpose. The MembraneMax™ Reagent provides proper folding and stability of the membrane protein becuase the expressed membrane protein is embedded in the lipid bilayer which prevents aggregation of the protein. According to the manufacturer's instructions, the DNA template must contain a T7 promoter and the gene of interest must contain an ATG initiation codon. Hence, *ompP2* fragments were cloned into the pEXP5-CT/TOPO vector which contains these elements. Primers P2CtHis_F and P2CtHis_ R (Table 2.1) were used to amplify *ompP2* and *ompP2*Δ*L2* from plasmids pNJO74 and pMSA4 respectively to yield 1.011 kb (*ompP2*) and 0.99 kb (*ompP2*Δ*L2*) amplicons (Figure 3.14A). These products were then cloned into pEXP5-CT/TOPO to yield pMSA18 and pMSA19 respectively. Constructs were confirmed by PCR (Figure 3.14B), restriction digestion and DNA sequencing (data not shown).

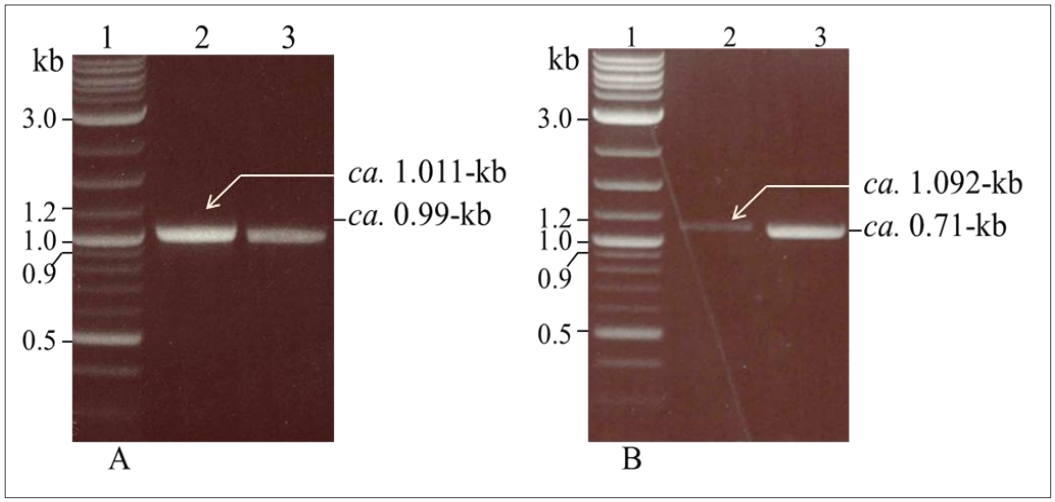

Figure 3.14. Generation of pMSA18 and pMSA19 constructs for cell-free protein expression. Agarose gel analysis of PCR products of (A) amplified fragment from templates pNJO74 (lane 2, *ca.* 1.011 kb) and pMSA4 (lane 3, *ca.* 0.99 kb) using P2CtHis_F and P2CtHis_R primers, (B) PCR-amplified fragments from pMSA18 (lane 2, *ca.* 1.092 kb) and pMSA19 (lane 3, *ca.* 1.071 kb) using T7_F and P2CtHis_R primers. In both panels, DNA markers are shown in lane 1.

3.2.10 Expression of OmpP2 and OmpP2ΔL2 Proteins Using the MembraneMax™ Protein Expression Kit

The MembraneMax^{TM} protein expression kit is designed for *in vitro* expression of soluble membrane proteins from template DNA. For proper expression in the MembraneMax^{TM} system, it is recommended that the template must contain the T7 promoter and the gene of interest must contain an ATG initiation codon. Therefore, the pEXP5-CT/TOPOR vector, which is ideally suited for use with MembraneMax™ Protein Expression Kits, was used.

Genes encoding OmpP2 and OmpP2ΔL2 were recombined pEXP5-CT/TOPO plasmid (Invitrogen) following the manufacturer's directions. In brief, the genes *ompP2* and *ompP2ΔL2* were PCR-amplified from plasmid pNJO74 and pMSA4

respectively using primers P2CtHis_F and P2CtHis_R (Table 2.1) and recombined into pEXP5-CT/TOPO to yield pMSA18 (encoding OmpP2) and pMSA19 (encoding OmpP2ΔL2) respectively, which were used to transform *E. coli* JM109. These primers amplify the whole gene of *ompP2* or *ompP2ΔL2*, incorporating the start codons and devoid of the stop codon of the genes.

The MembraneMax™ protein expression kit includes all the components and reagents needed for the production and solubilisation of desired recombinant membrane proteins. The membrane protein of interest is synthesized into an environment that mimics its cellular surroundings with consistent soluble structure and less aggregates or clumping.

pMSA18 and pMSA19 were purified from *E. coli* JM109 and used for protein expression using the MembraneMax^{TM} protein expression kit according to the manufacturer's instructions. Following the expression reaction, samples were analysed by SDS-PAGE (Figure 3.15A) and immunoblotting using anti-penta-his (Figure 3.15B) and anti-OmpP2 antibodies (Figure 3.15C). This analysis showed that expression of both proteins was successful using this approach. However, the yield of the protein was comparably low, and further purification steps would be required to remove the cell lysate of the *E. coli* slyD^{-} extract which was used in the reaction. To purify the amount of OmpP2 and OmpP2ΔL2 needed for the further investigation of LRP-binding, many expression kits would be required and the cost prohibitive. Hence, the purification of OmpP2 and OmpP2ΔL2 using this strategy was not pursued further.

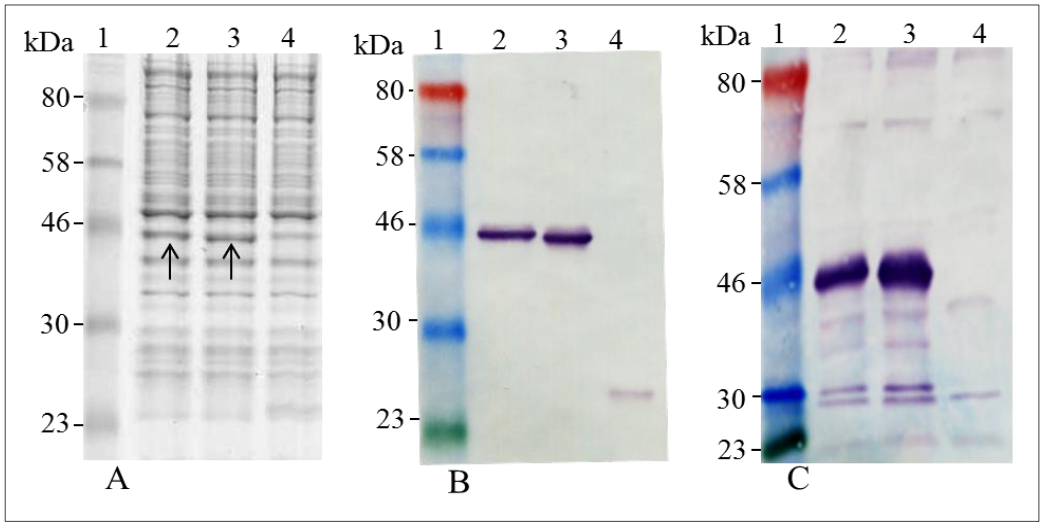

Figure 3.15. Expression and purification of OmpP2 and OmpP2ΔL2 using a cell-free protein purification system. SDS-PAGE (A) and immunoblot analysis (B; probed with α-His antibody, C; probed with α-OmpP2 antibody) of expressed proteins obtained using the MembraneMax™ Protein Expression Kit. Lane 2, OmpP2; lane 3, OmpP2ΔL2; lane 4, negative control, contains all additives except DNA template (pMSA18 or pMSA19). Broad range protein markers (6-175 kDa) are shown in all panels in lane 1.

3.3 Discussion

Invasive disease caused by Hib can affect many organ systems. The most common types of invasive disease are meningitis, epiglottitis, pneumonia, arthritis, and cellulitis. Meningitis is infection of the membranes covering the brain and is the most common clinical manifestation of invasive Hib disease. To cause meningitis, the bacteria have to cross the blood–brain barrier (BBB), but the precise mechanisms by which bacterial meningeal pathogens such as *N. meningitidis, S. pneumoniae,* and *H. influenzae* cross the BBB and gain access to the CNS and brain is not fully understood (Kim, 2006).

Recent work has shown that CbpA of *S. pneumoniae*, PorA and PilQ of *N. meningitidis* and OmpP2 of *H. influenzae* are LamR-binding ligands and enable these bacterial pathogens to bind to rodent and human brain microvascular endothelial cells of the BBB (Orihuela *et al.*, 2009).

OmpP2 is the most abundant protein in the outer membrane of *H. influenzae* and, besides its basic function as a porin, it has many activities associated with host cell interactions. For instance, Anderson *et al* found that mutation of *ompP2* caused reduced uptake of nicotinamide adenine dinucleotide (NAD) and nicotinamide mononucleotides (NMN) (Andersen *et al.*, 2003). Additionally, changes in the OmpP2 sequence led to differences in antibiotic sensitivity (Regelink *et al.*, 1999). Antibodies against OmpP2 were shown to be protective in the infant rat model of bacteremia (Chong *et al.*, 1993; Duim *et al.*, 1996).

In this chapter, the interaction between purified OmpP2 and rLRP was investigated using ELISA with the aim of defining the regions of OmpP2 required

for optimal rLRP binding. Initially, two truncated fragment of OmpP2 were expressed and purified. The first fragment corresponded to the N-terminal half of OmpP2 and including the first four extracellular loops of the molecule. The second part corresponded to the C-terminal half of OmpP2 including the last four extracellular loops of the protein. ELISA analysis suggested that the region of OmpP2 that interacts with rLRP was contained in the N-terminal part of OmpP2. In order to investigate which of the four extracellular loops contained in this fragment was important in the interaction of OmpP2 with rLRP, four plasmids were constructed in which the coding regions of these loops were individually removed from OmpP2. The truncated proteins encoded by these plasmids were then expressed and purified and the ability of the proteins to interact with rLRP was investigated. The data suggested that OmpP2 lacking loop 2 significantly reduces its binding to rLRP in comparison to the whole protein.

The work described in this chapter utilised OmpP2 derivatives purified under denaturing conditions. Attempts were also made to purify them under native conditions, so that the purified protein would more closely mimic the membrane-embedded OmpP2 protein produced by *H. influenzae.* This was performed using the MembraneMax™ Protein Expression Kit. SDS-PAGE analysis and immunoblotting confirmed expression of the recombinant proteins. However, the yield of expressed protein obtained from each reaction was low, and given the cost of the expression kit, it was not considered a viable option for purifying the amount of OmpP2 derivatives needed for further analysis of LR-binding.

The interaction between OmpP2 of *H. influenzae* and LamR has been shown to be important in the pathogenesis of this organism. To test the hypothesis that loop 2 of OmpP2 is important for the interaction of *H. influenzae* and LamR (rather than just OmpP2 alone), a specific mutant was then generated in *H. influenzae* in which this loop was deleted. This mutant was then be tested in assays for LamR-binding and additional models of virulence. This work is detailed in subsequent chapters of this thesis.

CHAPTER FOUR: Mutagenesis of *ompP2* and *ompP2ΔL2* of *H. influenzae*

CHAPTER FOUR

4. MUTAGENESIS OF *OMPP2* AND *OMPP2ΔL2* OF *H. INFLUENZAE*

4.1 Introduction

Initial investigations into the specific regions of OmpP2 mediating interactions with recombinant laminin receptor precursor protein (rLRP) were described in the previous chapter. Two fragments of OmpP2 were expressed in *Escherichia coli*: one corresponded to the N-terminal portion of OmpP2, and included loops 1-4 (OmpP2ΔL5-8); the second corresponded to the C-terminal portion, and included loops 5-8 (OmpP2ΔL1-4). ELISA experiments using purified rLRP showed that the region of OmpP2 which interacts with recombinant laminin receptor protein was contained in the first four loops of OmpP2. In contrast, the last four loops were unable to bind rLRP. Furthermore, deletion of loop 2 from full length recombinant OmpP2 expressed in *E. coli* significantly reduced its interaction with rLRP. These results suggest that loop 2 is important for the ability of OmpP2 to bind to rLRP, and thus, it is likely that loop 2 plays an important role in the pathogenesis of *Haemophilus influenzae*. A study carried out by Orihuela and colleagues suggested that the initiating step of invasion of the vascular endothelium of the blood-brain barrier by meningeal pathogens (including *Neisseria meningitidis*, *H. influenzae* and *Streptococcus pneumoniae*) is the interaction of outer membrane proteins of these microorganisms with the 37/67-kDa laminin receptor (LamR) on the surface of human brain microvascular endothelial cells (HBMECs) (Orihuela *et al.*, 2009). LamR was identified to be a

common receptor for all three species of meningeal pathogens (Orihuela *et al.*, 2009). Moreover, mutagenesis studies indicated that the bacterial LamR-binding adhesins were pneumococcal CbpA, meningococcal PilQ and PorA, and OmpP2 of *H. influenzae* (Orihuela *et al.*, 2009). It had already been shown that LamR acts as a receptor for a number of neurotrophic viruses, such as Sindbis virus and Dengue virus (Wang *et al.*, 1992), thus LamR may act as a common determinant in mediating the entry of viral and bacterial pathogens to the immunologically-privileged CNS.

To further characterize the role of OmpP2 loop 2 of *H. influenzae* in its interaction to LamR, *ompP2* and *ompP2ΔL2* null mutants were generated. The mutants will be utilized in subsequent characterization experiments to facilitate a study of the potential role of OmpP2 and its second loop in the pathogenesis of *H. influenzae*. In addition to mutating *ompP2* (*H. influenzae* Δ*ompP2*) and its loop 2-encoding region (*H. influenzae ompP2*Δ*L2*), the *H. influenzae ompP2::kanR* mutant was created, in which the kanamycin resistance cassette was inserted into the wild type *H. influenzae*, and was used as negative controls in experiments. Moreover, the surface location of the mutated OmpP2 protein was investigated using cell fractionation by a modification of the method of Nossal and Heppel (Nossal & Heppel, 1966). In this study interaction of *H. influenzae* and its derivative mutants to rLRP was investigated using a combination of molecular and immunological techniques, including ELISA, whole cell lysate pull-down assays, and flow cytometry. In addition, the proteins OmpP2 and OmpP2ΔL2 were purified under non-denatured conditions using ion exchange and gel filtration. Purified proteins

then tested to their binding with rLRP by enzyme-linked immunosorbant assay (ELISA).

4.2 Results

4.2.1 Generating a Mutant Lacking the Region of Loop 2 Gene Encoding OmpP2 Lack the loop 2 Peptides

Previous results indicated that the second loop of recombinant OmpP2 is important for OmpP2 interaction with rLRP. Therefore, the next aim was to construct a *H. influenzae* strain expressing OmpP2 with loop 2 deleted. This strain could then be tested for LamR-binding. In order to create a loop 2 knock-out mutant in *H. influenzae* strain Rd KW20, a region of DNA containing *ca.* 1-kb upstream and *ca.* 1-kb downstream of the *ompP2* gene sequence was successfully amplified by PCR from genomic DNA of *H. influenzae* Rd, Amplification was done by PCR using primers mP2_F and mP2_R (Table 2.1). The fragment containing *ompP2* plus flanking regions was amplified, A-tailed to facilitate T-cloning and then purified (Figures 4.1 and 4.2A).

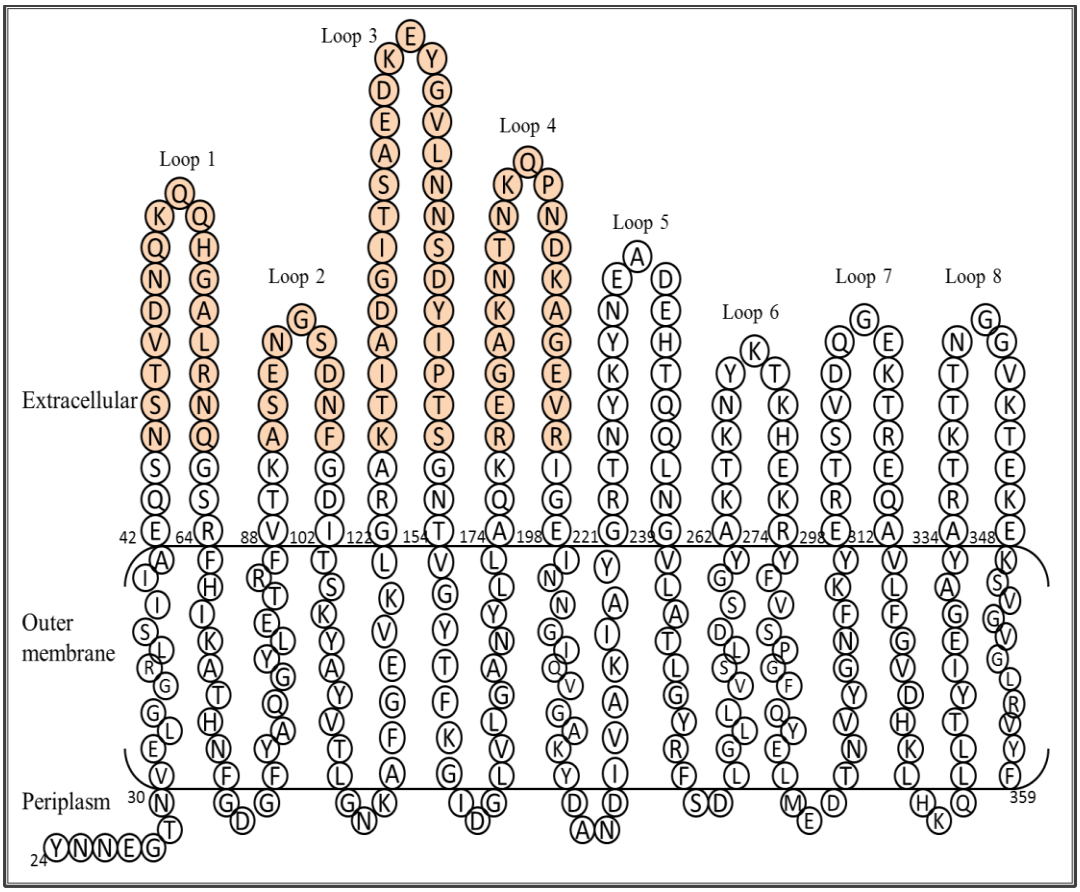

Figure 4.1. Topology of the OmpP2 protein in the *H. influenzae* cell envelope, based on the model of Galdiero *et al.* (2006). The highlighted sequences represent the separately deleted loops in this work.

The amplified fragment was then ligated into pGEM-T Easy (Promega) and used to transform *E. coli* JM109. The resulting colonies were screened for the presence of the desired insert by PCR using T7P and SP6 vector-specific primers. However, no product bands corresponding the expected size were generated despite repeating this experiment several times using a range of different conditions. Similar results were obtained when another set of primers: p2F3 and P2R3_3 (Table 2.1) was employed in conjunction with the alternative cloning vector.

It was hypothesized that the amplified region may be deleterious to *E. coli*. In particular, the gene upstream of *ompP2* (*rnh*), which encodes for ribonuclease H (an enzyme involved in DNA replication, recombination and repair) might also be harmful to *E. coli*. Therefore, new primers were designed: F1 and mP2_R (Table 2.1), which are predicted to yield a 2.72-kb amplicon (containing *ca.* 0.52-kb upstream and *ca.* 1.1-kb downstream of the *ompP2* gene sequence). A PCR product of the expected size was obtained using *H. influenzae* Rd KW20 chromosomal DNA as template (Figure 4.2B), purified, A-tailed, cloned into pGEM-T Easy and used to transform *E. coli* JM109. Transformants containing the desired insert were identified by blue white screening and confirmed by PCR and restriction digestion analysis. PCR analysis employed the plasmid pGEM-T Easy vector-specific primers T7P and SP6 to yield *ca.* 2.9-kb band (Figure 4.2C). Furthermore, restriction digestion using *EcoR*I produced the expected three bands of *ca.*3 kb, *ca.* 1.6 kb and *ca.*1.13kb (Figure 4.2D).

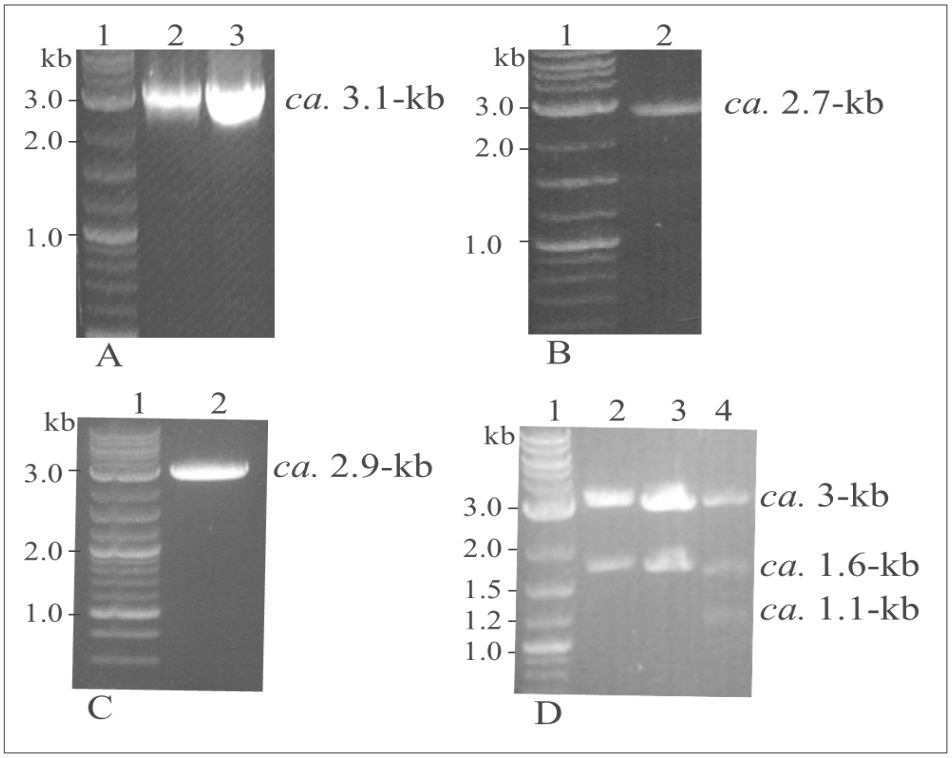

Figure 4.2. Agarose gel analysis showing (A) the PCR product amplified from *H. influenzae* using mP2_F and mP2_R primers (3.199-kb). Lanes: 1, 2-kb DNA marker; 2, 3 PCR product before and after gel purification, (B) the F1 and mP2_R PCR products lane 2. Lane 3 is A-tailed, purified F1 and mP2_R product (*ca.* 2.7-kb), (C) T7P and SP6 PCR products generated from *E. coli* JM109 transformants containing the F1 and mP2_R insert (expected size 2.9-kb), (D**)** pMSA8 restriction digestion fragments. Lane: 2-4 pMSA8 extracted plasmids digested with *Eco*RI. 2-kb DNA marker is shown in lane 1 in all panels.

PCR analysis and restriction digestion results demonstrated that only one of the tested colonies harboured the expected plasmid with the *ca.* 2.7-kb fragment generated by the F1 and mP2_R primers. Both approaches confirmed the successful ligation of the desired insert to pGEM-T Easy and this plasmid was designated pMSA8.

Following on from this characterization, the inserts from pMSA8 were sequenced to ensure they contained no errors. This analysis showed that the plasmid lacked a single adenine nucleotide in the *ompP2* coding region compared to the genome sequence (Figure 4.3).

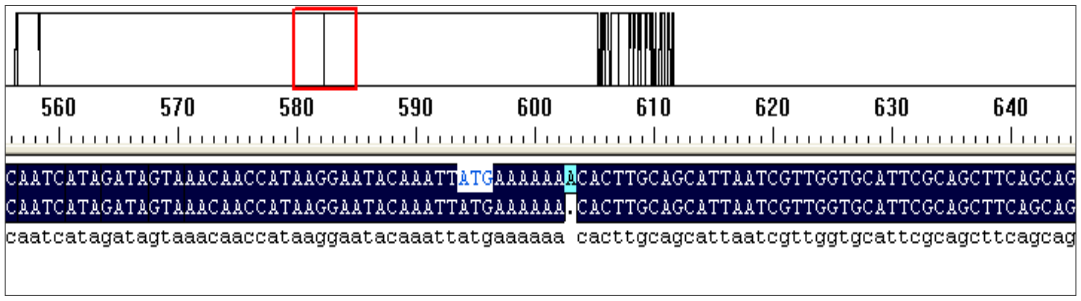

Figure 4.3. DNA sequencing data showing the missing adenine nucleotide in the ompP2 coding region compared to the *H. influenzae* type b genome. The alignment was generated using DNAMAN software and the wild type *H. influenzae* genome and the sequenced fragment of pMSA8 (carrying *ompP2* plus flanking regions). The start codon of *ompP2* is highlighted in white and the A nucleotide is shown in green which is missing in pMSA8.

4.2.2 Constructing Amplicon to Facilitate Deletion of OmpP2 Loop Using the Missing Nucleotide Construct (pMSA8)

Since the previously constructed plasmid pMSA8, which contained *ompP2* plus flanking regions, was missing a single adenine within the open reading frame (ORF) of *ompP2*, the protein OmpP2 would not be expected to be expressed in the transformant cells. Consequently, it was hypothesized that this construct could be manipulated and cloned in *E. coli* by avoiding the suspected problems with toxicity resulting from the introduction of the intact *ompP2* gene. A construct based on this plasmid was generated by amplifying using primers F1 and mP2_R to yield a *ca.* 2.7 kb amplicon (*ompP2* plus 0.5 kb upstream and 1.1 kb

downstream) and used to facilitate further constructions needed for deletion of the loop 2-encoding region of *ompP2* (Figures 4.4 and 4.5).

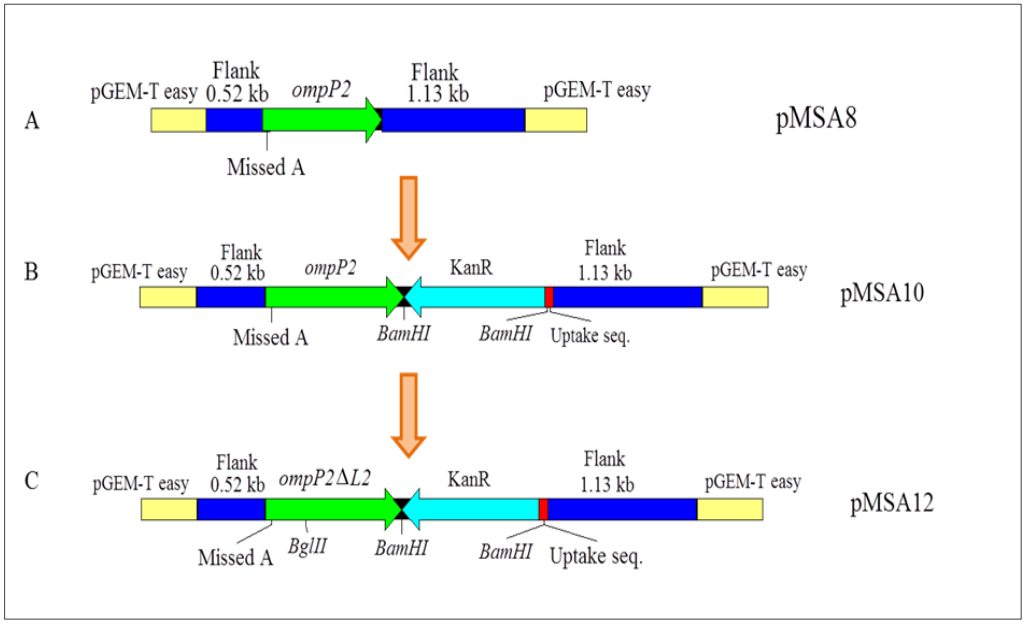

Figure 4.4. Schematic diagram representing steps used to generate designing mutagenic constructs using pMSA8 as a template. (A) pMSA8 plasmid comprising 3-kb pGEM-T easy, *ompP2* plus *ca.* 0.52-kb upstream flanking region and 1.113 kb downstream region. (B) plasmid derived from pMSA8 containing 3-kb pGEM-T easy, *ca.* 1.5-kb kanamycin resistance cassette and the *ompP*2 plus 0.52-kb upstream and 1.113-kb downstream flanking regions (pMSA10). (C) plasmid pMSA12 derived from pMSA10 comprising 3-kb pGEM-T easy, 1.5-kb kanamycin resistance cassette and the *ompP2ΔL2* plus 0.52-kb upstream and 1.113-kb downstream flanking regions.

pMSA8 was subjected to Inverse PCR (IPCR) using Omg_F and Omg_R primers (Figure 4.5A) incorporating *Bam*HI restriction sites in both sides of the product. A copy of the *H. influenzae* DNA uptake sequence (5'AAGTGCGGTCA3'), which is required for efficient DNA uptake and natural transformation of *H. influenzae* (Danner *et al.*, 1982; Smith *et al.*, 1995), was incorporated into the forward primer Omg_F and hence the amplified fragment. The PCR product was purified,

dephosphorylated and ligated with the 1.5-kb *Bam*HI-digested Kanamycin resistance cassette isolated from the vector pJMK30. Following transformation of *E. coli* JM109, putative transformant colonies were selected on kanamycin plates and analysed by PCR using the plasmid pGEM-T Easy vector-specific primers T7P and SP6 to yield an expected band of *ca.* 4.1-kb band (Figure 4.5B).

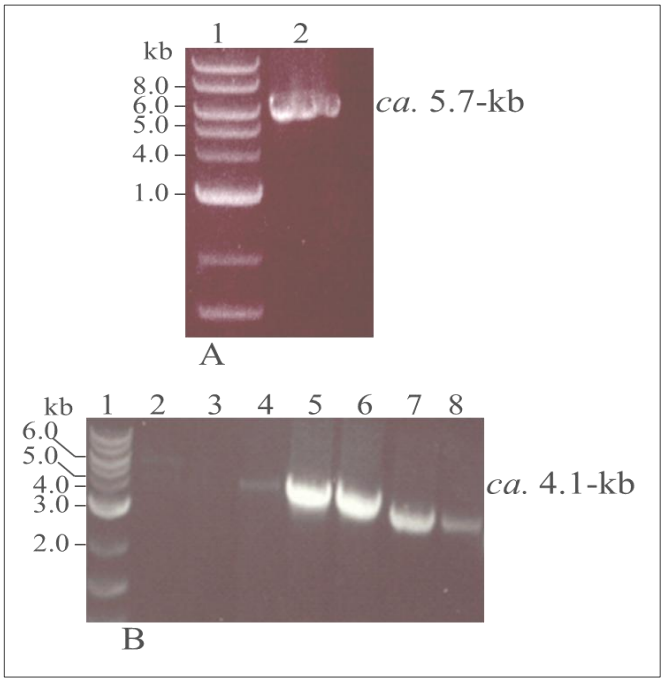

Figure 4.5. Construction of intermediate plasmid pMSA10. Agarose gel analysis of (A) *Bam*HI-digested purified PCR products. Product obtained from pMSA8 using Omg_F and Omg_R primers to yield a 5.7-kb product (pMSA8). (B) PCR products obtained from transformed cells with pMSA10 using primers T7P and SP6. Lanes 2-9: PCR products from seven colonies expected to harbour pMSA10 (expected size *ca.* 4.1-kb in total; *ca.* 2.6-kb plus *ca.* 1.5-kb). In both panels 2-kb DNA marker is shown in lane 1.

A transformant harbouring the expected product was selected, sequenced and named pMSA10. pMSA10 was subsequently used as a template for inverse PCR utilizing primers P2Δ2I_F and P2Δ2I_R (Table 2.1, Figure 4.6A), digestion with

*Bgl*II and self-ligation resulting in a construct lacking the DNA encoding loop 2, which was designated pMSA12. The plasmid was confirmed by restriction digestion using *Not*I and *Bgl*II (Figure 4.6B). Sequence analysis of both pMSA10 and pMSA12 confirmed that they contain no errors except the expected missing adenine nucleotide which was missing from the parent plasmid pMSA8. This deletion was located at the 5' end of *ompP2* and recombining this into the *H. influenzae* chromosome would yield an OmpP2-deficient strain, rather than one expressing OmpP2, but with loop 2 missing.

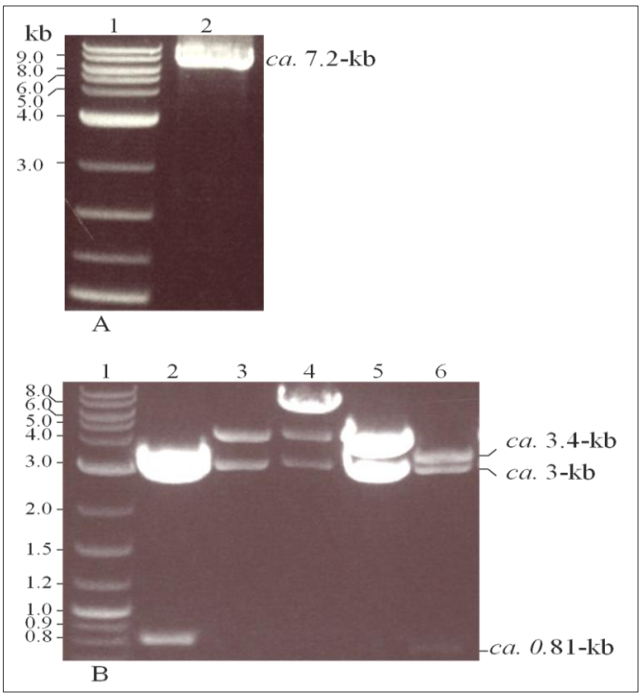

Figure 4.6. Constructing of mutagenic plasmid pMSA12. Agarose gel analysis of (A) IPCR products derived from pMSA10 utilizing P2Δ2I_F and P2Δ2I_R primers to yield 7.2-kb product followed by restriction digestion with *Bgl*II. (B) digested pMSA12 plasmids extracted from three *E. coli* JM109. Lanes 2-6 are double digestions using *Not*I and *Bgl*II of the five putative positive transformants with pMSA12. Positive result of the digestion yield 3 expected bands of 3, 3.4 and 0.81-kb as it is shown in lanes 2 and 6. Lane 1 is 2-kb DNA marker in both panels.

4.2.3 Correction of the Mutation in the *ompP2* Gene Cloned in pMSA12

Before plasmid pMSA12 could be used to mutate *H. influenzae* Rd KW20 it was necessary to correct the sequence. Site-directed mutagenesis was applied to correct the plasmid pMSA8 by inserting an adenine nucleotide in the construct (Figure 4.7). A fragment of DNA consisting of the 539 bp upstream region of the *ompP2* gene (including 7 consecutive adenine residues in *ompP2*) was amplified using MegaR and F1 primers from *H. influenzae* Rd KW20 chromosomal DNA (Table 2.1). This fragment was used in subsequent rounds of PCR as a forward mega primer in conjunction with the mP2_R reverse primers and pMSA12 as a template. The 2.7 kb product of this amplification included *ompP2* minus loop 2 region and flanking regions, and incorporated the kanamycin resistant cassette.

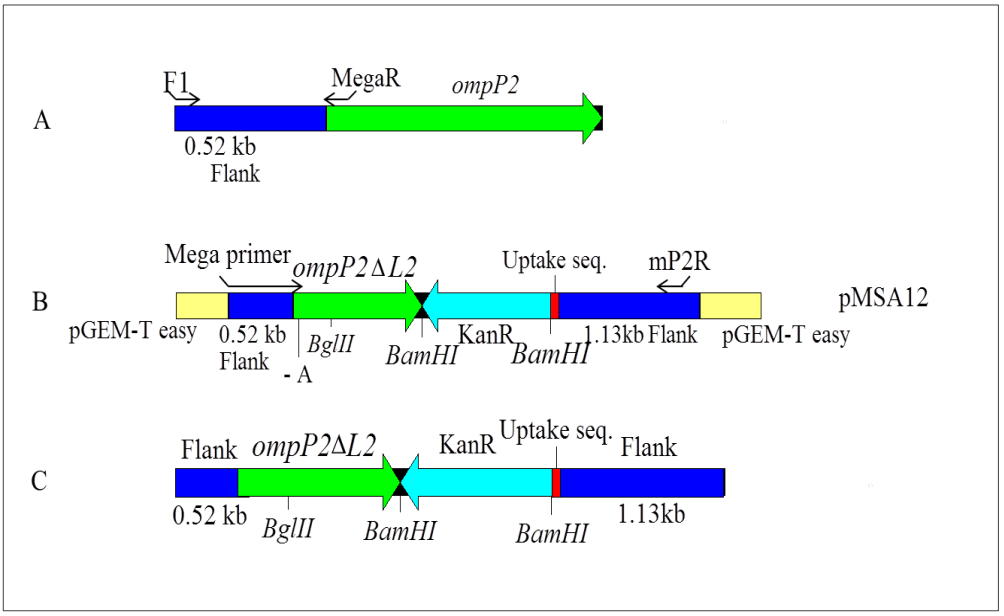

Figure 4.7. Schematic diagrams showing the steps of site-directed mutagenesis to add an adenine nucleotide to the pMSA12. A, a mega primer was amplified using the F1 and MegaR primers. B, the generated mega primer with mP2_R was used to amplify the corrected region indicated using pMSA12 as a template. C, the 4.1 kb product amplified from pMSA12, was used to transform *H. influenzae*.

The 0.539-kb mega primer fragment was amplified from *H. influenzae* using MegaR and R2 primers. The mega primer consists of part of the upstream region of *ompP2*, the ribonuclease H DNA metabolism gene (*rnh*), plus 7 nucleotides of *ompP2* totaling 539 bp (Figure 4.8). The amplicon (mega primer; 539 bp) was utilised in the PCR as a forward primer with the mP2_R reverse to yield 4.1 kb fragments from the plasmid pMSA12 (Figure 4.8B).

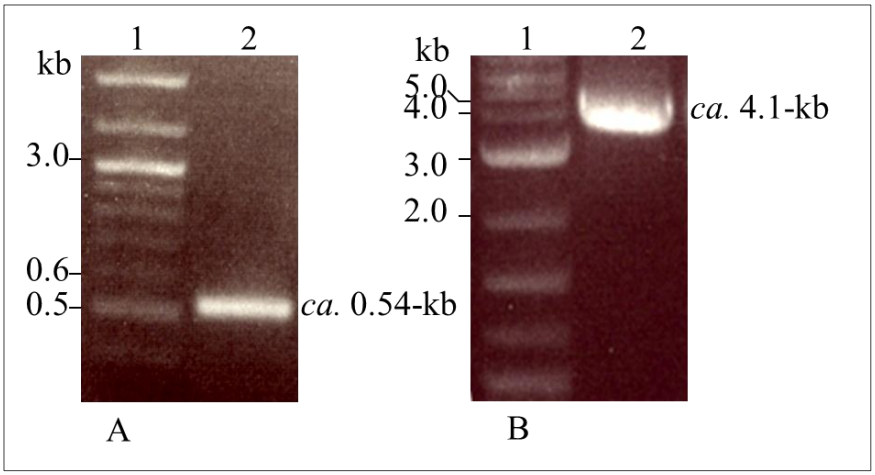

Figure 4.8. Generation of the mutagenic PCR amplicon for deletion of the loop 2-encoding region of *ompP2*. pMSA12 was used as a template to amplify the 539-bp mega primer using MegR and F1 primers (lane 1, A). (B) The 4.1 kb mutagenic PCR product was amplified using the mega primer and the mP2R (lane 2), lane 1 contains the 2 kb DNA marker.

4.2.4 Mutagenesis of *ompP2* in *H. influenzae* Rd KW20

H. influenzae cells were mutagenised using the PCR amplicon described above. Attempts to transform the cells by electro-transformation did not yield the desired mutants. Naturally transformed *H. influenzae* cells were grown on the selective media containing kanamycin and putative colonies were screened by PCR. Primers flanking the region of interest amplified a fragment that was *ca.* 1.5-kb larger than the wild type *H. influenzae* (*ca.* 2.2 kb for the wild type and *ca.* 3.7 kb in mutated cells), which corresponded to the size of the kanamycin resistance cassette (Figure 4.9).

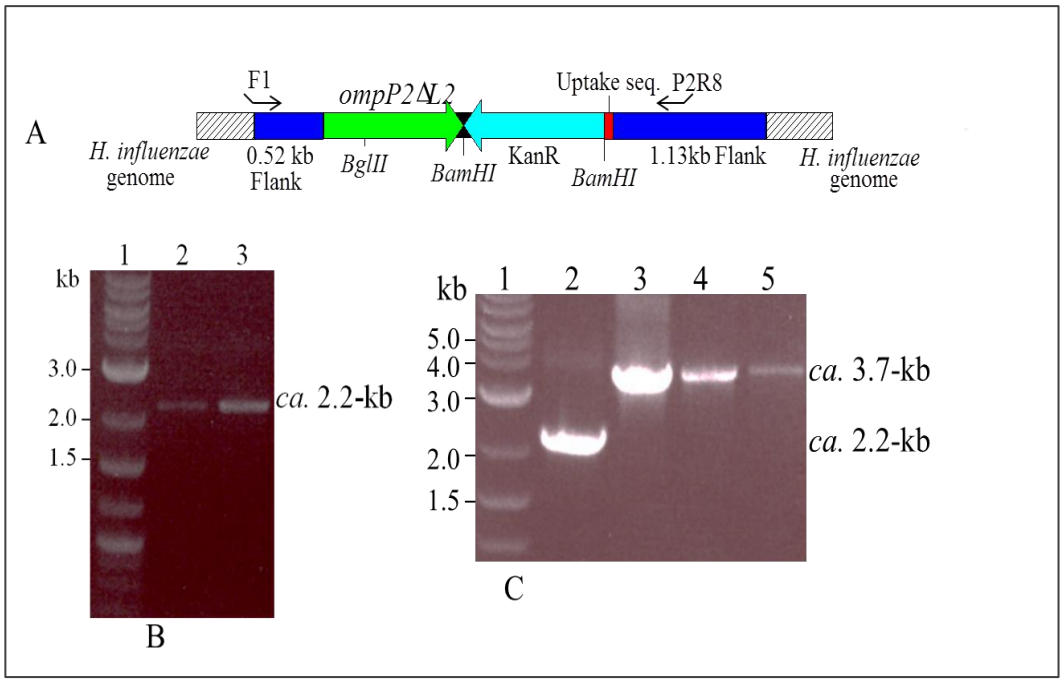

Figure 4.9. PCR analysis of electro and naturally-transformed *H. influenzae*. (A) Schematic diagram showing the positions of the primers relative to the region of interest. Chromosomal DNA of the (B) electro and (C) naturally-transformed *H. influenzae* colonies amplified with primers F1 and P2R8. Lane B, 2 represents the wild type *H. influenzae*; Lane B, 3 shows a band amplified from one of the putative mutant *H. influenzae* colonies; Lane C, 2 shows the amplified fragment from wild type *H. influenzae*; Lanes C, 3-5 are the amplified fragments from loop 2-mutated *H. influenzae* colonies. Molecular marker size in kb is shown in the lane 1.

For further confirmation of the mutagenesis primers mP2F and mP2R (both external to the mutagenic amplicon) were employed (Figure 4.10B). Amplicons of 4.1-kb for the mutated colonies and 3.2-kb for the wild type bacteria were obtained, confirming the insertion of the kanamycin resistance cassette. To determine the orientation of the kanamycin gene a PCR screen using the primers mP2F and Kan_CTR (C-terminal primer of the kanamycin cassette) was employed (Figure 4.10C). This showed that the kanamycin resistance cassette was

inserted in the reverse orientation on a chromosome with respect to the orientation of *ompP2* (Figure 4.10A).

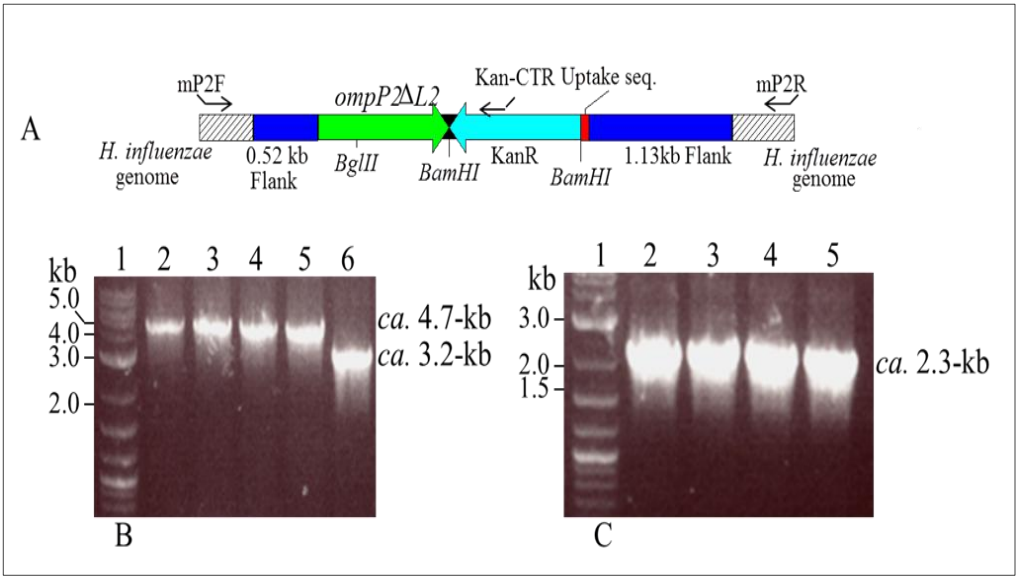

Figure 4.10. PCR analysis of mutated *H. influenzae* using mP2F and mP2R primers or mP2_F and Kan_CTR primers. (A) Schematic diagram showing the PCR reaction. Agarose gel electrophoresis analysis demonstrating PCR-amplified fragments with natural-transformed *H. influenzae* DNA, (B) mP2F and mP2R primers were used. Lane 6 is wild type. Lanes 2 to 5 are the mutated *H. influenzae* colonies. (C) mP2F and Kan_CTR primers were used. Lanes 2 to 5 are the PCR-fragments amplified from the loop 2 mutated *H. influenzae* colonies. Molecular marker size in kb is shown in the lane 1 of panels A and B.

To confirm the deletion of the loop 2-encoding region in the mutated cells the 2.267 kb amplicon amplified using primers mP2F and Kan_CTR was digested using *Bgl*II (a *Bgl*II site was incorporated after deletion the loop 2). Two fragments of *ca.* 1.26 and 1.0 kb were obtained (Figure 4.11) confirming that the loop 2-encoding region had been deleted in the mutated *H. influenzae*. The fragment amplified using primers mP2_F and Kan_CTR using DNA from the putatively mutated colony DNA was sequenced and shown to carry the intended

sequence which includes *ompP2* minus the second loop encoding region and the kanamycin resistance cassette.

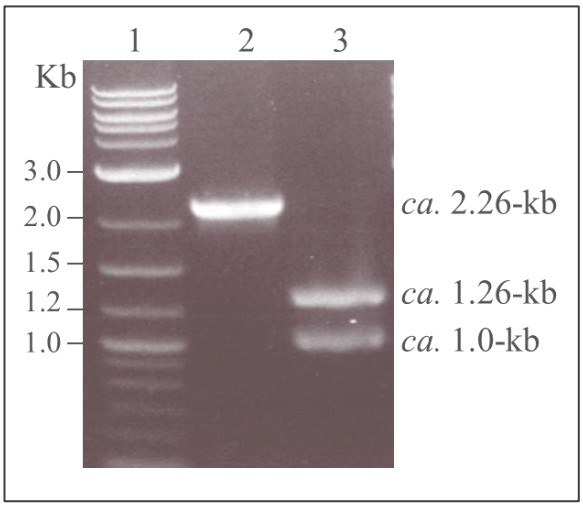

Figure 4.11. Agarose gel analysis showing the digested amplicon from the mutated *H. influenzae* DNA. Lanes: 1, 2kb DNA marker; 2, 2.267 kb fragment amplified using mP2_F and Kan-CTR; 3, digested amplicon with *Bgl*II, which yielded 2 bands corresponding to 1.26 and 1.0 kb.

4.2.5 OmpP2 Expression in the Wild type *H. influenzae* and Loop 2-Deleted Mutant

Expression of the OmpP2 protein in the loop 2-deleted *H. influenzae* (*ompP2ΔL2*) was analysed by SDS-PAGE. Overnight cultures of wild type, *ompP2ΔL2* and the *ompP2* deletion mutant grown in BHI broth overnight at 37°C and whole cell lysates analysed by SDS-PAGE. Bands corresponding to OmpP2 were observed in wild type and *ompP2ΔL2 H. influenzae*, but not in the negative control *ΔompP2 H. influenzae* (Figure 4.12A). Lysates were also analysed by immunobolotting and probed with anti-OmpP2 antibody. Bands corresponding to OmpP2 were only seen in the wild type and OmpP2ΔL2 extracts (Figure 4.12B).

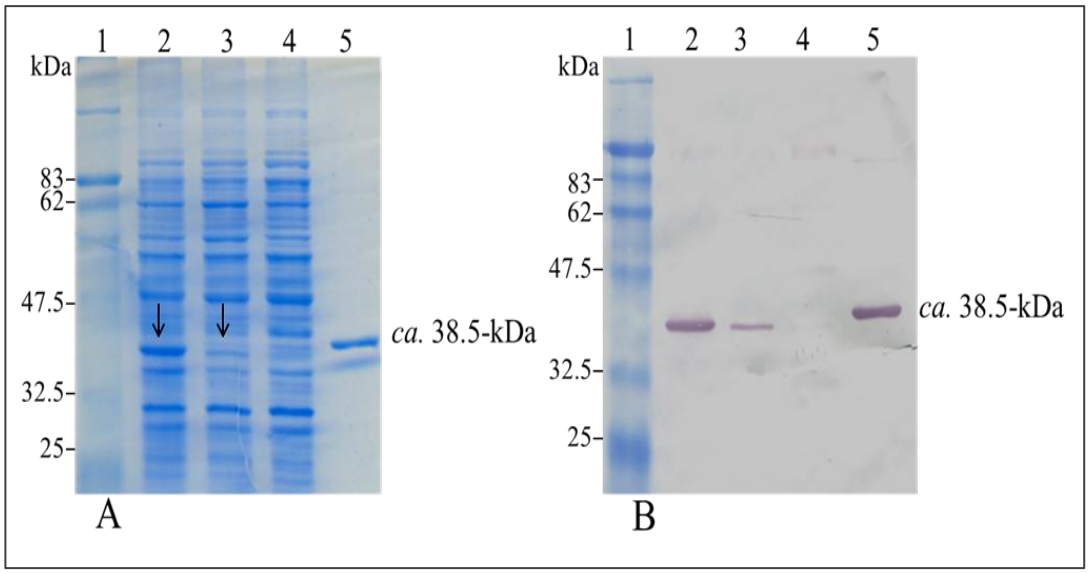

Figure 4.12. Expression of mutated OmpP2. (A) SDS-PAGE analysis of whole cell lysates from the mutated *H. influenzae*. Lane 1, Broad range protein marker (6-175 kDa); lane 2, Wild-type *H. influenzae*; lane 3, OmpP2ΔL2 mutant; lane 4, ΔOmpP2 mutant; lane 5, purified recombinant OmpP2. Arrows in panel A indicate the position of the OmpP2 protein. (B) Immunoblot of lysates as described for panel A and probed with anti-OmpP2 antibody. A band corresponding to OmpP2 is seen in wild type and OmpP2ΔL2 lysates, and purified OmpP2 only.

To determine whether the mutant and wild type OmpP2 proteins were expressed at similar levels, samples of whole cell lysates were taken at various times (7, 10.5 and 15 h of the growth; log and stationary phase) and analysed by SDS-PAGE (Figure 4.13). Expression of the OmpP2 derivative lacking loop 2 (Ala91-Phe99) was lower by comparison with expression of the wild type protein at each time point.

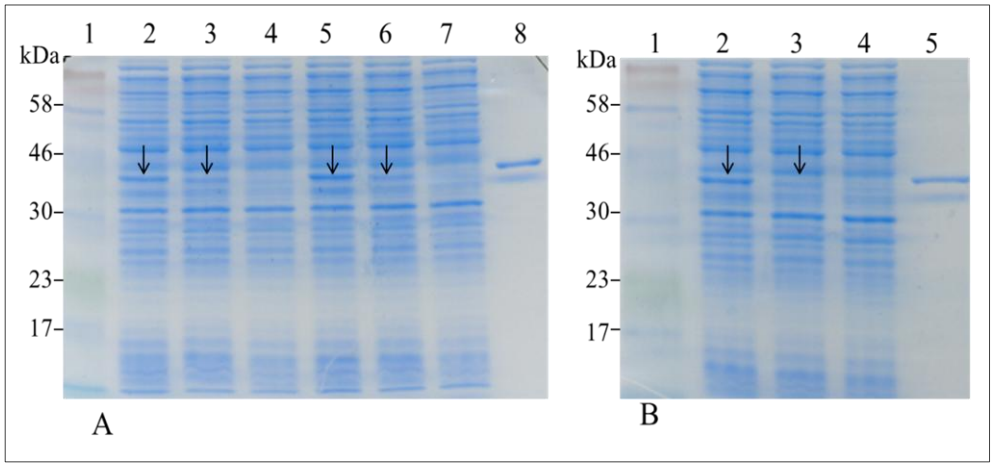

Figure 4.13. SDS- PAGE showing expressed OmpP2 in *H. influenzae*. (A) lanes 2-4 the 7 h cells culture of wild type, OmpP2ΔL2 mutant and ΔOmpP2 mutant respectively; 5-7, the 10.5 h cells culture of wild type, OmpP2ΔL2 mutant and ΔOmpP2 mutant respectively; (B) lanes 2-4, the 15 h cells culture of wild type, OmpP2ΔL2 mutant and ΔOmpP2 mutant respectively; 8 (A) and 5 (B) purified recombinant OmpP2 from *E. coli* JM109. A 36-42 kDa band corresponding to OmpP2 is seen in wild type, OmpP2ΔL2 lysates and purified OmpP2 only. The arrows indicate the position of the OmpP2 protein. Lane 1 in panel A and B, protein marker.

4.2.6 Construction of Mutants with Similar Levels of Protein Expression

OmpP2ΔL2 mutant was introduced in the *H. influenzae.* However, the amount of the expressed OmpP2ΔL2 protein was lower compared to the expression levels of OmpP2 in the wild type. This might be due to the fact that the orientation of the kanamycin resistance gene in the chromosome was in the opposite orientation of the *ompP2*. For this reason, the kanamycin resistance cassette was replaced with the Omega cassette, which encodes resistance to spectinomycin and streptomycin and is transcriptionally isolated as the resistance gene is flanked by transcription termination signals. Two plasmids pMSA13 and pMSA14 were derived from the

two previously designed plasmids pMSA10 and pMSA12 respectively. Plasmids pMSA10 and pMSA12 digested with *Bam*HI to eliminate kanamycin resistance cassette (Figure 4.14A). Digested plasmids were extracted from the gel and the purified bands were analysed on gel electrophoresis (Figure 4.14B). pMSA10 and pMSA12 products were extracted from the gel, dephosphorylated and ligated to the Omega cassette, which was obtained from *Bam*HI-digested pKG130 vector (Figure 4.15 C and D).

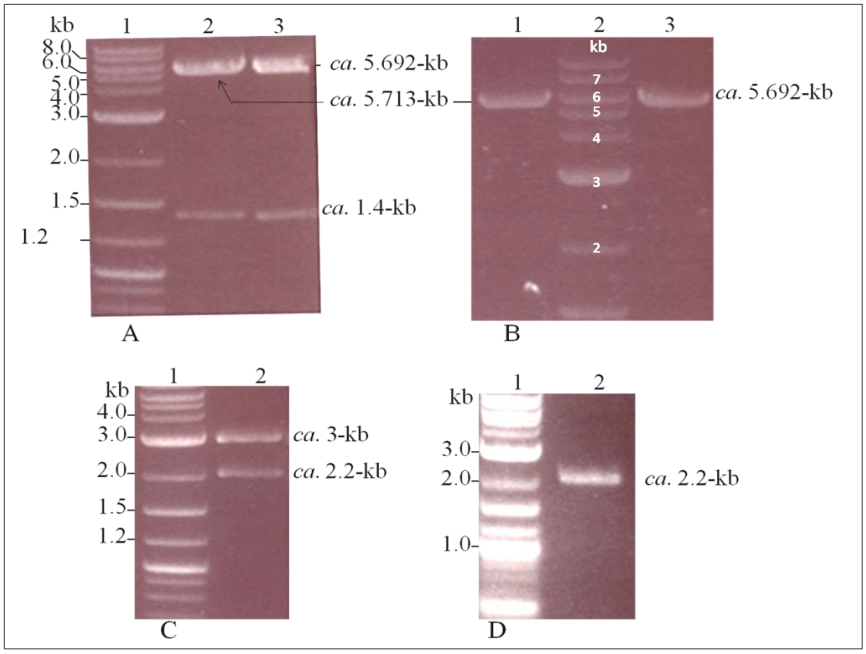

Figure 4.14. Construction of the mutagenic plasmids pMSA13 and pMSA14. Agarose gel analysis of (A) *Bam*HI-digested plasmids. Lane 2, digested pMSA10 to yield 5.713 kb and 1.4 kb (kanamycin resistance gene). Lane 3, digested pMSA12 to yield 5.692 kb and 1.4 kb (kanamycin resistance gene). (B) gel extracted fragments. Lanes: 1, the 5.713 kb released from *Bam*HI digested pMSA10. 3, the 5.692 kb fragment released from *Bam*HI-digested pMSA12. (C) *Bam*HI-digested pKG130 vector. Lane 2 digested pKG130 vector to yield 3 kb and 2.2 kb (Omega cassette). (D) gel extracted Omega cassette. 2-kb DNA marker is shown in lane 1 in panels A, C and D and in lane 2 in panel B.

*Bam*HI-digested pMSA10 and pMSA12 were ligated with the Omega cassette and named pMSA13 and pMSA14 respectively. *E. coli* cells were transformed with pMAS13 and pMSA14, isolated colonies were screened by PCR utilising P2Δ5-8I_F and R2 primers (Figure 4.15).

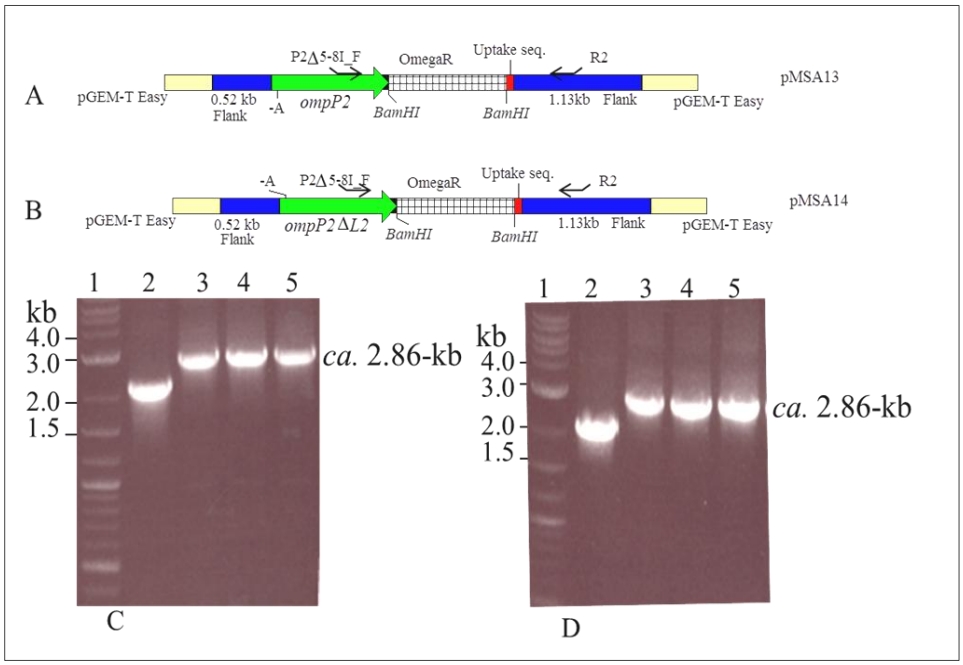

Figure 4.15. PCR analysis of pMSA13 and pMSA14. Schematic diagram demonstrating the PCR-amplified fragments from (A) pMSA13 (the 3-kb pGEM-T easy, the 2.2-kb Omega cassette and the. 1.1-kb *ompP2* plus *ca.* 0.52 kb upstream and *ca.* 1.1 kb downstream flanking region and (B) pMSA14 (the 3-kb pGEM-T easy, the *ca.* 2.2-kb Omega cassette and the 1.07-kb *ompP2ΔL2* plus *ca.* 0.52 kb upstream and 1.1 kb downstream flanking region) using primers P2Δ5-8I_F and R2. Both pMSA13 and pMSA14 plasmids were derived from pMSA10 and pMSA12 respectively by replacing kanamycin resistance cassette with Omega resistant cassette. Agarose gel electrophoresis demonstrating amplified PCR-fragments using primers P2Δ5-8I_F and R2 with pMSA13 (C) and pMSA14 (D). Panels: C, lanes 3-5 are PCR products of colonies transformed with pMSA13. B, lanes 3-5 are PCR products of transformed colonies with pMSA14. pMSA10 and pMSA12 used as control and are shown in the lane 2 in both A and B respectively. 2-kb DNA marker is shown in lane 1 in both panels.

pMSA13 and pMSA14 were confirmed by sequencing and the missing adenine nucleotide (known to be missing from their parent plasmids) was again corrected by site-directed mutagenesis using a mega primer approach as described above. Mutagenesis fragments were amplified using mega primer and mP2R (Figure 4.16). The amplified fragments were gel-extracted and used to transform *H. influenzae* by natural transformation. Several attempts to transform *H. influenzae* using these amplicons were unsuccessful.

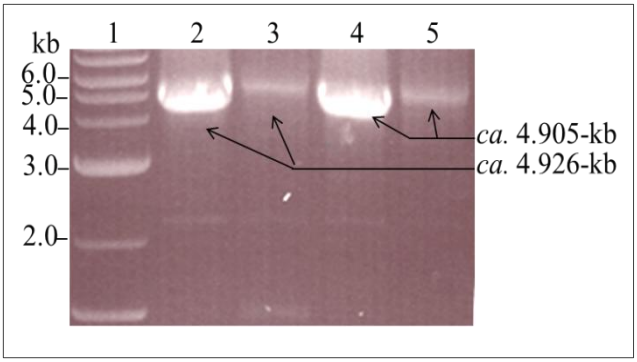

Figure 4.16. Gel agarose electrophoresis of the PCR products amplicons of pMSA13 and pMSA14. Lanes: 2, F1 and P2FR primers with pMSA10 template (control). 3, mega and P2FR primers with pMSA13. 4, F1 and P2FR primers with pMSA12 template (control). 5, using mega and R2 primers with pMSA14. 2 kb DNA marker is shown in lane 1.

4.2.7 Correct the Orientation of Kanamycin Resistance Cassette: Construction of Plasmids pMSA15 and pMSA16

Due to the fact that attempts to transform *H. influenzae* with plasmids pMSA13 and pMSA14, which contain the Omega cassette for selection, were unsuccessful, we aimed to produce mutants using the kanamycin resistance cassette, but in which the resistance gene was in the same orientation as the mutated gene. For this purpose, pMSA10 and pMSA12 plasmids, which were already prepared, were

employed. Kanamycin resistance cassettes were released from pMSA10 and pMSA12 using *Bam*HI restriction enzyme (Figure 4.17).

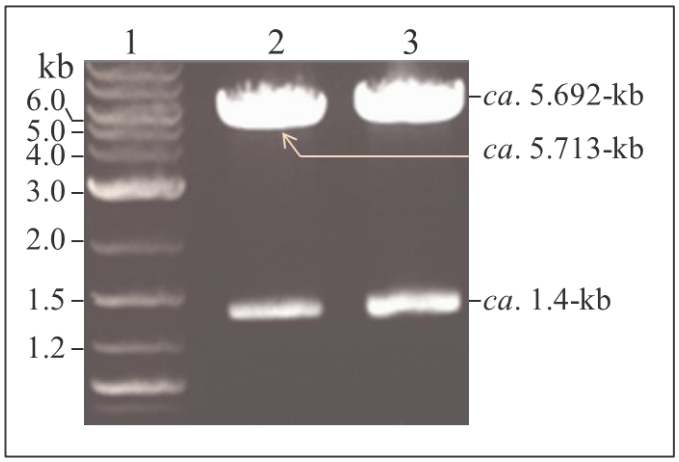

Figure 4.17. Agarose gel analysis of *Bam*HI-digested pMSA10 and pMSA12 plasmids. 2-kb DNA marker is shown in lane 1. Lane 2, digested pMSA10 to yield 5.713 kb and 1.4 kb (kanamycin resistance cassette). Lane 3, digested pMSA12 to yield 5.692 kb and 1.4 kb (kanamycin resistance cassette).

The resulting digests were re-ligated with kanamycin resistance cassette and used to transform *E. coli* JM109. Putative positive transformants were subjected to PCR analysis using F1 and mP2R primers then were selected and plasmids were extracted and designated pMSA15 and pMSA16 (Figure 4.18).

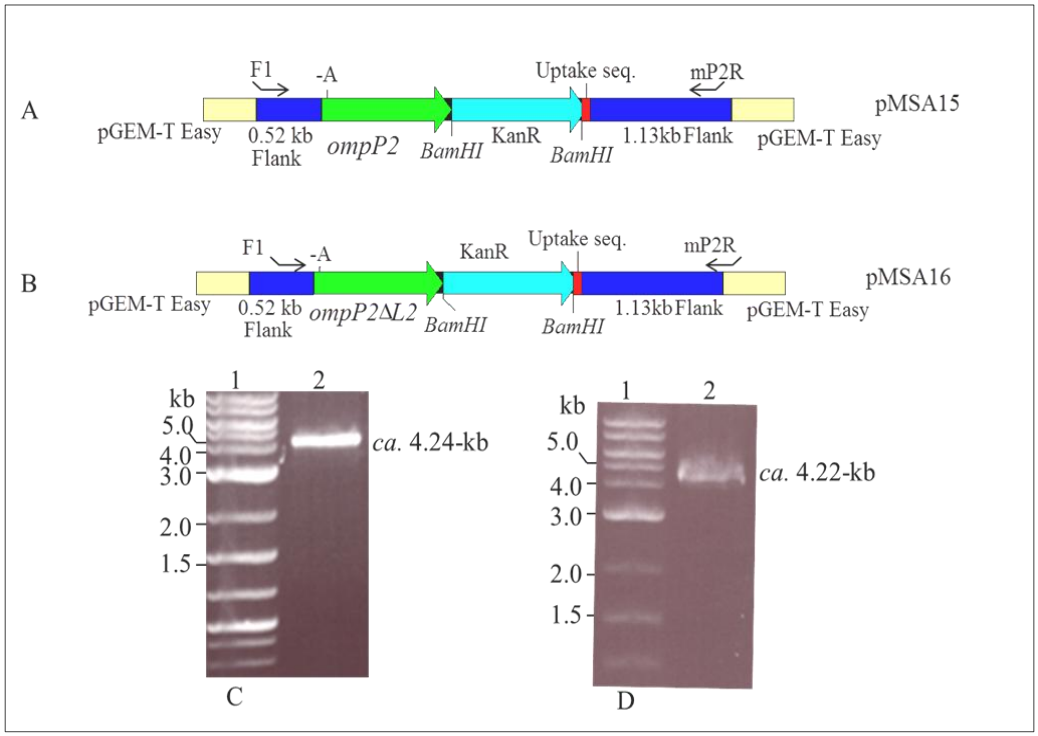

Figure 4.18. PCR analysis of pMSA15 and pMSA16 transformed into *E. coli* JM109. Schematic diagram showing the PCR-amplified using F1 and mP2R primers from pMSA15 (A) and pMSA16 (B). Gel electrophoresis analysis of PCR-amplified fragment by using F1 and mP2R primers from pMSA15 (4.240 kb) is shown in panel (C), and from pMSA16 (4.220 kb) is shown in panel D. pMSA15 and pMSA16 were derived from pMSA10 and pMSA12 respectively, in which kanamycin resistance cassettes orientation were corrected. 2-kb DNA marker is shown in the left.

The transformants were then scanned using PCR for the desired orientation of the kanamycin resistance cassette and plasmids in which the cassette was in the correct orientation. Colonies containing plasmids in which the resistance cassette was inserted in the desired orientation were identified and plasmids were isolated and designated as pMSA15 (3-kb pGEM-T easy, *ca.* 1.5-kb kanamycin resistance cassette and the *ompP*2 plus 0.52-kb upstream and 1.113-kb downstream flanking regions) and pMSA16 (3-kb pGEM-T easy, 1.5-kb kanamycin resistance cassette

and the *ompP2ΔL2* plus 0.52-kb upstream and 1.113-kb downstream flanking regions) (Figure 4.19).

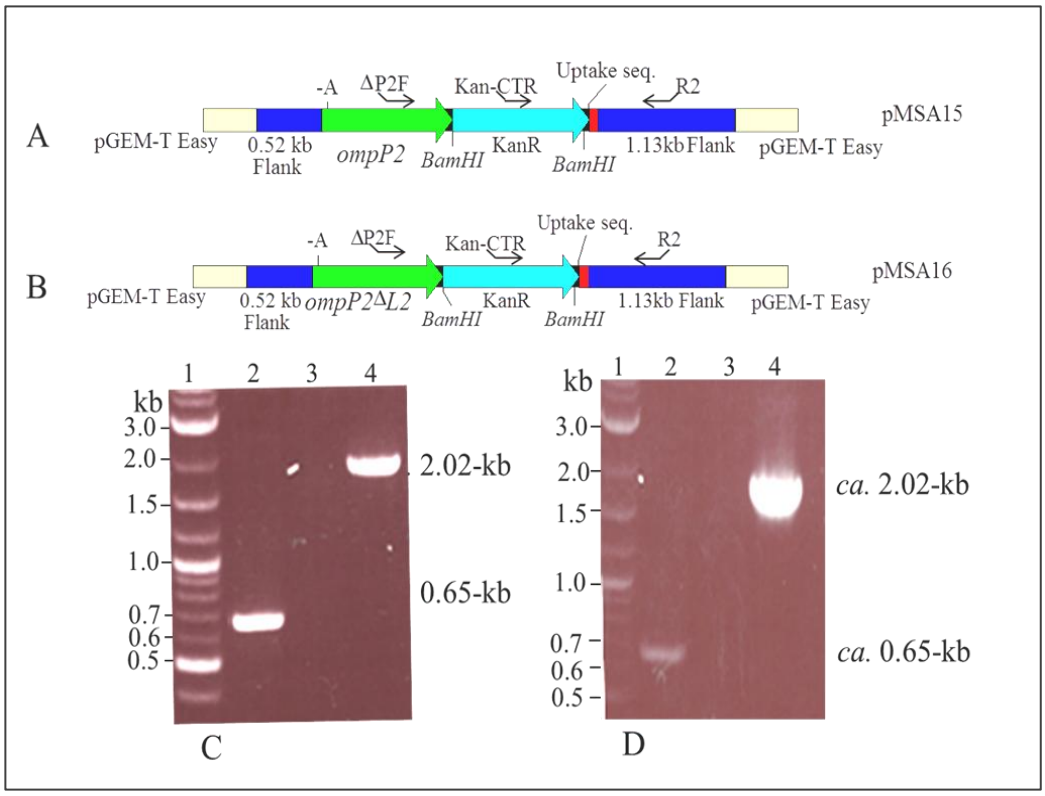

Figure 4.19. PCR analysis of the kanamycin resistance cassette orientation of pMSA15 and pMSA16. Schematic diagram representing the PCR-amplified fragments using primers ΔP2F, Kan_CTR and R2 with pMSA15 plasmid (A) and with pMSA16 plasmid (B). Agarose gel analysis of PCR products for different primers with pMSA15 (C) and pMSA16 (D). Lane 2, Kan_CTR and R2 (*ca.* 650 bp), lane 3, Kan_CTR and ΔP2F (no products for positive result), lane 4, R2 and ΔP2F (*ca.* 2377 bp). 2-kb DNA marker is shown in lane 1 in A and B.

4.2.8 Insertion of Single Adenine Nucleotide in the Constructs pMSA15 and pMSA16 Using Mega Primer

The data from the PCR analysis and DNA sequencing indicated that the screened colonies harboured the desired construct with the kanamycin resistance cassette in

the same orietation as *ompP2*. However, the constructs obtained from the plasmids pMSA15 and pMSA16 were missing a single adenine within the open reading frame (ORF) of the *ompP2*. Hence, a single adenine nucleotide was re-inserted in the constructs pMSA15 and pMSA16 by PCR using the mega primer (0.54-kb) in the PCR as a forward primer with the mP2R reverse primer (Figure 4.20).

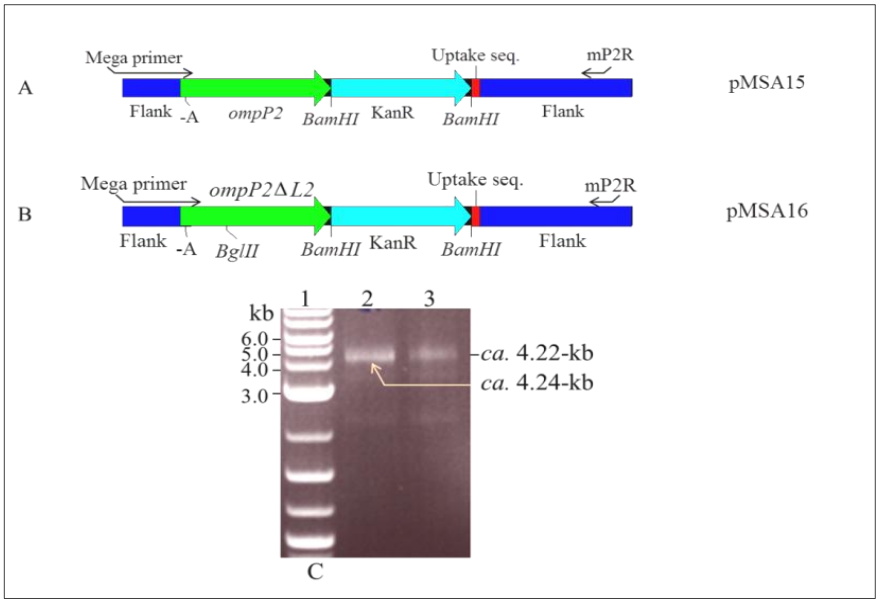

Figure 4.20. Insertion of single adenine nucleotide in the constructs pMSA15 and pMSA16 using mega primer. Schematic diagram showing PCR-amplified fragments using mega and mP2R primers from pMSA15 (A) and pMSA16 (B). 2-kb DNA marker is shown in the lane 1. (C) Agarose gel electrophoresis showing the PCR analysis using mega and mP2R primers with pMSA15 (lane 2, *ca.* 4.240 kb) and with pMSA16 (lane 3, *ca.*4.220 kb). 2-kb DNA marker is shown in the lane 1.

Next, the corrected constructs were used to mutate loop 2 *in vivo* in *H. influenzae* as well as to insert the kanamycin resistance cassette into the wild type *H. influenzae* in order to generate an appropriate control isolate. The constructs

which were amplified and corrected by mega primer were used as template for PCR to amplify the mutagenic fragments using F1 and P2FR (Figure 4.21).

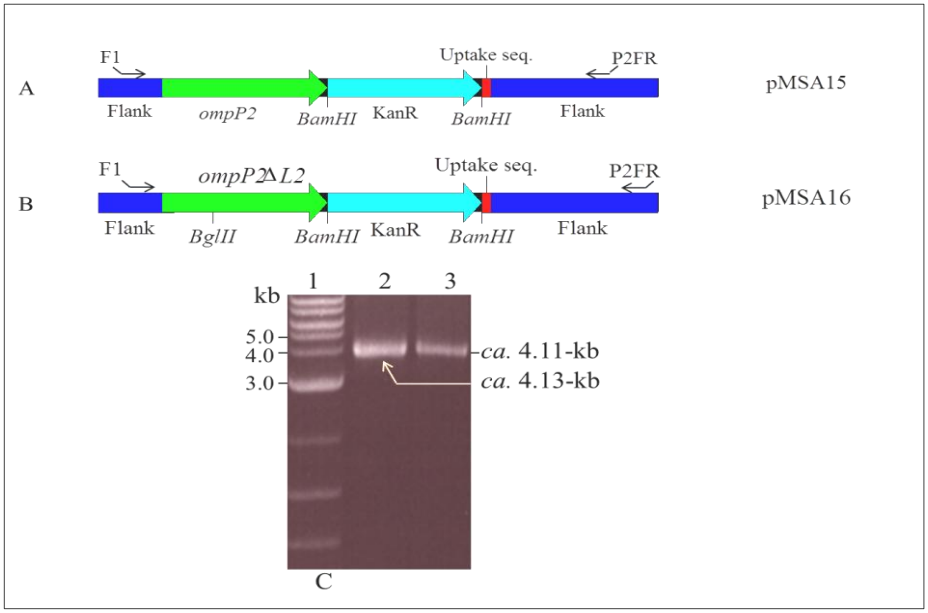

Figure 4.21. Amplifying mutagenic fragments from pMSA15 and pMSA16 using F1 and P2FR. Schematic diagram representing the amplified fragment by the PCR using F1 and P2FR primers from corrected pMSA15 (A) and pMSA16 (B). (C) Agarose gel analysis of PCR-amplified amplicon fragments using F1 and P2FR primers. Lane 2, *ca.* 4.110 kb fragment amplified from corrected pMSA15, lane 3, 4.110 kb fragment amplified from corrected pMSA16. 2-kb DNA marker is shown in the left.

4.2.9 Generation of OmpP2ΔL2 Mutants in *H. influenzae* Rd KW20 Cells

H. influenzae cells were naturally transformed with the 4.13 or 4.11-kb fragment (Figure 4.22). The mutagenic fragment (4.110-kb; derived from corrected pMSA16) was used to delete loop 2 of the *ompP2* and incorporate the kanamycin resistance cassette into the genome. The other amplified mutagenic fragment (4.130-kb; derived from corrected pMSA15) was used to insert the kanamycin

resistance cassette in the genome generating a control isolate. Putative transformant colonies were PCR-screened for the existence of the desired insert utilising primers F1 and P2FR (Table 2.1) as shown in figure 4.22A. Further checking for the deleted loop 2, was done by digestion reaction of amplified PCR products using *Bgl*II (Figure 4.22B).

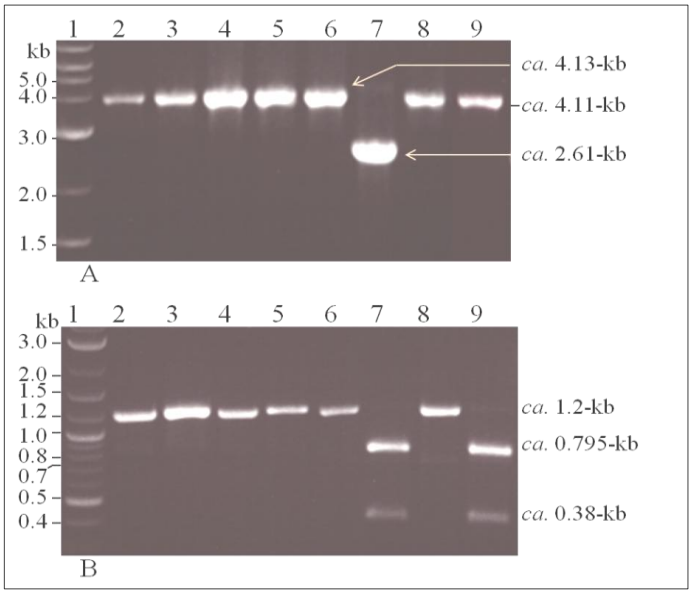

Figure 4.22. PCR and restriction digestion analysis of mutated *H. influenzae*. (A) PCR products of transformed *H. influenzae* with primers F1 and P2FR. Lanes 2-6: 4.130-kb PCR products of transformed *H. influenzae*, into which the kanamycin resistance cassette was inserted. Lane 7 shows the 2.615-kb PCR product of wild type cells. Lanes 8-9: 4.110 kb-PCR products of transformed cells, into which the kanamycin resistance cassette was inserted and loop 2 encoding region of *ompP2* was deleted. (B) *Bgl*II-digested PCR product amplified from deleted loop 2 *H. influenzae* using F1 and P2Δ5-8I_R primers. Lanes 2, 4, 6, 8: 1.2-kb fragment of PCR product of colonies 1, 2, 3, and 4, respectively, before digestion reaction. Lanes 3, 5, 7 and 9 are *Bgl*II-digested PCR product using F1 and P2Δ5-8I_R primers of colonies 1, 2, 3, 4, respectively, which yielded 2 bands: 759 and 380 bp (just colonies 3 and 4; lanes 7, 9; give positive result). 2-kb DNA markers are shown in the left.

4.2.10 Creation of a New Negative Control of *ompP2* Mutant

In order to generate a new *ompP2 H. influenzae* Rd KW20 mutant, that contains kanamycin resistant cassette, a new primer was designated: ΔP2F, and used with P2Δ2I_R primer in inverse PCR with the plasmid pMSA15 as template. This PCR resulted in deletion of approximately 796 bp of the *ompP2* gene from the start codon and amplification of a 6.4-kb amplicon (Figure 4.23). The IPCR product was gel-extracted, *Bgl*II-digested and self-ligated and used to transform *E. coli* JM109 cells. Putative transformants were selected and analysed by PCR (Figure 4.23C). The resulting plasmid was designated pMSA17.

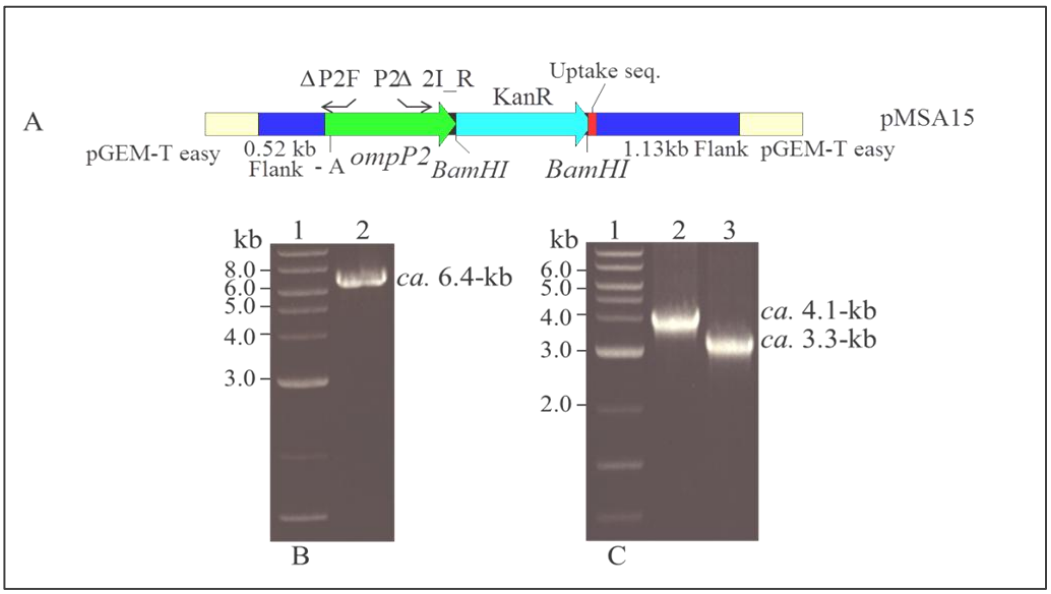

Figure 4.23. Generation of pMSA17 plasmid from pMSA15 by IPCR. (A) Schematic diagram demonstrating IPCR of the P2Δ2I_R and ΔP2F primers with pMSA15 plasmid. (B) Agarose gel electrophoresis of the IPCR product of pMSA15 plasmid. The 6.445 kb reaction products of a PCR using P2Δ2I_R and ΔP2F primers is shown in lane 2. (C) Agarose gel analysis of the PCR product using the primers F1 and P2FR. Lane 2: 4.130-kb fragment of PCR product of the plasmid pMSA15 (control); Lane 3: 3.334-Kb fragment of the PCR product of the plasmid pMSA17 transformed into *E. coli* JM109. Molecular mass markers are shown in lane1.

The band produced using F1 and P2FR primers using plasmid pMSA17 as a template (Figure 4.23C, lane 3) corresponding to the expected size of *ca.* 3.33-kb was extracted and used to transform *H. influenzae* cells to delete the *ompP2* region and introduce the kanamycin resistance cassette by natural transformation. DNA sequencing and PCR using F1 and Omg_R primers (Figure 4.24A and B) were used to confirm the mutagenesis (Figure 4.24C and D).

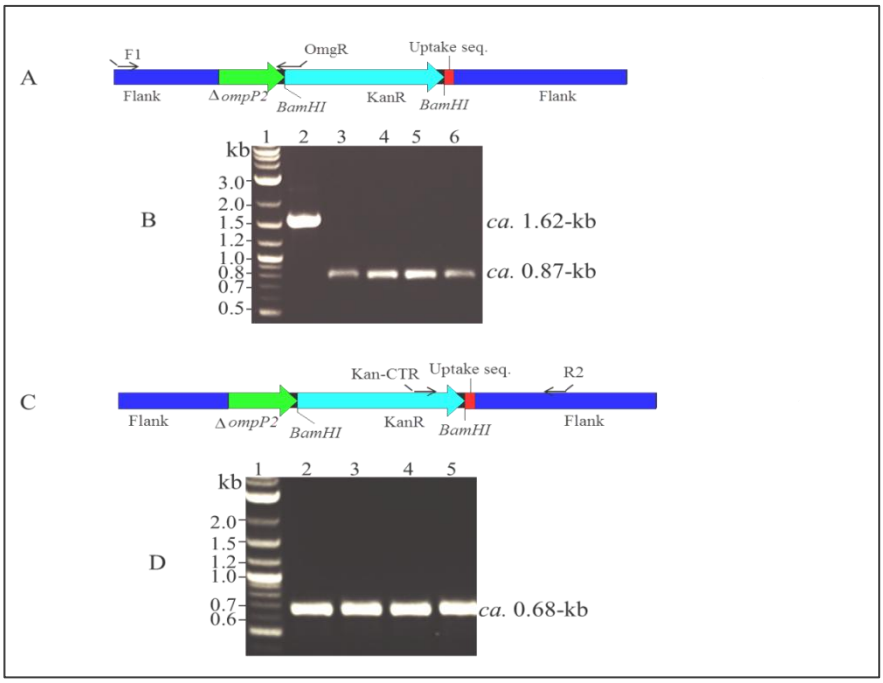

Figure 4.24. PCR analysis of knout-out ompP2 *H. influenzae*. PCR- amplified fragment of the mutated *H. influenzae* cells using F1and Omg_R primers (A) schematic diagram (B) Agarose gel analysis. Lane 2, fragment amplified from wild type *H. influenzae* cells (*ca.* 1.623 kb). Lane 3-6, fragments amplified from *ompP2* mutated cells (872 bp). (C) Diagrammatic representation of the amplified fragment of the *ompP2* mutated *H. influenzae* cells by the PCR using kan_CTR and R2 primers. (D) 1% agarose gel analysis of the PCR products of the *ompP2* mutated *H. influenzae* cells using Kan_CTR and R2 primers. Lane 2-5, fragment amplified from putative *ompP2* mutated *H. influenzae* cells. 2-kb DNA marker is shown in the lane 1 in B and C.

The mutation of *ompP2* was confirmed by SDS-PAGE and immunoblotting of whole cell lysates (Figure 4.25). Bands corresponding to OmpP2 were only seen in the wild type, *ompP2::kanR* and *ompP2ΔL2* extracts indicating that the OmpP2 is expressed in the wild type, *ompP2::kanR* and *ompP2ΔL2* but not in the Δ*ompP2* mutant. The expression levels of OmpP2 and OmpP2ΔL2 were similar. Moreover, there were no apparent differences in expression of other proteins in the generated mutants.

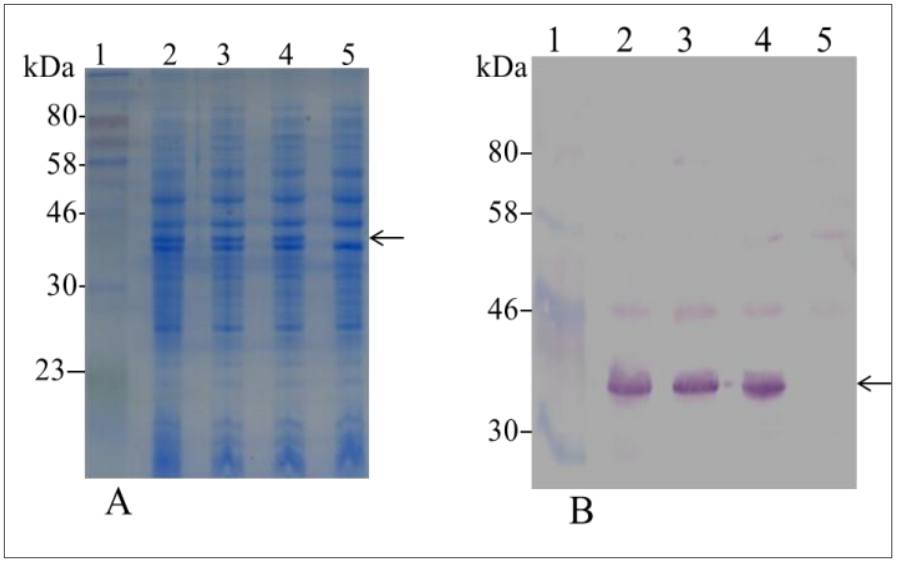

Figure 4.25. Expression of OmpP2 and OmpP2ΔL2. (A) SDS-PAGE analysis of whole cell proteins from the *H. influenzae* wild type and mutant strains. Lane 2: Wild-type; lane 3: *ompP2::kanR*; Lane 4: *ompP2ΔL2* mutant; lane 5: Δ*ompP2* mutant. (B) Immunoblot of *H. influenzae* cell lysates probed with anti-OmpP2 antibody. Lanes as for panel A. A *ca.* 36-42 kDa band corresponding to OmpP2 is seen in wild type, *ompP2::kanR*, OmpP2ΔL2 lysates only. Broad range protein marker (6-175 kDa) is shown in lane 1 in A and B. The arrows indicate the position of the OmpP2 protein.

4.2.11 Growth Characteristics of *H. influenzae* and Its Mutant Derivatives

Comparison of the *in vitro* growth of *H. influenzae* and its derivative mutants in liquid culture was performed before further analysis of the mutant strains. The wild-type *H. influenzae*, Δ*ompP2*, *ompP2*Δ*L2* and *ompP2::KanR* mutant strains were grown in BHI broth with an equal starting OD600. Growth curves were plotted based on the measurement at OD600 of samples that were removed from the culture at hourly intervals. Growth rates of the mutants were not substantially different to that observed for the wild-type *H. influenzae* strain (Figure 4.26).

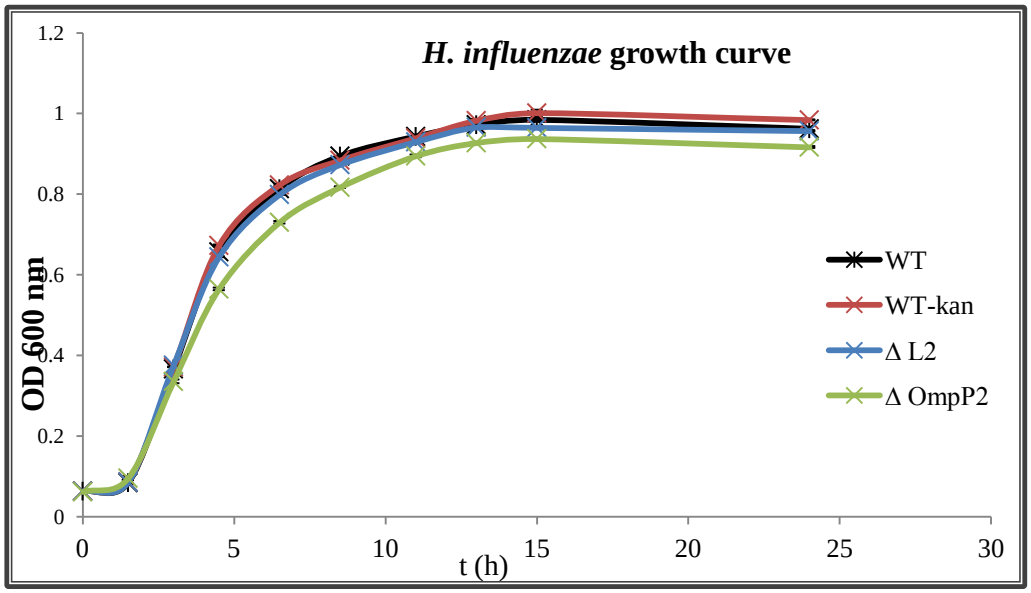

Figure 4.26. Comparison of the rate of *ompP2*Δ*L2* (ΔL2), Δ*ompP2*, *ompP2::kanR* mutants compared to the wild-type. Cultures were grown at 37°C in 15-ml tubes with vigorous aeration and OD_{600} reading was taken at hourly intervals for 24 h. Mean values from triplcate cultures are plotted.

4.2.12 OmpP2ΔL2 is Correctly Localised to the Outer Membrane

OmpP2 is an outer membrane protein that is transported from the cytoplasm across the inner membrane via the *sec* secretion system into the periplasm before reaching its final destination in the outer membrane. To investigate the sub-cellular localisation of OmpP2ΔL2 in *H. influenzae*, a previously described method of cell fractionation was used to separate inner and outer membrane fractions and the sub-cellular location of OmpP2 determined by immunoblotting using anti-OmpP2 antibody (Figure 4.27). Bands corresponding to OmpP2 or its mutant derivatives were seen in outer membrane fractions of wild type and OmpP2ΔL2 *H. influenzae*, respectively, but not in the *ompP2*-mutant. Furthermore, no bands were seen in the inner membrane fraction of any of these cells.

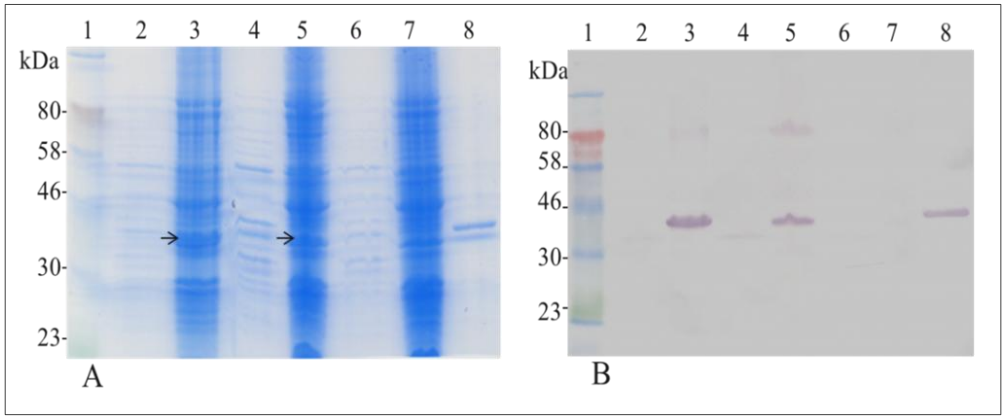

Figure 4.27. Localization of OmpP2ΔL2 in *H. influenzae*. SDS-PAGE (A) and immunoblot (B) of *H. influenzae* cell fractions. Lane 1: Broad range protein marker (6-175 kDa); lane 2- 3: IM and OM-enriched fractions, respectively, of Wild-type; lane 4-5: IM and OM-enriched fractions, respectively, of *ompP2ΔL2* mutant; lane 6-7: IM and OM-enriched fractions, respectively, of Δ*ompP2* mutant; lane 8, purified OmpP2. A 36-42 kDa band corresponding to OmpP2 is seen in OM fractions of wild type, OmpP2ΔL2 and purified OmpP2 only. The arrows indicate the position of the OmpP2 protein.

4.2.13 Interaction of *H. influenzae* and Its Derivative Mutants with Laminin Receptor

To investigate the interaction of wild-type *H. influenzae* Rd KW20 and the constructed mutants (*H. influenzae ompP2::kanR*, *H. influenzae ompP2*Δ*L2* and *H. influenzae* Δ*ompP2*) with LamR, bacteria cells were DIG-labelled and utilised in ELISA. rLRP-binding by *H. influenzae ompP2*Δ*L2* was significantly reduced compared to the wild-type ($p < 0.01$), albeit the reduction in rLRP-binding was not as great as that observed for the control strain lacking OmpP2 (Figure 4.28), perhaps indicating that additional residues of OmpP2 may play a role in optimizing rLRP-binding. The control strain with an antibiotic cassette inserted at the *ompP2* locus, but no modification to the *ompP2* coding sequence, showed no significant reduction in rLRP-binding, thus confirming the direct effect of removing or truncating *ompP2* on binding.

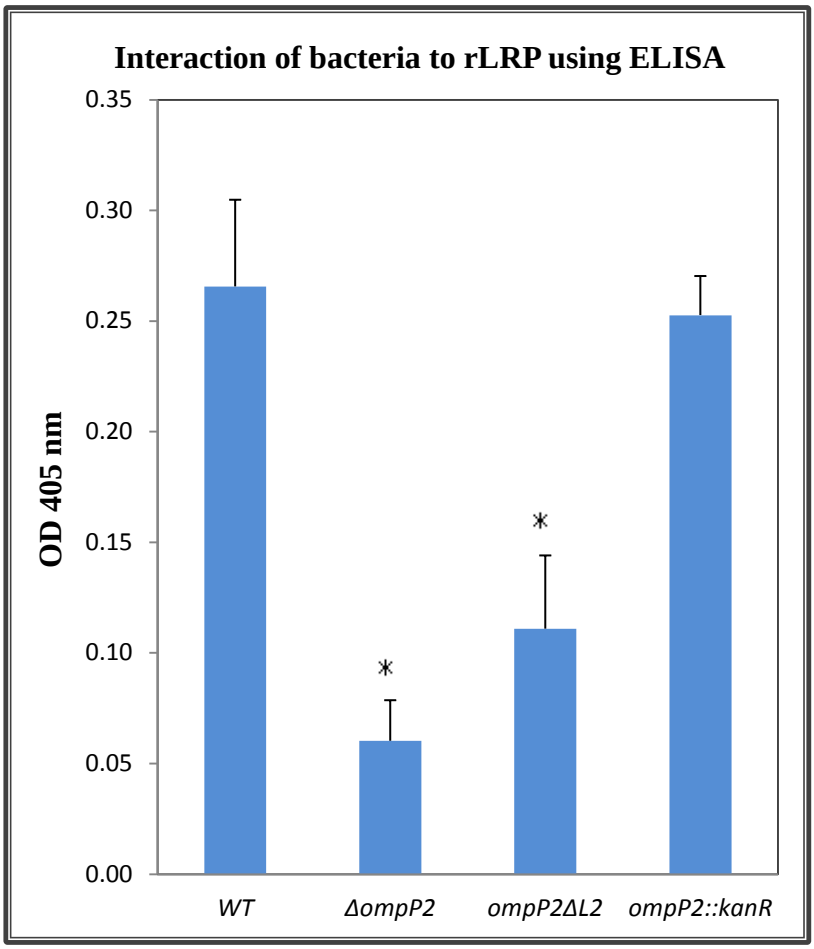

Figure 4.28. Deletion of OmpP2 loop 2 significantly reduces bacterial rLRP-binding. Binding of *H. influenzae* (WT), *H. influenzae* Δ*ompP2* (*ΔompP2*), *H. influenzae ompP2ΔL2* (*ompP2ΔL2*) or *H. influenzae ompP2::kanR* (*ompP2::kanR*) to rLRP. Specific binding of digoxigenin-labeled bacteria to rLRP-coated ELISA plates was determined by subtracting the absorbance in BSA-coated wells from that in rLRP-coated wells. Data shown are means from three independent experiments; in each experiment each sample was tested in triplicate. * $p < 0.01$ compared to wild-type. Error bars indicate SE.

To further investigate the interaction of wild type *H. influenzae* and its derivative mutants with rLRP, flow cytometry was employed using bacterial cells harvested during the logarithmic phase of growth. The rLRP was stained with fluorescein using Lightning-Link™ Atto680 Conjugation Kit (section 2.16). As an additional

control, wild type and Δ*porA*Δ*pilQ* double knock out *N. meningitidis* MC58 mutant cells were also examined using the same conditions. The combination of treated and non-treated cells with stained rLRP, demonstrated a clear difference in rLRP binding between wild-type cells and the mutants Δ*ompP2* and *ompP2*ΔL2 (Figure 4.29).

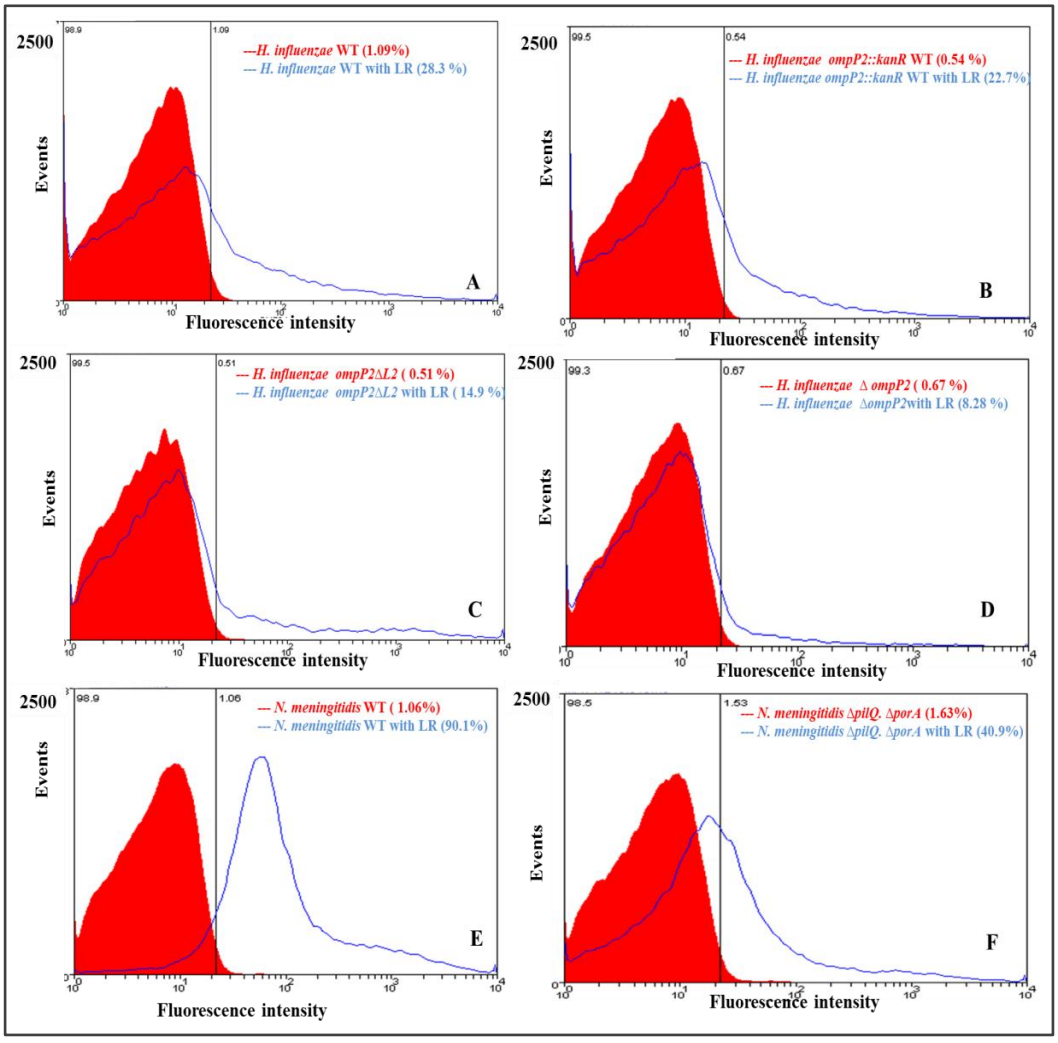

Figure 4.29. Flow cytometry analysis of treated and non-treated strains with fluorescein-conjugated rLRP. Panels A, *H. influenzae* wild-type. B, *H. influenzae ompP2::kanR*. C, *H. influenzae ompP2ΔL2.* D, *H. influenzae* Δ*ompP2*. E, *N. meningitidis* wild-type. F, *N. meningitidis* Δ*porA*Δ*pilQ*. Cells were incubated with fluorescein-conjugated rLRP or without rLRP (control). Mid-log phase bacterial samples were washed with PBS and adjusted to 2×10^7 CFU ml^{-1} aliquots. After centrifugation, fluorescein-conjugated rLRP was added (untreated cells were used as a control). After being incubated, the samples were washed with FACS buffer and finally samples were fixed in 1 ml PBS containing 0.5% formaldehyde. Samples were analysed for fluorescence using a Coulter Altra Flow Cytometer. The cells were detected using forward and log-side scatter dot plots, and a gating region was set to exclude cell debris and aggregates of bacteria. A total of 50, 000 bacteria (events) were analysed for fluorescence signals. The population of fluorescently labeled cells was displayed as a histogram.

Binding to rLR, expressed as the percentage of labeled cells exhibiting greater fluorescence than the cutoff, varied between the bacterial cell populations: 28.4% of the wild type *H. influenzae* bound to rLRP, which was approximately similar to the level observed in control cells in which the kanamycin resistance cassette had been inserted downstream of an intact *ompP2* gene (*H. influenzae* mutant, *ompP2::kanR*), of which 22.7% bound rLRP. The cutoff was set such that less than 2% of the unlabeled population of cells were recorded. The percentages of the cells were much lower for the *H. influenzae ompP2ΔL2* and *H. influenzae* Δ*ompP2* (14.9% and 8.28%, respectively). Similarly, the binding of *N. meningitidis ΔporAΔpilQ* cells bound rLRP 40.9% less than their wild type counterparts (90.1%), which were used as control in this experiment. Interaction of the *H. influenzae ompP2ΔL2* and *H. influenzae* Δ*ompP2* mutants with rLRP was significantly less than the interaction of either the wild type *H. influenzae* or *H. influenzae ompP2::kanR*. Binding of the *H. influenzae ompP2::kanR*, which was used for control purposes, was also less than the wild type, but this difference did not reach significance (Figure 4.30).

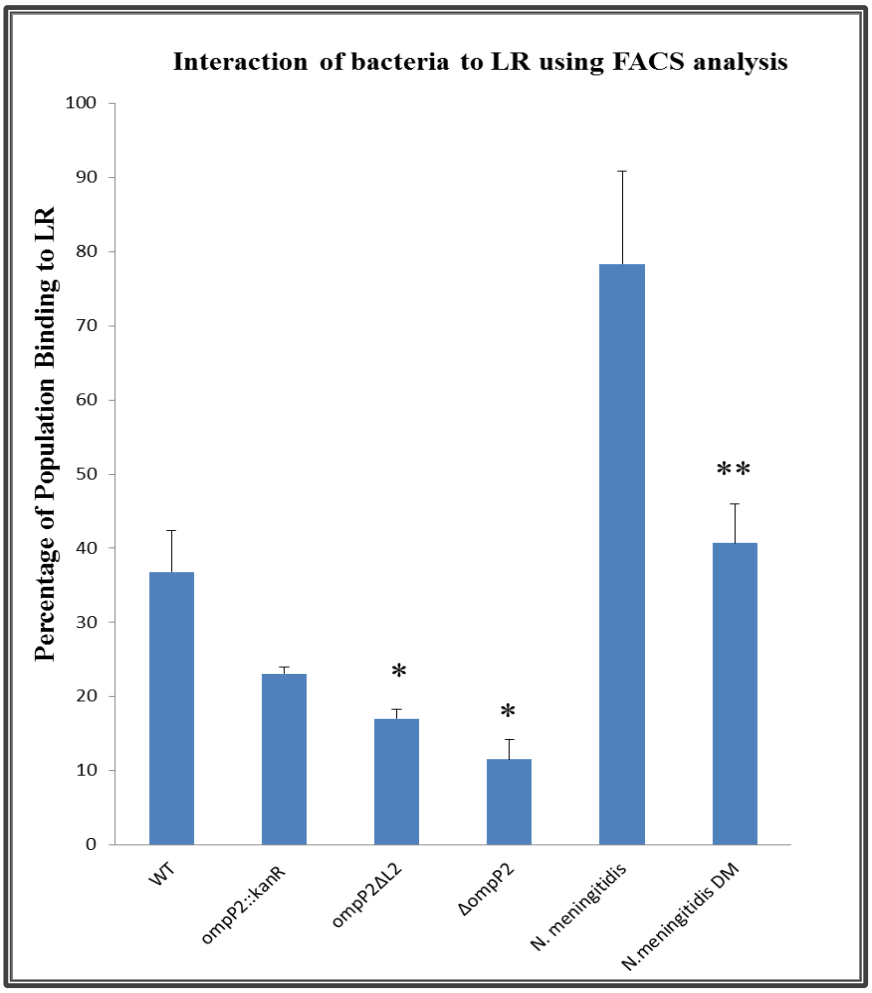

Figure 4.30. Interaction of the *H. influenzae* and its derived mutants with rLRP using FACS analysis. Mid-log phase bacteria were adjusted to 2 × 10^7 cfu/ml aliquots, centrifuged and 20 µg of fluorescein- conjugated rLRP was added in a total volume of 0.2 ml and incubated for 3 h, washed with FACS buffer fixed with 0.5% paraformaldehyde in PBS. Samples were analysed for fluorescence using a Coulter Altra Flow Cytometer. Student's *t*-test analysis showed that the different of the interaction with rLRP between wild type and *H. influenzae ompP2::kanR* (control mutant) was not significant and *p* value > 0.05. The interaction with rLRP was significantly reduced in the mutants *H. influenzae ompP2ΔL2* and *H. influenzae* Δ*ompP2* mutants compared with the wild type (WT), **p* value < 0.05. The binding of the double mutant *N. meningitidis* Δ*porA*Δ*pilQ* (DM) was significantly less than the wild type *N. meningitidis* (NM) which was used as a control, ***p* value < 0.05. Experiment was performed in triplicate. The experiment was repeated for three times on different occasions using similar conditions. Error bars indicate SE.

In order to provide confirmatory evidence for the interaction of rLRP with *H. influenzae* and the role of loop 2 of OmpP2 in this interaction, whole cell lysate pull-down assays were conducted. Bacterial cells (*H. influenzae, H. influenzae ompP2*Δ*L2*, and *H. influenzae* Δ*ompP2* mutants) were incubated with soluble purified rLRP, harvested by centrifugation, washed and re-suspended in SDS-PAGE loading buffer and analysed by SDS-PAGE and immunoblotting with anti-LR. Bands were scanned and quantitated by densitometry (Figure 4.31A). Bands corresponding to protein with an apparent molecular mass of *ca*. 44 kDa represent the rLR bound to the bacteria. A band with an apparent molecular mass of *ca.* 29 kDa was consistently observed; the identity of this protein is unknown. Band intensity was quantified by multiplying the total area of the band with the average density of the band (Figure 4.31B).

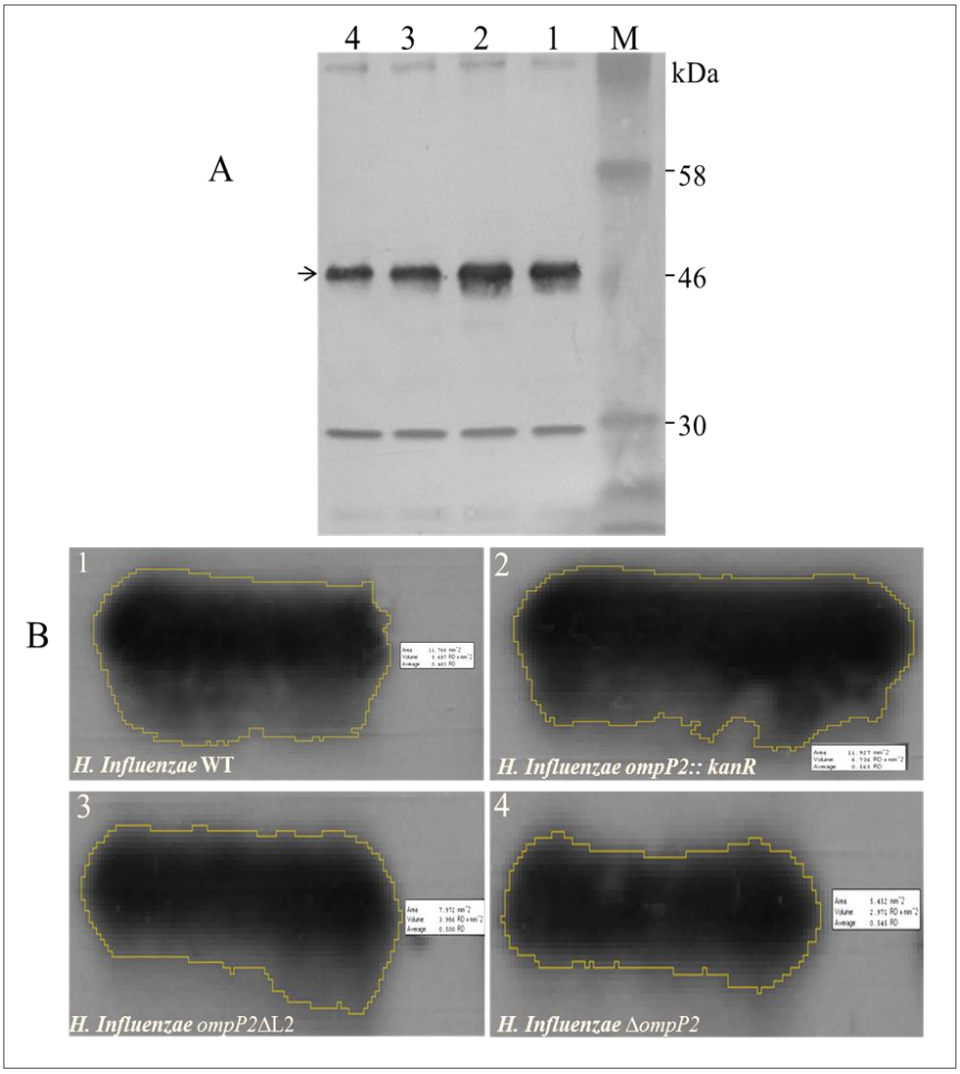

Figure 4.31. rLRP binding to whole cells detected using a whole cell pull-down assay. (A) rLRP bound to whole cells was detected after cell lysis and immunoblotting. Lysates of wild-type *H. influenzae* (1), *ompP2::kanR* (2), *ompP2ΔL2* (3), Δ*ompP2* (4) were probed with anti-LR and the membrane was scanned using a Bio-Rad GS-800 calibrated densitometer. rLRP binding was quantified by multiplying the area of the bands with the average band intensity. (B) Quantified regions are indicated for each band.

The experiment was repeated three times on different occasions with similar results (Figure 4.32). The interaction of the *H. influenzae ompP2ΔL2* and *H. influenzae* Δ*ompP2* mutants with rLRP was significantly lower than either the wild type *H. influenzae* or *H. influenzae ompP2::kanR.*

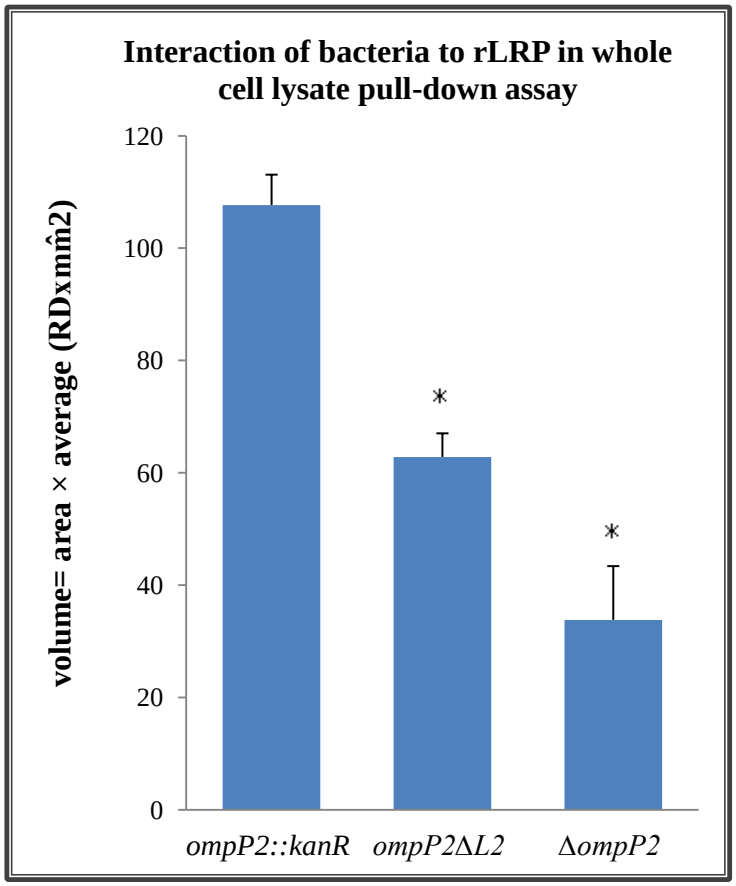

Figure 4.32. The interaction of rLRP to the bacteria determined by whole cell pull-down assay. The amount of rLRP interacting to the bacterial cells was determined by multiplying the total area of the band by the average band intensity. Values are expressed as a percentage of the binding's percentages were compared versus wild-type. Interaction of rLRP with the *H. influenzae ompP2ΔL2* and *H. influenzae* Δ*ompP2* mutants was significantly lower than with wild type cells (**p* value < 0.05). Experiments were performed in triplicate. Error bars indicate SE.

4.2.14 Interaction of OmpP2 and OmpP2ΔL2 Purified under non-Denatured Conditions with Laminin Receptor

Previous data demonstrating an interaction of OmpP2 and rLRP and the role played by loop 2, in these experiments the proteins were purified under denaturing conditions after being expressed in *E. coli*. In order to further investigate the role of OmpP2 and loop 2 in the interaction of the *H. influenzae* with rLRP, OmpP2 and OmpP2ΔL2 were purified under non-denaturing conditions directly from *H. influenzae* using detergent extraction, ion exchange and gel filtration. Overnight bacteria cultures were harvested and lysed in lysis buffer (50mM Tris-HCl, 30mM Zwittergent 3-12, pH 8.5 and 1:500 DNase I) at 4°C, cell lysates then were centrifuged. Supernatants were subjected to Capto Q cation exchange column chromatography and proteins then were eluted with a linear gradient of elution buffer 1 (50mM Tris-HCl, 30mM Zwittergent 3-12, 2M NaCl, pH 8.5) and samples analysed by SDS-PAGE (Figure 4.33). Fractions containing the porin (fractions 5 to 10; lanes 5-10 in figure 4.33 A and B) were then successfully further purified by gel filtration and again fractions were analysed SDS-PAGE and immunoblotting using anti-OmpP2 (Figure 4.34).

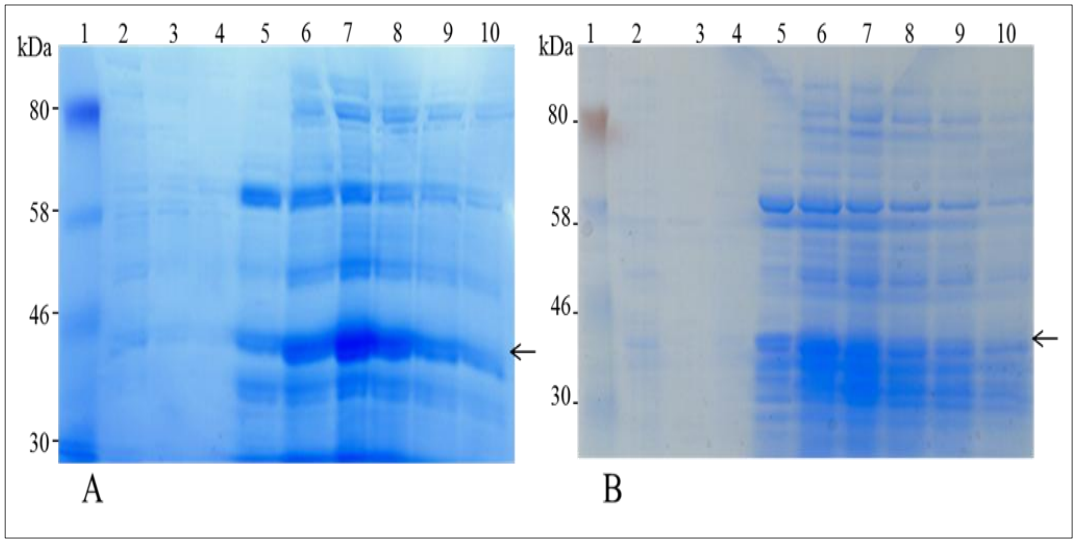

Figure 4.33. Purification of OmpP2 and OmpP2ΔL2. Fractions eluted from a Capto Q ion exchange column loaded with detergent extracts of *H. influenzae* (A) or *H. influenzae ompP2ΔL2* (B) were analysed by SDS-PAGE. In both panels lane 1 contains protein marker; lane 2: detergent extract of whole cells; lane 3: flow through; lane 4: wash; lanes 5-10 are fractions 5 to 10 respectively. Arrows show the expected size of the protein of interest.

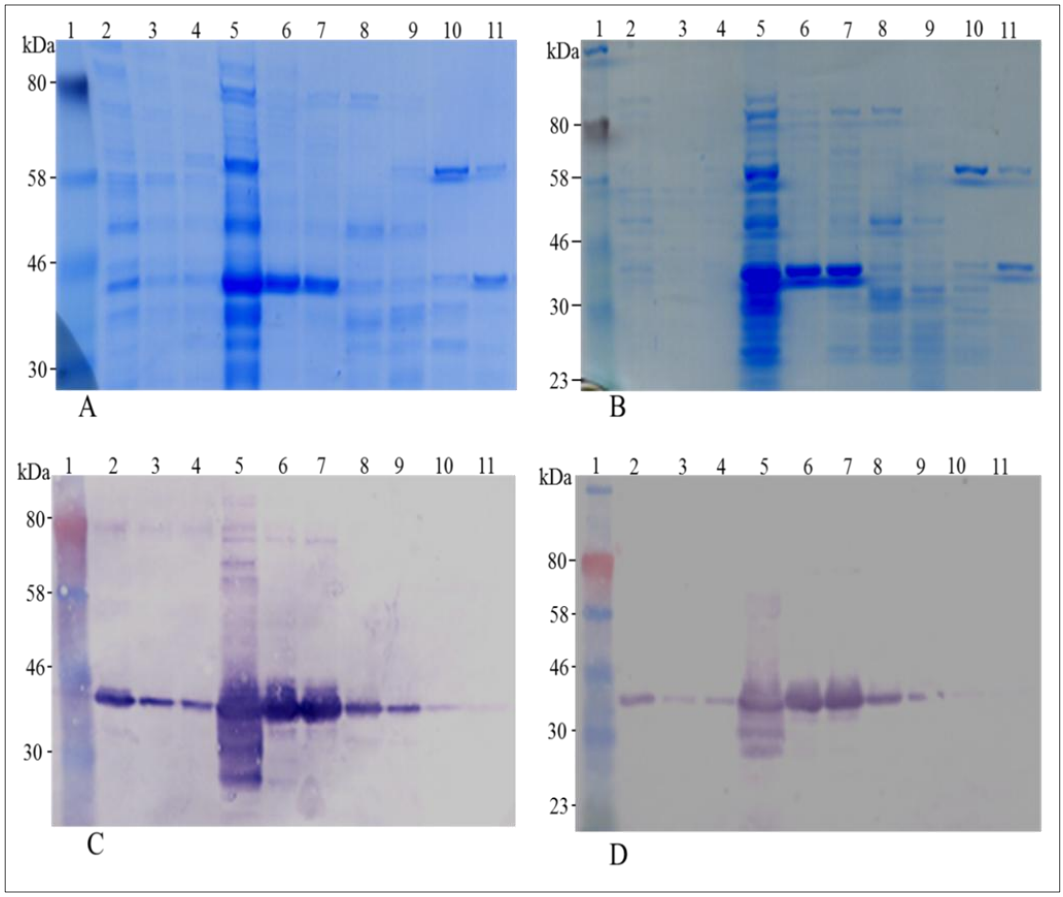

Figure 4.34. Gel filtration purification of OmpP2 and OmpP2ΔL2. Eluted fractions of proteins of *H. influenzae* (A) or *H. influenzae ompP2ΔL2* (B) were analysed by SDS-PAGE. The fractions then of *H. influenzae* (C) or *H. influenzae ompP2ΔL2* (D) were analysed by blotting (probed with anti OmpP2). In all panels lane 1 contains protein marker; lane 2: soluble; lane 3: flow through; lane 4: wash; lane 5: mixture of fraction 6-10 of ion exchange elution; lane 6-11 are fractions 5 to 10 respectively.

Purified native OmpP2 (lanes 6 and 7 in panels A and C; figures 4.34) and OmpP2ΔL2 (lanes 6 and 7 in panels B and D; figures 4.34) proteins (lanes 6 and 7 in figures 4.34) were tested in ELISA assays to determine their ability to bind rLRP. Both OmpP2 and OmpP2ΔL2 bound rLRP but binding by the mutant protein was significantly less than the wild type protein ($p < 0.01$) (Figure 4.35).

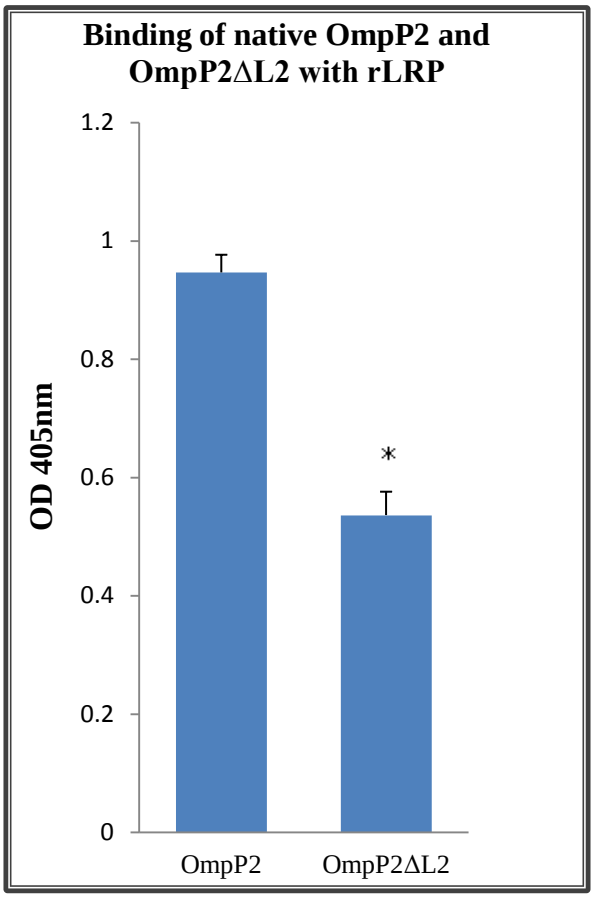

Figure 4.35. Binding of native OmpP2 and OmpP2ΔL2 to rLRP. An ELISA plate was coated with native OmpP2 and OmpP2ΔL2 at a concentration of 5 µg ml^{-1}. BSA-coated wells were included as a negative control. Wells were subsequently incubated with rLRP (5µg ml^{-1}) followed with rabbit anti-LR and then anti-rabbit IgG-AP. Bound rLRP was detected after adding AP substrate in an ELISA plate reader. Specific binding of rLRP to OmpP2 and OmpP2ΔL2-coated ELISA plates was determined by subtracting the absorbance in BSA-coated wells from that in OmpP2 and OmpP2ΔL2-coated wells. Data shown are the means of three independent experiments, with each sample tested in triplicate. *p value < 0.01 compared to wild-type. Error bars indicate SE.

4.3 Discussion

The laminin receptor protein is an important protein in the microbial infection pathway of a number of pathogens, which appear to target this protein as a means to enter host cells (Nelson *et al.*, 2008). It was demonstrated that 67LR present on the human brain microvascular epithelial cells (HBMECs) membrane and serves as a cell-surface receptor facilitating *E. coli* K1 internalization of HBMECs. This interaction is mediated by interaction of cytotoxic necrotizing factor-1 (CNF1) with the 37/67-kDa laminin receptor (Chung *et al.*, 2003). Many cell-binding and internalization studies proved evidence that the LamR has been reported to serve as target for many viruses and it is a receptor for the binding and internalization of infectious prions into neuronal or non-neuronal cells (Ludwig *et al.*, 1996; Gauczynski *et al.*, 2006; Gauczynski *et al.*, 2001). Furthermore, it has been reported that LamR acts as the PrP^{Sc} receptor at the cell surface in cultured neuronal cells (Leucht *et al.*, 2003).

Porin P2 purified from *H. influenzae* type b (Hib) contributes to signaling of the inflammatory cascade as in the rat model of meningitis and it was revealed that inoculation of OmpP2 of Hib into the fourth stimulated the expression of 1L-1 α, TNF- α, and macrophage inflammatory protein 2 (MIP-2) (Galdiero *et al.*, 2001). Concomitantly, Galdiero *et al.*, found that the release of IL-6 and TNF-α was increased in human monocytic cell line THP-1 cells stimulated with Hib porin. Moreover, Hib porin-induced IL-6 and TNF-α in THP1 cells is mediated by the CD14 and TLR2 pathway (Galdiero *et al.*, 2004). Similarly, stimulation of U937 cells by synthetic peptides corresponding to externally exposed loops L5, L6, and L7 of OmpP2 porin from Hib induced IL-6 and TNF-α production. Moreover, this

production mediated by activation of JNK and p38 mitogen-activated protein kinase (MAPK) phosphorylation. L7 and L2 induced IL-6 and TNF- cytokine to approximately 40% and 20%, respectively, in comparison to the entire OmpP2 protein. Loop 7 was identified to be the most active derivative among these loops (Galdiero *et al.*, 2006; Neary *et al.*, 2001).

The work described in the previous chapter using purified recombinant OmpP2 and its derivatives implicated the second extracellular loop of the porin in its rLRP binding activity. To extend these observations, a *H. influenzae* mutant strain expressing OmpP2, with the apex of loop 2 removed (Ala91-Phe99) was constructed and the binding of this strain to rLRP compared to the binding of the cognate wild-type strain. This mutant was constructed using bacterial transformation and allelic exchange. Initial attempts to clone *ompP2* and its flanking region in *E. coli* JM109 failed; perhaps due to toxicity to the *E. coli* cells and a subsequent clone obtained using a smaller amplicon contained a frameshift mutation, suggesting that expression of the full-length porin gene (including the N-terminal signal sequence, which was absent in the pQE-based expression plasmids) might also be toxic to *E. coli*. This clone was used to facilitate further steps toward construction of the desired mutagenic amplicon and the point mutation had to be corrected using site-directed mutagenesis (Chapnik *et al.*, 2008), this was achieved using a megaprimer (Kammann *et al.*, 1989). Expression levels of OmpP2 in the first OmpP2ΔL2 strain constructed were greatly reduced compared to wild-type, this could be due to the kanamycin resistance cassette which was inserted in the reverse orientation to *ompP2*; transcription from the *kanR* gene could interfere with transcription of *ompP2* and thus reduce *ompP2*

gene expression. The kanamycin resistance cassette was therefore replaced with the Omega cassette, but this construct could not be successfully introduced into *H. influenzae.* The reason for this was not clear. Therefore a new mutant, *ompP2ΔL2* was created by removing and re-inserting the kanamycin resistance cassette in the forward orientation. In addition to the deleted loop 2 *H. influenzae* mutants, other mutants, Δ*ompP2* and *ompP2::kan,* were generated for control purposes.

Due to the fact that a specific gene manipulation might cause several phenotypic changes compared to the parent strain, it was first essential to demonstrate that genetic alterations did not significantly affect the growth rate of *H. influenzae*. All generated mutants were tested for their growth with comparison to the wild type. All the mutated cells showed similar growth rate to the wild type *H. influenzae*. In contrast, in 2006, Murphy and colleagues showed that during mutation of outer membrane protein P6, which plays a structural function in the bacterial cell, several changes would resulted including: morphological alteration; larger cell size, vesicle formation, and reduction in cell wall integrity compared to the parent cells. Moreover, the growth of the mutated cells was slower, susceptibility to the antibiotics and complement-mediated killing by human serum increased (Murphy *et al.*, 2006).

OmpP2 is translocated to the outer membrane via the inner membrane and the periplasmic space. Therefore, the ability of OmpP2ΔL2 to localise to the outer membane was checked to exclude this as a possible explanation for reduced LR-binding. The result obtained from the SDS-PAGE staining and blotting of the cell fractions (enriched for the inner and outer membrane proteins) indicated that the

mutated protein was still able to localise to the outer membrane as efficiently as the wild-type protein.

Next, the role of OmpP2 L2 in the *H. influenzae* binding to rLRP was studied by flow cytometery analysis and whole cell pull-down assays. Furthermore, the native protein OmpP2 and OmpP2ΔL2 were purified natively from *H. influenzae* directly using ion exchange and gel filtration. Natively purified proteins were again investigated for its binding to the rLRP in ELISA. Mutation of the OmpP2 loop 2 resulted in a marked reduction of binding to recombinant LRP as shown by flow cytometry and whole cell lysate pull-down assay as well as ELISA. However, the data showed that the *ompP2* knockout still had some residual LR binding actvity. This may suggest that there is another binding protein that is not yet identified and further screening would be needed to identify this protein. Taken together, the experimental data presented herein show that loop 2 (Ala91-Phe99) has an important role amongst the eight loops of OmpP2 in its binding to rLRP.

This work confirms the identification of OmpP2 as a ligand for LamR. Furthermore, the second extracellular loop of this protein has been demonstrated to be important for binding to the human receptor. This data builds on previous reports that indicated some of the surface-exposed loops are involved in recognition of ligands, including small molecule nutrients, bacteriophages and eukaryotic target cells (Galdiero *et al.*, 2003). Vitiello and colleagues pointed out that OmpP2 loops are capable of different biological activities such as activation of TNF, MEK1-MEK2/MAP, IL-6 and JNK (Vitiello *et al.*, 2008).

In a newborn mouse model, *E. coli* K1 mutants missing the extracellular loops 1 and 2 regions from OmpA were unable to cause meningitis. These regions were found to be responsible for survival of the pathogen inside neutrophils and dendritic cells and loop regions 1 and 3 are needed for survival the pathogen in macrophages. Loop 2 (MPYKGSVENGA) was involved in the majority of the interactions and represents an interesting target for immunization. Levels of TNF-α, IL-1, IL-6, and IL-12 were decreased in the brains of mice infected with loop 1 and loop 2 mutants compared with animals infected with loop 3 and loop 4 mutants or $OmpA^{+}$ *E. coli* K1 (Mittal *et al.*, 2011). The results may lead to a better understanding of the mechanism of *H. influenzae* invading of the BBB and then getting access to the HBMECs and in turn to the development of potential vaccines to prevent infection.

CHAPTER FIVE: Role of the Second Extracellular Loop of OmpP2 in Binding to Human Microvascular Endothelial Cells

CHAPTER FIVE

5. ROLE OF THE SECOND EXTRACELLULAR LOOP OF OMPP2 IN BINDING TO HUMAN MICROVASCULAR ENDOTHELIAL CELLS

5.1 Introduction

H. influenzae has many virulence factors which contribute to its pathogenicity. For example, in a rats bacterial meningitis model it was found that inoculation of animals with live *H. influenzae*, bacterial LPS or outer membrane vesicles induced meningeal inflammation and resulted in both dose- and time-dependent increases in cerebrospinal fluid (CSF) white blood cells (WBC) and blood-brain barrier permeability (Mustafa *et al.*, 1989; Wispelwey *et al.*, 1989). *In vivo* and *in vitro* model systems were showed that capsular polysaccharide and lipopolysaccharide (LPS) are important for the ability of *H. influenzae* to traverse the nasopharynx and localize in the cerebrospinal fluid and meninges. Also it was identified that lipopolysaccharide plays a role in enhancing the efficiency of bacterial translocation from the nose to the blood, and in facilitating intravascular survival (Moxon, 1992). A study of nasopharyngeal carriage in an infant rat model indicated that phosphorylcholine (ChoP) plays a role in *H. influenzae* colonization (Weiser *et al.*, 1998). ChoP is present on the cell surface of the major pathogens residing in the human respiratory tract including *S. pneumoniae*, *H. influenzae*, and *Neisseria meningitidis* (Gould & Weiser, 2002). Studies have revealed that ChoP is expressed on *H. influenzae* lipopolysaccharide (LPS) and it is subjected to phase variation (Weiser *et al.*, 1989; Weiser *et al.*, 1998; Lysenko

et al., 2000). Moreover, it was verified that the expression and phase variation of ChoP on *H. influenzae* LPS is mediated by four genes in the *lic1* locus: *licA, licB, licC,* and *licD* (Weiser *et al.*, 1997; Weiser *et al.*, 1990a). It was showed that the first gene *licA* is mediated phase variation (Weiser *et al.*, 1998). This gene has multiple tandem repeats of the sequence 5'-CAAT-3' within the coding region of the first open reading frame which provides a mechanism for phase variable expression (Weiser *et al.*, 1997; Weiser *et al.*, 1990a). By shifting the upstream initiation codons in or out of phase with the remainder of the open reading frame, could switch on or off the translation of downstream genes (Cope *et al.*, 1990). Moreover, it was shown that ChoP mediates the interaction of *H. influenzae* with the PAF receptor (Swords *et al.*, 2000). In addition, the phosphorylcholine (ChoP) is a target for C-reactive protein (CRP) (Weiser & Pan, 1998; Lysenko *et al.*, 2000) which, in the presence of complement against *H. influenzae* expressing ChoP, will have bactericidal activity against the organism (Gould & Weiser, 2002; Weiser *et al.*, 1990b). *H. influenzae* has the ability to switch off expression of ChoP, which eliminates binding of CRP suggesting that the biological role of the $ChoP^+$ phenotype might be evasion of CRP-mediated clearance (Weiser *et al.*, 1997).

In a study performed by Reddy *et al.*, (1996) to determine the mechanism of binding between mucin and OMPs of NTHi, an overlay binding assay was performed and the OMPs P2 and P5 of NTHi were found to function as adhesins for purified human nasopharyngeal mucin (HNM). Moreover, the sialic acid-containing oligosaccharides of HNM appear to be the receptors for NTHi (Prasadarao *et al.*, 1996). It was demonstrated in a new born rat meningitis model

that a prominent outer membrane protein, OmpA, of *Escherichia coli* is essential for interaction with GlcNAcb1-4GlcNAc epitopes of BMEC glycoproteins and entry of $OmpA^+$ *E. coli* into the central nervous system was inhibited by soluble GlcNAcβ1-4GlcNAc oligomers (Prasadarao *et al.*, 1996).

Outer membrane protein P2 (OmpP2) is the major outer membrane (porin) protein of *H. influenzae* type b (Hansen *et al.*, 1989; Galdiero *et al.*, 2006). The molecular mass of OmpP2 is 38.5 kDa and the structure is composed of 16 transmembrane regions separating eight large surface-exposed loops on the external surface of the bacterial membrane, seven short periplasmic loops and periplasmic N and C termini (Munson & Tolan, 1989; Srikumar *et al.*, 1992b; Srikumar *et al.*, 1997; Galdiero *et al.*, 2006). There is increasing evidence to show that OmpP2 of *H. influenzae* plays a significant role in the pathogenesis of the *H. influenzae* (Duim *et al.*, 1996; Yi & Murphy, 1997; Murphy & Bartos, 1988; Chong *et al.*, 1993; Andersen *et al.*, 2003). In comparison with the wild-type parent strain, the OmpP2 mutant Hib was unable to generate bacteremia in infant rats after intraperitoneal challenge (Cope *et al.*, 1990).

The mechanisms responsible for microbial invasion and traversal of the microvascular endothelial cell of blood–brain barrier are poorly understood. However, previous work indicated that these pathogens required interaction with LamR on the surface of HBMECs as a first step to initiate invasion of the BBB (Orihuela *et al.*, 2009). OmpP2 of the *H. influenzae* was shown to be the bacterial adhesion responsible for interaction with LamR (Orihuela *et al.*, 2009). Notably, LamR has been shown to act as a receptor for a number of bacterial ligands (Kim

et al., 2005) as well as neurotrophic viruses, such as Sindbis virus and Dengue virus (Wang *et al.*, 1992), and is also required for internalization of prion proteins (Nelson *et al.*, 2008).

It was shown that the cytotoxic necrotizing factor 1 (CNF1) of *E. coli* K1 interaction with 37/67-kDa laminin receptor (LamR) is the initial step required for bacterial uptake into eukaryotic cells including HBMEC and HEp-2 by mediating RhoA activation. Exogenous 37-kDa laminin receptor precursor (LRP) or LRP antisense oligodeoxynucleotides blocked the CNF1-mediated RhoA activation and bacterial uptake, whereas they were increased in LRP overexpressing cells (Chung *et al.*, 2003).

Work described in chapter four identified that recombinant loop 2 of *H. influenzae* OmpP2 as being important for the interaction of *H. influenzae* and LamR. Hence, it is likely that possession of this loop plays an important role in the pathogenesis of *H. influenzae*. To test this hypothesis, the interaction of synthetic peptides based on the loop 2 sequence with rLRP and HBMECs was investigated. In addition, the potential roles of OmpP2 and loop 2 in *H. influenzae* adhesion to, and invasion of, cultured HBMECs and HEp-2 are discussed. The final aim discussed in this chapter was to explore whether OmpP2 or loop 2 have the ability to activate RhoA.

5.2 Results

5.2.1 Binding of Synthetic Peptides Corresponding to OmpP2 Loop 2 with Laminin Receptor

The mutagenesis study of *H. influenzae* indicated that loop 2 of OmpP2 is the most important region of this protein for rLRP-binding. Further characterization of the role of this loop in interactions with rLRP was undertaken using synthetic peptides. The surface-exposed amino acid sequence corresponding to the 9-amino acid apical region of OmpP2 loop 2 (residues 91-99) were synthesized including additional terminal cysteine residues; under oxidizing conditions cysteine sulfhydryl groups spontaneously form disulfide bonds, thus allowing the peptides to more closely mimic the native loop structures seen in outer membrane-embedded proteins. ELISA assays were performed to determine the interaction between rLRP and the OmpP2 loop 2 synthetic peptide and another two synthetic peptides; the 34-amino acids corresponding to the fourth loop of *N. meningitidis* PorA (residues 185-218) and the 39 amino acids corresponding to the first loop of PorA (residues 31-70) served as positive and negative controls, respectively. OmpP2 loop 2 and PorA loop 4 both bound rLR to a significantly higher degree than PorA loop 1 (Figure 5.1). This observation confirms that *H. influenzae* OmpP2 binding to rLRP is governed by its second loop and this loop directly binds to rLRP.

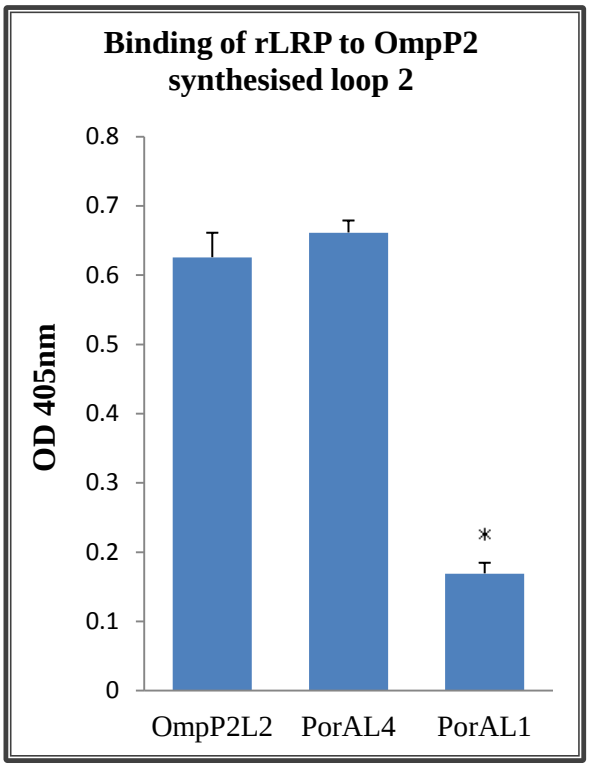

Figure 5.1. Binding of synthetic OmpP2 loop 2 to rLRP. Synthetic loop 2 (5 µM) was used to coat the wells of an ELISA plate and rLRP was added to the plates (5 µM). Following incubation, bound rLRP was detected with rabbit anti-LR and then anti-rabbit IgG-AP antibody. PorA loop 4 and loop 1-coated wells were included as comparative positive and negative controls respectively. To correct for non-specific background binding, the absorbance in BSA-coated wells was subtracted from that in OmpP2 loop 2, PorA loop 4 and PorA loop 1-coated wells. Each data point represents the means of three independent experiments; in each experiment each sample was tested in triplicate. * $p <$ 0.01 compared with synthesised OmpP2L2. Error bars indicate SE.

5.2.2 OmpP2 Loop 2 Interacts with HBMECs

Synthetic loop 2 interacts with rLRP in the ELISA. Further study was undertaken in order to identify whether this loop can bind directly to HBMECs, which are known to express LamR on the cell surface. Synthetic loop 2 peptides were coupled to micro-beads and the ability of the synthetic loop 2 to mediate adherence of the beads to HBMECs was characterised. This showed that

interaction of the micro-beads with HBMECs was enhanced if the micro-beads were first coupled to synthetic loop 2 compared to BSA-coated control beads (Figure 5.2). After being rinsed with PBS, cells were fixed with 4% paraformaldehyde, washed and blocked with BSA/PBS. Anti-IHLR and Mluc5 IgM mouse antibodies were then added to detect the 37LR and 67LR respectively. Cells were rinsed with PBS and then incubated with anti rabbit Alexa 488 (to detect IHLR), anti-mouse IgM 647 (to detect Mluc5) and Hoechst 33258 (to detect dsDNA). Adhesion of loop2-coated micro-beads to HBMECs was viewed using the Leica inverted confocal microscope (DM IRE2). Only micro-beads coated with loop 2 were observed to bind HBMECs (Figure 5.2).

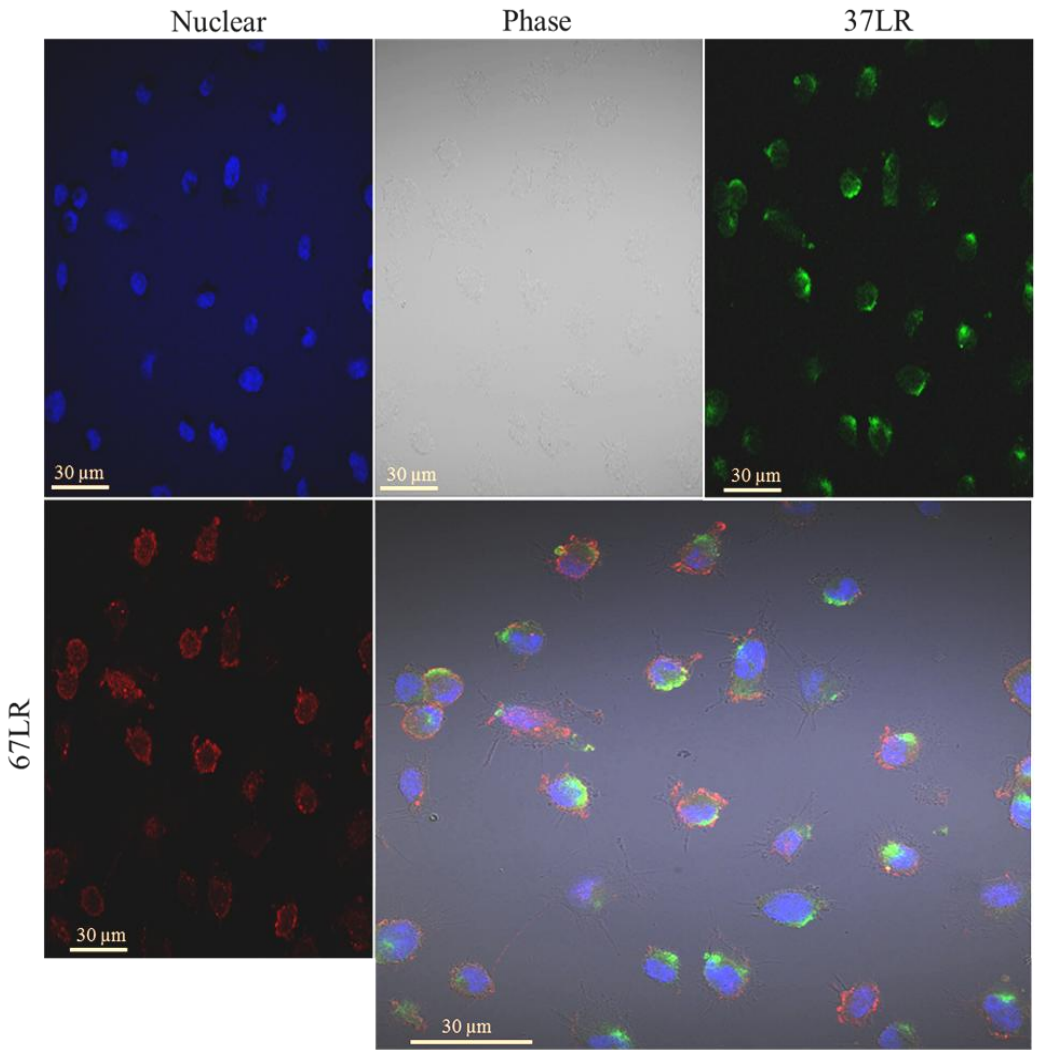
Nuclear
Phase
37LR
67LR
30 µm
30 µm
30 µm
30 µm
30 µm
A
Merged images

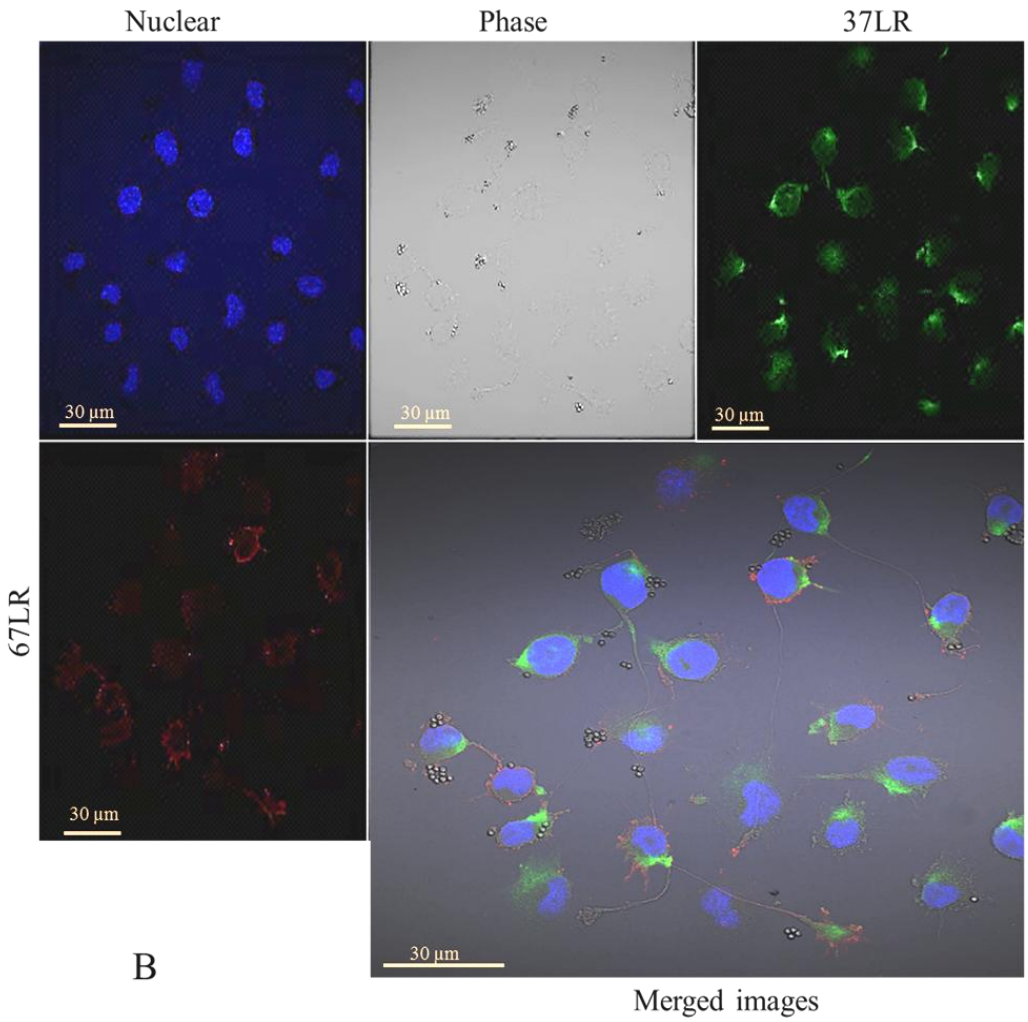

Figure 5.2. Representative confocal microscopy images of (A) BSA- and (B) loop2-coated micro-bead adhesion to HBMECs. To determine whether loop 2 of OmpP2 binds to HBMECs, HBMECs seeded onto sterile coverslips. Synthetic loop 2 coupled-beads and BSA-coupled beads (control) were incubated with HBMECs at 4°C for 1 h. HBMECs were then rinsed with PBS and fixed with 4% paraformaldehyde. Cells were then washed and blocked with BSA/PBS. Localization of 37LR in HBMEC was detected with anti-37LR (anti-IHLR) monoclonal antibody, followed with anti-rabbit Alexa-488 conjugated secondary antibody (green). Localization of 67LR in HBMEC was detected with anti-67LR (MLuC5) monoclonal antibody, followed with anti-mouse IgM 647 conjugated secondary antibody (red). Nuclear DNA was detected with Hoechst 0033258 (blue). Images were captured using a Leica inverted confocal microscope (DM IRE2).

5.2.3 Adhesion of OmpP2, OmpP2ΔL2 and Loop 2-coated Micro-Beads to HBMECs

Synthetic OmpP2 loop 2 was shown by confocal microscopy to bind to HBMEC monolayers. Further experiments were performed to determine the specificity of this reaction by comparing the interaction of the synthetic loop 2 with a scrambled sequence based on the loop 2 sequence and the *N. meningitidis* PorA loop 1 sequence. Moreover, the micro-beads assay was performed to assess whether the deletion of loop 2 from intact OmpP2 affects its ability to bind HBMECs. OmpP2 and OmpP2ΔL2 were purified from *H. influenzae* under non-denatured conditions employing detergent extraction, ion exchange and gel filtration. Purified proteins and synthetic peptides were utilised to coat micro beads and then coupled protein-beads were incubated with HBMEC monolayers. Subsequently, the micro-beads adhesion assay slides were read and the beads coated with OmpP2, OmpP2ΔL2, OmpP2L2, PorAL1, scrambled loop 2 and BSA adhering to monolayers were counted. All beads interacted with HBMECs except the negative control (BSA-coated) beads. Loop 2-coated micro-beads adhered at higher levels compared to the scrambled loop 2 and PorAL1 coated control beads. In addition, deletion of loop 2 from OmpP2 (OmpP2ΔL2) reduced its ability to adhere to the HBMECs compared to the wild type OmpP2 (Figure 5.3). These findings confirm that loop 2 of OmpP2 interacts with HBMEC and it is the most important region of this protein that facilitates its binding to the HBMECs.

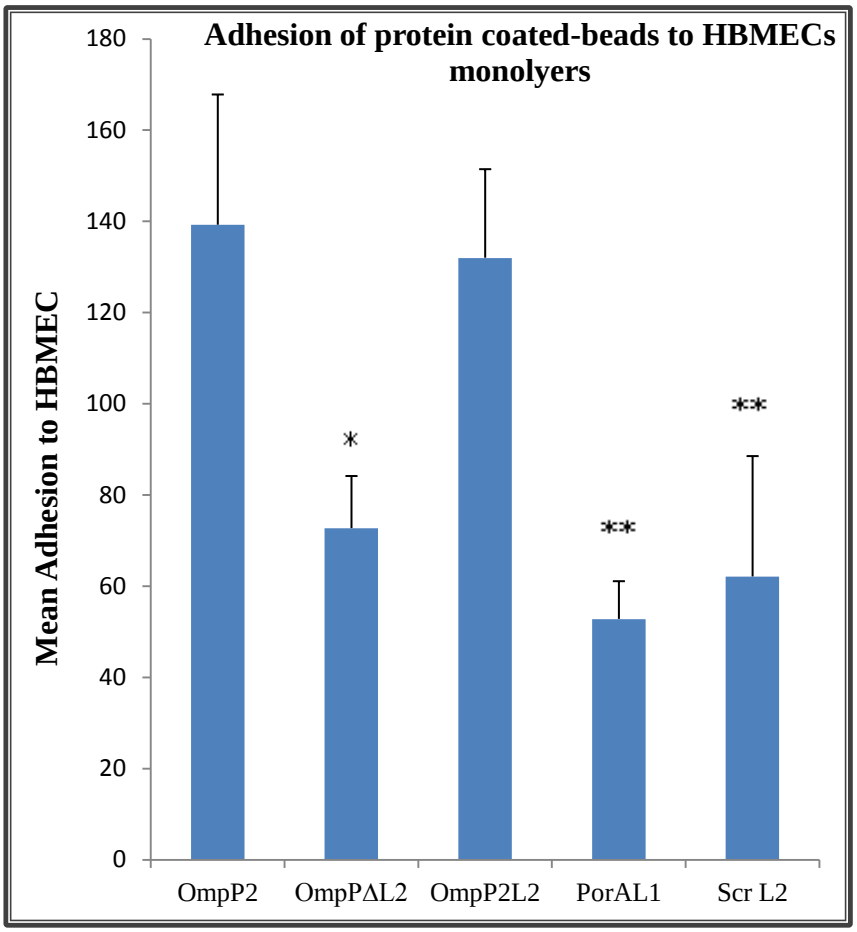

Figure 5.3. Adhesion of OmpP2-, OmpP2ΔL2-, OmpP2L2, PorAL1 or scrambled OmpP2L2-coated micro-beads to HBMEC monolayers. Human brain microvascular endothelial cells were grown in the 12-well plate containing fibronectin-coated covers slips. Coupled protein-beads (5 µl per well) were added for 1 h incubation duration at 4°C. After being washed with PBS, the cells were fixed with 4% PFA/PBS. Following the washing with the PBS and blocking with 4% BSA/PBS the coverslips were then mounted on microscopic slides and examined under light microscope. Employing a blind method of reading the slides, micro-beads were counted from 15 random fields per slide at 400 × magnification. BSA-coated beads were included as negative controls, and the mean value obtained from these controls was subtracted from all other data points. The micro-beads attached to HBMECs were counted and the mean total adhesion of micro-beads were analysed. Data shown are the means of three independent experiments experiments * $p <$ 0.1 compared to adhering of the OmpP2 and ** $p <$ 0.1 compared to adhering of OmpP2L2. Error bars indicate mean SE.

5.2.4 Role of OmpP2 in Association and Invasion of HBMECs and HEp-2 Cells by *H. influenzae*

To investigate the potential role of *H. influenzae* OmpP2 in general, and its second loop in particular, in adhesion and invasion to epithelial and endothelial cells, viable counts of bacteria associated with homogenized infected monolayers were determined to compare the capacity of wild-type and *ompP2* and *ompP2*Δ*L2* mutant strains to associate with and invade either HBME or HEp-2 cells. Adhesion and invasion assays were performed essentially based on the previously described employing HBME or HEp-2 monolayers (Section 2.23, 2.24) (Oldfield *et al.*, 2007). For association assays, confluent monolayers of HBMECs or HEp-2 cells were grown in a 24-well tissue culture plate format. Cells were infected with bacteria and, following the incubation period, non-adherent bacteria were removed by washing and monolayers were permeabilised with 0.1% Saponin. Dilutions of the homogenized suspensions were plated on chocolate agar plates and numbers of colony forming units determined. To determine the number of bacteria entering the cells of HBMECs or HEp-2 monolayers, invasion assays were performed essentially as described above except that after the initial 3 h incubation, monolayers were washed with PBS and incubated for another 2 h with culture medium containing gentamicin, a bactericidal antibiotic that is unable to enter eukaryotic cells. Therefore, bacteria adherent to epithelial cells are killed, whilst internalized bacteria are protected (St Geme & Falkow, 1990). After washing, monolayers were disrupted and homogenized as before for plate counting (Figures 5.4 and 5.5). To exclude the possibility that any observed changes in the ability of the mutants to adhere or invade monolayers might be due

to the presence of the kanamycin resistance cassette, which was inserted into the *H. influenzae* genome during generating the mutants, an additional mutant, *ompP2::kanR,* was used as a control. OmpP2-deficient cells had a significantly reduced capacity to adhere to monolayers of HEp-2 in comparison to both parental strain and the *ompP2::kanR* mutant. There was also slightly reduced adhesion to HBMEC cells but this reduction did not reach statistical significance (Figure 5.4). Although it was not statistically significant, the *ompP2* and *ompP2*Δ*L2* mutants exhibited a decrease in invasion of both HEp-2 and HBMECs. Taken together, the above data demonstrate that OmpP2, and specifically its second extracellular loop contribute to the ability of *H. influenzae* to bind and invade HEp-2 and HBMEC.

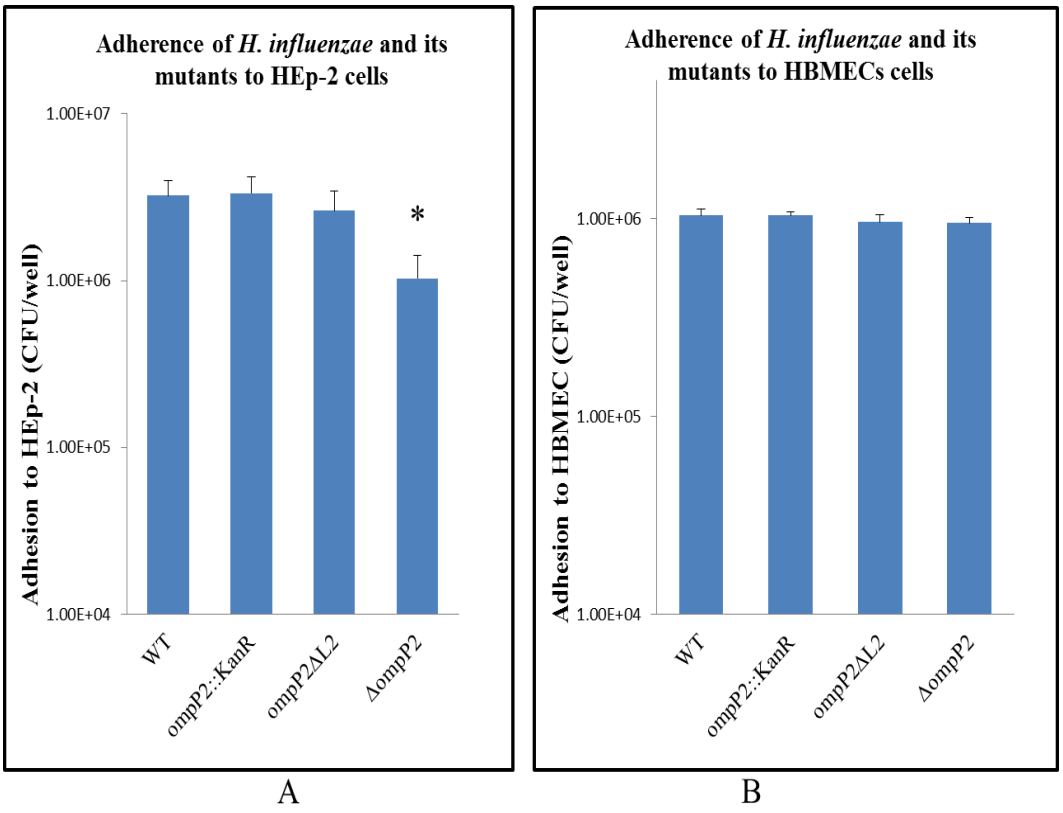

Figure 5.4. Adherence of *H. influenzae* and its mutants to human HEp-2 and HBMEC cell. Bacterial cells, *H. influenzae* and its mutants, Δ*ompP2, ompP2ΔL2 and ompP2::kanR*, were adjusted to 1×10^7 CFU ml^{-1} (confirmed retrospectively by plating out aliquots of serially diluted inoculums) and were allowed to associate with confluent monolayers of HEp-2 (A) and HBMEC (B) cells for 3 h. After incubation, monolayers were washed with 1 × PBS to remove non adherent bacteria and cells were disrupted and homogenized in 0.1% saponin. 10 µl spots of serial 10-fold dilutions of the homogenized suspensions, were plated out and incubated overnight. The viable count plates yielded the number of cell-associated bacteria per monolayer (CFU/well per strain). Statistically significant differences are represented by ***** for $p < 0.05$. In (A) mean levels shown from five independent experiments, four wells were used in each experiments. Bars denote standard error from the mean samples from five experiments. In (B) mean levels shown from a representative of one of two repeated experiments on separate occasions using quadruplicate wells, with consistent results. Bars denote standard error from the mean of quadruplicate samples from one experiment. CFU denotes colony forming units.

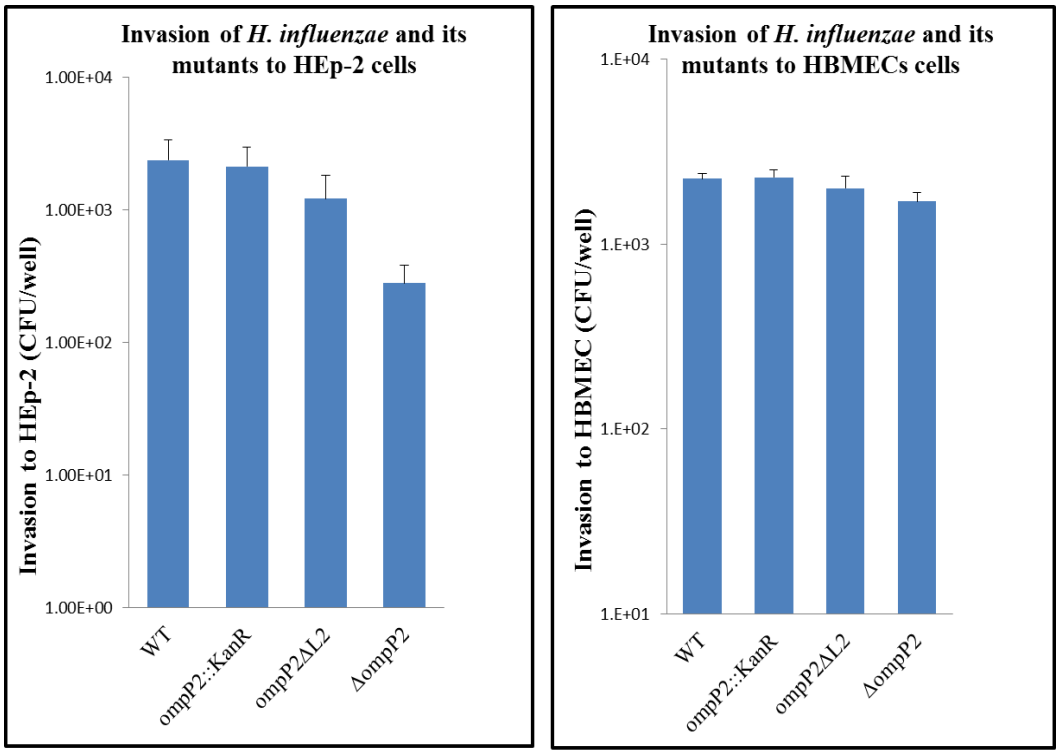

Figure 5.5. Invasion of *H. influenzae* strains into human HEp-2 and HBMEC cells. *H. influenzae* and derivatives were incubated with confluent monolayers of HEp-2 (A) and HBMEC (B) cells for 3 h. Following washing, the monolayers were then re-incubated for 2 h with medium containing 100 µg ml^{-1} gentamycin to kill attacheded bacteria. Monolayers then disrupted and homogenized in 0.1% saponin. Dilutions of the homogenized suspensions were plated out on a chocolate agar plates and incubated overnight. The number of cell-internalised bacteria per monolayer (CFU/well per strain) was measured by viable count. In (A) mean levels are shown from three independent experiments, each using four wells. Bars denote standard error from the mean samples from three experiments. In (B) mean levels shown from one of two repeated experiments on separate occasions using quadruplicate wells, with consistent results. Bars denote standard error from the mean of quadruplicate samples. CFU denotes colony forming units. Bars denote standard error.

5.2.5 *H. influenzae* OmpP2 Contributes to Activation of RhoA in HBMECs

The LR-binding protein CNF1 of *E. coli* K1 can activate RhoA, which in turn induces host cell cytoskeleton rearrangement and enhances bacterial uptake in epithelial cells and human brain microvascular endothelial cells (Flatau *et al.*, 1997; Chung *et al.*, 2003). Moreover, it was identified that the CNF1 interaction with LRP is the initial step required for CNF1-mediated RhoA activation and bacterial uptake into eukaryotic cells (Chung *et al.*, 2003). The role of OmpP2, and specifically its loop 2, in the possible activation of RhoA was investigated in HBMECs using the G-LISA^{TM} RhoA activation assay. Monolayers of HBMECs were allowed to grow to 50-60% confluency, serum starved and treated with OmpP2, OmpP2ΔL2 or loop 2. Thrombin was also used as a positive control (Chung *et al.*, 2003). In addition to the positive control, OmpP2 activated the RhoA-GTP in treated HBMECs (Figure 5.6). OmpP2ΔL2 also induced the RhoA activation; albeit it this activity was lower than the wild type protein. The synthetic loop 2 peptide did not induce a statistically significant increase in RhoA activation.

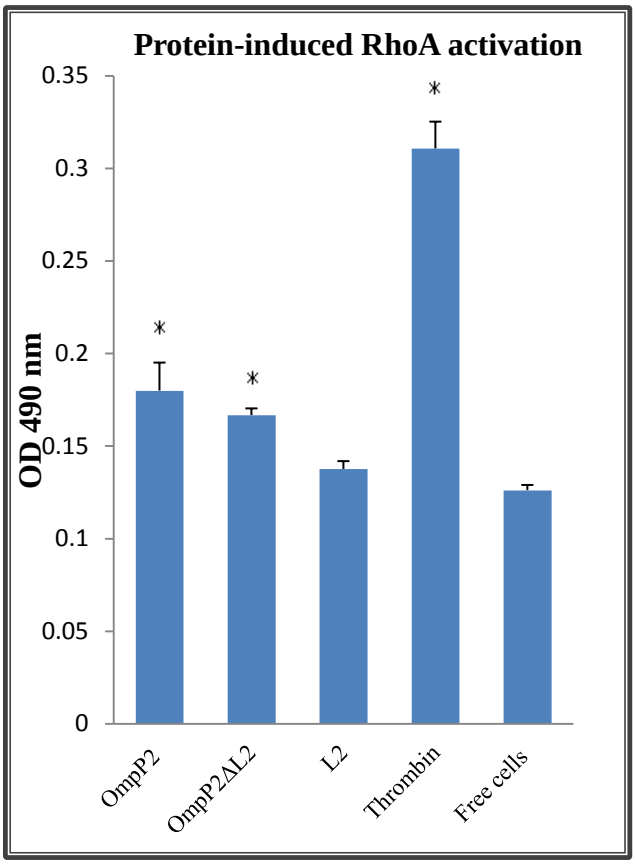

Figure 5.6. G-LISATM assay showing activation of RhoA-GTP in the HBMECs. HBMECs monolayers were incubated with 5 µM OmpP2, OmpP2ΔL2, loop 2 of OmpP2 and thrombin (which was used as a positive control) for 30 min. Cells were lysed and samples were run employing G-LISA, the amount of RhoA-GTP was detected with anti-RhoA antibody and measured by microplate spectrophotometer. Non-treated cells were used as a negative control. Data shown are the means of three independent experiments, with each sample tested in triplicate. * $p < 0.01$ compared with non-treated cells (free cells). Error bars indicate SE.

5.2.6 Binding of Alanine-substituted Synthetic Peptides of L2 to Laminin Receptor

Full length synthetic loop 2 was able to bind rLRP in ELISA experiments. To define the amino acids within OmpP2 loop 2 required for optimal rLRP binding 9

synthetic peptides (designated L2-1 to L2-9) were synthesized (Table 2.2). In each synthetic peptide a single amino acid was substituted with alanine (A). The ability of the derivative peptides to bind purified recombinant LRP protein was analyzed by ELISA. Synthetic peptides were immobilized in microtitre wells and rLRP added. Loops 1 and 4 of *N. meningitidis* PorA were included as negative and positive controls, respectively. After washing, bound rLRP was detected and quantified (Figure 5.7). Two of the peptides (L2-4; N94A, and L2-8; N98A) showed significantly reduced rLR-binding compared to wild-type loop 2 peptide. As expected, the control non-rLRP binding control peptide (PorA loop 1) also showed significantly less binding to rLRP compared to loop 2. The highest rLRP-binding was exhibited by positive control (PorA loop 4). Taken together our data suggested the key residue(s) mediating rLRP binding are the two asparagine (N) amino acids within the loop 2 sequence.

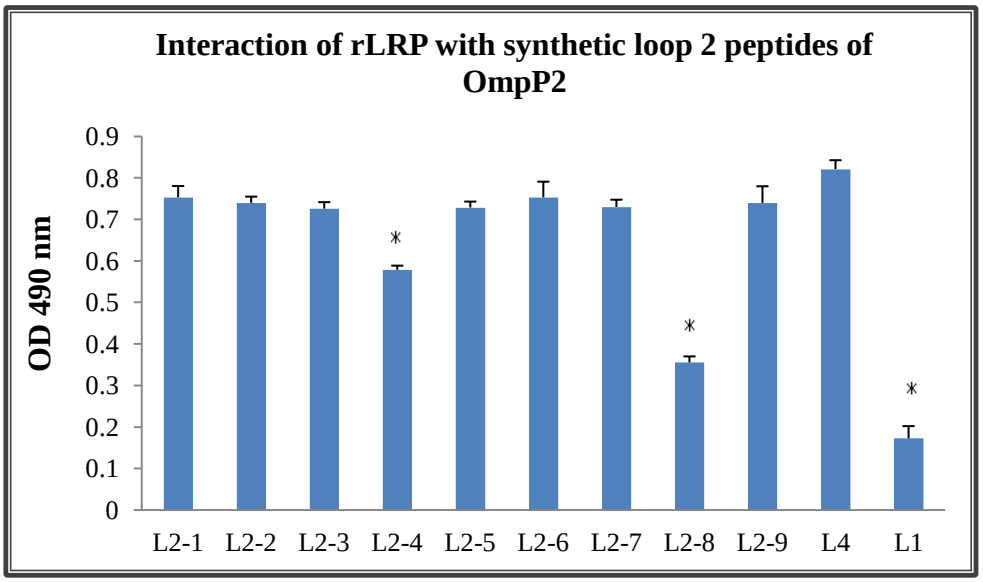

Figure 5.7. Binding of synthetic OmpP2 loop 2 and its derivatives to rLRP. Loop 2 (L2) and its alanine substitued varients (5 µM) were used to coat the wells of an ELISA plate and rLRP was added (5 µM). Following incubation, bound rLRP was detected with polyclonal rabbit anti-LR and then anti-rabbit IgG-AP antibodies. Synthetic peptides L4 and L1 of PorA were used as positive and negative control respectively. Specific binding was determined by subtracting the absorbance in BSA-coated wells from other wells. Each data point represents the means of three independent experiments, in each experiment each sample was tested in triplicate. * $p < 0.01$ compared with whole loop 2 (L2-1). Error bars indicate SE.

5.2.7 Variability of OmpP2 and its Loop 2 in *H. influenzae* Strains

Further analysis of the OmpP2 and loop 2 sequences was performed to determine the degree of conservation of these sequences among 50 sequence isolates of *H. influenzae* (Appendix 2A). OmpP2 was at least 62% identical among these isolates and 33 isolates were at least 80% identical (Appendix 2B-C). However, within the loop 2 region identity of 50% or more was found in only 20 sequences (Adppendix 2D-E). Furthermore, 4 typeable and 10 NTHi *H. influenzae* strains were examined; the identity of the loop 2 amino acids sequence was highly

conserved (98%) among the typable isolates compared to the NTHi isolates (76%) (Table 5.1).

Table 5.1. Amino acid sequences of loop 2 of OmpP2 among different *H. influenzae* strains

Strain	OmpP2 Loop 2 sequences	Ref.
H. influenzae type b Rd	TKASENGSDNFGDI	(Srikumar *et al.*, 1992b)
Hib DL42	TKASENGSDNFGDI	(Hansen *et al.*, 1989)
Hib ATCC 9795	TKASENGSDNPGDI	(Galdiero *et al.*, 2006)
Minna	TKASENGSDNFGDI	(Munson & Tolan, 1989)
Identity percentage for typeable strains	98.21%	
NTHi 12085	SAQSGTESDNFGHI	(Bell *et al.*, 1994)
NTHi 3232	SAQSGTESDNFGHI	(Bell *et al.*, 1994)
NTHi 2019	SAQSGTESDNFGHI	
NTHi 12	AAQSGTKSDDFGHI	(Bell *et al.*, 1994)
NTHi 12049	SSYDGENTDGFGGI	(Bell *et al.*, 1994)
NTHi 1479	SKASKEKADQFADI	(Sikkema & Murphy, 1992)
NTHi TN106	SAQSGTESDNFGHI	(Sanders *et al.*, 1993)
NTHi H05-19	SDASKNGSDNFGDI	(Sanders *et al.*, 1993)
NTHi H04-06	SDYTKKKSDHFGDI	(Sanders *et al.*, 1993)
NTHi H99-115	SAQSGTESDNFGHI	(Sanders *et al.*, 1993)
Identity percentage for NTHi strains	76.43%	

5.3 Discussion

Based on experimental data presented in previous chapters OmpP2 was shown to harbor a LRP-binding domain within the loop 2 region. Experiments were undertaken to further characterize the role of this region. Maximal rLRP binding was initially localized to the region between amino acids 91-99 (ASENGSDNF), which corresponds to loop 2. The ability of this sequence to bind rLRP and to epithelial and endothelial human cell was investigated. This was addressed by producing this region synthetically and incorporating a terminal cysteine residue at each end to form a bridge between the peptide ends and thus to stimulate the loop structure of this region within the native protein. Binding of the synthetic loop 2 to rLRP was tested in ELISA. Synthetic loops 1 and 4 of *N. meningitidis* PorA were used as negative and positive controls, respectively, as *N. meningitidis* PorA loop 4 had been shown previously to bind to rLRP, while no such activity was demonstrated for loop 1 (N. Abouseada, personal communication). OmpP2 loop 2 and PorA loop 4 both bound rLRP in these assays. The binding was statistically significant in comparison to the negative controls BSA or synthetic loop 1 of PorA.

In this study, HBMEC cells, which are known to express LamR at the cell surface, were used to address whether synthetic loop 2 of OmpP2 of *H. influenzae* was able to mediate adherence to these cells *in vitro*. Initially, confocal microscopy images showed that loop 2 but not BSA- coated beads were able to bind HBMECs. Furthermore, the loop 2-coated beads co-localised to 37LR or 67LR proteins. Subsequently, images were captured by light microscopy and binding of the

OmpP2, OmpP2ΔL2 and synthetic peptide-coated beads to the HBMEC monolayers were counted and then the adherence was analysed. Although the micro-beads adhesion assay showed that all protein and peptides-coated beads can adhere to the HBMECs, there were obvious differences among the adherence of these beads. Deletion of loop 2 from OmpP2 significantly reduced the binding to the cells. Additionally, the loop 2-coated micro-beads adhered at significantly higher levels compared to the negative control PorA loop 1 or scrambled loop 2. Taken together, the data suggest that loop 2 has the ability to interact with the HBMECs.

Adherence to respiratory epithelium is generally assumed to be the first step in carriage and the pathogenesis of diseases by encapsulated and nonencapsulated *H. influenzae* (van Alphen *et al.*, 1991b). The ability of bacteria to colonize their hosts and cause infection is often related to their ability to express several different adhesins with different receptor specificities (Scarselli *et al.*, 2006). Here, the potential roles of *H. influenzae* OmpP2 and its second loop in adhesion to, and invasion into, host cells was characterised using the HBMEC and HEp-2 cell models.

Experiments using HEp-2 cells were carried out five times for adhesion and three times for invasion. However, due to time and material constraints, adhesion and invasion experiments using HBMECs cells were carried out only twice and ideally they should be repeated at least three times at different occasions to allow statistical significance to be fully assessed. Wild type *H. influenzae* and its mutants: Δ*ompP2*, *ompP2*Δ*L2* and *ompP2::kanR* (control), were tested for their

ability to adhere to and invade HBMEC and HEp-2 cells. In both cell lines models the *ompP2::kanR* mutant strain of *H. influenzae* did not display a statistically significant difference in its ability to association with and invade HEp-2 or HBMEC cells compared to the wild type *H. influenzae*. Adherence of Δ*ompP2 H. influenzae* to monolayers of HEp-2 was significantly attenuated in comparison with both the wild type parent and the *ompP2::kanR* mutant strain ($p < 0.05$). However, adherence of *ompP2*Δ*L2* to HEp-2 was not statistically significantly reduced. This could be explained by the fact that residues outside of the deleted loop 2 of OmpP2 region may also play a role in adherence to these cells. While the adherence level to HBMECs was also lower than the wild type but this difference did not reach statistical significance. No significant changes in invasion were observed in either of the mutants.

Rho guanosine triphosphatases (Rho GTPases) are molecular switches that control a wide variety of regulation various cellular processes involving actin filaments, signal transduction pathways, and play a key role in the initiation and regulation of cell migration (Lemonnier *et al.*, 2007). Rho proteins play essential roles in host cell invasion by bacteria and GTP-binding proteins are major targets for bacterial toxins acting inside eukaryotic cells, these GTPases appear to be of major importance for the entry of bacteria into eukaryotic host cells (Aktories, 1997).

Here, the potential role of OmpP2 and its second loop in mediating activation of RhoA-GTP in HBMECs was investigated. To assess the activation, OmpP2 and OmpP2ΔL2 were purified under non-denaturing conditions from *H. influenzae*

and its *ompP2ΔL2* mutant derivative. HBMECs were treated with the purified proteins, as well as the synthetic loop 2. OmpP2 and OmpP2ΔL2 significantly increased the activated RhoA level. Deletion of loop 2 from OmpP2 decreased RhoA activation compared to OmpP2 but the difference was not significant. Activation of RhoA by synthetic loop 2 was not statistically significant. These data suggest that *H. influenzae* OmpP2 may contribute to activation of RhoA but the mechanism of this induction may not involve LamR, since the removal of the LamR-binding domain did not significantly reduce activation. Further work is needed to clarify this.

In the present work, the surface-exposed amino acid sequence of *H. influenzae* OmpP2 loop 2 was identified to be important for OmpP2 interaction with host cells. Substitution of amino acids within synthetic peptides corresponding to loop 2 identified the asparagine residues at positions L2-4 and L2-8 as being important for rLRP binding, which was reduced by 23% and 52% respectively in peptides in which these residues were replaced by alanine. Substitution of alanine for other amino acids within the loop 2 sequence had no significant effect on the binding. The surface-exposed epitopes of OmpP2 protein have been shown to vary markedly among NTHi strains. Sikkema and Murphy characterized the OmpP2 proteins from three NTHi strains and indicated that antigenic differences reside in four hypervariable regions of the porin protein (Sikkema & Murphy, 1992). In contrast analysis of nucleotide sequences of *ompP2* genes have demonstrated that the OmpP2 proteins of type b strains are conserved among strains (Munson *et al.*, 1989a; Munson & Tolan, 1989). Although NTHi strains are frequently implicated in non-invasive infections, Hib is a major cause of bacterial meningitis and other

invasive infection such as epiglottitis, osteomyelitis, septic arthritis, septicaemia, cellulitis, and pericarditis (Collee *et al.*, 1996; Peltola, 2000; William *et al.*, 2005). Our findings demonstrate that loop 2 is important for OmpP2-rLRP binding and this loop was identified to be conserved motif within the OmpP2 of Hib strains.

CHAPTER SIX: General Discussion

CHAPTER SIX

6. GENERAL DISCUSSION

Acute bacterial meningitis is one of the most severe infectious diseases, causing an estimated 171,000 deaths worldwide per year and neurologic sequelae in up to 30% of the survivors (Grimwood *et al.*, 1995; WHO, 2000). Until the introduction of conjugated vaccines, the leading agents of bacterial meningitis were *Haemophilus influenzae* type b (Hib), *Streptococcus pneumoniae*, and *Neisseria meningitidis* (Ceyhan *et al.*, 2008; Harvey *et al.*, 1999; Pong & Bradley, 1999).

In recent years, the introduction of modern methods of treatment, effective antibiotics and approved vaccines that targeted some serogroups of these meningeal pathogens has resulted in a significant decline in mortality (Harvey *et al.*, 1999; Bilukha *et al.*, 2005; Morris *et al.*, 2008). However, there is still a high incidence of meningitis which is caused by *S. pneumoniae*, Hib, and *N. meningitidis* (McVernon *et al.*, 2003a; Ceyhan *et al.*, 2008; Flores-Cordero *et al.*, 2003). Currently there is no available vaccine against *N. meningitidis* serogroup B, which is responsible for the majority of cases in the United States and Europe (Milonovich, 2007). It was documented that Hib causes at least three million cases of serious disease every year as well as approximately 386,000 deaths (WHO, 2006).

Hib conjugate vaccines, PRP-HbOC, PRP-OMP, PRP-T, PRP-D, have dramatically reduced the incidence of Hib. Nevertheless, failures have been reported in fully immunized infants in different areas, such as England, Ireland, Wales and Canada (Heath *et al.*, 2000; McVernon *et al.*, 2004a; Scheifele *et al.*,

2005). In addition, the vaccine for Hib is directed against its type-specific polysaccharide capsule, it has no ability to prevent infections caused by nonencapsulated NTHi (Foxwell *et al.*, 1998). Therefore, understanding interactions between bacteria and cells of the blood–brain and blood–CSF barrier may allow the development of new strategies to prevent meningitis by blocking bacterial adherence.

Hib is the most pathogenic of the six recognised capsular serotypes (a, b, c, d, e and f). *H. influenzae* pathogenesis begins with colonisation of the nasopharynx. This colonisation may be transitory or bacteria may remain for several months without affecting the host (asymptomatic carriage). Bacterial adherence to the respiratory epithelium represents a mechanism to circumvent clearance, whereas invasion into host cells and the mucosa of the upper respiratory tract may allow evasion of immune function and subsequent entry into the blood. The passage of bacteria through mucosal epithelium and penetration of sub-epithelial blood vessels represents a key step in the pathogenesis of meningitis. Entry of bacteria into the central nervous system requires passage across the blood-brain barrier (BBB). The major anatomical sites of the BBB are the cerebral microvascular endothelium of the arachnoid membrane and the choroid plexus epithelium (Polin & Harris, 2001). The attachment of bacteria to microvascular endothelial cells is promoted by receptors for these pathogens on endothelial cells (Stins *et al.*, 1994). Following attachment, bacteria gain entry to the central nervous system by disrupting tight junctions, active or passive movement across the endothelial cell, or carriage by leukocytes entering the nervous system (Leib & Tauber, 1999b; Tuomanen, 1996).

Outer membrane proteins (OMPs) of Gram-negative bacteria have diverse functions and are directly involved in the interaction with various environments encountered by pathogenic organisms. Thus, OMPs represent important virulence factors and play essential roles in bacterial adaptation to host niches, which are usually hostile to invading pathogens (Galdiero, 2007; Srikumar *et al.*, 1992b; Vachon *et al.*, 1985). Understanding the structure and functions of bacterial OMPs may facilitate the design of novel antimicrobial drugs and vaccines.

The LamR proteins role as a laminin receptor makes it an important molecule both in host cell adhesion to the basement membrane and in signal transduction following this binding event. In addition to these functions, LamR has additional roles. It was shown that the reduction of LamR expression reduced developing tumours in HT1080 human fibrosarcoma cell line (Scheiman *et al.*, 2010). Moreover, it was proposed that the suppression of 37LBP/p40 expression reduces tumour formation of lung cancer cells *in vivo* (Satoh *et al*., 1999). Also, LamR is known to be receptor to many virus and bacteria (Wang *et al.*, 1992; Thepparit & Smith, 2004; Huang & Jong, 2009). Understanding the molecular basis of these interactions will certainly increase our knowledge of bacterial pathogenesis and allow the development of new strategies to prevent diseases, such as meningitis caused by *H. influenzae* and others agents by blocking the adherence of the pathogens to their receptors.

The OmpP2 protein is a homotrimeric porin that constitutes approximately one-half of the total protein content of the outer membrane. Each monomer consists of 16 antiparallel β strands that spanning the outer membrane, eight short

periplasmic turns and eight outer loops of variable size (Galdiero *et al.*, 2003). The effect of loop 2 on LRP-binding of the whole bacterium was tested by deletion of the loop 2-region from *ompP2*. Flow cytometry, whole cell lysate pull-down assays and ELISA experiments showed that the interaction of *ompP2ΔL2* mutant *H. influenzae* to LamR was significantly reduced compared to the wild type. The recent published data showed that pneumococcus, meningococcus, and *H. influenzae* adhere to the BMECs via LamR, and the same study identified that the corresponding LamR-binding adhesins were CbpA, PilQ and PorA, and OmpP2 respectively (Orihuela *et al.*, 2009; Abouseada, 2009). These species target a common carboxy-terminal recognition site on LamR (amino acids 263–282), since antibodies recognizing this sequence or a peptide corresponding to LamR residues 263–282 could inhibit bacterial binding to microvascular endothelial cells. Moreover, it was identified that the CbpA LamR-binding region mapped to a highly conserved surface-exposed loop (residues ^{391}EPRNEEK^{397}) linking the second and third anti-parallel α-helices of the R2 domain. Pneumococci expressing a CbpAP392GR393G derivative showed significantly reduced binding to recombinant LamR and endothelial cells. Importantly, in a mouse model of pneumococcal meningitis, strains expressing CbpAP392G-R393G rarely caused meningitis compared to strains expressing wild-type CbpA (Orihuela *et al.*, 2009; Abouseada, 2009). Similarly, it was identified that the fourth extra-cellular loop of PorA was the LamR-binding domains of this protein (Abouseada, 2009). Residues 192-208 (AYTPAYYTKNTNNNLTL) in the apex of loop 4 were found to be particularly important for LamR-binding (Abouseada, 2009). In this study, the second extra-cellular loop of OmpP2 (amino acids

ASENGSDNF) was identified as the LamR-binding domain of this protein (Abouseada *et al.*, 2012). Increased knowledge of the structural motifs of bacterial ligands that interact with LamR may facilitate the design of therapeutic interventions which could disrupt or modulate the interaction of neuroinvasive bacteria with LamR and engender protection against bacterial meningitis.

To define the region(s) of OmpP2 that are responsible for binding of the protein to LamR, a series of OmpP2 truncated proteins were characterized and assessed for rLRP binding. The *ompP2* mutant *H. influenzae* Rd KW20 was provided from a different laboratory (J. Reidl and J. McCullers) and, although it was the same strain as the wild type available in our laboratory, it is possible that different passage histories of these isolates may have led to changes in the genetic background in addition to the defined mutation. Therefore, we generated a new *ompP2* mutant using our own stock of *H. influenzae* Rd. All the mutated cells showed similar growth rate to the wild type *H. influenzae*. In addition, the truncated OmpP2 was still able to localise to the outer membrane. This is in agreement with the findings of a study performed to investigate the role of surface-exposed loops of OmpA in *E. coli*, as the deletion of specific loops from the whole protein did not hinder its assembling into the outer membrane of the bacterial cells (Koebnik, 1999). In the current study, we obtained three lines of evidence: flow cytometry and whole cell lysate pull-down assay as well as ELISA that the binding domain responsible for adherence of *H. influenzae* to rLRP resides within the second loop 2 of OmpP2.

It is known that surface-exposed loops L1, L2, and L4 of OmpP2 of *H. influenzae* are important for monomer-monomer interactions within the porin trimer; loop L3 is internal; loops L5, L6, and L7 are superficial; loop L8 contributes to form the channel opening on the external side (Galdiero *et al.*, 2006; Galdiero *et al.*, 2003). In addition, these loops were identified to have several functions during pathogenesis. By utilising seven murine monoclonal anti-Hib porin antibodies, the surface-exposed epitopes loops 4 and 8 were identified as antigenic determinants on Hib porin (Srikumar *et al.*, 1992a). In another study, Haase *et al.* proposed that the surface-exposed loops L5 and L8 of the OmpP2 of the NTHi are potentially an immunodominant region of the molecule (Haase *et al.*, 1994). Accordingly, Yi and Murphy published that a MAb specific for loop 5 of the OmpP2 molecule was bactericidal and a mutant with minor amino acid changes in this loop lost susceptibility to this bactericidal activity (Yi & Murphy, 1994). It was shown that immunizing rabbits with peptides corresponding to a conserved loop 6 sequence of the gene that encodes the P2 porin of NTHi results in bactericidal activity against multiple strains (Neary & Murphy, 2006).

Prior to employing the *H. influenzae* mutants in association and invasion experiments, *in vitro* assessment of synthetic loop 2 peptide, recombinant OmpP2 and OmpP2ΔL2 was undertaken to determine whether they can bind directly to the HBMECs using coated micro-beads in an adhesion assay. Data showed that loop 2 is essential for OmpP2 to interact with HBMECs. Since loop 2 peptide-coated beads adhered to the HBMECs. In addition, deletion of loop 2 from OmpP2 significantly reduced its interaction to the HBMECs in comparison to the whole OmpP2-coated beads. To investigate OmpP2 and the contribution made by

loop 2 to *H. influenzae* colonization, the various strains of the *H. influenzae* were compared in an *in vitro* cell infection model for their ability to adhere to and invade into HEp-2 and HBMECs. Both *H. influenzae* mutant strains (ΔOmpP2 and OmpP2ΔL2) were consistently impaired in their ability to adhere to and invade into HBMECs and HEp-2 cells compared to *H. influenzae* wild-type strain. The adherence level of the ΔOmpP2 mutants to HEp-2 (but not HBMECs) was significantly reduced when compared to the parental strain. Although the invasion rate of ΔOmpP2 and OmpP2ΔL2 mutant strains to either HBMECs or HEp-2 cell lines model was less than the parental strain, it was not statistically significant. It is perhaps not surprising since a variety of bacterial factors, such as the polysaccharide capsule, the lipooligosaccharide (LOS), pili, HMW1, influence *H. influenzae* adherence to and entry into mammalian cells (van Alphen *et al.*, 1991b; van Alphen & van Ham, 1994; Noel *et al.*, 1994; van Alphen *et al.*, 1996).

Deletion of loop 2 (Ala91-Phe99) from OmpP2 significantly reduced its interaction with rLRP (Abouseada *et al.*, 2012). Thus, these amino acids are pivotal in the ability of the OmpP2 to bind to rLRP. Therefore, it is likely that possession of this loop plays an important role in the pathogenesis of *H. influenzae*. To further study the role of OmpP2 and its loop 2 to activate RhoA in HBMECs was investigated using a G-LISA^{TM} assay. This was based on the previously published data proposing that the CNF1 interaction with 37-kDa LRP is the initial step required for CNF1-mediated RhoA activation and *E. coli* K1 uptake in HBMECs cells (Chung *et al.*, 2003). Furthermore, in a separate study, the region(s) of CNF1 that are responsible for binding to LRP were investigated; two receptor-binding domains were identified, the first located in the N terminus

(amino acids 135 to 164) and the second located in the C-terminal portion of CNF1 (amino acids 683 to 730) (Rieger *et al.*, 1997). G-LISA™ assay was employed in order to assess the ability of OmpP2 and its loop 2 in activation the RhoA-GTP in the HBMECs. Despite the fact that synthetic loop 2 peptide and both recombinant OmpP2 and OmpP2ΔL2 protein activated the RhoA-GTP, the activation was not statistically significant compared with non-treated HBMECs cells. In addition, no significant differences in RhoA activation were observed between HBMECs cells treated with OmpP2 or OmpP2ΔL2, indicating that OmpP2L2 has little effect on RhoA activation.

Bacterial pathogens utilize several strategies to modulate the organization of the actin cytoskeleton. Some bacterial toxins catalyze the covalent modification of actin or the Rho GTPases, which are involved in the control of the actin cytoskeleton (Barbieri *et al.*, 2002). In one study, invasion of HBMECs by *E. coli* K1 was found to be mediated by RhoA activation and subsequent remodelling of the host-cell actin cytoskeleton; a Δ*cnf1* mutant caused decreased RhoA activation and invasion HBMECs compared to its wild type parent (Khan *et al.*, 2002). CNF-1 activates Rho, Rac, and Cdc42 by deamidating Gln-63 (of Rho) or Gln-61 (Rac and CDC42), converting a Gln to a glutamate (Hopkins *et al.*, 2003). Deamination of glutamine 63 or 61 locks the intrinsic or the GTPase activating protein (GAP)-induced hydrolysis of GTP leading to the permanent activation of the GTPase (Boquet, 2001).

To further determine the exact site of the interaction between the LamR and loop 2, several synthetic peptides corresponding to OmpP2 loop 2-region were

synthesised, in each one a single amino acid was substituted with alanine (Table 2.2). These synthetic peptides were analysed by ELISA assay for their ability to bind rLRP. Two of the mutated loop 2 peptides (L2-4, L2-8), in both of which the asparagine was replaced to alanine, showed markedly less interaction to rLRP comparing to the original loop 2.

Extracellular loops of outer membrane porins, including OmpP2, contribute to the pathogenesis of bacteria (Neary & Murphy, 2006; Severino *et al.*, 2010; Maruvada & Kim, 2011). It was found that loop L7 or porin OmpP2 intravenous injection induced an increased release of IL-6 and TNF-α and elicited hyperglycaemia (Vitiello *et al.*, 2008). Thus, OmpP2 loop 2 bears the potential for being a suitable vaccine candidate, but the effect of the variability of this loop on *H. influenzae* binding to LamR has to be evaluated before considering loop 2 for vaccine production.

One reason of the fact that the pathogen can reinfect the host despite a prior immune response to other strains of the same organism is due to variations within the surface-exposed hypervariable regions. Thus the organism can evade the immune system (Brunham *et al.*, 1993). The ability of NTHi to cause recurrent infections is in part attributable to antigenic variability in several surface-exposed loops of major OmpP2 (Bell *et al.*, 1994; Sikkema & Murphy, 1992). The surface-exposed epitopes of OmpP2 protein are variable among NTHi strains, whereas OmpP2 proteins of type b strains are conserved among strains (Munson *et al.*, 1989a; Munson & Tolan, 1989). The derived amino acid sequences of the OmpP2 proteins from the eight *H. influenzae* strains were aligned (7 NTHi and the

OmpP2 sequence from the serotype b strain MinnA). The amino acid identity was between 76% and 94%. The OmpP2 proteins from the NTHi strains were 79% to 84% identical to the OmpP2 protein from *H. influenzae* type b strain MinnA (Bell *et al.*, 1994). These amino acid changes resulted in altered reactivity of murine monoclonal antibodies directed against a surface exposed epitope in the L4 loop of OmpP2 (Bell *et al.*, 1994).

Work by van Alphen and colleagues, has demonstrated that regions of the *ompP2* gene encoding surface exposed loops undergo point mutations under immune selective pressure (van Alphen *et al.*, 1991a). This observation raises the possibility that point mutations could occur in conserved loops targeted as vaccine antigens and render a vaccine useless (van Alphen *et al.*, 1991a; Duim *et al.*, 1996).

Comparison of the sequences of the *ompP2* genes of various nonencapsulated *H. influenzae* strains revealed highly conserved sequences coding for the membrane-spanning regions and highly variable sequences coding for surface-exposed loops (Sikkema & Murphy, 1992). Therefore, the antibodies against these peptides will be only strain-specific. Using OmpP2 as an immunogen against *H. influenzae*-induced infection would likely ultimately prove to be problematic for all the above cited reasons. To overcome this obstacle, conserved antigenic domains within these proteins and/or use multiple short linear peptides could be used. In the current study, sequences of OmpP2 and its second loop from different *H. influenzae* strains were analysed and it was revealed that the amino acid identity of OmpP2 was 62% conserved among all analysed strains and more than 80%

among 33 of the 50 isolates examined. However, the amino acids sequences of loop 2 of OmpP2 among strains were highly variable. Additional analysis showed that the amino acid sequences were highly conserved among typeable *H. influenzae* strains (98.21%) while it was more variable among NTHi strains (76.43%). The second asparagine residues in loop 2 sequence (L2-8; N98A), which was found to be important for rLRP binding, is only present in the sequence of around 50% (26 of 50) OmpP2 sequences. Hib is responsible for most invasive infections (90%) such as meningitis, but NTHi is responsible for 10% of the invasive infections such as epiglottitis, septic arthritis, osteomyelitis, pneumonia and cellulitis and it is responsible for about 90% of noninvasive diseases such as otitis media, sinusitis and conjunctivitis (Slack, 2007). Hence, these findings may be useful in the development of alternative therapies aimed at reducing excessive inflammatory responses during Hib infections.

In conclusion, this study has shown that the second surface-exposed loop of OmpP2 is the most significant region that contributes to binding to LRP. Moreover, recombinant OmpP2 and its synthesised loop 2 were shown to bind directly to HBMECs. We also showed that this loop plays a role in the interaction of *H. influenzae* with rLRP. However, OmpP2 and its second loop did not contribute significantly in the adhesion to and invasion of HEp-2 and HBMECs cell lines by *H. influenzae*, suggesting that there are different factors are mediating host cells adhering and invasion. The importance of these newly identified results may lead to a better understanding of the mechanism of host-pathogen interaction and in turn to the development of potential vaccines to prevent infection.

Future Directions

This study has provided greater insights into the role of outer membrane extracellular loops of the *H. influenzae* porin OmpP2 in LamR-binding. Further study is needed to map region(s) of LamR to which loop 2 of OmpP2 binds. Truncated protein fragments of LamR can be generated and purified and their binding to loop 2 studied. Moreover, inhibition assays can be performed to assess whether loop 2 can inhibit the LamR-binding of *H. influenzae* and other meningeal pathogens. Two residues of loop 2 were found to be especially important for the interaction; to identify whether these residues are important in the context of the whole organism, new mutant strains with these two residues substituted could be generated and their binding to LamR can be investigated.

Although this study has demonstrated the central role of OmpP2, and specifically its second extracellular loop, for LamR-binding, the *ompP2* knockout strain retained residual LamR binding activity. This may suggest there is another binding protein, reminiscent of the situation in *N. meningitidis*, in which two distinct LamR-binding proteins have been described. In future experiments, different independent approaches, such as cross-linking or immunoprecipation, may facilitate identification of such protein(s).

It will be necessary to determine what role loop 2 plays during infection. The *in vivo* mouse model of *H. influenzae* type b meningitis may be useful in this respect, although it should be noted that the murine model will not necessarily reflect the situation in human patients in all details. Additional *in vitro* assays employing

human cells might also be useful in determining the role of this region in infection.

OmpP2 loop 2 region is found to be important for LamR-bacteria binding and thus loop 2 bears the potential for being a suitable vaccine candidate as antibodies directed against this region may block the LamR-bacterial interaction, which could prevent adhesion or invasion of the BBB by the *H. influenzae* and thus prevent bacterial meningitis. As the loop is surface-accessible, it might also be a target for bactericidal antibodies. Bactericidal assays should be performed using bacteria grown under *in vivo* conditions (in the mouse model for example) and antibodies raised against the loop 2 could be assessed for serum bactericidal activity.

Given that loop 2 is expressed by a wide range of isolates and is highly conserved, among Hib strains, but variable among NTHi strains, it will be of interest to investigate and compare the LamR-binding of the equivalent loop in different strains of typeable *H. influenzae* and NTHi. Furthermore, further studies are required to evaluate the possible consequences of LamR binding by loop 2 in signal transduction cascades occurring after bacterial association with host cells.

BIBLIOGRAPHY

BIBLIOGRAPHY

Abouseada, N.M., M.S. Assafi, J. Mahdavi, N.J. Oldfield, L.M. Wheldon, K.G. Wooldridge & D.A. Ala'aldeen, (2012) Mapping the Laminin Receptor Binding Domains of Neisseria meningitidis PorA and Haemophilus influenzae OmpP2. *PloS one* **7**: e46233.

Abouseada, N.M.A., (2009) Role of 37/67-kDa laminin receptor in binding of bacteria causing meningitis. Doctor of Philosophy PhD Thesis. The Universirty of Nottingham, pp.

Adhikari, M., Y.M. Coovadia & D. Singh, (1995) A 4-year study of neonatal meningitis: clinical and microbiological findings. *J Trop Pediatr* **41**: 81-85.

Akache, B., D. Grimm, K. Pandey, S.R. Yant, H. Xu & M.A. Kay, (2006) The 37/67-kilodalton laminin receptor is a receptor for adeno-associated virus serotypes 8, 2, 3, and 9. *J Virol* **80**: 9831-9836.

Aktories, K., (1997) Rho proteins: targets for bacterial toxins. *Trends Microbiol* **5**: 282-288.

al-Saleh, W., P. Delvenne, F.A. van den Brule, S. Menard, J. Boniver & V. Castronovo, (1997) Expression of the 67 KD laminin receptor in human cervical preneoplastic and neoplastic squamous epithelial lesions: an immunohistochemical study. *J Pathol* **181**: 287-293.

Andersen, C., E. Maier, G. Kemmer, J. Blass, A.-K. Hilpert, R. Benz & J. Reidl, (2003) Porin OmpP2 of *Haemophilus influenzae* Shows Specificity for Nicotinamide-derived Nucleotide Substrates. *J. Biol. Chem.* **278**: 24269-24276.

Anderson, P., D.L. Ingram, M.E. Pichichero & G. Peter, (2000) A high degree of natural immunologic priming to the capsular polysaccharide may not prevent *Haemophilus influenzae* type b meningitis. *The Pediatric infectious disease journal* **19**: 589-591.

Ardini, E., G. Pesole, E. Tagliabue, A. Magnifico, V. Castronovo, M.E. Sobel, M.I. Colnaghi & S. Menard, (1998) The 67-kDa laminin receptor originated from a ribosomal protein that acquired a dual function during evolution. *Mol Biol Evol* **15**: 1017-1025.

Auth, D. & G. Brawerman, (1992) A 33-kDa polypeptide with homology to the laminin receptor: component of translation machinery. *Proceedings of the National Academy of Sciences of the United States of America* **89**: 4368-4372.

Bar-Zeev, N. & J.P. Buttery, (2006) Combination conjugate vaccines. *Expert Opin Drug Saf* **5**: 351-360.

Barbieri, J.T., M.J. Riese & K. Aktories, (2002) Bacterial toxins that modify the actin cytoskeleton. *Annu Rev Cell Dev Biol* **18**: 315-344.

Barenkamp, S.J., (1996) Immunization with high-molecular-weight adhesion proteins of nontypeable *Haemophilus influenzae* modifies experimental otitis media in chinchillas. *Infection and immunity* **64**: 1246-1251.

Barenkamp, S.J. & J.W. St Geme, 3rd, (1994) Genes encoding high-molecular-weight adhesion proteins of nontypeable *Haemophilus influenzae* are part of gene clusters. *Infection and Immunity* **62**: 3320-3328.

Barenkamp, S.J. & J.W. St Geme, 3rd, (1996) Identification of a second family of high-molecular-weight adhesion proteins expressed by non-typable *Haemophilus influenzae*. *Molecular microbiology* **19**: 1215-1223.

Barsky, S.H., C.N. Rao, J.E. Williams & L.A. Liotta, (1984) Laminin molecular domains which alter metastasis in a murine model. *The Journal of clinical investigation* **74**: 843-848.

Bedford, H., J. de Louvois, S. Halket, C. Peckham, R. Hurley & D. Harvey, (2001) Meningitis in infancy in England and Wales: follow up at age 5 years. *BMJ* **323**: 533-536.

Bell, J., S. Grass, D. Jeanteur & R.S. Munson, Jr., (1994) Diversity of the P2 protein among nontypeable *Haemophilus influenzae* isolates. *Infection and immunity* **62**: 2639-2643.

Ben, R.J., S. Kung, F.Y. Chang, J.J. Lu, N.H. Feng & Y.D. Hsieh, (2008) Rapid diagnosis of bacterial meningitis using a microarray. *J Formos Med Assoc* **107**: 448-453.

Bertani, G., (2004) Lysogeny at mid-twentieth century: P1, P2, and other experimental systems. *J Bacteriol* **186**: 595-600.

Bilukha, O., R.A. Hahn, A. Crosby, M.T. Fullilove, A. Liberman, E. Moscicki, S. Snyder, F. Tuma, P. Corso, A. Schofield & P.A. Briss, (2005) The

effectiveness of early childhood home visitation in preventing violence: a systematic review. *Am J Prev Med* **28**: 11-39.

Bisgard, K.M., A. Kao, J. Leake, P.M. Strebel, B.A. Perkins & M. Wharton, (1998) *Haemophilus influenzae* invasive disease in the United States, 1994-1995: near disappearance of a vaccine-preventable childhood disease. *Emerging infectious diseases* **4**: 229-237.

Black, S.B., H.R. Shinefield, B. Fireman, R. Hiatt, M. Polen & E. Vittinghoff, (1991) Efficacy in infancy of oligosaccharide conjugate *Haemophilus influenzae* type b (HbOC) vaccine in a United States population of 61,080 children. The Northern California Kaiser Permanente Vaccine Study Center Pediatrics Group. *The Pediatric infectious disease journal* **10**: 97-104.

Booy, R., S. Hodgson, L. Carpenter, R.T. Mayon-White, M.P. Slack, J.A. Macfarlane, E.A. Haworth, M. Kiddle, S. Shribman, J.S. Roberts & et al., (1994) Efficacy of *Haemophilus influenzae* type b conjugate vaccine PRP-T. *Lancet* **344**: 362-366.

Booy, R., S.A. Hodgson, M.P. Slack, E.C. Anderson, R.T. Mayon-White & E.R. Moxon, (1993) Invasive *Haemophilus influenzae* type b disease in the Oxford region (1985-91). *Arch Dis Child* **69**: 225-228.

Boquet, P., (2001) The cytotoxic necrotizing factor 1 (CNF1) from *Escherichia coli*. *Toxicon : official journal of the International Society on Toxinology* **39**: 1673-1680.

Bortoluzzi, S., F. d'Alessi, C. Romualdi & G.A. Danieli, (2001) Differential expression of genes coding for ribosomal proteins in different human tissues. *Bioinformatics* **17**: 1152-1157.

Brouwer, M.C., A.R. Tunkel & D. van de Beek, (2010) Epidemiology, diagnosis, and antimicrobial treatment of acute bacterial meningitis. *Clin Microbiol Rev* **23**: 467-492.

Bruant, G., N. Gousset, R. Quentin & A. Rosenau, (2002) Fimbrial *ghf* Gene Cluster of Genital Strains of Haemophilus spp. *Infection and immunity* **70**: 5438-5445.

Brunham, R.C., F.A. Plummer & R.S. Stephens, (1993) Bacterial antigenic variation, host immune response, and pathogen-host coevolution. *Infect Immun* **61**: 2273-2276.

Bulkow, L.R., R.B. Wainwright, G.W. Letson, S.J. Chang & J.I. Ward, (1993) Comparative immunogenicity of four *Haemophilus influenzae* type b conjugate vaccines in Alaska Native infants. *The Pediatric infectious disease journal* **12**: 484-492.

Buto, S., E. Tagliabue, E. Ardini, A. Magnifico, C. Ghirelli, F. van den Brule, V. Castronovo, M.I. Colnaghi, M.E. Sobel & S. Menard, (1998) Formation of the 67-kDa laminin receptor by acylation of the precursor. *J Cell Biochem* **69**: 244-251.

Campagne, G., A. Schuchat, S. Djibo, A. Ousseini, L. Cisse & J.P. Chippaux, (1999) Epidemiology of bacterial meningitis in Niamey, Niger, 1981-96. *Bull World Health Organ* **77**: 499-508.

Campbell, H., R. Borrow, D. Salisbury & E. Miller, (2009) Meningococcal C conjugate vaccine: the experience in England and Wales. *Vaccine* **27 Suppl 2**: B20-29.

Castronovo, V., (1993) Laminin receptors and laminin-binding proteins during tumor invasion and metastasis. *Invasion Metastasis* **13**: 1-30.

Castronovo, V., G. Taraboletti & M.E. Sobel, (1991) Functional domains of the 67-kDa laminin receptor precursor. *The Journal of biological chemistry* **266**: 20440-20446.

CDC, (2002) Centers for Disease Control and Prevention. Progress toward elimination of *Haemophilus influenzae* type b invasive disease among infants and children: United States, 1998–2000. MMWR Morb Mortal Wkly Rep. **51**: 234-239.

Ceyhan, M., I. Yildirim, P. Balmer, R. Borrow, B. Dikici, M. Turgut, N. Kurt, A. Aydogan, C. Ecevit, Y. Anlar, O. Gulumser, G. Tanir, N. Salman, N. Gurler, N. Hatipoglu, M. Hacimustafaoglu, S. Celebi, Y. Coskun, E. Alhan, U. Celik, Y. Camcioglu, G. Secmeer, D. Gur & S. Gray, (2008) A prospective study of etiology of childhood acute bacterial meningitis, Turkey. *Emerging infectious diseases* **14**: 1089-1096.

Chang, C.J., W.N. Chang, L.T. Huang, S.C. Huang, Y.C. Chang, P.L. Hung, C.H. Lu, C.S. Chang, B.C. Cheng, P.Y. Lee, K.W. Wang & H.W. Chang, (2004) Bacterial meningitis in infants: the epidemiology, clinical features, and prognostic factors. *Brain Dev* **26**: 168-175.

Chapnik, N., H. Sherman & O. Froy, (2008) A one-tube site-directed mutagenesis method using PCR and primer extension. *Anal Biochem* **372**: 255-257.

Chaudhuri, J.D., (2000) Blood brain barrier and infection. *Medical science monitor : international medical journal of experimental and clinical research* **6**: 1213-1222.

Chen, X.L. & L. Jiang, (2011) Recurrent bacterial meningitis caused by an occult basilar skull fracture. *World J Pediatr* **7**: 179-181.

Chiba, N., S.Y. Murayama, M. Morozumi, E. Nakayama, T. Okada, S. Iwata, K. Sunakawa & K. Ubukata, (2009) Rapid detection of eight causative pathogens for the diagnosis of bacterial meningitis by real-time PCR. *Journal of infection and chemotherapy : official journal of the Japan Society of Chemotherapy* **15**: 92-98.

Chong, P., Y.P. Yang, R. Fahim, P. McVerry, C. Sia & M. Klein, (1993) Immunogenicity of overlapping synthetic peptides covering the entire sequence of *Haemophilus influenzae* type b outer membrane protein P2. *Infection and immunity* **61**: 2653-2661.

Chung, J.W., S.J. Hong, K.J. Kim, D. Goti, M.F. Stins, S. Shin, V.L. Dawson, T.M. Dawson & K.S. Kim, (2003) 37-kDa laminin receptor precursor modulates cytotoxic necrotizing factor 1-mediated RhoA activation and bacterial uptake. *The Journal of biological chemistry* **278**: 16857-16862.

Claesson, B.A., (1993) Epidemiology of invasive *Haemophilus influenzae* type b disease in Scandinavia. *Vaccine* **11 Suppl 1**: S30-33.

Collee, J.G., A.G. Fraser, B.P. Marmion & A. Simmons, (1996) *Mackie and MacCarty Practical Medical Microbiology*. Churchill Livingstone.

Cope, L.D., S.E. Pelzel, J.L. Latimer & E.J. Hansen, (1990) Characterization of a mutant of *Haemophilus influenzae* type b lacking the P2 major outer membrane protein. *Infection and immunity* **58**: 3312-3318.

Coutinho, A. & G. Moller, (1973) Mitogenic properties of the thymus-independent antigen pneumococcal polysaccharide S3. *European journal of immunology* **3**: 608-613.

Cowgill, K.D., M. Ndiritu, J. Nyiro, M.P. Slack, S. Chiphatsi, A. Ismail, T. Kamau, I. Mwangi, M. English, C.R. Newton, D.R. Feikin & J.A. Scott, (2006) Effectiveness of *Haemophilus influenzae* type b Conjugate vaccine introduction into routine childhood immunization in Kenya. *JAMA* **296**: 671-678.

Cown, K. & K.P. Talaro, (2009) *Microbiology a System Approach*. McGraw-Hill Companies, Inc.

Crosson, F.J., Jr., J.A. Winkelstein & E.R. Moxon, (1976) Participation of complement in the nonimmune host defense against experimental *Haemophilus influenzae* type b septicemia and meningitis. *Infection and immunity* **14**: 882-887.

Cutter, D., KathrynÂ W. Mason, AlanÂ P. Howell, DoranÂ L. Fink, BruceÂ A. Green & JosephÂ W. St.Â GemeÂ Iii, (2002) Immunization with *Haemophilus influenzae* Hap Adhesin Protects against Nasopharyngeal Colonization in Experimental Mice. *The Journal of infectious diseases* **186**: 1115-1121.

Daly, J.A., W.M. Gooch, 3rd & J.M. Matsen, (1985) Evaluation of the Wayson variation of a methylene blue staining procedure for the detection of microorganisms in cerebrospinal fluid. *Journal of clinical microbiology* **21**: 919-921.

Danner, D.B., H.O. Smith & S.A. Narang, (1982) Construction of DNA recognition sites active in Haemophilus transformation. *Proceedings of the National Academy of Sciences of the United States of America* **79**: 2393-2397.

Dawid, S., S. Grass & J.W. St Geme, 3rd, (2001) Mapping of binding domains of nontypeable *Haemophilus influenzae* HMW1 and HMW2 adhesins. *Infection and immunity* **69**: 307-314.

Daza, P., R. Banda, K. Misoya, A. Katsulukuta, B.D. Gessner, R. Katsande, B.R. Mhlanga, J.E. Mueller, C.B. Nelson, A. Phiri, E.M. Molyneux & M.E. Molyneux, (2006) The impact of routine infant immunization with *Haemophilus influenzae* type b conjugate vaccine in Malawi, a country with high human immunodeficiency virus prevalence. *Vaccine* **24**: 6232-6239.

de Louvois, J., J. Blackbourn, R. Hurley & D. Harvey, (1991) Infantile meningitis in England and Wales: a two year study. *Arch Dis Child* **66**: 603-607.

Dery, M.A. & R. Hasbun, (2007) Changing epidemiology of bacterial meningitis. *Current infectious disease reports* **9**: 301-307.

Doran, L.F., Z.B. Amy, G. Bruce, F. Phillip & W.S.G. Joseph, (2003) The *Haemophilus influenzae* Hap autotransporter mediates microcolony formation and adherence to epithelial cells and extracellular matrix via

binding regions in the C-terminal end of the passenger domain. *Cellular microbiology* **5**: 175-186.

Duim, B., L. Vogel, W. Puijk, H.M. Jansen, R.H. Meloen, J. Dankert & L. van Alphen, (1996) Fine mapping of outer membrane protein P2 antigenic sites which vary during persistent infection by *Haemophilus influenzae*. *Infection and immunity* **64**: 4673-4679.

Durand, M.L., S.B. Calderwood, D.J. Weber, S.I. Miller, F.S. Southwick, V.S. Caviness, Jr. & M.N. Swartz, (1993) Acute bacterial meningitis in adults. A review of 493 episodes. *N Engl J Med* **328**: 21-28.

Edwards, J.S. & B.O. Palsson, (1999) Systems properties of the *Haemophilus influenzae* Rd metabolic genotype. *The Journal of biological chemistry* **274**: 17410-17416.

Fernaays, M.M., A.J. Lesse, X. Cai & T.F. Murphy, (2006) Characterization of *igaB*, a Second Immunoglobulin A1 Protease Gene in Nontypeable *Haemophilus influenzae*. *Infection and immunity* **74**: 5860-5870.

Fink, D.L., L.D. Cope, E.J. Hansen & J.W. St. Geme, III, (2001) The *Haemophilus influenzae* Hap autotransporter is a chymotrypsin clan serine protease and undergoes autoproteolysis via an intermolecular mechanism. *J. Biol. Chem.*: M106913200.

Fink, D.L., B.A. Green & J.W. St. Geme Iii, (2002) The *Haemophilus influenzae* Hap Autotransporter Binds to Fibronectin, Laminin, and Collagen IV. *Infection and immunity* **70**: 4902-4907.

Fitzgerald, M., M. Canny & D. O'Flanagan, (2005) Vaccination catch-up campaign in response to recent increase in Hib infection in Ireland. *Euro Surveill* **10**: E050929 050922.

Flatau, G., E. Lemichez, M. Gauthier, P. Chardin, S. Paris, C. Fiorentini & P. Boquet, (1997) Toxin-induced activation of the G protein p21[thinsp]Rho by deamidation of glutamine. *Nature* **387**: 729-733.

Fleischmann, R.D., M.D. Adams, O. White, R.A. Clayton, E.F. Kirkness, A.R. Kerlavage, C.J. Bult, J.F. Tomb, B.A. Dougherty, J.M. Merrick & et al., (1995) Whole-genome random sequencing and assembly of *Haemophilus influenzae* Rd. *Science* **269**: 496-512.

Flores-Cordero, J.M., R. Amaya-Villar, M.D. Rincon-Ferrari, S.R. Leal-Noval, J. Garnacho-Montero, A.C. Llanos-Rodriguez & F. Murillo-Cabezas, (2003)

Acute community-acquired bacterial meningitis in adults admitted to the intensive care unit: clinical manifestations, management and prognostic factors. *Intensive Care Med* **29**: 1967-1973.

Fogarty, J., A.C. Moloney & J.B. Newell, (1995) The epidemiology of *Haemophilus influenzae* type b disease in the Republic of Ireland. *Epidemiology and infection* **114**: 451-463.

Fontanini, G., S. Vignati, S. Chine, M. Lucchi, A. Mussi, C.A. Angeletti, S. Menard, V. Castronovo & G. Bevilacqua, (1997) 67-Kilodalton laminin receptor expression correlates with worse prognostic indicators in non-small cell lung carcinomas. *Clin Cancer Res* **3**: 227-231.

Foxwell, A.R., J.M. Kyd & A.W. Cripps, (1998) Nontypeable *Haemophilus influenzae*: pathogenesis and prevention. *Microbiology and molecular biology reviews : MMBR* **62**: 294-308.

Galdiero, M., M. D'Amico, F. Gorga, C. Di Filippo, M. D'Isanto, M. Vitiello, A. Longanella & A. Tortora, (2001) *Haemophilus influenzae* Porin Contributes to Signaling of the Inflammatory Cascade in Rat Brain. *Infection and immunity* **69**: 221-227.

Galdiero, M., E. Finamore, F. Rossano, M. Gambuzza, M.R. Catania, G. Teti, A. Midiri & G. Mancuso, (2004) *Haemophilus influenzae* porin induces Toll-like receptor 2-mediated cytokine production in human monocytes and mouse macrophages. *Infection and immunity* **72**: 1204-1209.

Galdiero, S., D. Capasso, M. Vitiello, M. D'Isanto, C. Pedone & M. Galdiero, (2003) Role of surface-exposed loops of *Haemophilus influenzae* protein P2 in the mitogen-activated protein kinase cascade. *Infection and immunity* **71**: 2798-2809.

Galdiero, S., Galdiero, M. & Pedone, C. , (2007) Beta-barrel membrane bacterial proteins: structure, function, assembly and interaction with lipids. . *Curr.Protein Pept. Sci. 8, 63–82* **8**: 63–82.

Galdiero, S., M. Vitiello, P. Amodeo, M. D'Isanto, M. Cantisani, C. Pedone & M. Galdiero, (2006) Structural requirements for proinflammatory activity of porin P2 Loop 7 from *Haemophilus influenzae*. *Biochemistry* **45**: 4491-4501.

Galiza, E.P. & P.T. Heath, (2009) Improving the outcome of neonatal meningitis. *Curr Opin Infect Dis* **22**: 229-234.

Garcia-Hernandez, M., E. Davies & P.E. Staswick, (1994) Arabidopsis p40 homologue. A novel acidic protein associated with the 40 S subunit of ribosomes. *The Journal of biological chemistry* **269**: 20744-20749.

Garner, D. & V. Weston, (2003) Effectiveness of vaccination for *Haemophilus influenzae* type b. *Lancet* **361**: 395-396.

Garpenholt, O., S. Hugosson, H. Fredlund, J. Giesecke & P. Olcen, (2000) Invasive disease due to *Haemophilus influenzae* type b during the first six years of general vaccination of Swedish children. *Acta Paediatr* **89**: 471-474.

Garty, B., S. Berliner, E. Liberman & Y. Danon, (1997) Cerebrospinal fluid leukocyte aggregation in meningitis. *The Pediatric infectious disease journal* **16**: 647-651.

Gauczynski, S., D. Nikles, S. El-Gogo, D. Papy-Garcia, C. Rey, S. Alban, D. Barritault, C.I. Lasmezas & S. Weiss, (2006) The 37-kDa/67-kDa laminin receptor acts as a receptor for infectious prions and is inhibited by polysulfated glycanes. *J Infect Dis* **194**: 702-709.

Gauczynski, S., J.M. Peyrin, S. Haik, C. Leucht, C. Hundt, R. Rieger, S. Krasemann, J.P. Deslys, D. Dormont, C.I. Lasmezas & S. Weiss, (2001) The 37-kDa/67-kDa laminin receptor acts as the cell-surface receptor for the cellular prion protein. *EMBO J* **20**: 5863-5875.

Geiseler, P.J., K.E. Nelson, S. Levin, K.T. Reddi & V.K. Moses, (1980) Community-acquired purulent meningitis: a review of 1,316 cases during the antibiotic era, 1954-1976. *Rev Infect Dis* **2**: 725-745.

Gilsdorf, J.R., K.W. McCrea & C.F. Marrs, (1997) Role of pili in *Haemophilus influenzae* adherence and colonization. *Infection and immunity* **65**: 2997-3002.

Goering, R.V., D.H. Dockrell, D. Wakelin, M. Zuckerman, P.L. Chiodin, I.M. Roitt & C. Mims, (2008) *Mims' Medical Microbiology*. China.

Gould, J.M. & J.N. Weiser, (2002) The inhibitory effect of C-reactive protein on bacterial phosphorylcholine platelet-activating factor receptor-mediated adherence is blocked by surfactant. *J Infect Dis* **186**: 361-371.

Gray, L.D. & D.P. Fedorko, (1992) Laboratory diagnosis of bacterial meningitis. *Clin Microbiol Rev* **5**: 130-145.

Grimwood, K., V.A. Anderson, L. Bond, C. Catroppa, R.L. Hore, E.H. Keir, T. Nolan & D.M. Roberton, (1995) Adverse outcomes of bacterial meningitis in school-age survivors. *Pediatrics* **95**: 646-656.

Haase, E.M., K. Yi, G.D. Morse & T.F. Murphy, (1994) Mapping of bactericidal epitopes on the P2 porin protein of nontypeable *Haemophilus influenzae*. *Infection and immunity* **62**: 3712-3722.

Hallstrom, T., A.M. Blom, P.F. Zipfel & K. Riesbeck, (2009) Nontypeable *Haemophilus influenzae* protein E binds vitronectin and is important for serum resistance. *J Immunol* **183**: 2593-2601.

Hallstrom, T., H. Jarva, K. Riesbeck & A.M. Blom, (2007) Interaction with C4b-binding protein contributes to nontypeable *Haemophilus influenzae* serum resistance. *J Immunol* **178**: 6359-6366.

Hallstrom, T. & K. Riesbeck, (2010) *Haemophilus influenzae* and the complement system. *Trends in microbiology* **18**: 258-265.

Hallstrom, T., E. Trajkovska, A. Forsgren & K. Riesbeck, (2006) *Haemophilus influenzae* Surface Fibrils Contribute to Serum Resistance by Interacting with Vitronectin. *J Immunol* **177**: 430-436.

Hallstrom, T., P.F. Zipfel, A.M. Blom, N. Lauer, A. Forsgren & K. Riesbeck, (2008) *Haemophilus influenzae* interacts with the human complement inhibitor factor H. *J Immunol* **181**: 537-545.

Hansen, E.J., C. Hasemann, A. Clausell, J.D. Capra, K. Orth, C.R. Moomaw, C.A. Slaughter, J.L. Latimer & E.E. Miller, (1989) Primary structure of the porin protein of *Haemophilus influenzae* type b determined by nucleotide sequence analysis. *Infection and immunity* **57**: 1100-1107.

Harvey, D., D.E. Holt & H. Bedford, (1999) Bacterial meningitis in the newborn: a prospective study of mortality and morbidity. *Semin Perinatol* **23**: 218-225.

Hauck, C.R. & T.F. Meyer, (1997) The lysosomal/phagosomal membrane protein h-lamp-1 is a target of the IgA1 protease of *Neisseria gonorrhoeae*. *FEBS letters* **405**: 86-90.

Heath, P.T., (1998) *Haemophilus influenzae* type b conjugate vaccines: a review of efficacy data. *The Pediatric infectious disease journal* **17**: S117-122.

Heath, P.T., R. Booy, H. Griffiths, E. Clutterbuck, H.J. Azzopardi, M.P. Slack, J. Fogarty, A.C. Moloney & E.R. Moxon, (2000) Clinical and immunological risk factors associated with *Haemophilus influenzae* type b conjugate vaccine failure in childhood. *Clinical infectious diseases : an official publication of the Infectious Diseases Society of America* **31**: 973-980.

Hendrixson, D.R., M.L. de la Morena, C. Stathopoulos & J.W. St Geme, 3rd, (1997) Structural determinants of processing and secretion of the *Haemophilus influenzae* hap protein. *Molecular microbiology* **26**: 505-518.

Hendrixson, D.R. & J.W. St Geme, 3rd, (1998) The *Haemophilus influenzae* Hap serine protease promotes adherence and microcolony formation, potentiated by a soluble host protein. *Mol Cell* **2**: 841-850.

Hoda Abdel, H., G.W. Karl, R. Karen & A.A.A.A. Dlawer, (2001) Identification and characterization of App: an immunogenic autotransporter protein of *Neisseria meningitidis*. *Molecular microbiology* **41**: 611-623.

Holt, G.J., N.R. Krieg, P.H.A. Sneath, J.T. Staley & S.T. Williams, (1994) *Bergey's Manual of Determinative Bacteriology*. Williams & Wilkins.

Hopkins, A.M., S.V. Walsh, P. Verkade, P. Boquet & A. Nusrat, (2003) Constitutive activation of Rho proteins by CNF-1 influences tight junction structure and epithelial barrier function. *J Cell Sci* **116**: 725-742.

Howie, S.R., M. Antonio, A. Akisanya, S. Sambou, I. Hakeem, O. Secka & R.A. Adegbola, (2007) Re-emergence of *Haemophilus influenzae* type b (Hib) disease in The Gambia following successful elimination with conjugate Hib vaccine. *Vaccine* **25**: 6305-6309.

Huang, S.H. & A. Jong, (2009) Evolving role of laminin receptors in microbial pathogenesis and therapeutics of CNS infection. *Future Microbiol* **4**: 959-962.

Huang, S.H., M.F. Stins & K.S. Kim, (2000) Bacterial penetration across the blood-brain barrier during the development of neonatal meningitis. *Microbes and infection / Institut Pasteur* **2**: 1237-1244.

Jamieson, K.V., S.R. Hubbard & D. Meruelo, (2011) Structure-guided identification of a laminin binding site on the laminin receptor precursor. *Journal of molecular biology* **405**: 24-32.

Jin, Z., S. Romero-Steiner, G.M. Carlone, J.B. Robbins & R. Schneerson, (2007) Haemophilus influenzae type a infection and its prevention. *Infect Immun* **75**: 2650-2654.

Johnson, N.G., J.U. Ruggeberg, G.F. Balfour, Y.C. Lee, H. Liddy, D. Irving, J. Sheldon, M.P. Slack, A.J. Pollard & P.T. Heath, (2006) *Haemophilus influenzae* type b reemergence after combination immunization. *Emerging infectious diseases* **12**: 937-941.

Joiner, K.A., (1988) Complement evasion by bacteria and parasites. *Annu Rev Microbiol* **42**: 201-230.

Joseph, W.S.G., III & C. David, (1995) Evidence that surface fibrils expressed by *Haemophilus influenzae* type b promote attachment to human epithelial cells. *Molecular microbiology* **15**: 77-85.

Kammann, M., J. Laufs, J. Schell & B. Gronenborn, (1989) Rapid insertional mutagenesis of DNA by polymerase chain reaction (PCR). *Nucleic Acids Res* **17**: 5404.

Kaplan, S.L., (1999) Clinical presentations, diagnosis, and prognostic factors of bacterial meningitis. *Infect Dis Clin North Am* **13**: 579-594, vi-vii.

Kazmin, D.A., T.R. Hoyt, L. Taubner, M. Teintze & J.R. Starkey, (2000) Phage display mapping for peptide 11 sensitive sequences binding to laminin-1. *Journal of molecular biology* **298**: 431-445.

Khan, N.A., Y. Wang, K.J. Kim, J.W. Chung, C.A. Wass & K.S. Kim, (2002) Cytotoxic Necrotizing Factor-1 Contributes to Escherichia coli K1 Invasion of the Central Nervous System. *Journal of Biological Chemistry* **277**: 15607-15612.

Kim, D.W., P.E. Kilgore, E.J. Kim, S.A. Kim, D.D. Anh & M. Seki, (2011) Loop-mediated isothermal amplification assay for detection of *Haemophilus influenzae* type b in cerebrospinal fluid. *Journal of clinical microbiology* **49**: 3621-3626.

Kim, K.J., J.W. Chung & K.S. Kim, (2005) 67-kDa laminin receptor promotes internalization of cytotoxic necrotizing factor 1-expressing *Escherichia coli* K1 into human brain microvascular endothelial cells. *The Journal of biological chemistry* **280**: 1360-1368.

Kim, K.S., (2006) Microbial translocation of the blood-brain barrier. *International Journal for Parasitology* **36**: 607-614.

Kim, K.S., (2008) Mechanisms of microbial traversal of the blood-brain barrier. *Nat Rev Micro* **6**: 625-634.

Kim, K.S., (2010) Acute bacterial meningitis in infants and children. *Lancet Infect Dis* **10**: 32-42.

Kinoshita, K., Y. Kaneda, M. Sato, Y. Saeki, M. Wataya-Kaneda & A. Hoffmann, (1998) LBP-p40 binds DNA tightly through associations with histones H2A, H2B, and H4. *Biochem Biophys Res Commun* **253**: 277-282.

Kline, M.W. & S.L. Kaplan, (1988) Computed tomography in bacterial meningitis of childhood. *The Pediatric infectious disease journal* **7**: 855-857.

Koebnik, R., (1999) Structural and Functional Roles of the Surface-Exposed Loops of the beta -Barrel Membrane Protein OmpA from *Escherichia coli*. *J. Bacteriol.* **181**: 3688-3694.

Kotilainen, P., J. Jalava, O. Meurman, O.P. Lehtonen, E. Rintala, O.P. Seppala, E. Eerola & S. Nikkari, (1998) Diagnosis of meningococcal meningitis by broad-range bacterial PCR with cerebrospinal fluid. *Journal of clinical microbiology* **36**: 2205-2209.

Kroll, J.S., I. Hopkins & E.R. Moxon, (1988) Capsule loss in *H. influenzae* type b occurs by recombination-mediated disruption of a gene essential for polysaccharide export. *Cell* **53**: 347-356.

Kroll, J.S., B. Loynds, L.N. Brophy & E.R. Moxon, (1990) The bex locus in encapsulated *Haemophilus influenzae*: a chromosomal region involved in capsule polysaccharide export. *Molecular microbiology* **4**: 1853-1862.

Kroll, J.S., B.M. Loynds & E.R. Moxon, (1991) The *Haemophilus influenzae* capsulation gene cluster: a compound transposon. *Molecular microbiology* **5**: 1549-1560.

Kubiet, M., R. Ramphal, A. Weber & A. Smith, (2000) Pilus-Mediated Adherence of *Haemophilus influenzae* to Human Respiratory Mucins. *Infection and immunity* **68**: 3362-3367.

Laemmli, U.K., (1970) Cleavage of structural proteins during the assembly of the head of bacteriophage T4. *Nature* **227**: 680-685.

Lagos, R., O.S. Levine, A. Avendano, I. Horwitz & M.M. Levine, (1998) The introduction of routine *Haemophilus influenzae* type b conjugate vaccine

in Chile: a framework for evaluating new vaccines in newly industrializing countries. *The Pediatric infectious disease journal* **17**: S139-148.

Landowski, T.H., E.A. Dratz & J.R. Starkey, (1995) Studies of the structure of the metastasis-associated 67 kDa laminin binding protein: fatty acid acylation and evidence supporting dimerization of the 32 kDa gene product to form the mature protein. *Biochemistry* **34**: 11276-11287.

Leib, S.L. & M.G. Tauber, (1999a) Pathogenesis of bacterial meningitis. *Infect Dis Clin North Am* **13**: 527-548.

Leib, S.L. & M.G. Tauber, (1999b) Pathogenesis of bacterial meningitis. *Infect Dis Clin North Am* **13**: 527-548, v-vi.

Lemonnier, M., L. Landraud & E. Lemichez, (2007) Rho GTPase-activating bacterial toxins: from bacterial virulence regulation to eukaryotic cell biology. *FEMS Microbiol Rev* **31**: 515-534.

Lesot, H., U. Kuhl & K. Mark, (1983) Isolation of a laminin-binding protein from muscle cell membranes. *EMBO J* **2**: 861-865.

Leucht, C., S. Simoneau, C. Rey, K. Vana, R. Rieger, C.I. Lasmezas & S. Weiss, (2003) The 37 kDa/67 kDa laminin receptor is required for PrP(Sc) propagation in scrapie-infected neuronal cells. *EMBO Rep* **4**: 290-295.

Lorenzen, D.R., F. Dux, U. Wolk, A. Tsirpouchtsidis, G. Haas & T.F. Meyer, (1999) Immunoglobulin A1 protease, an exoenzyme of pathogenic Neisseriae, is a potent inducer of proinflammatory cytokines. *J Exp Med* **190**: 1049-1058.

Ludwig, G.V., J.P. Kondig & J.F. Smith, (1996) A putative receptor for Venezuelan equine encephalitis virus from mosquito cells. *J Virol* **70**: 5592-5599.

Luong, D.C., N. Ishiwada, T. Nobue & Y. Kohno, (2004) Serotype of *Haemophilus influenzae* Strains Isolated from Pediatric Patients with Respiratory Tract Infection. *Tohoku J. Exp. Med.* **202**: 245-254.

Lysenko, E., J.C. Richards, A.D. Cox, A. Stewart, A. Martin, M. Kapoor & J.N. Weiser, (2000) The position of phosphorylcholine on the lipopolysaccharide of *Haemophilus influenzae* affects binding and sensitivity to C-reactive protein-mediated killing. *Molecular microbiology* **35**: 234-245.

Mace, S.E., (2008) Acute Bacterial Meningitis. *Emergency medicine clinics of North America* **26**: 281-317.

Mahon, C.R. & G. Manuselis, (2000) *Textbookof Diagnostic Microbiology*. W.B. Saunders Company.

Malinda, K.M. & H.K. Kleinman, (1996) The laminins. *Int J Biochem Cell Biol* **28**: 957-959.

Malinoff, H.L. & M.S. Wicha, (1983) Isolation of a cell surface receptor protein for laminin from murine fibrosarcoma cells. *J Cell Biol* **96**: 1475-1479.

Marrs, C.F., G.P. Krasan, K.W. McCrea, D.L. Clemans & J.R. Gilsdorf, (2001) *Haemophilus influenzae* - human specific bacteria. *Front Biosci* **6**: E41-60.

Martignone, S., S. Menard, R. Bufalino, N. Cascinelli, R. Pellegrini, E. Tagliabue, S. Andreola, F. Rilke & M.I. Colnaghi, (1993) Prognostic significance of the 67-kilodalton laminin receptor expression in human breast carcinomas. *J Natl Cancer Inst* **85**: 398-402.

Maruvada, R. & K.S. Kim, (2011) Extracellular Loops of the Eschericia coli Outer Membrane Protein A Contribute to the Pathogenesis of Meningitis. *Journal of Infectious Diseases* **203**: 131-140.

McCrea, K.W., J.L. St. Sauver, C.F. Marrs, D. Clemans & J.R. Gilsdorf, (1998) Immunologic and Structural Relationships of the Minor Pilus Subunits among *Haemophilus influenzae* Isolates. *Infection and immunity* **66**: 4788-4796.

McCrea, K.W., W.J. Watson, J.R. Gilsdorf & C.F. Marrs, (1994) Identification of hifD and hifE in the pilus gene cluster of *Haemophilus influenzae* type b strain Eagan. *Infection and immunity* **62**: 4922-4928.

McCrea, K.W., W.J. Watson, J.R. Gilsdorf & C.F. Marrs, (1997) Identification of two minor subunits in the pilus of *Haemophilus influenzae*. *Journal of bacteriology* **179**: 4227-4231.

McVernon, J., N. Andrews, M.P.E. Slack & M.E. Ramsay, (2003a) Risk of vaccine failure after *Haemophilus influenzae* type b (Hib) combination vaccines with acellular pertussis. *The Lancet* **361**: 1521-1523.

McVernon, J., P.D. Johnson, A.J. Pollard, M.P. Slack & E.R. Moxon, (2003b) Immunologic memory in *Haemophilus influenzae* type b conjugate vaccine failure. *Arch Dis Child* **88**: 379-383.

McVernon, J., N.A. Mitchison & E.R. Moxon, (2004a) T helper cells and efficacy of *Haemophilus influenzae* type b conjugate vaccination. *The Lancet Infectious Diseases* **4**: 40-43.

McVernon, J., N.A. Mitchison & E.R. Moxon, (2004b) T helper cells and efficacy of *Haemophilus influenzae* type b conjugate vaccination. *Lancet Infect Dis* **4**: 40-43.

McVernon, J., C.L. Trotter, M.P. Slack & M.E. Ramsay, (2004c) Trends in *Haemophilus influenzae* type b infections in adults in England and Wales: surveillance study. *BMJ* **329**: 655-658.

Menard, S., V. Castronovo, E. Tagliabue & M.E. Sobel, (1997) New insights into the metastasis-associated 67 kD laminin receptor. *J Cell Biochem* **67**: 155-165.

Ménard, S., E. Tagliabue & M. Colnaghi, (1998) The 67 kDa laminin receptor as a prognostic factor in human cancer. *Breast Cancer Research and Treatment* **52**: 137-145.

Mendsaikhan, J., J.P. Watt, O. Mansoor, N. Suvdmaa, K. Edmond, D.J. Litt, P. Nymadawa, Y. Baoping, D. Altantsetseg & M. Slack, (2009) Childhood bacterial meningitis in Ulaanbaatar, Mongolia, 2002-2004. *Clinical infectious diseases : an official publication of the Infectious Diseases Society of America* **48 Suppl 2**: S141-146.

Milonovich, L.M., (2007) Meningococcemia: epidemiology, pathophysiology, and management. *J Pediatr Health Care* **21**: 75-80.

Mistry, D. & R.A. Stockley, (2006) IgA1 protease. *The International Journal of Biochemistry & Cell Biology* **38**: 1244-1248.

Mitchell, M.A., K. Skowronek, L. Kauc & S.H. Goodgal, (1991) Electroporation of *Haemophilus influenzae* is effective for transformation of plasmid but not chromosomal DNA. *Nucl. Acids Res.* **19**: 3625-3628.

Mittal, R., S. Krishnan, I. Gonzalez-Gomez & N.V. Prasadarao, (2011) Deciphering the roles of outer membrane protein A extracellular loops in the pathogenesis of *Escherichia coli* K1 meningitis. *The Journal of biological chemistry* **286**: 2183-2193.

Molyneux, E.M., A.L. Walsh, H. Forsyth, M. Tembo, J. Mwenechanya, K. Kayira, L. Bwanaisa, A. Njobvu, S. Rogerson & G. Malenga, (2002)

Dexamethasone treatment in childhood bacterial meningitis in Malawi: a randomised controlled trial. *Lancet* **360**: 211-218.

Montuori, N., F. Muller, S. De Riu, G. Fenzi, M.E. Sobel, G. Rossi & M. Vitale, (1999) Laminin receptors in differentiated thyroid tumors: restricted expression of the 67-kilodalton laminin receptor in follicular carcinoma cells. *J Clin Endocrinol Metab* **84**: 2086-2092.

Morris, S.K., W.J. Moss & N. Halsey, (2008) *Haemophilus influenzae* type b conjugate vaccine use and effectiveness. *Lancet Infect Dis* **8**: 435-443.

Moxon, E.R., (1992) Molecular basis of invasive *Haemophilus influenzae* type b disease. *The Journal of infectious diseases* **165 Suppl 1**: S77-81.

Munson, R., Jr., C. Bailey & S. Grass, (1989a) Diversity of the outer membrane protein P2 gene from major clones of *Haemophilus influenzae* type b. *Molecular microbiology* **3**: 1797-1803.

Munson, R., Jr. & R.W. Tolan, Jr., (1989) Molecular cloning, expression, and primary sequence of outer membrane protein P2 of *Haemophilus influenzae* type b. *Infection and immunity* **57**: 88-94.

Munson, R.S., Jr., M.H. Kabeer, A.A. Lenoir & D.M. Granoff, (1989b) Epidemiology and prospects for prevention of disease due to *Haemophilus influenzae* in developing countries. *Rev Infect Dis* **11 Suppl 3**: S588-597.

Murphy, T.F. & L.C. Bartos, (1988) Purification and analysis with monoclonal antibodies of P2, the major outer membrane protein of nontypable *Haemophilus influenzae*. *Infection and immunity* **56**: 1084-1089.

Murphy, T.F., C. Kirkham & A.J. Lesse, (2006) Construction of a mutant and characterization of the role of the vaccine antigen P6 in outer membrane integrity of nontypeable *Haemophilus influenzae*. *Infection and immunity* **74**: 5169-5176.

Mustafa, M.M., O. Ramilo, G.A. Syrogiannopoulos, K.D. Olsen, G.H. McCracken, Jr. & E.J. Hansen, (1989) Induction of meningeal inflammation by outer membrane vesicles of *Haemophilus influenzae* type b. *The Journal of infectious diseases* **159**: 917-922.

Mwangi, I., J. Berkley, B. Lowe, N. Peshu, K. Marsh & C.R. Newton, (2002) Acute bacterial meningitis in children admitted to a rural Kenyan hospital: increasing antibiotic resistance and outcome. *The Pediatric infectious disease journal* **21**: 1042-1048.

Naiman, H.L. & W.L. Albritton, (1980) Counterimmunoelectrophoresis in the Diagnosis of Acute Infection. *Journal of Infectious Diseases* **142**: 524-531.

Neary, J.M. & T.F. Murphy, (2006) Antibodies directed at a conserved motif in loop 6 of outer membrane protein P2 of nontypeable *Haemophilus influenzae* recognize multiple strains in immunoassays. *FEMS immunology and medical microbiology* **46**: 251-261.

Neary, J.M., K. Yi, R.J. Karalus & T.F. Murphy, (2001) Antibodies to loop 6 of the P2 porin protein of nontypeable Haemophilus influenzae are bactericidal against multiple strains. *Infection and immunity* **69**: 773-778.

Nelson, J., N.V. McFerran, G. Pivato, E. Chambers, C. Doherty, D. Steele & D.J. Timson, (2008) The 67 kDa laminin receptor: structure, function and role in disease. *Biosci Rep* **28**: 33-48.

Nikles, D., K. Vana, S. Gauczynski, H. Knetsch, H. Ludewigs & S. Weiss, (2008) Subcellular localization of prion proteins and the 37 kDa/67 kDa laminin receptor fused to fluorescent proteins. *Biochim Biophys Acta* **1782**: 335-340.

Noel, G.J., A. Brittingham, A.A. Granato & D.M. Mosser, (1996) Effect of amplification of the Cap b locus on complement-mediated bacteriolysis and opsonization of type b *Haemophilus influenzae*. *Infection and immunity* **64**: 4769-4775.

Noel, G.J., S. Katz & P.J. Edelson, (1988) Complement-mediated early clearance of *Haemophilus influenzae* type b from blood is independent of serum lytic activity. *The Journal of infectious diseases* **157**: 85-90.

Noel, G.J., D.C. Love & D.M. Mosser, (1994) High-molecular-weight proteins of nontypeable *Haemophilus influenzae* mediate bacterial adhesion to cellular proteoglycans. *Infection and immunity* **62**: 4028-4033.

Nossal, N.G. & L.A. Heppel, (1966) The release of enzymes by osmotic shock from *Escherichia coli* in exponential phase. *The Journal of biological chemistry* **241**: 3055-3062.

Odio, C.M., (1995) Cefotaxime for treatment of neonatal sepsis and meningitis. *Diagnostic microbiology and infectious disease* **22**: 111-117.

Oldfield, N.J., S.J. Bland, M. Taraktsoglou, F.J. Dos Ramos, K. Robinson, K.G. Wooldridge & D.A. Ala'Aldeen, (2007) T-cell stimulating protein A

(TspA) of Neisseria meningitidis is required for optimal adhesion to human cells. *Cell Microbiol* **9**: 463-478.

Orihuela, C.J., J. Mahdavi, J. Thornton, B. Mann, K.G. Wooldridge, N. Abouseada, N.J. Oldfield, T. Self, D.A.A. Ala'Aldeen & E. Tuomanen, (2009) Laminin receptor initiates bacterial contact with the blood brain barrier in experimental meningitis models. *The Journal of Clinical Investigation* **0**: 0-0.

Ozaki, I., K. Yamamoto, T. Mizuta, S. Kajihara, N. Fukushima, Y. Setoguchi, F. Morito & T. Sakai, (1998) Differential expression of laminin receptors in human hepatocellular carcinoma. *Gut* **43**: 837-842.

Pelkonen, T., I. Roine, L. Monteiro, M. Correia, A. Pitkaranta, L. Bernardino & H. Peltola, (2009) Risk factors for death and severe neurological sequelae in childhood bacterial meningitis in sub-Saharan Africa. *Clinical Infectious Diseases* **48**: 1107-1110.

Pelosi, G., F. Pasini, E. Bresaola, G. Bogina, P. Pederzoli, S. Biolo, S. Menard & G. Zamboni, (1997) High-affinity monomeric 67-kD laminin receptors and prognosis in pancreatic endocrine tumours. *J Pathol* **183**: 62-69.

Peltola, H., (2000) Worldwide *Haemophilus influenzae* Type b Disease at the Beginning of the 21st Century: Global Analysis of the Disease Burden 25 Years after the Use of the Polysaccharide Vaccine and a Decade after the Advent of Conjugates. *Clin. Microbiol. Rev.* **13**: 302-317.

Peltola, H., H. Kayhty, A. Sivonen & H. Makela, (1977) *Haemophilus influenzae* type b capsular polysaccharide vaccine in children: a double-blind field study of 100,000 vaccinees 3 months to 5 years of age in Finland. *Pediatrics* **60**: 730-737.

Peltola, H., E. Salo & H. Saxen, (2005) Incidence of *Haemophilus influenzae* type b meningitis during 18 years of vaccine use: observational study using routine hospital data. *BMJ* **330**: 18-19.

Pittman, M., (1931) Variation and Type Specificity in the Bacterial Species *Hemophilus Influenzae*. *J Exp Med* **53**: 471-492.

Polin, R.A. & M.C. Harris, (2001) Neonatal bacterial meningitis. *Semin Neonatol* **6**: 157-172.

Pollard, A.J., K.P. Perrett & P.C. Beverley, (2009) Maintaining protection against invasive bacteria with protein-polysaccharide conjugate vaccines. *Nat Rev Immunol* **9**: 213-220.

Pong, A. & J.S. Bradley, (1999) Bacterial meningitis and the newborn infant. *Infect Dis Clin North Am* **13**: 711-733, viii.

Poppert, S., A. Essig, B. Stoehr, A. Steingruber, B. Wirths, S. Juretschko, U. Reischl & N. Wellinghausen, (2005) Rapid diagnosis of bacterial meningitis by real-time PCR and fluorescence in situ hybridization. *Journal of clinical microbiology* **43**: 3390-3397.

Prasadarao, N.V., E. Lysenko, C.A. Wass, K.S. Kim & J.N. Weiser, (1999) Opacity-associated protein A contributes to the binding of *Haemophilus influenzae* to chang epithelial cells. *Infection and immunity* **67**: 4153-4160.

Prasadarao, N.V., C.A. Wass & K.S. Kim, (1996) Endothelial cell GlcNAc beta 1-4GlcNAc epitopes for outer membrane protein A enhance traversal of *Escherichia coli* across the blood-brain barrier. *Infection and immunity* **64**: 154-160.

Prescott, L.M., J.P. Harley & K.D. A., (2005) *Microbiology*. McGraw-Hill Companies, Inc.

Quagliarello, V. & W.M. Scheld, (1992) Bacterial meningitis: pathogenesis, pathophysiology, and progress. *N Engl J Med* **327**: 864-872.

Ramsay, M.E., J. McVernon, N.J. Andrews, P.T. Heath & M.P. Slack, (2003) Estimating *Haemophilus influenzae* type b vaccine effectiveness in England and Wales by use of the screening method. *The Journal of infectious diseases* **188**: 481-485.

Rao, C.N., V. Castronovo, M.C. Schmitt, U.M. Wewer, A.P. Claysmith, L.A. Liotta & M.E. Sobel, (1989) Evidence for a precursor of the high-affinity metastasis-associated murine laminin receptor. *Biochemistry* **28**: 7476-7486.

Rao, N.C., S.H. Barsky, V.P. Terranova & L.A. Liotta, (1983) Isolation of a tumor cell laminin receptor. *Biochem Biophys Res Commun* **111**: 804-808.

Reddy, M.S., J.M. Bernstein, T.F. Murphy & H.S. Faden, (1996) Binding between outer membrane proteins of nontypeable *Haemophilus influenzae* and human nasopharyngeal mucin. *Infection and immunity* **64**: 1477-1479.

Regelink, A.G., D. Dahan, L.V. Moller, J.W. Coulton, P. Eijk, P. Van Ulsen, J. Dankert & L. Van Alphen, (1999) Variation in the composition and pore function of major outer membrane pore protein P2 of *Haemophilus influenzae* from cystic fibrosis patients. *Antimicrobial agents and chemotherapy* **43**: 226-232.

Rieger, R., F. Edenhofer, C.I. Lasmezas & S. Weiss, (1997) The human 37-kDa laminin receptor precursor interacts with the prion protein in eukaryotic cells. *Nat Med* **3**: 1383-1388.

Rijkers, G.T., P.E. Vermeer-de Bondt, L. Spanjaard, M.A. Breukels & E.A.M. Sanders, (2003) Return of *Haemophilus influenzae* type b infections. *The Lancet* **361**: 1563-1564.

Robbins, J.B., R. Schneerson, P. Anderson & D.H. Smith, (1996) The 1996 Albert Lasker Medical Research Awards. Prevention of systemic infections, especially meningitis, caused by *Haemophilus influenzae* type b. Impact on public health and implications for other polysaccharide-based vaccines. *JAMA* **276**: 1181-1185.

Rodriguez, C.A., V. Avadhanula, A. Buscher, A.L. Smith, J.W. St. Geme Iii & E.E. Adderson, (2003) Prevalence and Distribution of Adhesins in Invasive Non-Type b Encapsulated *Haemophilus influenzae*. *Infection and immunity* **71**: 1635-1642.

Rosenstein, N.E., B.A. Perkins, D.S. Stephens, T. Popovic & J.M. Hughes, (2001) Meningococcal disease. *N Engl J Med* **344**: 1378-1388.

Rubin, L.G. & E.R. Moxon, (1983) Pathogenesis of bloodstream invasion with *Haemophilus influenzae* type b. *Infection and immunity* **41**: 280-284.

Rubin, L.L. & J.M. Staddon, (1999) The cell biology of the blood-brain barrier. *Annu Rev Neurosci* **22**: 11-28.

Saez-Llorens, X. & G.H. McCracken, Jr., (2003) Bacterial meningitis in children. *Lancet* **361**: 2139-2148.

Salih, M.A., H.S. Ahmed, Y. Hofvander, D. Danielsson & P. Olcen, (1989) Rapid diagnosis of bacterial meningitis by an enzyme immunoassay of cerebrospinal fluid. *Epidemiology and infection* **103**: 301-310.

Sambrook, J.F.E. & T. Maniatis, (1989) *Molecular Cloning: A Laboratory Manual*. Cold Spring Harbor, NY.

Sanders, J.D., L.D. Cope, G.P. Jarosik, I. Maciver, J.L. Latimer, G.B. Toews & E.J. Hansen, (1993) Reconstitution of a porin-deficient mutant of *Haemophilus influenzae* type b with a porin gene from nontypeable *H. influenzae*. *Infection and immunity* **61**: 3966-3975.

Sanjuan, X., P.L. Fernandez, R. Miquel, J. Munoz, V. Castronovo, S. Menard, A. Palacin, A. Cardesa & E. Campo, (1996) Overexpression of the 67-kD laminin receptor correlates with tumour progression in human colorectal carcinoma. *J Pathol* **179**: 376-380.

Sato, M., K. Kinoshita, Y. Kaneda, Y. Saeki, A. Iwamatsu & K. Tanaka, (1996) Analysis of nuclear localization of laminin binding protein precursor p40 (LBP/p40). *Biochem Biophys Res Commun* **229**: 896-901.

Satoh, K., K. Narumi, T. Abe, T. Sakai, T. Kikuchi, M. Tanaka, T. Shimo-Oka, M. Uchida, F. Tezuka, M. Isemura & T. Nukiwa, (1999) Diminution of 37-kDa laminin binding protein expression reduces tumour formation of murine lung cancer cells. *Br J Cancer* **80**: 1115-1122.

Scarselli, M., D. Serruto, P. Montanari, B. Capecchi, J. Adu-Bobie, D. Veggi, R. Rappuoli, M. Pizza & B. Arico, (2006) *Neisseria meningitidis* NhhA is a multifunctional trimeric autotransporter adhesin. *Molecular microbiology* **61**: 631-644.

Scheifele, D., S. Halperin, B. Law, A. King, R. Morris, C.A. Janeway, P. Dery, M. Lebel, D. Moore, N. Le Saux, E. Ford-Jones, B. Tan, T. Jadavji, W. Vaudry, W. Walop, J. Embree & J. Waters, (2005) Invasive *Haemophilus influenzae* type b infections in vaccinated and unvaccinated children in Canada, 2001-2003. *CMAJ* **172**: 53-56.

Scheiman, J., J.C. Tseng, Y. Zheng & D. Meruelo, (2010) Multiple functions of the 37/67-kd laminin receptor make it a suitable target for novel cancer gene therapy. *Mol Ther* **18**: 63-74.

Schlech, W.F., 3rd, J.I. Ward, J.D. Band, A. Hightower, D.W. Fraser & C.V. Broome, (1985) Bacterial meningitis in the United States, 1978 through 1981. The National Bacterial Meningitis Surveillance Study. *JAMA* **253**: 1749-1754.

Schnaitman, C.A., (1971) Solubilization of the Cytoplasmic Membrane of *Escherichia coli* by Triton X-100. *J. Bacteriol.* **108**: 545-552.

Schneider, M.C., R.M. Exley, S. Ram, R.B. Sim & C.M. Tang, (2007) Interactions between *Neisseria meningitidis* and the complement system. *Trends in microbiology* **15**: 233-240.

Schuchat, A., K. Robinson, J.D. Wenger, L.H. Harrison, M. Farley, A.L. Reingold, L. Lefkowitz & B.A. Perkins, (1997) Bacterial meningitis in the United States in 1995. Active Surveillance Team. *N Engl J Med* **337**: 970-976.

Severino, V., A. Chambery, M. Vitiello, M. Cantisani, S. Galdiero, M. Galdiero, L. Malorni, A. Di Maro & A. Parente, (2009) Proteomic Analysis of Human U937 Cell Line Activation Mediated by Haemophilus influenzae Type b P2 Porin and Its Surface-Exposed Loop 7. *Journal of Proteome Research* **9**: 1050-1062.

Severino, V., A. Chambery, M. Vitiello, M. Cantisani, S. Galdiero, M. Galdiero, L. Malorni, A. Di Maro & A. Parente, (2010) Proteomic analysis of human U937 cell line activation mediated by *Haemophilus influenzae* type b P2 porin and its surface-exposed loop 7. *Journal of proteome research* **9**: 1050-1062.

Sikkema, D.J. & T.F. Murphy, (1992) Molecular analysis of the P2 porin protein of nontypeable *Haemophilus influenzae*. *Infection and immunity* **60**: 5204-5211.

Singh, B., F. Jalalvand, M. Morgelin, P. Zipfel, A.M. Blom & K. Riesbeck, (2011) *Haemophilus influenzae* protein E recognizes the C-terminal domain of vitronectin and modulates the membrane attack complex. *Molecular microbiology* **81**: 80-98.

Singleton, R., L. Hammitt, T. Hennessy, L. Bulkow, C. DeByle, A. Parkinson, T.E. Cottle, H. Peters & J.C. Butler, (2006) The Alaska *Haemophilus influenzae* Type b Experience: Lessons in Controlling a Vaccine-Preventable Disease. *Pediatrics* **118**: e421-429.

Slack, M.P., H.J. Azzopardi, R.M. Hargreaves & M.E. Ramsay, (1998) Enhanced surveillance of invasive *Haemophilus influenzae* disease in England, 1990 to 1996: impact of conjugate vaccines. *The Pediatric infectious disease journal* **17**: S204-207.

Slack, M.P.E., (2007) Haemophilus: Respiratory infections; meningitis; chancroid. *[Online], Available at http://www.medicaltextbooksrevealed.com/files/11219-53.pdf [2 August, 2012]*.

Smith, A.L., (1987) Pathogenesis of *Haemophilus influenzae* meningitis. *The Pediatric infectious disease journal* **6**: 783-786.

Smith, D.H., G. Peter, D.L. Ingram, A.L. Harding & P. Anderson, (1973) Responses of children immunized with the capsular polysaccharide of *Hemophilus influenzae*, type b. *Pediatrics* **52**: 637-644.

Smith, H.O., J.F. Tomb, B.A. Dougherty, R.D. Fleischmann & J.C. Venter, (1995) Frequency and distribution of DNA uptake signal sequences in the *Haemophilus influenzae* Rd genome. *Science* **269**: 538-540.

Sobel, M.E., (1993) Differential expression of the 67 kDa laminin receptor in cancer. *Semin Cancer Biol* **4**: 311-317.

Srikumar, R., A.C. Chin, V. Vachon, C.D. Richardson, M.J. Ratcliffe, L. Saarinen, H. Kayhty, P.H. Makela & J.W. Coulton, (1992a) Monoclonal antibodies specific to porin of *Haemophilus influenzae* type b: localization of their cognate epitopes and tests of their biological activities. *Molecular microbiology* **6**: 665-676.

Srikumar, R., D. Dahan, F.F. Arhin, P. Tawa, K. Diederichs & J.W. Coulton, (1997) Porins of *Haemophilus influenzae* type b mutated in loop 3 and in loop 4. *The Journal of biological chemistry* **272**: 13614-13621.

Srikumar, R., D. Dahan, M.F. Gras, M.J. Ratcliffe, L. van Alphen & J.W. Coulton, (1992b) Antigenic sites on porin of *Haemophilus influenzae* type b: mapping with synthetic peptides and evaluation of structure predictions. *Journal of bacteriology* **174**: 4007-4016.

St Geme, J.W., 3rd, (1994) The HMW1 adhesin of nontypeable *Haemophilus influenzae* recognizes sialylated glycoprotein receptors on cultured human epithelial cells. *Infection and immunity* **62**: 3881-3889.

St Geme, J.W., 3rd, D. Cutter & S.J. Barenkamp, (1996) Characterization of the genetic locus encoding *Haemophilus influenzae* type b surface fibrils. *Journal of bacteriology* **178**: 6281-6287.

St Geme, J.W., 3rd & S. Falkow, (1990) *Haemophilus influenzae* adheres to and enters cultured human epithelial cells. *Infection and immunity* **58**: 4036-4044.

St Geme, J.W., 3rd & S. Falkow, (1993) Isolation, expression, and nucleotide sequencing of the pilin structural gene of the Brazilian purpuric fever

clone of *Haemophilus influenzae* biogroup aegyptius. *Infection and immunity* **61**: 2233-2237.

Steele, R.W., J.R. McConnell, R.F. Jacobs & J.R. Mawk, (1985) Recurrent bacterial meningitis: coronal thin-section cranial computed tomography to delineate anatomic defects. *Pediatrics* **76**: 950-953.

Stins, M.F., N.V. Prasadarao, L. Ibric, C.A. Wass, P. Luckett & K.S. Kim, (1994) Binding characteristics of S fimbriated *Escherichia coli* to isolated brain microvascular endothelial cells. *The American journal of pathology* **145**: 1228-1236.

Sukupolvi-Petty, S., S. Grass & J.W. St Geme, 3rd, (2006) The *Haemophilus influenzae* Type b hcsA and hcsB gene products facilitate transport of capsular polysaccharide across the outer membrane and are essential for virulence. *Journal of bacteriology* **188**: 3870-3877.

Sutton, A., R. Schneerson, S. Kendall-Morris & J.B. Robbins, (1982) Differential Complement Resistance Mediates Virulence of *Haemophilus influenzae* Type b. *Infection and immunity* **35**: 95-104.

Swords, W.E., B.A. Buscher, K. Ver Steeg Ii, A. Preston, W.A. Nichols, J.N. Weiser, B.W. Gibson & M.A. Apicella, (2000) Non-typeable *Haemophilus influenzae* adhere to and invade human bronchial epithelial cells via an interaction of lipooligosaccharide with the PAF receptor. *Molecular microbiology* **37**: 13-27.

Swords, W.E., M.R. Ketterer, J. Shao, C.A. Campbell, J.N. Weiser & M.A. Apicella, (2001) Binding of the non-typeable *Haemophilus influenzae* lipooligosaccharide to the PAF receptor initiates host cell signalling. *Cellular microbiology* **3**: 525-536.

Taylor, S.W., E. Fahy, B. Zhang, G.M. Glenn, D.E. Warnock, S. Wiley, A.N. Murphy, S.P. Gaucher, R.A. Capaldi, B.W. Gibson & S.S. Ghosh, (2003) Characterization of the human heart mitochondrial proteome. *Nat Biotechnol* **21**: 281-286.

Terranova, V.P., C.N. Rao, T. Kalebic, I.M. Margulies & L.A. Liotta, (1983) Laminin receptor on human breast carcinoma cells. *Proceedings of the National Academy of Sciences of the United States of America* **80**: 444-448.

Thadepalli, H., P.K. Gangopadhyay, A. Ansari, G.D. Overturf, V.K. Dhawan & A.K. Mandal, (1982) Rapid differentiation of bacterial meningitides by

direct gas-liquid chromatography. *The Journal of clinical investigation* **69**: 979-984.

Thepparit, C. & D.R. Smith, (2004) Serotype-specific entry of dengue virus into liver cells: identification of the 37-kilodalton/67-kilodalton high-affinity laminin receptor as a dengue virus serotype 1 receptor. *J Virol* **78**: 12647-12656.

Thigpen, M.C., C.G. Whitney, N.E. Messonnier, E.R. Zell, R. Lynfield, J.L. Hadler, L.H. Harrison, M.M. Farley, A. Reingold, N.M. Bennett, A.S. Craig, W. Schaffner, A. Thomas, M.M. Lewis, E. Scallan & A. Schuchat, (2011) Bacterial meningitis in the United States, 1998-2007. *N Engl J Med* **364**: 2016-2025.

Tio, P.H., W.W. Jong & M.J. Cardosa, (2005) Two dimensional VOPBA reveals laminin receptor (LAMR1) interaction with dengue virus serotypes 1, 2 and 3. *Virol J* **2**: 25.

Tortora, G.J. & C.L. Case, (2009) Microbiology: an Introduction. In. Canada: Benjamin Cummings, pp.

Trollfors, B., T. Lagergard, B.A. Claesson, E. Thornberg, J. Martinell & R. Schneerson, (1992) Characterization of the serum antibody response to the capsular polysaccharide of *Haemophilus influenzae* type b in children with invasive infections. *The Journal of infectious diseases* **166**: 1335-1339.

Trotter, C.L., J. McVernon, M.E. Ramsay, C.G. Whitney, E.K. Mulholland, D. Goldblatt, J. Hombach & M.-P. Kieny, (2008) Optimising the use of conjugate vaccines to prevent disease caused by *Haemophilus influenzae* type b, *Neisseria meningitidis* and *Streptococcus pneumoniae*. *Vaccine* **26**: 4434-4445.

Trotter, C.L. & M.E. Ramsay, (2007) Vaccination against meningococcal disease in Europe: review and recommendations for the use of conjugate vaccines. *FEMS Microbiol Rev* **31**: 101-107.

Trotter, C.L., M.E. Ramsay & M.P. Slack, (2003) Rising incidence of *Haemophilus influenzae* type b disease in England and Wales indicates a need for a second catch-up vaccination campaign. *Commun Dis Public Health* **6**: 55-58.

Tunkel, A.R. & W.M. Scheld, (1993) Pathogenesis and pathophysiology of bacterial meningitis. *Clin. Microbiol. Rev.* **6**: 118-136.

Tunkel, A.R. & W.M. Scheld, (1995) Acute bacterial meningitis. *Lancet* **346**: 1675-1680.

Tunkel, A.R., B. Wispelwey, V.J. Quagliarello, S.W. Rosser, A.J. Lesse, E.J. Hansen & W.M. Scheld, (1992) Pathophysiology of blood-brain barrier alterations during experimental *Haemophilus influenzae* meningitis. *The Journal of infectious diseases* **165 Suppl 1**: S119-120.

Tuomanen, E., (1996) Entry of pathogens into the central nervous system. *FEMS Microbiol Rev* **18**: 289-299.

Ulanova, M. & R.S. Tsang, (2009) Invasive *Haemophilus influenzae* disease: changing epidemiology and host-parasite interactions in the 21st century. *Infection, genetics and evolution : journal of molecular epidemiology and evolutionary genetics in infectious diseases* **9**: 594-605.

Unkmeir, A., K. Latsch, G. Dietrich, E. Wintermeyer, B. Schinke, S. Schwender, K.S. Kim, M. Eigenthaler & M. Frosch, (2002) Fibronectin mediates Opc-dependent internalization of *Neisseria meningitidis* in human brain microvascular endothelial cells. *Molecular microbiology* **46**: 933-946.

Vachon, V., D.J. Lyew & J.W. Coulton, (1985) Transmembrane permeability channels across the outer membrane of *Haemophilus influenzae* type b. *Journal of bacteriology* **162**: 918-924.

Vadheim, C.M., D.P. Greenberg, S. Partridge, J. Jing & J.I. Ward, (1993) Effectiveness and safety of an *Haemophilus influenzae* type b conjugate vaccine (PRP-T) in young infants. Kaiser-UCLA Vaccine Study Group. *Pediatrics* **92**: 272-279.

van Alphen, L., P. Eijk, L. Geelen-van den Broek & J. Dankert, (1991a) Immunochemical characterization of variable epitopes of outer membrane protein P2 of nontypeable *Haemophilus influenzae*. *Infection and immunity* **59**: 247-252.

van Alphen, L., P. Eijk, H. Kayhty, J. van Marle & J. Dankert, (1996) Antibodies to *Haemophilus influenzae* type b polysaccharide affect bacterial adherence and multiplication. *Infection and immunity* **64**: 995-1001.

van Alphen, L., L. Geelen-van den Broek, L. Blaas, M. van Ham & J. Dankert, (1991b) Blocking of fimbria-mediated adherence of *Haemophilus influenzae* by sialyl gangliosides. *Infection and immunity* **59**: 4473-4477.

van Alphen, L., L. Spanjaard, A. van der Ende, I. Schuurman & J. Dankert, (1997) Effect of nationwide vaccination of 3-month-old infants in The Netherlands with conjugate *Haemophilus influenzae* type b vaccine: high efficacy and lack of herd immunity. *J Pediatr* **131**: 869-873.

van Alphen, L. & S.M. van Ham, (1994) Adherence and invasion of *Haemophilus influenzae*. *Reviews in Medical Microbiology* **5**: 245-255.

Van Eldere, J., L. Brophy, B. Loynds, P. Celis, I. Hancock, S. Carman, J.S. Kroll & E.R. Moxon, (1995) Region II of the *Haemophilus influenzae* type be capsulation locus is involved in serotype-specific polysaccharide synthesis. *Molecular microbiology* **15**: 107-118.

Virkola, R., M. Brummer, H. Rauvala, L. van Alphen & T.K. Korhonen, (2000) Interaction of Fimbriae of *Haemophilus influenzae* Type B with Heparin-Binding Extracellular Matrix Proteins. *Infection and immunity* **68**: 5696-5701.

Vitiello, M., E. Finamore, M. Cantisani, P. Bevilacqua, N. Incoronato, A. Falanga, E. Galdiero & M. Galdiero, (2011) P2 porin and loop L7 from *Haemophilus influenzae* modulate expression of IL-6 and adhesion molecules in astrocytes. *Microbiology and immunology* **55**: 347-356.

Vitiello, M., S. Galdiero, M. D'Isanto, M. D'Amico, C. Di Filippo, M. Cantisani, M. Galdiero & C. Pedone, (2008) Pathophysiological changes of gram-negative bacterial infection can be reproduced by a synthetic peptide mimicking loop L7 sequence of *Haemophilus influenzae* porin. *Microbes and infection / Institut Pasteur* **10**: 657-663.

Vitovski, S., K.T. Dunkin, A.J. Howard & J.R. Sayers, (2002) Nontypeable *Haemophilus influenzae* in carriage and disease: a difference in IgA1 protease activity levels. *JAMA* **287**: 1699-1705.

Wang, K.S., R.J. Kuhn, E.G. Strauss, S. Ou & J.H. Strauss, (1992) High-affinity laminin receptor is a receptor for Sindbis virus in mammalian cells. *J Virol* **66**: 4992-5001.

Wang, X., C. Moser, J.P. Louboutin, E.S. Lysenko, D.J. Weiner, J.N. Weiser & J.M. Wilson, (2002) Toll-like receptor 4 mediates innate immune responses to *Haemophilus influenzae* infection in mouse lung. *J Immunol* **168**: 810-815.

Ward, K.N., A.C. McCartney & B. Thakker, (2009) *Notes on Medical Microbiology* Churchill Livingstone Elsevier.

Weiser, J.N., S.T. Chong, D. Greenberg & W. Fong, (1995) Identification and characterization of a cell envelope protein of *Haemophilus influenzae* contributing to phase variation in colony opacity and nasopharyngeal colonization. *Molecular microbiology* **17**: 555-564.

Weiser, J.N., J.M. Love & E.R. Moxon, (1989) The molecular mechanism of phase variation of *H. influenzae* lipopolysaccharide. *Cell* **59**: 657-665.

Weiser, J.N., D.J. Maskell, P.D. Butler, A.A. Lindberg & E.R. Moxon, (1990a) Characterization of repetitive sequences controlling phase variation of *Haemophilus influenzae* lipopolysaccharide. *Journal of bacteriology* **172**: 3304-3309.

Weiser, J.N. & N. Pan, (1998) Adaptation of *Haemophilus influenzae* to acquired and innate humoral immunity based on phase variation of lipopolysaccharide. *Molecular microbiology* **30**: 767-775.

Weiser, J.N., N. Pan, K.L. McGowan, D. Musher, A. Martin & J. Richards, (1998) Phosphorylcholine on the lipopolysaccharide of *Haemophilus influenzae* contributes to persistence in the respiratory tract and sensitivity to serum killing mediated by C-reactive protein. *J Exp Med* **187**: 631-640.

Weiser, J.N., M. Shchepetov & S.T. Chong, (1997) Decoration of lipopolysaccharide with phosphorylcholine: a phase-variable characteristic of *Haemophilus influenzae*. *Infection and immunity* **65**: 943-950.

Weiser, J.N., A. Williams & E.R. Moxon, (1990b) Phase-variable lipopolysaccharide structures enhance the invasive capacity of *Haemophilus influenzae*. *Infection and immunity* **58**: 3455-3457.

Wenger, J.D., (1998) Epidemiology of *Haemophilus influenzae* type b disease and impact of *Haemophilus influenzae* type b conjugate vaccines in the United States and Canada. *The Pediatric infectious disease journal* **17**: S132-136.

Wenger, J.D., A.W. Hightower, R.R. Facklam, S. Gaventa & C.V. Broome, (1990) Bacterial meningitis in the United States, 1986: report of a multistate surveillance study. The Bacterial Meningitis Study Group. *The Journal of infectious diseases* **162**: 1316-1323.

Wewer, U.M., L.A. Liotta, M. Jaye, G.A. Ricca, W.N. Drohan, A.P. Claysmith, C.N. Rao, P. Wirth, J.E. Coligan, R. Albrechtsen & et al., (1986) Altered levels of laminin receptor mRNA in various human carcinoma cells that have different abilities to bind laminin. *Proceedings of the National Academy of Sciences of the United States of America* **83**: 7137-7141.

WHO, (2000) World Health Organization. The world health report. 2000 [cited 2012May 1]. Available from http://www.who.int/whr/2000/en/whr00_en.pdf. htm.

WHO, (2006) WHO position paper on *Haemophilus influenzae* type b conjugate vaccines. (Replaces WHO position paper on Hib vaccines previously published in the Weekly Epidemiological Record. Weekly Epidemiological Record. **81**: 445-452.

WHO, (2008) WHO vaccine-preventable diseases: monitoring system

William, I., B. Tim & A. Dlawer, (2005) *Medical Microbilogy*. Taylor and Francis Group

Winn, W., Jr, S. Allen, W. Janda, E. Koneman, G. Procop, P. Schreckenberger & G. woods, (2006) *Koneman's Color Atlas and Textbook of Diagnostic Microbiology*. Lippincott Williams & Wilkins, Philadelphia.

Wispelwey, B., E.J. Hansen & W.M. Scheld, (1989) *Haemophilus influenzae* outer membrane vesicle-induced blood-brain barrier permeability during experimental meningitis. *Infection and immunity* **57**: 2559-2562.

Yeo, H.J., S.E. Cotter, S. Laarmann, T. Juehne, J.W. St Geme, 3rd & G. Waksman, (2004) Structural basis for host recognition by the *Haemophilus influenzae* Hia autotransporter. *EMBO J* **23**: 1245-1256.

Yi, K. & T.F. Murphy, (1994) Mapping of a strain-specific bactericidal epitope to the surface-exposed loop 5 on the P2 porin protein of non-typeable *Haemophilus influenzae*. *Microbial pathogenesis* **17**: 277-282.

Yi, K. & T.F. Murphy, (1997) Importance of an immunodominant surface-exposed loop on outer membrane protein P2 of nontypeable *Haemophilus influenzae*. *Infection and immunity* **65**: 150-155.

Zhang, J.R. & E. Tuomanen, (1999) Molecular and cellular mechanisms for microbial entry into the CNS. *J Neurovirol* **5**: 591-603.

Zwahlen, A., J.S. Kroll, L.G. Rubin & E.R. Moxon, (1989) The molecular basis of pathogenicity in *Haemophilus influenzae*: comparative virulence of genetically-related capsular transformants and correlation with changes at the capsulation locus cap. *Microbial pathogenesis* **7**: 225-235.

APPENDIX.

Appendix 1. Formula of Commonly Used Buffers and Solutions

Sodium dodecyl sulfate (SDS)-resolving buffer; (36.34 g Tris base, 8 ml 10% SDS add deionised waster (dH2O) up to 200 ml, pH at 8.8).

SDS-staking buffer; (12.114 g Tris base, 8 ml 10% SDS) add dH2O up to 200 ml, pH at 6.8.

SDS running buffer (10 ×); dissolve 30.3 g (0.25 M) Tris base, 187.7 g (2.5 M) Glycine, in 950 ml dH2O, add 10 g SDS (1%), made up to 1000 ml with dH2O, mix well.

SDS-sample buffer (5 ×); 0.62 M Tris-Cl (pH 6.8), 5% SDS, 25% glycerol, 12.5% β-meracaptoethanol, 0.002% Bromophenol blue, or 7.8125 ml (2 M) Tris-Cl, 1.25 g SDS, 6.25 ml glycerol, 3.125 ml β-meracaptoethanol, tip of pipette Bromophenol blue, made up to 25 ml with dH2O.

Resolving (separating) gel; 1.7 ml SDS-resolving buffer, 2.33 ml Acrylamide/Bis-Acrylamide (30%), 2.88 ml dH2O, 30 µl 10% Ammonium persulfate (APS) and 30 µl Tetramethyl ethylenediamine (TEMED).

Staking gel; 1 ml SDS-stacking buffer, 0.8 ml Acrylamide/Bis-Acrylamide (30%), 2.18 ml dH2O, 30 µl 10% APS and 30 µl TEMED.

Semi-dry blotting buffer; 5.82 g Tris base, 2.93 g Glycine, 3.75ml 10% SDS, 200 ml methanol and make up to 1000 ml with dH2O.

Phosphate buffered saline solution (PBS); 1 × PBS was prepared by dissolving 1 tablet of Phosphate buffered saline (Dulbaco A, Oxoid) in 100 ml dH2O and autoclave, this gives Sodium chloride 0.16 mol, Potassium chloride 0.003 mol, Disodium hydrogen phosphate 0.008 mol and Potassium dihydrogen phosphate 0.001 mol with a pH value of 7.3.

BSA; (Albumin from bovine serum, Sigma A3912) as lyophilized powder (M W *c.* 66 kDa) was prepared in sterile PBS according to the concentration needed.

Blocking buffer; 2.52 g skimmed milk powder, 50 ml PBS/0.05% Tween-20 (400 ml PBS with 200 µl Tween-20); or add 1 g BSA to 100 ml of PBS (1% BSA in PBS).

PBS-Tween washing buffer; 400 ml PBS/200 µl Tween-20.

Buffers used for protein purification under denature condition (Ni-NTA column technique); 100 mM NaH_2PO_4, 10 mM Tris-Cl, and 8 M urea, adjusts

the pH, lysis Buffer (buffer B) at pH 8.0, wash Buffer (buffer C) at pH 6.3 and elution Buffer (buffer E) at pH 4.3.

Antibiotics; prepare according to the recommended concentrations, sterilise by filtration and store at 4°C.

Lysogeny broth (LB); Tryptone 10 g, Yeast extract 5 g and Sodium chloride 10 g for 1000 ml dH2O.

LB agar; Tryptone 10 g, Yeast extract 5 g, Sodium chloride 10 g, Microbial tested agar 15 g for 1000 ml of dH2O, pH 7.0 ± 0.2 at 25°C.

LB ampicillin/IPTG/X-gal agar; LB agar at 50°C, 100 µg ml-1 Ampicillin, 40 µg ml-1 IPTG and 50 µg ml-1 X-gal, mix and pour (0.5 mM IPTG and 20 µg ml-1 X-gal).

IPTG (Isopropyl-β-D thiogalactopyranoside [FW 238.8]); 1 M solution stock solution was prepared by dissolving 0.23 g of IPTG in 1 ml dH2O, sterilize by filtration and store at -20°C.

DNA loading dye (6 ×); 10 mM Tris-HCl (pH 7.6), 0.03% Bromophenol blue, 0.03% xylene cyanol FF, 60% glycerol, 60 mM Ethylenediamine tetraacetic acid (EDTA).

TAE buffer (50 × stock); 2 M Tris base (242 g) (life technologies), 2 M Acetic acid (57.1 ml glacial acetic acid [Fisher chemicals]) 50 mM EDTA (18.6 g) (pH 8.0) made up to 1000 ml with dH2O.

Agarose gel; 0.8-1.0 % agarose was prepared by dissolving 0.8-1 g of agarose powder (sigma), 2 ml 50 × TAE buffer and made up to 100 ml with dH2O; melt and add 5 µl ethidium bromide (10 mg ml^{-1}).

ELISA coating (carbonate) buffer; 142 mM sodium bicarbonate, 8 mM sodium carbonate [pH 9.4]) to 5µg ml^{-1}).

Alkaline phosphatase buffer; 15.7 g Tris-HCl, 5.8 g NaCl , 0.2 g Mgcl2.6H2O , 1000 ml dH2O, and adjust the pH to 9.5.

Appendix 2

A-OmpP2 Amino Acids Sequences in Different Strains of *H. influenzae*

(http://www.uniprot.org/uniprot/?query=ompP2&offset=0&sort=score)

1- *H. influenzae* strain: B1, B2, B3, B4 and D1.

AVVYNNEGTNVELGGRLSIITEQSNSTVDDQEQQHGALRNAGSRFHIKATHNFGDGFYAQGYLETRLVSDYPESSSDHFGGITTKYAYVTLGNKAFGEVKLGRAKTIADGITSAED
KEYGVLNNKKYIPTNGNTVGYTYKGIDGLDGLVLGANYLLAQSRVPGGPSPFPRKQGEVYPQQISNGVQVGAKYDANNIIAGIAFGRTNYKTAGADFDPYGDFGLGRKEQVEGV
LSTLGYRFSDLGLLVSLDSGYAKTKYYTTTDSSSGSQTITNPAYDEKRSFVSPGFQYELMEDTNVYGNFKYERTSVNQGKNTREQAVLFGVDHKLHKQVLTYIEGAYARTKTNDK
GKTEKTGKEKSVGVGLRVYF

2- *H. influenzae* strain: Serotype B.

AVVYNNEGTNVELGGRLSIIAEQSNSTVDNQKQQHGALRNQGSRFHIKATHNFGDGFYAQGYLETRFVTKASENGSDNFGDITSKYAYVTLGNKAFGEVKLGRAKTIADGITSAE
DKEYGVLNNSDYIPTSGNTVGYTFKGIDGLVLGANYLLAQKREGAKGENKRPNDKAGEVRIGEINNGIQVGAKYDANDIVAKIAYGRTNYKYNESDEHKQQLNGVLATLGYRFS
DLGLLVSLDSGYAKTKNYKIKHEKRYFVSPGFQYELMEDTNVYGNFKYERTSVDQGEKTREQAVLFGVDHKLHKQLLTYIEGAYARTRTTETGKGVKTEKEKSVGVGLRVYF

3- *H. influenzae* strain: D2, D3, D3R and D4.

AVVYNNEGTNVELGGRLSIITEQSNSTVDDQEQQHGALRNAGSRFHIKATHNFGDGFYAQGYLETRLVSDYPGSSSDHFGGITTKYAYVTLGNKAFGEVKLGRAKTIADGITSAED
KEYGVLNNKKYILTNGNTVGYTYKGIDGLDGLVLGANYLLAQSRVPGGPGLFPRKQGEVYPQQISNGVQVGAKYDANNIIAGIAFGRTNYKTAGADFDFSDAFGLGRKEQVEGV
LSTLGYRFSDLGLLVSLDSGYAKTKYHTTTTDSDDGRQTITNPAYDEKRSFVSPGFQYELMEDTNVYGNFKYERTSVNQGKNTREQAVLFGVDHKLHKQVLTYIEGAYARTKTN
DKGKTEKTGKEKSVGVGLRVYF

4- *H. influenzae* strain: T1 and T2.

AVVYNNEGSKVELGGRLSVIAEQSNNTVDDQKQQHGALRNQGSRFHIKATHNFGDGFYAQGYLETRFISHYQDNADHFDDITTKYAYVTLGNKAFGEVKLGRAKTIADDITSAE
DKEYGVLNNSKYIRTNGNTVGYTFKGIDGLVLGANYLLAQARDTANPGKKGEVAAQSISNGVQVGAKYDANNIVAGIAYGRTNYRKNIIAPKQNLGRKDQVEGVLSTLGYHFSD
LGLLVSLDSGYAKTKYYEQQQQQRSSPTKPRYDEKRYFVSPGFQYELMEDTNVYGNFKYERTSSDEGKKTREQAVLFGVDHKLHKQVLTYIEGAYARTKTNGKGKAETTGKEKS
VGVGLRVYF

5- *H. influenzae* strain: A1/A850043.

AVVYNNEGTNVELGGRLSVIAEQSNSTRKDQKQQHGELRNAGSRFHIKATHNFGDGFYAQGYLETRLVSDYQSSSDNFGNIITKYAYVTLGNKGFGEVKLGRAKTISDGITSAEDK
EYGVLENKEYIPKDGNSVGYTFKGIDGLVLGANYLLAQKREAYKTATATPGEVIAQVISNGVQVGAKYDANNIIAGIAYGRTNYREDLATQDKSGKKQQVNGALSTLGYRFSDLG
LLVSLDSGYAKTKNYKDKHEKRYFVSPGFQYELMEDTNVYGNFKYERNSVDQGKKAREHAVLFGVDHKLHKQVLTYIEGAYARTRTNDKGKTEKTEKEKSVGVGLRVYF

6- *H. influenzae* strain: AG30010.

AVVYNNEGTNVELGGRLSIIAEQSNSTIKDQKQQHGALRNQSSRFHIKATHNFGDGFYAQGYLETRLVSAQSGTESDNFGHIITKYAYVTLGNKALGEVKLGRAKTIADGITSAED
KEYGVLNNSKYIPIDGNTVGYTFKGIDGLVLGANYLLAQERYKYTTAAAAGAAGAAGAVAGEVYPQKISNGVQVGAKYDANNIIAGIAYGRTNYREDIASPDLGKKQQVNGALS
TLGYRFSDLGLLVSLDSGYAKTKNYKDKHEKSYFVSPGFQYELMEDTNVYGNFKYERDSVDQGKKTREQAVLFGVDHKLHKQVLTYIEGAYARTRTTESKKGVKTEKEKSVGV
GLRVYF

7- *H. influenzae* strain: 321GC.

AVVYNNEGTKVELGGRVSIIAEQSTSNRKDQKHQHGSLRNQGSRFNIKVTHNLGDGYYALGYYETRFINKDIDGNEKNIGSGFGSITTKLAYAGLGNKELGEATFGLQKTIADKIST
AEDKEYGVIEKNSYIPTEGNAIAYTYKGIEGLTLGASYVFGGRNFSDYEITDGKVSNAVQVGAKYDANNIVAGFAYGRTNYKAQQAKTQQVNGALATLGYHFDDLGLLISLDSGY
AKTKNKADKHEKRYFVSPGFQYELMEDTNLYGNLKYERINSVDQGEKVREHAVLFGIDHKLHKQVLTYIEGAYARTRTNDKGKTEKTEKEKSVGVGLRVYF

8- *H. influenzae* strain: 3185A.

AVVYNNEGTNVELGGRLSVIAEQSNSTRKDQKQQHGELRNAGSHFHIKATHNFGDGFYAQGYLETRLVSDYQSSSDNFGNIITKYAYVTLGNKGFGEVKLGRAKTIADGITSAED
KEYGVLENKEYIPKDGNSVGYTFKGIDGLVLGANYLLAQKREAYKTDAATPGEVIAQAISNGVQVGAKYDANNIIAGIAYGRTNYREDLAELGNKSGKKQQVNGALSTLGYRFS
DLGLLVSLDSGYAKTKNYKDKHEKRYFVSPGFQYELMEDTNVYGNFKYERNSVDQGKKAREHAVLFGVDHKLHKQVLTYIEGAYARTRTNDKDKTEKTEKEKSVGVGLRVYF

9- *H. influenzae* strain: 3224A.

AVVYNNEGTNVELGGRLSIIAEQSNSTIKDQKQQHGALRNQSSRFHIKATHNFGDGFYAQGYLETRLVSAQSGTESDNFGHIITKYAYVTLGNKAFGEVKLGRAKTIADGITSAED
KEYGVLNNSKYIPTNGNTVGYTFKGIDGLVLGANYLLAQERYKYGGAAGGAGGAGAVAGEVYPQKISNGVQVGAKYDANNIIAGIAYGRTNYRESIHEKDLGKKQQVNGALST
LGYRFSDLGLLVSLDSGYAKTKNYKDKHEKSYFVSPGFQYELMEDTNFYGNFKYERNSVDQGKKEREQAVLFGIDHKLHKQVLTYIEGAYARTRTNDKSKAEKTEKEKSVGVGL
RVYF

10- *H. influenzae* strain: 3230B.

AVVYNNEGTNVELGGRLSIIAEQSNSTIKDQKQQHGALRNQSSRFHIKATHNFGDGFYAQGYLETRLVSAQSGTESDNFGHIITKYAYVTLGNKAFGEVKLGRAKTIADGITSAED
KEYGVLNNSKYIPTNGNTVGYTFKGIDGLVLGANYLLAQERNKYGTGVGEVTSQSISNGVQVGAKYDANNIIVGIAYGRTNYREDVSQQDDAGKKQQVNGALSTLGYRFSDLGL
LVSLDSGYAKTKNYKDKHEKRYFVSPGFQYELMEDTNLYGNFKYERNSVDQGKKEREHAVLFGVDHKLHKQVLTYIEGAYARTRTTTRDTTKNTSTVKTEKEKSVGVGLRVYF

11- *H. influenzae* strain: ATCC 51907 / DSM 11121 / KW20 / Rd.

AVVYNNEGTNVELGGRLSIIAEQSNSTVDNQKQQHGALRNQGSRFHIKATHNFGDGFYAQGYLETRFVTKASENGSDNFGDITSKYAYVTLGNKAFGEVKLGRAKTIADGITSAE
DKEYGVLNNSDYIPTSGNTVGYTFKGIDGLVLGANYLLAQKREGAKNTNKQPNDKAGEVRIGEINNGIQVGAKYDANDIVAKIAYGRTNYKYNEADEHTQQLNGVLATLGYRFS
DLGLLVSLDSGYAKTKNYKTKHEKRYFVSPGFQYELMEDTNVYGNFKYERTSVDQGEKTREQAVLFGVDHKLHKQLLTYIEGAYARTKTTNGGVKTEKEKSVGVGLRVYF

12- *H. influenzae* strain: 86-028NP.

AVVYNNEGTNVELGGRLSIIAEQSNSTIKDQKQQHGALRNQSSRFHIKATHNFGDGFYAQGYLETRLVSAQSGTESDNFGHIITKYAYVTLGNKALGEVKLGRAKTIADGITSAED
KEYGVLNNSKYIPTNGNTVGYTFKGIDGLVLGANYLLAQERHKYTTAAGTRAVTVAGEVYPQKISNGVQVGAKYDANNIIAGIAYGRTNYREDIVDPDLGKKQQVNGALSTLGY
RFSDLGLLVSLDSGYAKTKNYKDKHEKSYFVSPGFQYELMEDTNVYGNFKYERDSVDQGKKTREQAVLFGVDHKLHKQVLTYIEGAYARTRTTEQAKGVKTEKEKSVGVGLRV
YF

13- *H. influenzae* strain: 2019.

AVVYNNEGTNVELGGRLSIIAEQSNSTIKDQKQQHGALRNQSSRFHIKATHNFGDGFYAQGYLETRLVSAQSGTESDNFGHIITKYAYVTLGNFAKGEVKLGRAKTIADGIISAEDK
EYGVLNNSKYIPTNGNTVGYTFKGIDGLVLGANYLLAQQRHKYTAAAAAAAAAGGARAVAGEVYPQKISNGVQVGAKYDANNIIAGIAYGRTNYREDITITPADKLGKKQQVNG
ALSTLGYRFSDLGLLVSLDSGYAKTKNYKAKHEKSYFVSPGFQYELMEDTNVYGNFKYERNSVDQGEKEREQAVLFGIDHKLHKQVLTYIEGAYSRTRTTTVGSKTNASKVKTE
KEKSVGVGLRVYF

14- *H. influenzae* strain: 23P2H1.

AVVYNNEGTKVELGGRVSIIAEQSTSNKKGQKHQHGSLRNQGSRFNIKVTHNLGDGYYALGYYETRFMNKNIDSTENSIGSGFGTITTKLAYAGLGNKELGEATFGLQKTIADIIST
AEDKEYGVIDKKPYIPTEGNAIAYTYKGIEGLTLGASYVFGGRNFYDYEIANGKISNAVQVGAKYDANNIVAGIAYGRTNYKAEQGKTQQVNGALATLGYHFDDLGLLISLDSGY
AKTKNKAAKHEKRYFVSPGFQYELMENTNVYGNFKYERSSVDQGEKEREHAVLFGVDHKLHKQVLTYIEGAYARTRTTE

15- *H. influenzae* strain: 23P4H1.

AVVYNNEGTKVELGGRVSIIAEQSTSNKKGQKHQHGSLRNQGSRFNIKVTHNLGDGYYALGYYETRFMNKNIDSTENSIGSGFGTITTKLAYAGLGNKELGEATFGLQKTIADIIST
AEDKEYGVIDKKPYIPTEGNAIAYTYKGIEGLTLGASYVFGGRNFYDYEIANGKISNAVQVGAKYDANNIVAGIAYGRTNYKAEQGKTQQVNGALATLGYHFDDLGLLISLDSGY
AKTKNKAAKHEKRYFVSPGFQYELMENTNVYGNFKYERSSVDQGEKEREHAVLFGVDHKLHKQVLTYIEGAYARTRTTEQAKGV

16- *H. influenzae* strain: 5657.

AVVYNNEGTKVELGGRLTIIAEQSSNTLDDQKQQHGALRNQGSRFHIKATHNFGDGFYAQGYLETRFVSKYKDNADHFDSITTKYAYVTLGNKALGEVKLGRAKTIADGITSAED
KEYGVLNNSKYIPTNGNTVGYTFEGIDGLVLGANYLLAQQRNAHGSTAGEVVAQVISNGVQVGAKYDANNIIAGIAYGRTNYREDLAAQGDSDKKQQVNGALSTLGYRFSDLGL
LVSLDSGYAKTKNYKDKHEKRYFVSPGFQYELMEDTNVYGNFKYERNSVDQGKKAREHAVLFGVDHKLHKQVLTYIEGAYARTRTNDKGKTEKTEKEKSVGVGLRVYF

17- *H. influenzae* Strain: 73P4H1.

AVVYNNEGTNVELGGRLSVIAEQSNSTRKDQKQQHGELRNAGSRFHIKATHNFGDGFYAQGYLETRLVSDYESRSDNFGNIITKYAYVTLGNKGFGEVKLGRAKTISDGITSAEDK
EYGVLKNKEYIPKDGNSVGYTFKGIDGLVLGANYLLAQKREAYKTATATPGEVTSQSISNGVQVGAKYDANNIIVGIAYGRTNYREDVPQQNDVGKKQQVNGALSTLGYRFSDL
GLLVSLDSGYAKTKNYKDKHEKRYFVSPGFQYELMEDTNLYGNFKYERNSVDQGKKEREQAVLFGIDHKLHKQVLTYIEGAYARTRTTMHDTKKTSTVKTEKEKSVGVGLRVY
F

18- *H. influenzae* strain: 31P12H1.

AVVYNNEGTNVELDGHLSVIAEQSSNTLDDQKQQHGALRNQGSRFHIKATHNFGDGFYAQGYLETRFVSKYKDNADHFDSITTKYAYVTLGNKALGEVKLGRAKTIADGITSAE
DKEYGVLNNSKYIPTNGNTVGYTFEGIDGLVLGANYLLAQQRNAHSGAAGEVVAQAISNGVQVGAKYDANNIIAGIAYGRTNYREDLAIQDKSGKKQQVNGALSTLGYRFSDLG
LLVSLDSGYAKTKNYKDKHEKRYFVSPGFQYELMEDTNVYGNFKYERNSVDQGKKAREHAVLFGVDHKLHKQVLTYIEGAYARTRTNDKGKTEKTEKEKSVGVGLRVYF

19- *H. influenzae* strain: 14P5H1.

AVVYNNEGTKVELGGRLSVIAEQSSNTLDDQKQQHGALRNQGSRFHIKATHNFGDGFYAQGYLETRLVTNPNGFTHEDRDGFGDITTKYAYVTLGNKALGEVKLGRAKTIADGI
TSAEDKEYGVLNNSKYVPTNGNTAGYTFKGIDGLVLGANYLLAQKYDNAGVNDGEVQKQSISNGVQVGAKYDANNIVAAIAFGRTNYKEDNSPSASKRKEQLKGVLSTLGYRFS
DLGLLVSLDSGYAKTKNHKKHRPAAAAYDEKRYFVSPGFQYELMEDTNVYGNFKYERNSSDQGKKTHEQAVLFGVDHKLHKQVLTYIEGAYARTKTNEKGQTEKTEKEKSGG
VGLRVYF

20- *H. influenzae* strain: 14P14H1.

AVVYNNEGTKVELGGRLSVIAEQSSNTLDDQKQQHGALRNQGSRFHIKATHNFGDGFYAQGYLETRLVTNPNGFTHEDRDGFGDITTKYAYVTLGNKALGEVKLGRAKTIADGI
TSAEDKEYGVLNNSKYVPTNGNTAGYTFKGIDGLVLGANYLLAQKYDNAGANDGEVQKQSISNGVQVGAKYDANNIVAAIAFGRTNYKEDNSPCASKRKEQLKGVLSTLGYRF
SDLGLLVSLDSGYAKTKNHKKHIPAAAAAAAAAAYDEKRYFVSPGFQYELMEDTNVYGNFKYERNSSDQGKKTHEQAVLFGVDHKLHKQVLTYIEGAYARTKTNEKGQTEKTE
KEKSVGVGLRVYF

21- *H. influenzae* strain: 3232.

AVVYNNEGTNVELGGRLSIIAEQSNSTIKDQKQQHGALRNQSSRFHIKATHNFGDGFYAQGYLETRLVSAQSGTESDNFGHIITKYAYVTLGNKAFGEVKLGRAKTISDGITSAEDK
EYGVLNNSKYIPTNGNTVGYTFKGIDGLVLGANYLLAQERYKYGGAAGGAGAVAGEVYPQKISNGVQVGAKYDANNIIAGIAYGRTNYRESIHEKDLGKKQQVNGALSTLGYRF
SDLGLLVSLDSGYAKTKNYKDKHEKSYFVSPGFQYELMEDTNFYGNFKYERNSVDQGKKEREQAVLFGIDHKLHKQVLTYIEGAYARTRTNDKSKAEKTEKEKSVGVGLRVYF

22- *H. influenzae* strain: 12085.

AVVYNNEGTNVELGGRLSIIAEQSNSTIKDQKQQHGALRNQGSRFHIKATHNFGDGFYAQGYLETRLVSAQSGTESDNFGHIITKYAYVTLGNKALGEVKLGRAKTIADGITSAED
KEYGVLNNSKYIPTDGNTVGYTFKGIDGLVLGANYLLAQERHKYTGAGAGAVAGEVYQQKISNGVQVGAKYDANNIIAGIAYGRTNYREDIIAGSDSGKKQQVNGALSTLGYRF
SDLGLLVSLDSGYAKTKNYKAKHEKSYFVSPGFQYELMEDTNFYGNFKYERNSVDQGKKEREHAVLFGVDHKLHKQVLTYIEGAYARTRTTQATGTKVKTEKEKSVGVGLRVY
F

23- *H. influenzae* strain: 13P24H1s.

AVVYNNEGTNVELGGRLSIIAEQSNSTIKDQKQQHGALRNQGSRFHIKATHNFGDGFYAQGYLETRLVSAQSGTESDNFGHIITKYAYVTLGNKALGEVKLGRAKTIADGITSAED
KEYGVLNNSKYIPTDGNTVGYTFKGIDGLVLGANYLLAQERHKYTGAGAGAVAGEVYQQKISNGVQVGAKYDANNIIAGIAYGRTNYREDIIAGSDSGKKQQVNGALSTLGYRF
SDLGLLVSLDSGYAKTKNYKAKHEKSYFVSPGFQYELMEDTNFYGNFKYERNSVDQGKKEREHAVLFGVDHKLHKQVLTYIEGAYARTRTTQATGTKVKTEKEKSVGVGLRVY
F

24- *H. influenzae* strain: 1479.

AVVYNNEGTKVELGGRLSVIAEQSSSTEDNQEQQHGALRNQGSRFHIKATHNFGDGFYAQGYLETRFVSKASKEKADQFADIVNKYAYLTLGNNTFGEVKLGRAKTIADEITTAE
DKEYGLLNSKKYIPTNGNTVGYTFNGIDGLVLGANYLLAQERDLRTLDSRTNPTKSGEVTVGEVSNGIQVGAKYDANNIIVAIAYGRTNYKDSNHSYTQKIPKANAADADTDTTII
YPHHGKKQEVNGALASLGYRFSDLGLLVSLDSGYAKTKNYKAKHEKSYFVSPGFQYELMEDTNVYGNFKYERNSVDQGEKEREQALLFGIDHKLHKQVLTYIEGAYSRTRTTSV
GDKQVASKVKTEKEKSVGVGLRVYF

25- *H. influenzae* strain: 74P4H1.

AVVYNNEGTNVELGGRLSIIAEQSNSTIKDQKQQHGALRNQSSRFHIKATHNFGDGFYAQGYLETRLVSAQSGTESDNFGHIITKYAYVTLGNNALGEVKLGRAKTIADGITSAED
KEYGVLNNSKYIPTNGNTVGYTFKGIDGLVLGANYLLAQERHKYTAAAAGGARAVAGEVYPQKISNGVQVGAKYDANNIIAGIAYGRTNYREDITITPAYKLGKKQQVNGALST
LGYRFSDLGLLVSLDSGYAKTKNYKAKHEKSYFVSPGFQYELMEDTNVYGNFKYERNSVDQGEKEREQAVLFGIDHKLHKQVLTYIEGAYSRTRTTTVGSKTNASKVKTEKEKS
VGVGLRVYF

26- *H. influenzae* strain: 13P36H1.

AVVYNNEGTNVELGGRLSIIAEQSNSTIKDQKQQHGALRNQGSRFHIKATHNFGDGFYAQGYLETRLVSAQSGTESDNFGHIITKYAYVTLGNKALGEVKLGRAKTIADGITSAED
KEYGVLNNSKYIPTDGNTVGYTFKGIDGLVLGANYLLAQERHKYTGAGAGAVAGEVYQQKISNGVQVGAKYDANNIIAGIAYGRTNYREDIIAGSDSGKKQQVNGALSTLGYRF
SDLGLLVSLDSGYAKTKNYKAKHEKSYFVSPGFQYELMEDTNFYGNFKYERNSVDQGKKEREHAVLFGVDHKLHKQVLTYIEGAYARTRTTQATGTKVKTEKEKSVGVGLRVY
F

27- *H. influenzae* strain: 5P30H1.

AVVYNNEGTNVELGGRLSVIAEQSNSTRKDQKQQHGELRNAGSRFHIKATHNFGDGFYAQGYLETRLVSDYESRSDNFGNIITKYAYVTLGNKGFGEVKLGRAKTISDGITSAEDK
EYGVLKNKEYIPKDGNSVGYTFKGIDGLVLGANYLLAQERVAYSSNGNTPGEVSTQKISNGVQVGAKYDANNIIAGIAYGRTNYREDLAAPQAKSGKKQQVNGALSTLGYRFSD
LGLLVSLDSGYAKTKNYKDKHEKRYFVSPGFQYELMEDTNLYGNFKYERNSVDQGKKAREHAVLFGVDHKLHKQVLTYIEGAYARTRTNDKGKTEKTEKEKSVGVGLRVYF

28- *H. influenzae* strain: 47P12H1.

AVVYNNEGTNVELGGRLSVIAEQSNSTADDQKQQHGALRNQGSRFHIKATHNFGDGFYAQGYLETRFVTKASENGSDNFGDITTKYAYVTLGNKAFGEVKLGRAKTIADGITSAE
DKEYGVIKNSKYIPTNGNTIGYTFKGIDGLVLGANYLLAQERYEGEVNPQKISNGVQVGAKYDANNIIAGIAYGRTNYRENTIGIPGLGKKQQVNGALSTLGYRFSDLGLLVSLDSG
YAKTKNYKAKHEKRYFLSPGFQYELMEDTNVYGNFKYERNSVDQGKKTREHAVLFGVDHKLHKQLLTYIEGAYARTRTTSGTNVTTEKEKSVGVGLRVYF

29- *H. influenzae* strain: 14P1H1.

AVVYNNEGTKVELGGRLSVIAEQSSNTLDDQKQQHGALRNQGSRFHIKATHNFGDGFYAQGYLETRLVTNPNGFTHEDRDGFGDITTKYAYVTLGNKALGEVKLGRAKTIADGI
TSAEDKEYGVLNNSKYVPTNGNTAGYTFKGIDGLVLGANYLLAQKYDNAGVNDGEVQKQSISNGVQVGAKYDANNIVAAIAFGRTNYKEDNSPSASKRKEQLKGVLSTLGYRFS
DLGLLVSLDSGYAKTKNHKKHRPAAAAYDEKRYFVSPGFQYELMEDTNVYGNFKYERNSSDQGKKTHEQAVLFGVDHKLHKQVLTYIEGAYARTKTNEKGQTEITEKEKSVGV
GLRVYF

30- *H. influenzae* strain: 48P29H1.

AVVYNNEGTNVELGGRLSIIAEQSNSTIKDQKQQHGALRNQSSRFHIKATHNFGDGFYAQGYLETRLVSAQSGTESDNFGHIITKYAYVTLGNKALGEVKLGRAKTIADGITSAED
KEYGVLNNSKYIPTNGNTVGYTFKGIDGLVLGANYLLAQERYKYTAAAAVPGAVPGAVAGEVYPQKISNGVQVGAKYDANNIIAGIAYGRTNYREDIITGSDSGKKQQVNGALS
TLGYRFSDLGLLVSLDSGYAKTKNYKAKHEKSYFVSPGFQYELMEDTNFYGNFKYERNSVDQGKKEREQAVLFGIDHKLHKQVLTYIEGAYARTRTNDKSKAEKTEKEKSVGVG
LRVYF

31- *H. influenzae* strain: 12.

AVVYNNEGTKVELGGRLSIIAEQSNSTVNDQKQQHGALRNQGSRFHIKATHNFGDGFYAQGYLETRFVAAQSGTKSDDFGHIITKYAYVTLGNKAFGEVKLGRAKTIADGITSAE
DKEYGVLNNSKYIPTDGNTVGYTFKGIDGLVLGANYLLAQDRSKYTASGSVAGEVTPQSISNGVQVGAKYDANNIIIGIAYGRTNYREDIISKQLNNLVGTKQQVNGALSTLGYRF
SDLGLLVSLDSGYAKTKNYKAKHEKSYFVSPGFQYELMEDTNVYGNFKYERDSVDQGKKAREHAVLFGVDHKLHKQVLTYIEGAYARTRTTESKKGVKTEKEKSVGVGLRVYF

32- *H. influenzae* strain: 74P15H1.

AVVYNNEGTNVELGGRLSIIAEQSNSTIKDQKQQHGALRNQSSRFHIKATHNFGDGFYAQGYLETRLVSAQSGTESDNFGHIITKYAYVTLGNNALGEVKLGRAKTIADGITSAED
KEYGVLNNSKYIPTNGNTVGYTFKGIDGLVLGANYLLAQERHKYTAAAAAAAGGARAVAGEVYPQKISNGVQVGAKYDANNIIAGIAYGRTNYREDITITPAYKLGKKQQVNGA
LSTLGYRFSDLGLLVSLDSGYAKTKNYKAKHEKSYFVSPGFQYELMEDTNVYGNFKYERNSVDQGEKEREQAVLFGIDHKLHKQVLTYIEGAYSRTRTTTVGSKTNASKVKTEKE
KSVGVGLRVYF

33- *H. influenzae* strain: not presented.

AVVYNNEGTNVELGGRLSIIAEQSNSTVNDQKQQHGALRNQGSRFHIKATHNFGDGFYAQGYLETRFVADQSGTESDHFGHIITKYAYVTLGNKAFGEVKLGRAKTIADGITSAED
KEYGVLNNSKYIPTNGNTVGYTFKGIDGLVLGANYLLAQERHKYTGVGVGAAGAVAGEVYPQKISNGVQVGAKYDANNIIAGIAYGRTNYREDIHKEDLGKKQQVNGALSTLG
YRFSDLGLLVSLDSGYAKTKNYKDKHEKHYFVSPGFQYELMEDTNVYGNFKYERNSVDQGKKAREHAVLFGVDHKLHKQVLTYIEGAYARTRTNDQGKTEKTEKEKSVGVGL
RVYF

34- *H. influenzae* strain: 14P23H1.

AVVYNNEGTKVELGGRLSVIAEQSSNTLDDQKQQHGALRNQGSRFHIKATHNFGDGFYAQGYLETRLVTNPNGFTHEDRDGFGDITTKYAYVTLGNKALGEVKLGRAKTIADGI
TSAEDKEYGVLNNSKYVPTNGNTAGYTFKGIDGLVLGANYLLAQKYDNAGANDGEVQKQSISNGVQVGAKYDANNIVAAIAFGRTNYKEDNSPCASKRKEQLKGVLSTLGYRF
SDLGLLVSLDSGYAKTKNHKKHIPAAAAAAAAAAYDEKRYFVSPGFQYELMEDTNVYGNFKYERNSSDQGKKTHEQAVLFGVDHKLHKQVLTYIEGAYARTKTNEKGQTEKTE
KEKSVGVGLRVYF

35- *H. influenzae* strain: 48P45H1.

AVVYNNEGTNVELGGRLSIIAEQSNSTIKGQKQQHGALRNQSSRFHIKATHNFGDGFYAQGYLETRLVSAQSGTESDNFGHIITKYAYVTLGNKALGEVKLGRAKTIADGITSAED
KEYGVLNNSKYIPTNGNTVGYTFKGIDGLVLGANYLLAQERYKYTAAAVPGAGAGAVAVAGEVYPQKISNGVQVGAKYDANNIIAGIAYGRTNYREDITGSDLGKKQQVNGAL
STLGYRFSDLGLLVSLDSGYAKTKNYKAKHEKSYFVSPGFQYELMEDTNFYGNFKYERNSVDQGKKEREQAVLFGIDHKLHKQVLTYIEGAYARTRTNDKSKAEKTEKEKSVGV
GLRVYF

36- *H. influenzae* strain: 74P1H1.

AVVYNNEGTNVELGGRLSIIAEQSNSTIKDQKQQHGALRNQSSRFHIKATHNFGDGFYAQGYLETRLVSAQSGTESDNFGHIITKYAYVTLGNNALGEVKLGRAKTIADGITSAED
KEYGVLNNSKYIPTNGNTVGYTFKGIDGLVLGANYLLAQERHKYTAAAAAAAAGGARAVAGEVYPQKISNGVQVGAKYDANNIIAGIAYGRTNYREDITITPAYKLGKKQQVNGA
LSTLGYRFSDLGLLVSLDSGYAKTKNYKAKHEKSYFVSPGFQYELMEDTNVYGNFKYERNSVDQGEKEREQAVLFGIDHKLHKQVLTYIEGAYSRTRTTTVGSKTNASKVKTEKE
KSVGVGLRVYF

37- *H. influenzae* strain: 73P2H1.

AVVYNNEGTNVELGGRLSVIAEQSNSTRKDQKQQHGELRNAGSRFHIKATHNFGDGFYAQGYLETRLVSDYESRSDNFGNIITKYAYVTLGNKGFGEVKLGRAKTISDGITSAEDK
EYGVLKNKEYIPKDGNSVGYTFKGIDGLVLGANYLLAQKREAYKTATATPGEVTSQSISNGVQVGAKYDANNIIVGIAYGRTNYREDVPQQNDVGKKQQVNGALSTLGYRFSDL
GLLVSLDSGYAKTKNYKDKHEKRYFVSPGFQYELMEDTNLYGNFKYERNSVDQGKKEREQAVLFGIDHKLHKQVLTYIEGAYARTRTTMHDTKKTSTVKTEKEKSVGVGLRVY
F

38- *H. influenzae* strain: 5P41H1.

AVVYNNEGTNVELGGRLSVIAEQSNSTRKDQKQQHGELRNAGSRFHIKATHNFGDGFYAQGYLETRLVSDYESRSDNFGNIITKYAYVTLGNKGFGEVKLGRAKTISDGITSAEDK
EYGVLKNKEYIPKDGNSVGYTFKGIDGLVLGANYLLAQERVAYSSNGNTPGEVSTQKISNGVQVGAKYDANNIIAGIAYGRTNYREDLAAPQAKSGKKQQVNGALSTLGYRFSD
LGLLVSLDSGYAKTKNYKDKHEKRYFVSPGFQYELMEDTNLYGNFKYERNSVDQGKKAREHAVLFGVDHKLHKQVLTYIEGAYARTRTRTRTNDKGKTEKTEKEKSVGVGLRV
YF

39- *H. influenzae* strain:18P4H1.

AVVYNNEGTNVELGGRLSVIAEQSTNTLDDQEQQHGALRNQGSRFHIKATHNLGDGFYAQGYLETRFVTDITKDKSDHFGDITTEYAYVTLGNKAFGEVKLGRAETIAGGITSAE
DKEYGVLNNSKYIPTNGNTAGYTFKGIDGLVLGANYLLAQQRDVYHTVGKPGEVYPQSISNGVQVGAKYDANNIVAGIAYGRTNYRENIRLTALSPSRKEQVEGVLSTLGYHFSD
LGLLVSLDSGYAKTKNHMKPAITTTTTTAAAEPAYDEKRYFVSPGFQYELMEDTNVYGNFKYERTYVNQGKKTHEQAVLFGVDHKLHKQVLTYIEGAYARTKTNDKGKAEKTG
KEKSMGVGLRVYF

40- *H. influenzae* strain: 22P5H1.

AVVYNNEGTKVELGGRLSIIAEQSTNTEKDQKQQHGTLRNQGSRFHIKATHNFGDDFYAQGYLETRFVADQSGTESDHFGHIITKYAYVTLGNKAFGEVKLGRAKTIADGITSAED
KEYGVLNNSKYIPTNGNTVGYTFKGIDGLVLGANYLLAQERHKYTAGSDTVAGEVYPQKISNGVQVGAKYDANNIIAGIAYGRTNYREDLSTTKDLGKKQQVNGALSTLGYRFS
DLGLLVSLDSGYAKTKNYKDKHEKRYFVSPGFQYELMEDTNVYGNFKYERNSVDQGKKAREHAVLFGVDHKLHKQVLTYIEGAYARTRTNDKGKTEKTEKEKSVGVGLRVYF

41- *H. influenzae* strain: not present.

AVVYNNEGTKVELGGRLSIIAEQSNSTIKDQKQQHGALRNQGSRFHIKATHNFGDGFYAQGYLETRFVAAQSGTGSDDFGHIITKYAYVTLGNKAFGEVKLGRAKTIADGITSAED
KEYGVLNNSKYIPTNGNTVGYTFKGIDGLVLGTNYLLAQDRYKYAATGSFAGEVTPQSISNGVQVGAKYDANNIIIGIAYGRTNYREDIVTAPGGDLAGTKQQVNGALSTLGYRFS
DLGLLVSLDSGYAKTKNYKDKHEKRYFVSPGFQYELMEDTNVYGNFKYERNSVDQGKKAREHAVLFGVDHKLHKQVLTYIEGAYARTRTNDKGKTEKTEKEKSVGVGLRVYF

42- *H. influenzae* strain: 18P1H1.

AVVYNNEGTNVELGGRLSVIAEQSTNTLDDQEQQHGALRNQGSRFHIKATHNLGDGFYAQGYLETRFVTDITKDKSDHFGDITTEYAYVTLGNKAFGEVKLGRAETIAGGITSAE
DKEYGVLNNSKYIPTNGNTAGYTFKGIDGLVLGANYLLAQQRDVYHTVGKPGEVYPQSISNGVQVGAKYDANNIVAGIAYGRTNYRENIRLTVLSPSRKEQVEGVLSTLGYHFSD
LGLLVSLDSGYAKTKNHMKPAITTTAATTAAEPAYDEKRYFVSPGFQYELMEDTNVYGNFKYERTYVNQGKKTHEQAVLFGVDHKLHKQVLTYIEGAYARTKTNDKGKAEKTG
KEKSMGVGLRVYF

43- *H. influenzae* strain: 31P7H7.

AVVYNNEGTNVELDGHLSVIAEQSSNTLDDQKQQHGALRNQGSRFHIKATHNFGDGFYAQGYLETRFVSKYKDNADHFDSITTKYAYVTLGNKALGEVKLGRAKTIADGITSAE
DKEYGVLNNSKYIPTNGNTVGYTFEGIDGLVLGANYLLAQQRNAHSGAAGEVVAQAISNGVQVGAKYDANNIIAGIAYGRTNYREDLAIQDKSGKKQQVNGALSTLGYRFSDLG
LLVSLDSGYAKTKNYKDKHEKRYFVSPGFQYELMEDTNVYGNFKYERNSVDQGKKAREHAVLFGVDHKLHKQVLTYIEGAYARTRTNDKGKTEKTEKEKSVGVGLRVYF

44- *H. influenzae* strain: 22P1H1.

AVVYNNEGTKVELGGRLSIIAEQSTNTEKDQKQQHGTLRNQGSRFHIKATHNFGDDFYAQGYLETRFVADQSGTESDHFGHIITKYAYVTLGNKAFGEVKLGRAKTIADGITSAED
KEYGVLNNSKYIPTNGNTVGYTFKGIDGLVLGANYLLAQERHKYTAGSDTVAGEVYPQKISNGVQVGAKYDANNIIAGIAYGRTNYREDLSTTKDLGKKQQVNGALSTLGYRFS
DLGLLVSLDSGYAKTKNYKDKHEKRYFVSPGFQYELMEDTNVYGNFKYERNSVDQGKKAREHAVLFGVDHKLHKQVLTYIEGAYARTRTNDKGKTEKTEKEKSVGVGLRVYF

45- *H. influenzae* strain: 12049.

AVVYNNEGTKVELGGRLSVIAEQSNTTVDDQKQQHGALRNQGSRFHIKATHNFSDGFYAQGYLETRLISSYDGENTDGFGGIVTRYAYVTLGNKAFGEVKLGRAKTIADGITSAE
DKEYGVLNNSKYIPTNGNTAGYTFKGIDGLVLGANYLLAQKYDTAGVAGEVQRQSISNGVQVGAKYDANNIVAAIAFGRTNYKESSVIALGRKEQLKGVLSTLGYRFSDLGLLVS
LDSGYAKTKNHKELNKPTGAKPAYDEKRYFVSPGFQYELMEDTNVYGNFKYERTSSDEGKKTHEQAVLFGVDHKLHKQVLTYIEGAYARTKTNDKNKPEKTGKEKSVGVGLRV
YF

46- *H. influenzae* strain: 54P24H1.

AVVYNNEGTNVELGGRLSVIAEQSNSTADDQKQQHGALRNQGSRFHIKATHNFGDGFYAQGYLETRFVTKASENGSDNFGDITTKYAYVTLGNKAFGEVKLGRAKTIADGITSAE
DKEYGVIKNSKYIPTNGNTIGYTFKGIDGLVLGANYLLAQERYEGEVNPQKISNGVQVGAKYDANNIIAGIAYGRTNYRENTIGIPDLGKKQQVNGALSTLGYRFSDLGLLVSLDSG
YAKTKNYKAKHEKRYFVSPGFQYELMEDTNVYGNFKYERNSVDQGKKTREHAVLFGVDHKLHKQLLTYIEGAYARTRTTSGTNVTTEKEKSVGVGLRVYF

47- *H. influenzae* strain: 54P33H1.

AVVYNNEGTNVELGGRLSVIAEQSNSTADDQKQQHGALRNQGSRFHIKATHNFGDGFYAQGYLETRFVTKASENGSDNFGDITTKYAYVTLGNKAFGEVKLGRAKTIADGITSAE
DKEYGVIKNSKYIPTNGNTIGYTFKGIDGLVLGANYLLAQERYEGEVNPQKISNGVQVGAKYDANNIIAGIAYGRTNYRENTIGIPDLGKKQQVNGALSTLGYRFSDLGLLVSLDSG
YAKTKNYKAKHEKRYFVSPGFQYELMEDTNVYGNFKYERNSVDQGKKTREHAVLFGVDHKLHKQLLTYIEGAYARTRTTSGTNVTTEKEKSVGVGLRVYF

48- *H. influenzae* strain: 54P33H1.

AVVYNNEGTNVELGGRLSVIAEQSNSTADDQKQQHGALRNQGSRFHIKATHNFGDGFYAQGYLETRFVTKASENGSDNFGDITTKYAYVTLGNKAFGEVKLGRAKTIADGITSAE
DKEYGVIKNSKYIPTNGNTIGYTFKGIDGLVLGANYLLAQERYEGEVNPQKISNGVQVGAKYDANNIIAGIAYGRTNYRENTIGIPDLGKKQQVNGALSTLGYRFSDLGLLVSLDSG
YAKTKNYKAKHEKRYFVSPGFQYELMEDTNVYGNFKYERNSVDQGKKTREHAVLFGVDHKLHKQLLTYIEGAYARTRTTSGTNVTTEKEKSVGVGLRVYF

49- *H. influenzae* strain: R2846 / 12.

AVVYNNEGTKVELGGRLSIIAEQSNSTVNDQKQQHGALRNQGSRFHIKATHNFGDGFYAQGYLETRFVAAQSGTKSDDFGHIITKYAYVTLGNKAFGEVKLGRAKTIADGITSAE
DKEYGVLNNSKYIPTDGNTVGYTFKGIDGLVLGANYLLAQDRSKYTASGSVAGEVTPQSISNGVQVGAKYDANNIIIGIAYGRTNYREDIISKQLNNLVGTKQQVNGALSTLGYRF
SDLGLLVSLDSGYAKTKNYKAKHEKSYFVSPGFQYELMEDTNVYGNFKYERDSVDQGKKAREHAVLFGVDHKLHKQVLTYIEGAYARTRTTESKKGVKTEKEKSVGVGLRVYF

50- *H. influenzae* strain: R2866.

AVVYNNEGSKVELGGRLSVIAEQSNNTVDDQKQQHGALRNQGSRFHIKATHNFGDGFYAQGYLETRFVSHYQDNADHFDDITTKYAYVTLGNKAFGEVKLGRAKTIADGITSAE
DKEYGVLNNSKYIRTNGNTVGYTFKGIDGLVLGANYLLAQARDTANPSKEGEVATQSISNGVQVGAKYDANNIVAGIAYGRTNYRKNIITPKQDLGRKDQVEGVLSTLGYHFSDL
GLLVSLDSGYAKTKYYEQQQQSNSTKPRYDEKRYFVSPGFQYELMEDTNVYGNFKYERTSSDEGKKTHEQAVLFGVDHKLHKQVLTYIEGAYARTKTNGKGKAETTGKEKSVG
VGLRVYF

B- Variability of OmpP2 Amino Acids in Different Strains of *H. influenzae*

Multi-way Protein alignment.
Sequences: 50. Scoring matrix: BLOSUM 62

Sequence	Start	End	#Match	NonMatch	%Match
1	1	365	282	90	75
2	1	341	280	79	77
3	1	366	280	93	75
4	1	351	276	84	76
5	1	340	296	53	84
6	1	349	300	53	84
7	1	333	230	127	64
8	1	341	296	53	84
9	1	347	304	49	86
10	1	343	300	56	84
11	1	339	277	82	77
12	1	345	302	50	85
13	1	358	298	61	83
14	1	311	221	130	62
15	1	316	223	128	63
16	1	337	293	58	83
17	1	344	291	63	82
18	1	337	293	58	83
19	1	347	278	79	77
20	1	353	279	84	76
21	1	344	303	47	86
22	1	344	300	51	85
23	1	344	300	51	85
24	1	370	267	109	71
25	1	353	299	55	84
26	1	344	300	51	85
27	1	341	295	54	84
28	1	332	291	55	84
29	1	347	278	79	77
30	1	349	304	50	85
31	1	344	295	55	84
32	1	356	299	58	83
33	1	345	302	48	86
34	1	353	279	84	76
35	1	349	303	50	85
36	1	356	299	58	83
37	1	344	291	63	82
38	1	345	295	58	83
39	1	356	275	89	75
40	1	342	300	47	86
41	1	344	301	49	86
42	1	356	275	89	75
43	1	337	293	58	83
44	1	342	300	47	86
45	1	345	276	85	76
46	1	332	292	54	84
47	1	332	292	54	84
48	1	332	292	54	84
49	1	344	295	55	84
50	1	349	277	81	77

C- Alignments of OmpP2 Amino Acids in Different Strains of *H. influenzae*

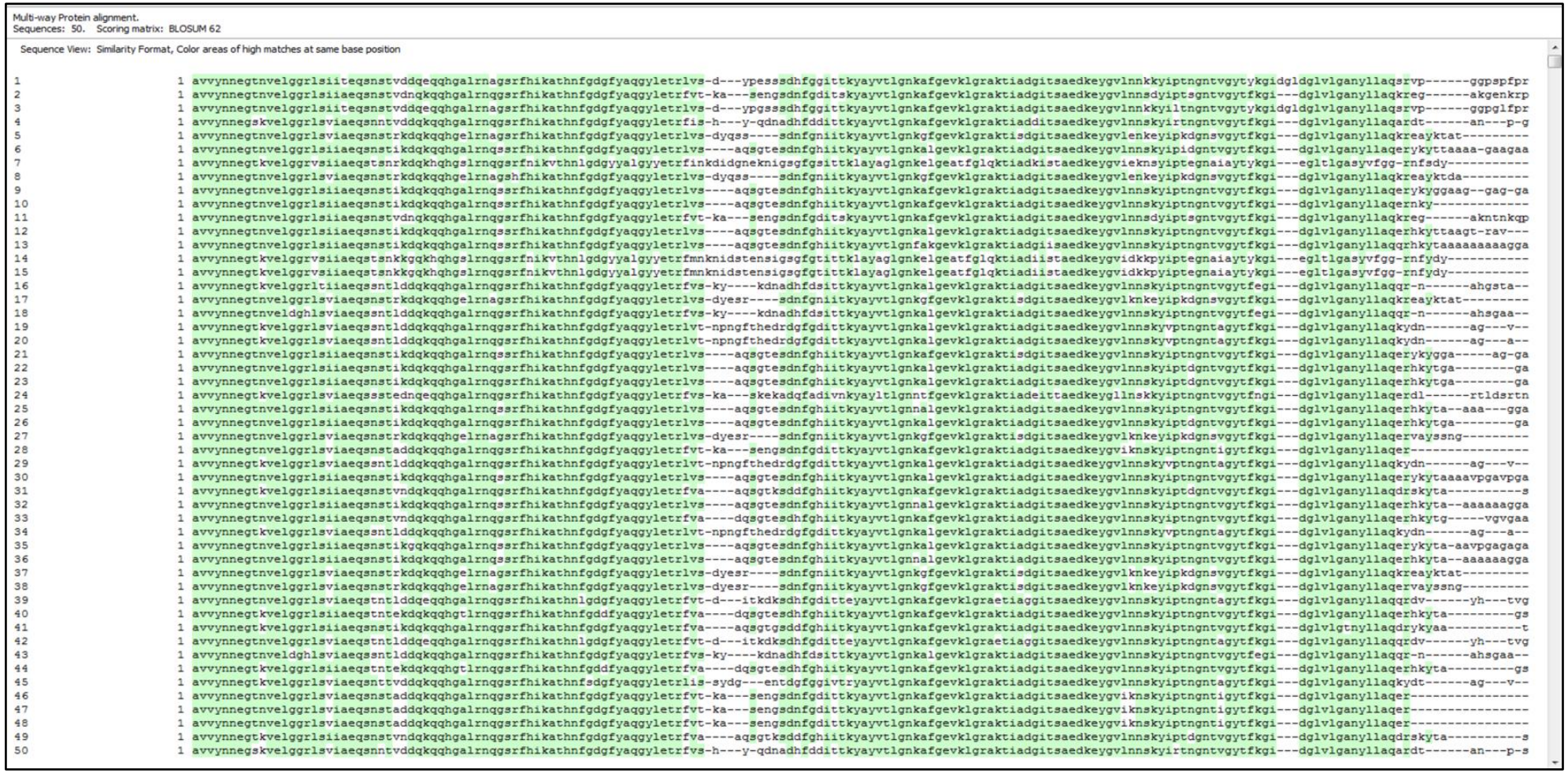

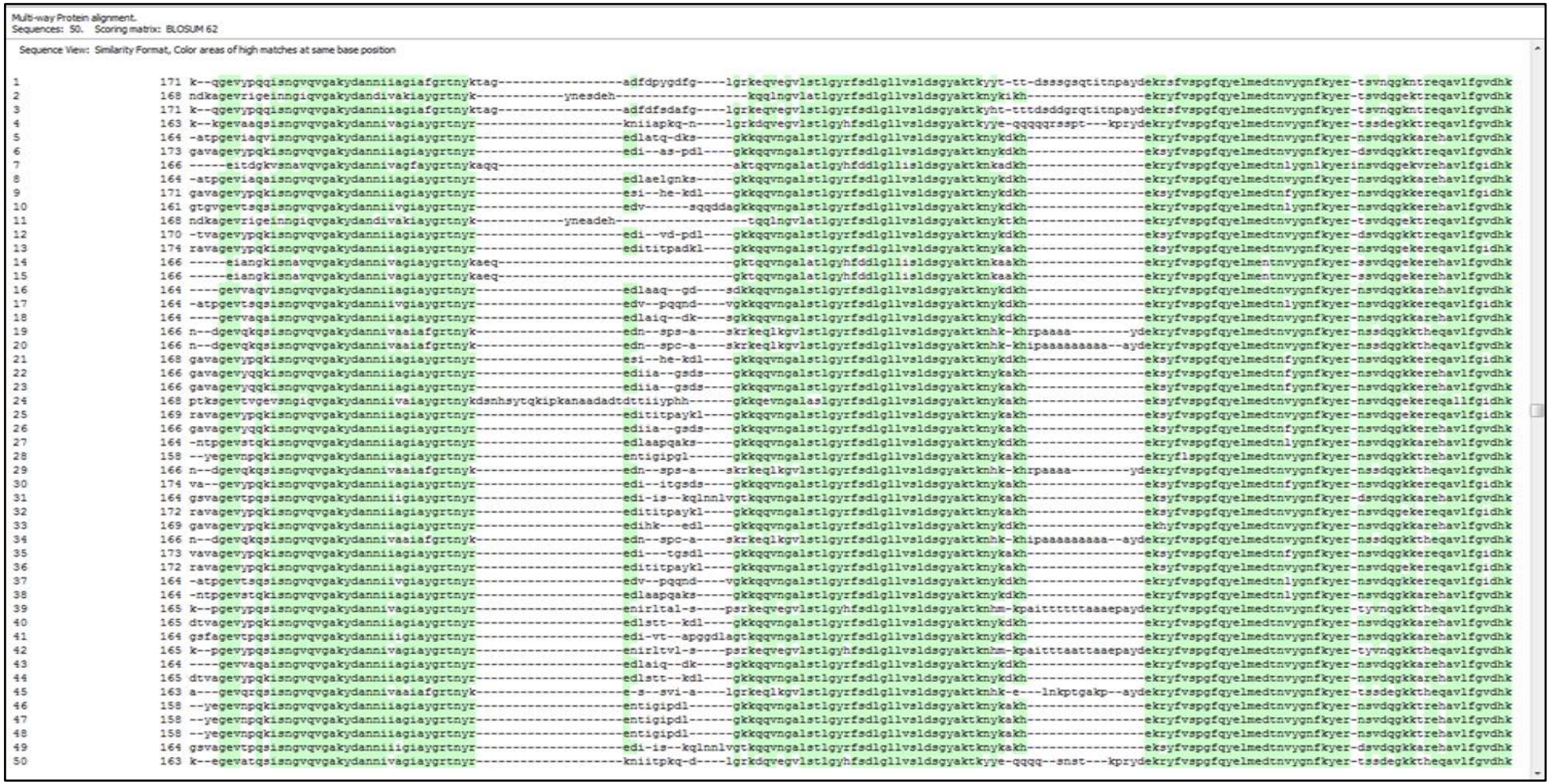
Multi-way Protein alignment.
Sequences: 50. Scoring matrix: BLOSUM 62
Sequence View: Similarity Format, Color areas of high matches at same base position

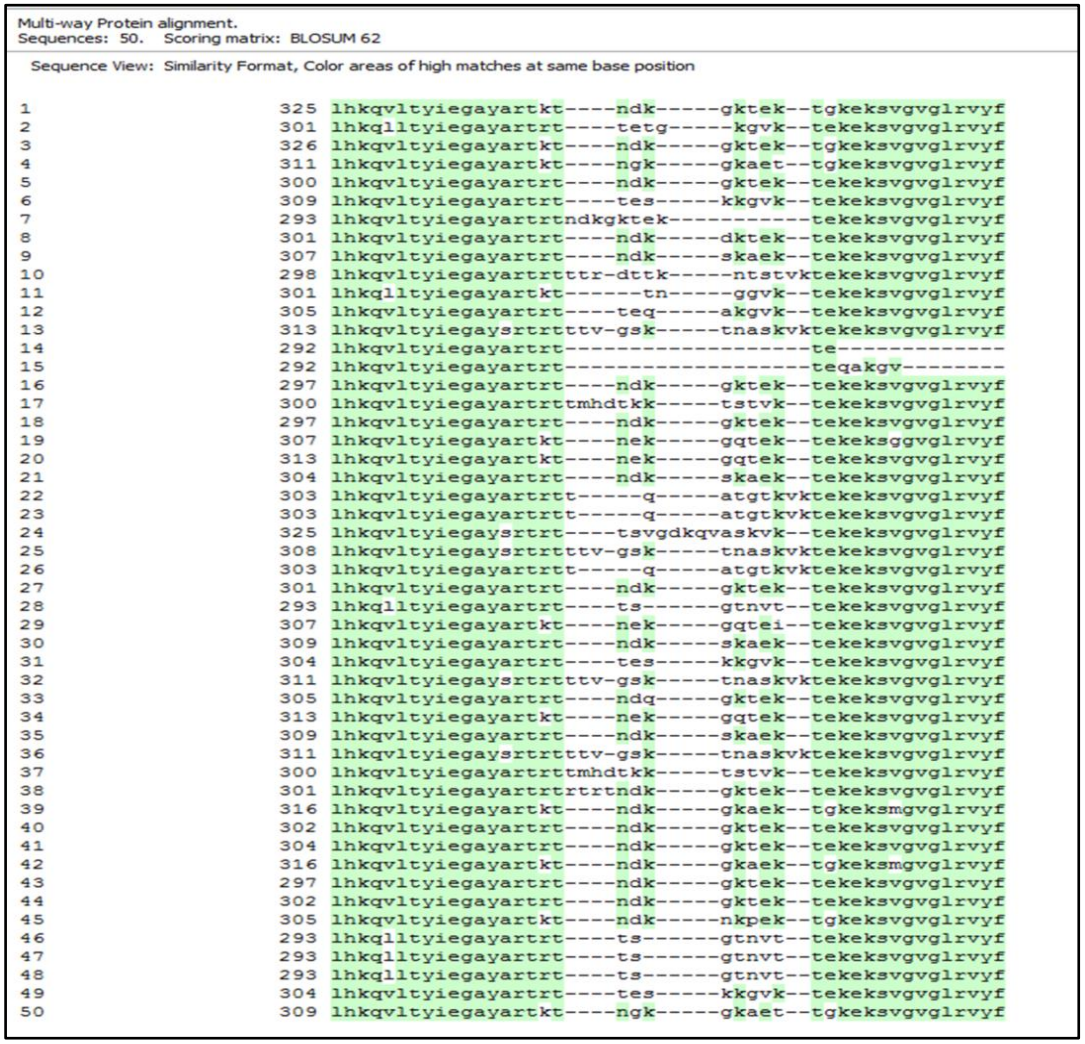
Multi-way Protein alignment.
Sequences: 50. Scoring matrix: BLOSUM 62
Sequence View: Similarity Format, Color areas of high matches at same base position
1 325 lhkqvltyiegayartkt----ndk-----gktek--tgkeksvgvglrvyf
2 301 lhkqlltyiegayartrt----tetg-----kgvk--tekeksvgvglrvyf
3 326 lhkqvltyiegayartkt----ndk-----gktek--tgkeksvgvglrvyf
4 311 lhkqvltyiegayartkt----ngk-----gkaet--tgkeksvgvglrvyf
5 300 lhkqvltyiegayartrt----ndk-----gktek--tekeksvgvglrvyf
6 309 lhkqvltyiegayartrt----tes-----kkgvk--tekeksvgvglrvyf
7 293 lhkqvltyiegayartrtndkgktek----------tekeksvgvglrvyf
8 301 lhkqvltyiegayartrt----ndk-----dktek--tekeksvgvglrvyf
9 307 lhkqvltyiegayartrt----ndk-----skaek--tekeksvgvglrvyf
10 298 lhkqvltyiegayartrtttr-dttk-----ntstvktekeksvgvglrvyf
11 301 lhkqlltyiegayartkt------tn-----ggvk--tekeksvgvglrvyf
12 305 lhkqvltyiegayartrt----teq-----akgvk--tekeksvgvglrvyf
13 313 lhkqvltyiegaysrtrtttv-gsk-----tnaskvktekeksvgvglrvyf
14 292 lhkqvltyiegayartrt--------------------te----------
15 292 lhkqvltyiegayartrt--------------------teqakgv--------
16 297 lhkqvltyiegayartrt----ndk-----gktek--tekeksvgvglrvyf
17 300 lhkqvltyiegayartrttmhdtkk-----tstvk--tekeksvgvglrvyf
18 297 lhkqvltyiegayartrt----ndk-----gktek--tekeksvgvglrvyf
19 307 lhkqvltyiegayartkt----nek-----gqtek--tekeksggvglrvyf
20 313 lhkqvltyiegayartkt----nek-----gqtek--tekeksvgvglrvyf
21 304 lhkqvltyiegayartrt----ndk-----skaek--tekeksvgvglrvyf
22 303 lhkqvltyiegayartrtt-----q-----atgtkvktekeksvgvglrvyf
23 303 lhkqvltyiegayartrtt-----q-----atgtkvktekeksvgvglrvyf
24 325 lhkqvltyiegaysrtrt----tsvgdkqvaskvk--tekeksvgvglrvyf
25 308 lhkqvltyiegaysrtrtttv-gsk-----tnaskvktekeksvgvglrvyf
26 303 lhkqvltyiegayartrtt-----q-----atgtkvktekeksvgvglrvyf
27 301 lhkqvltyiegayartrt----ndk-----gktek--tekeksvgvglrvyf
28 293 lhkqlltyiegayartrt----ts------gtnvt--tekeksvgvglrvyf
29 307 lhkqvltyiegayartkt----nek-----gqtei--tekeksvgvglrvyf
30 309 lhkqvltyiegayartrt----ndk-----skaek--tekeksvgvglrvyf
31 304 lhkqvltyiegayartrt----tes-----kkgvk--tekeksvgvglrvyf
32 311 lhkqvltyiegaysrtrtttv-gsk-----tnaskvktekeksvgvglrvyf
33 305 lhkqvltyiegayartrt----ndq-----gktek--tekeksvgvglrvyf
34 313 lhkqvltyiegayartkt----nek-----gqtek--tekeksvgvglrvyf
35 309 lhkqvltyiegayartrt----ndk-----skaek--tekeksvgvglrvyf
36 311 lhkqvltyiegaysrtrtttv-gsk-----tnaskvktekeksvgvglrvyf
37 300 lhkqvltyiegayartrttmhdtkk-----tstvk--tekeksvgvglrvyf
38 301 lhkqvltyiegayartrtrtrtndk-----gktek--tekeksvgvglrvyf
39 316 lhkqvltyiegayartkt----ndk-----gkaek--tgkeksmgvglrvyf
40 302 lhkqvltyiegayartrt----ndk-----gktek--tekeksvgvglrvyf
41 304 lhkqvltyiegayartrt----ndk-----gktek--tekeksvgvglrvyf
42 316 lhkqvltyiegayartkt----ndk-----gkaek--tgkeksmgvglrvyf
43 297 lhkqvltyiegayartrt----ndk-----gktek--tekeksvgvglrvyf
44 302 lhkqvltyiegayartrt----ndk-----gktek--tekeksvgvglrvyf
45 305 lhkqvltyiegayartkt----ndk-----nkpek--tgkeksvgvglrvyf
46 293 lhkqlltyiegayartrt----ts------gtnvt--tekeksvgvglrvyf
47 293 lhkqlltyiegayartrt----ts------gtnvt--tekeksvgvglrvyf
48 293 lhkqlltyiegayartrt----ts------gtnvt--tekeksvgvglrvyf
49 304 lhkqvltyiegayartrt----tes-----kkgvk--tekeksvgvglrvyf
50 309 lhkqvltyiegayartkt----ngk-----gkaet--tgkeksvgvglrvyf

D-Variability of OmpP2L2 Amino Acids in Different Strains of *H. influenzae*

Multi-way Protein alignment.
Sequences: 50. Scoring matrix: BLOSUM 62

Sequence	Start	End	#Match	NonMatch	%Match
1	1	15	5	13	27
2	1	15	8	7	53
3	1	15	5	13	27
4	1	15	3	16	15
5	1	15	6	13	31
6	1	15	8	7	53
7	1	15	0	19	0
8	1	15	5	15	25
9	1	15	8	7	53
10	1	15	8	7	53
11	1	15	8	7	53
12	1	15	8	7	53
13	1	15	8	7	53
14	1	15	1	18	5
15	1	15	1	19	5
16	1	15	3	16	15
17	1	15	6	13	31
18	1	15	3	16	15
19	1	15	2	17	10
20	1	15	2	17	10
21	1	15	8	7	53
22	1	15	8	7	53
23	1	15	8	7	53
24	1	15	5	10	33
25	1	15	8	7	53
26	1	15	8	7	53
27	1	15	6	13	31
28	1	15	8	7	53
29	1	15	2	17	10
30	1	15	8	7	53
31	1	15	7	8	46
32	1	15	8	7	53
33	1	15	7	8	46
34	1	15	2	17	10
35	1	15	8	7	53
36	1	15	8	7	53
37	1	15	6	13	31
38	1	15	6	13	31
39	1	15	6	9	40
40	1	15	7	8	46
41	1	15	7	8	46
42	1	15	6	9	40
43	1	15	3	16	15
44	1	15	7	8	46
45	1	15	4	14	22
46	1	15	8	7	53
47	1	15	8	7	53
48	1	15	8	7	53
49	1	15	7	8	46
50	1	15	3	16	15

E-Alignments of OmpP2L2 Amino Acids in Different Strains of *H. influenzae*